

LITHUANIAN UNIVERSITY OF HEALTH SCIENCES
MEDICAL ACADEMY

Marius Kubilius

**DENTAL IMPLANT TREATMENT
PLANNING: IMPROVEMENT IN CLINICAL
AND RADIOLOGICAL DIAGNOSIS**

Doctoral Dissertation
Biomedical Sciences,
Odontology (07B)

Kaunas, 2016

Dissertation has been prepared at the Department of Maxillofacial Surgery of Medical Academy of Lithuanian University of Health Sciences during the period of 2010–2016.

Scientific Supervisor:

Prof. Dr. Gintaras Juodžbalys (Lithuanian University of Health Sciences, Medical Academy, Biomedical Sciences, Odontology – 07B)

Dissertation is defended at the Odontology Research Council of the Lithuanian University of Health Sciences.

Chairperson

Prof. Dr. Vita Mačiulskienė (Lithuanian University of Health Sciences, Medical Academy, Biomedical Sciences, Odontology – 07B)

Members:

Prof. Dr. Antanas Šidlauskas (Lithuanian University of Health Sciences, Medical Academy, Biomedical Sciences, Odontology – 07B)

Prof. Dr. Algirdas Basevičius (Lithuanian University of Health Sciences, Medical Academy, Biomedical Sciences, Medicine – 06B)

Assoc. Prof. Dr. Jonas Peter Becktor (University of Malmö, Biomedical Sciences, Odontology – 07B)

Assoc. Prof. Dr. Thomas Jensen (Aalborg University, Biomedical Sciences, Odontology – 07B)

Dissertation will be defended at the open session of Lithuanian University of Health Sciences on the 29th of August 2016, at 09:00 a.m. in the Museum of History of Lithuanian Medicine and Pharmacy of Lithuanian University of Health Sciences.

Address: Rotušės 28, LT-44279 Kaunas, Lithuania.

LIETUVOS SVEIKATOS MOKSLŲ UNIVERSITETAS
MEDICINOS AKADEMIJA

Marius Kubilius

**DANTŲ IMPLANTACIJOS PLANAVIMAS:
KLINIKINĖS IR RADIOLOGINĖS
DIAGNOSTIKOS TOBULINIMAS**

Daktaro disertacija
Biomedicinos mokslai,
odontologija (07B)

Kaunas, 2016

Disertacija rengta 2010–2016 metais Lietuvos sveikatos mokslų universiteto Medicinos akademijos Odontologijos fakulteto Veido ir žandikaulių chirurgijos klinikoje.

Mokslinis vadovas

Prof. dr. Gintaras Juodžbalys (Lietuvos sveikatos mokslų universitetas, Medicinos akademija, biomedicinos mokslai, odontologija – 07B)

Disertacija ginama Lietuvos sveikatos mokslų universiteto Medicinos akademijos odontologijos mokslo krypties taryboje:

Pirmininkas

Prof. dr. Vita Mačiulskienė (Lietuvos sveikatos mokslų universitetas, Medicinos akademija, biomedicinos mokslai, odontologija – 07B)

Nariai:

Prof. dr. Antanas Šidlauskas (Lietuvos sveikatos mokslų universitetas, Medicinos akademija, biomedicinos mokslai, odontologija – 07B)

Prof. dr. Algidas Basevičius (Lietuvos sveikatos mokslų universitetas, Medicinos akademija, biomedicinos mokslai, medicina – 06B)

Doc. dr. Jonas Peter Beكتور (Malmės universitetas, biomedicinos mokslai, odontologija – 07B)

Doc. dr. Thomas Jensen (Alborgo universitetas, biomedicinos mokslai, odontologija – 07B)

Disertacija bus ginama viešame Lietuvos sveikatos mokslų universiteto Medicinos akademijos Odontologijos mokslo krypties tarybos posėdyje 2016 m. rugpjūčio 29 d. 9 val. Lietuvos sveikatos mokslų universiteto Lietuvos medicinos ir farmacijos istorijos muziejuje.

Disertacijos gynimo vietos adresas: Rotušės a. 28, LT-44279 Kaunas, Lietuva.

CONTENTS

ABBREVIATIONS	9
INTRODUCTION	12
AIM AND GOALS.....	14
SCIENTIFIC NOVELTY	15
1. LITERATURE REVIEW.....	17
1.1. Study I.....	17
1.2. Study II	18
1.3. Study III.....	19
1.4. Study IV	21
1.4.1. Classifications of jaw bone anatomy	21
1.4.2. Radiological examination.....	24
1.4.3. Inferior alveolar nerve injury risk.....	26
1.4.4. Aesthetic considerations.....	27
1.5. Study V	28
2. METHODS AND MATERIALS	32
2.1. Study I.....	32
2.1.1. Patient selection	32
2.1.2. Panoramic radiographs.....	32
2.1.3. MC visibility and JDS evaluation protocol	33
2.1.4. MC visibility analysis.....	34
2.1.5. Morphometric analysis	36
2.1.6. Densitometric analysis	37
2.2. Study II	39
2.3. Study III.....	41
2.3.1. Panoramic/Frontal view evaluations	41
2.3.1.1. The alveolar bone height and sinus membrane thickness measurements in mm.	41
2.3.1.2. Single or multi-rooted tooth/teeth in mm	42
2.3.1.3. The morphology of the sinus membrane	42
2.3.1.4. Vital and non-vital teeth classification for single tooth and multiple teeth loss with scoring system.....	42
2.3.1.5. Sinus augmentation classification for single tooth and multiple teeth loss with scoring.....	43
2.3.1.6. Sinus septa morphology in single tooth or multiple teeth loss	43
2.3.1.7. Sinus septa classification in single and multiple tooth loss with scoring.....	43
2.3.2. Sagittal view evaluations.....	43
2.3.2.1. Maxillary sinus ostium pattern in all sinus regions evaluated with scoring.....	43

2.3.2.2.	The vertical thickness of the sinus membrane morphological classification in all sinus regions evaluated with scoring	44
2.3.2.3.	Sinus membrane thickness measurement.....	44
2.3.2.4.	Sinus membrane thickness classification of single tooth loss and multiple teeth loss	44
2.3.2.5.	The location of the PSAA	44
2.3.2.6.	The diameter of the PSAA.....	45
2.3.2.7.	Bone length between the lower border of the PSAA to the alveolar ridge	45
2.3.2.8.	Buccal bone thickness at the upper border of the PSAA	45
2.3.2.9.	The height of the alveolar ridge.....	45
2.3.2.10.	The width of the alveolar ridge.....	45
2.3.2.11.	The width of the maxillary sinus	46
2.3.2.12.	The edentulous sites will also be classified according to ridge height with a scoring system	46
2.3.2.13.	Sinus septa morphology numbering and measurements	46
2.3.2.14.	Sinus septa classification with a scoring system.....	46
2.3.3.	Coronal/Transverse view evaluations.....	46
2.3.3.1.	Maxillary sinus has relation to with a scoring system	46
2.3.3.2.	Maxillary sinus ostium pattern with a scoring.....	47
2.4.	Study IV	47
2.5.	Study V.....	47
2.5.1.	Patient selection.....	47
2.5.2.	Study stages.....	48
2.5.3.	CBCCT, panoramic, and periapical radiography	49
2.5.4.	Preoperative stage (Appendix 1)	50
2.5.5.	Intraoperative stage (Appendix 2)	50
2.5.6.	Early postoperative stage (Appendix 2).....	51
2.5.7.	Late postoperative stage (Appendix 3)	51
3.	RESULTS	53
3.1.	Study I.....	53
3.1.1.	MC visibility analysis results.....	53
3.1.2.	Morphometric analysis results and relations to MC visibility scoring.....	55
3.1.3.	Morphometric analysis relations to MC visibility scoring.....	56
3.1.4.	Densitometric analysis results in relation to MC visibility scoring	56
3.1.5.	Vertical densitometric analysis in relation to MC visibility scoring.....	58
3.1.6.	Horizontal densitometric analysis in relation to MC visibility scoring.....	60
3.2.	Study II	60
3.3.	Study III	64
3.3.1.	The subgroup of single tooth loss.....	64
3.3.2.	The subgroup of multiple teeth loss.....	70
3.4.	Study IV	77
3.4.1.	Non aesthetic zone.....	78
3.4.1.1.	The height of the alveolar process (H).....	78
3.4.1.2.	The width of the alveolar process (W).....	80
3.4.1.3.	The length of the EJS (L)	81
3.4.1.4.	Alveolar ridge vertical position (RVP).....	82

3.4.2.	Aesthetic zone	82
3.4.2.1.	The height of the alveolar process (H)	82
3.4.2.2.	The width of alveolar process (W)	83
3.4.2.3.	The length of the EJS (L)	83
3.4.2.4.	Alveolar ridge vertical position (RVP).....	84
3.4.2.5.	Mesial and distal interdental bone peak height (BPH)	84
3.4.2.6.	Mandibular canal walls (MCW) and jaw bone quality (JBQ) type identification	85
3.5.	Study V	86
3.5.1.	Radiological EJS assessment during preoperative stage according to study protocol	87
3.5.2.	Risk degree evaluation for proper implantation	89
3.5.3.	Evaluation of the surgery during intraoperative and early postoperative stages according to study protocol: reliability of new proposed classification evaluation	89
3.5.4.	Implant treatment success evaluation at final crown placement	90
4.	DISCUSSION	92
4.1.	Study I.....	92
4.2.	Study II	96
4.3.	Study III	99
4.4.	Study IV and V	99
	CONCLUSIONS	104
	RECOMMENDATIONS FOR CLINICAL PRACTICE	105
	RECOMMENDATIONS FOR RESEARCH	106
	REFERENCES	107
	LIST OF THE AUTHOR 'S PUBLICATIONS	119
	Publications related to the results of dissertation	119
	Other publications	119
	Abstracts at scientific conferences	119
	MANUSCRIPTS	121
	Manuscript I related to study I	121
	Manuscript II related to study II.....	132
	Manuscript III related to study IV	139
	SANTRAUKA (SUMMARY IN LITHUANIAN).....	156

APPENDICES	166
Appendix 1	166
Appendix 2	169
Appendix 3	171
Appendix 4	172
Appendix 5	173
CURRICULUM VITAE.....	174
ACKNOWLEDGEMENT	176

ABBREVIATIONS

AC	–	alveolar crest
AC-IB-V	–	vertical densitometric measurement from the alveolar crest in the trabecular bone to the end of the inferior cortical bone
AC-MC-Ho	–	horizontal densitometric measurement 2.0 mm above the MC
AC-MC-HoP	–	horizontal densitometric measurement 2.0 mm below the superior cortical bone of the edentulous JDS (or mathematical average of horizontal measurements in mesial and distal parts of the dentate JDS trabecular bone 2.0 mm below the superior cortical bone) when visibility of the MC superior border is poor
AC-MC-V	–	vertical densitometric measurement from the alveolar crest in the trabecular bone to the bone 2.0 mm over the MC
α	–	confidence level
β	–	power of the study
CBCT	–	cone-beam computed tomography
CEI	–	complex aesthetic index
CEJ	–	cement-enamel junction
CI	–	confidence interval
CT	–	computed tomography
D	–	bone quality type
DI	–	distal inferior
DI BPH	–	distal bone peak height
DPR	–	digital panoramic radiograph
DS	–	distal superior
EJS	–	edentulous jaw segment
H	–	height
H-AC-IB	–	the height of the mandible
H-AC-MC	–	the height from the alveolar crest to the MC dark ribbon, including the superior MC border
H-IB	–	the height of the inferior cortical bone
H-MC	–	the height of MC, corresponding to the MC dark ribbon height
H-MC-IB	–	the height from the lowest point of the MC dark ribbon to the superior border of the inferior cortical bone (IB)
Ho	–	horizontal

HU	–	Hounsfield Unit
IAN	–	inferior alveolar nerve
IB	–	inferior cortical bone
IB-Ho	–	horizontal densitometric measurement in the region of the inferior cortical bone;
IB-V	–	vertical densitometric measurement in the inferior cortical bone region
IMCP	–	vertical densitometric measurement at the inferior MC peak corresponding to the border of the MC
JBQ	–	jaw bone quality
JDS	–	jaw dental segment
κ	–	Cohen's kappa coefficient
L	–	length
LLC	–	lateral lingual canal-foramen
M1	–	first molar
M2	–	second molar
M3	–	third molar
MC	–	mandibular canal
MC-IB-Ho	–	horizontal densitometric measurement in the trabecular bone below the MC
MC-IB-V	–	vertical densitometric measurement from the trabecular bone below the MC to the superior border of the inferior cortical bone
MC-Ho	–	horizontal densitometric measurement in the MC region
MC-V	–	vertical densitometric measurement in the MC region
MCW	–	mandibular canal wall
ME BPH	–	mesial interdental bone peak height
MI	–	mesial inferior
MLC	–	median lingual canal-foramen
MS	–	mesial superior
MSR	–	maxillary sinus region
N	–	total sample size
n	–	representative sample size
OR	–	odds ratio
p	–	p value
PM1	–	first premolar
PM2	–	second premolar
PSAA	–	posterior superior alveolar artery
RVP	–	alveolar ridge vertical position
SD	–	standard deviation
SE	–	standard error

- SMCP – vertical densitometric measurement at the superior MC peak corresponding to the border of the MC
- V – vertical
- W – width
- 2D – 2 dimensional
- 3D – 3 dimensional

INTRODUCTION

Dental implant treatment is among the most successful treatment methods, with the success rate over 90% [1], but it can involve many complications. Injury to the inferior alveolar nerve (IAN) is one of the most serious complications in implant dentistry. IAN injury is a predominantly iatrogenic complication with incidence of up to 40% [2]. Furthermore, IAN is the most commonly injured peripheral branch of the trigeminal nerve (64.4%) [3]. Preoperative radiological planning is obligatory for interventions in the posterior mandible to minimize the IAN injury rate. The use of digital panoramic imaging is becoming widespread due to improvements to image quality and after the introduction of dedicated software for image manipulation (even densitometric analysis tools are suggested). Quality of panoramic radiography is influenced by possible positioning, image-taking, and processing errors as well as errors due to anatomic abnormalities, but these images commonly have normal or higher-level quality [4] and are recommended for diagnostic examination in implant dentistry. While MC visibility changes throughout the course of the MC, the more precise evaluation of specific tooth related jaw dental segments (JDSs) by means of dedicated digital panoramic radiographs (DPRs) could provide more details with regard to MC visibility. It would be a significant advantage in MC and surrounding bone diagnostics if morphometric and densitometric assessment value changes could be the guide for detecting the MC and its walls, even in cases of poor visibility.

Bleeding can be one of the severe complications, during implant placement or other surgeries. The average size of lingual artery in the anterior mandible is about 1.41 mm and blood flow is about 2.92 ml/min to understand life-threatening complications even in the relatively safe symphysis [5]. Moreover there is an existing osseous concavity, sublingual fossa, extending to the first premolar region. The clinician can observe lingual vascular canal during surgery. It is crucial to evaluate anatomical peculiarities at presurgical stage by means of the most informative diagnostic method. The promising new method – cone-beam computed tomography (CBCT) could be tested with a large sample group internationally, to represent lingual foramina providing useful data for mandibular implant surgeries.

Anatomic peculiarities of the maxilla could be also related to increased rate of complications during implant treatment. Sufficient bone quality and quantity are important factors for an adequate dental implant insertion. Rehabilitation of the maxillary bone is usually problematic due to the pneumatization of maxillary sinus into the alveolar process, causing vertical bone

deficiency, which may cause serious problems during dental implant surgery. Understanding the normal maxillary sinus anatomy and possible variations are key factors for a successful sinus augmentation surgery. Prior and during sinus augmentation procedures, the surgeon should be aware of the several structures located in the sinus area, including posterior superior alveolar artery (PSAA), maxillary ostium, sinus mucosa, septum structures [6–18]. Existing literature review concerning the clinical imaging studies revealed the low number of samples measured. Furthermore, most of them were clinical series. Based on limited publications evaluating human participants with CBCT, the clarification about maxillary sinus anatomy, variations and pathologies of the sinus cavity and surrounding bony area, and further evaluating the volumetric pattern of the maxillary sinus seem to be essential before sinus augmentation and/or implant surgery.

The naturally arising idea is to combine the literature review results of the existing studies and own clinical experience to provide clinically important suggestions to improve dental implant treatment planning. The classification or decision tree could be that tool in daily practice. The first three parallel studies were performed to assess mandibular and maxillary anatomy peculiarities in relation to implant treatment planning. The further step was to provide comprehensive classification system of the jaw bone anatomy in endosseous dental implant treatment combining existing literature data with performed studies results and own clinical experience. The MC visibility evaluation, morphometric and densitometric analysis of mandibular JDSs, and vascular canals assessment were completed during creation process of comprehensive classification system. Previous classifications demonstrated lack of MC/bone quality evaluation, maxillary sinus region assessment, and main aesthetic parameters introduction additionally to main morphometric parameters. The validation of suggested classification would be necessary step for reproducibility and reliability confirmation.

Before exposing an individual to the treatment process, thorough clinical and radiologic investigations are taken with the aim to provide optimal treatment plan to the patient with significant predictability. Indeed, the core importance are the initial or planning steps affecting treatment results in short- and long-term periods together with increase of the patient's satisfaction and good clinical practice.

The rationale of this thesis outlines the essence of dental implant surgery on the various diagnostic imaging techniques highlighted in biomedical literature while assessing the need for improved radiological and clinical diagnostic methods for jaw bone tissues.

AIM AND GOALS

Aim

The aim of present study was to evaluate and upgrade clinical and radiological diagnostic methods' accuracy/efficacy in endosseous dental implant treatment planning for particular mandibular and maxillary sites determination, vital structures identification.

Goals:

1. To assess the visibility of the mandibular canal morphology in different jaw dental segments in relation to morphometric and densitometric parameters on digital panoramic radiographs.
2. To evaluate the diagnostic accuracy of CBCT in detection of the lingual vascular canals and define their anatomical characteristics in the mandibular bone.
3. To evaluate diagnostic accuracy of CBCT in detection of the maxillary sinus and surrounding bone anatomical structures.
4. To suggest a new clinical and radiological classification system of the jaw bone anatomy in endosseous dental implant treatment planning.
5. To assess reliability and validity of the suggested clinical and radiological classification system of the jaw bone anatomy in dental implant treatment planning.

Principal hypothesis

Comprehensive evaluation of EJS's anatomy improves diagnostics and treatment planning in endosseous dental implant therapy.

SCIENTIFIC NOVELTY

Complex and related studies were completed to evaluate and upgrade clinical and radiological diagnostic methods' efficacy in endosseous dental implant treatment planning.

There is lack of comprehensive, DPRs' accuracy related studies for MC visibility evaluation. Precise evaluation of jaw dental segments (JDSs) using DPRs evaluation tools were used to provide more details regard MC visibility possibilities. Unique evaluation of the MC visibility in four places of each JDS was provided with numerous tested variables for possible influence on MC visibility (**study I** [Descriptive study of mandibular canal visibility: morphometric and densitometric analysis for digital panoramic radiographs]).

Small vascular canals of the mandible were not investigated using large sample group during dental implant treatment planning on CBCT. International study (**study II** [Evaluation of mandibular lingual foramina related to dental implant treatment with computerized tomography: a multicenter clinical study]) was made with large sample size to examine visualization of the lingual vascular canals of the mandible. It provides useful data for preoperative surgery planning and gives wide conclusions on CBCT diagnostic accuracy.

CBCT diagnostic accuracy for assessment of the anatomical structures in the region of maxillary sinus was evaluated by other investigators. However, limited number of studies are published evaluating human participants with CBCT. The main drawbacks of previous studies are the low size of the samples and limited number of investigated anatomical parameters. Various anatomical parameters of the maxillary sinus region were evaluated (**study III** [Evaluation of maxillary sinus and surrounding bone anatomy with cone beam computed tomography]). Diagnostically important aspects related to dental implant treatment planning were highlighted.

Comprehensive classification was suggested for assessment of the jaws' anatomy based on literature data and our studies results for diagnostic efficacy improvement in dental implant treatment planning (**study IV** [Clinical and radiological classification of the jaw bone anatomy in endosseous dental implant treatment]). Furthermore, MC identification with bone quality evaluation and risk of inferior alveolar nerve injury, aesthetic considerations in aesthetic zone were discussed.

International pilot clinical study was performed to assess validity and reliability of the published classification. Limitations of the classification were analysed. The classification was updated taking on account the newest pilot study results (**study V** [Validation of the therapeutic anatomy oriented classification in endosseous dental implant treatment: a pilot study]).

1. LITERATURE REVIEW

1.1. Study I

Dental implant surgery is a widely accepted and increasingly frequent treatment method in dentistry, but it can involve many complications. Injury to the inferior alveolar nerve (IAN) is one of the most serious complications in implant dentistry. IAN injury is a predominantly iatrogenic complication with reported incidence of up to 40% [2]. Furthermore, IAN is the most commonly injured peripheral branch of the trigeminal nerve (64.4%) [3]. Intraoperative pain, bleeding, and temporary or permanent postoperative anaesthesia, paraesthesia, hypoesthesia, or dysesthesia can follow such an injury. Preoperative radiological planning is obligatory for interventions in the posterior mandible to minimize the IAN injury rate.

Opinion leaders and responsible organizations worldwide periodically provide guidelines for the application of diagnostic imaging in implant dentistry [19, 20]. The guidelines have been adapted many times in particular countries or regions based on particular scientific data, laws. The authors of the present study operated according to guidelines set forth by the European Commission and European Association for Osseointegration [19, 21].

Panoramic imaging has a wide range of applications and is accepted for the evaluation of mandibular canal (MC) visibility despite the existence of more accurate investigation methods (e. g. cone beam computed tomography (CBCT)) [22]. Panoramic imaging lacks three-dimensional visualization and suffers from vertical and horizontal magnification [23]. A previous panoramic radiography quality evaluation study [4] discusses possible positioning, image-taking, and processing errors as well as errors due to anatomic abnormalities, but these images commonly have normal or higher-level quality [4] and are recommended for examination in implant dentistry. Despite the possible shortcomings of panoramic imaging, accurate endosseous dental implant planning by means of panoramic radiographs reduces the risk for IAN injury and subsequent function impairment to a non-significant level [24, 25]. Treatment planning is exclusively unique because MC location and course are individual. MC visibility on panoramic radiographs changes from the mandibular foramen to the mental foramen [26]. The identification of fine anatomical structures on radiographs in the implant site is a delicate task for dental professionals. Juodzbaly et al. [27] proposed to use the term “jaw dental segment” (JDS) for more accurate jaw segment identification and related investigations.

The use of digital panoramic imaging is becoming widespread due to improvements to image quality and after the introduction of dedicated software for image manipulation [28]. While MC visibility changes throughout the course of the MC, the more precise evaluation of JDS by means of dedicated digital panoramic radiographs (DPRs) could provide more details with regard to possibilities for MC visibility. Manufacturers even provide tools for the densitometric analysis of bone density on panoramic radiographs. The clinician hopes to benefit from these technologies. Unfortunately, we could not find in the literature even one source for comprehensive MC region assessment with DPR using vertical morphometric measurements of MC and surrounding bone, nor could we find a source using vertical or horizontal densitometric measurements of MC and neighbouring regions to allow identification of the acquired parameters' relation to MC visibility. Therefore, the present study was initiated to assess whether the morphometric measurements of MC and surrounding bone and specific patterns of densitometric value changes could be the guide for detecting the MC and its walls, even in cases of poor visibility.

The aim of the present study was to assess the visibility of the MC morphology in different JDSs in relation to morphometric and densitometric parameters on DPRs.

1.2. Study II

Interforaminal region is a good choice for the implant placement to support fixed partial dentures or overdentures. Symphysis is one of the autologous donor graft area in the oral cavity in need of excessive ridge augmentations [29, 30]. Submental branch of the facial artery and sublingual branch of the lingual artery supplies this area, including the sublingual gland, mylohyoid, geniohyoid and genioglossus muscles, mucous membranes of the mouth floor, and the lingual gingiva [31, 32]. The submental artery supplies the lymph nodes of the submandibular triangle, the anterior belly of the digastric muscle, and the mylohyoid muscle [31, 33]. Important arterial anastomoses are formed between sublingual and submental arteries and between sublingual and incisive arteries through multiple accessory lingual foramina [34]. Mental artery, the branch of the inferior alveolar artery, was found to communicate with sublingual artery in the mental region of the internal mandible [35]. Although interforaminal region is a relatively safe area to place implants, perforation of the lingual cortex while placing dental implants can cause severe hemorrhage [36–45]. Additionally with the arterial wound, if drilling ruptures lingual periosteum, damage to anatomical structure

res in the sublingual space may enhance the bleeding, resulting in the hematoma of the floor of the mouth [36]. Besides the interforaminal region, the presence of lingual foramen in molar area has been reported as well [46]. Severe hemorrhage was reported during drilling in molar and premolar areas [47, 48]. Lingual vascular canals of the mandible have been investigated anatomically or by means of computerized tomography (CT) [49–63]. Cadaver studies depicted that both submental and sublingual arteries perforate into the mandible through lingual foramen/foramina [32, 58]. Longoni et al. [62] examined the interforaminal area in 100 CTs of the Caucasian patients. They reported 61% vascular canals ranging in entrance diameters between 0.3 and 1.1 mm (mean, 0.6 ± 0.2 mm) [62]. Katakami et al. [46] reported the presence of arterial in the molar area and measured a mean diameter of 0.88 ± 0.2 mm. Position of the foramen was reported to be 7.06 mm from the border of the mandible [46]. Some authors classified the lingual foramina of the mandible as median lingual canal-foramen (MLC) and lateral lingual canal-foramen (LLC) [33, 49, 62, 63]. LLC diameters were found slightly lower than the midline values [33, 34, 50].

After tooth extraction, bone loss is primarily horizontal from the labial side. This resorption pattern results in a linguallly angulated trajectory of mandible. If atrophic inclined mandible is not considered well before implant placement, risk of lingual perforations may increase. Moreover, there is an existing osseous concavity, sublingual fossa, extending to the first premolar region. Dental CT is a well-known and frequently used imaging technique to depict bony architecture and surrounding anatomical structures. It is a valuable tool for ridge mapping and diagnosis of pathologies of the jaws, teeth, and maxillofacial area [64]. Presurgical 3-dimensional assessment of the area is highly suggested to achieve favorable prosthetic angulations and avoid complications [52, 65].

1.3. Study III

Sufficient bone quality and quantity are important for an acceptable dental implant insertion. Rehabilitation of the maxillary bone is usually problematic due to the pneumatization of maxillary sinus into the alveolar bone cavity, causing vertical bone deficiency, which may cause serious problems during dental implant procedures. Hence, sinus augmentation procedure was proposed to overcome the vertical bone deficiency. Understanding the normal maxillary sinus anatomy and possible variations are keys for a successful sinus augmentation surgery. Maxillary sinus is the largest of the paranasal sinuses, and it is a pyramid-shaped cavity surroun-

ded by its base-the alveolar bone, zygomatic bone, inferior orbital surface of maxilla and the nasal cavity, which drains into the middle meatus of the nose by maxillary ostium or maxillary hiatus. The sinus cavity is lined with a thin continuous mucosa called Schneiderian membrane. Several surgical interventions were developed to increase the local bone volume to achieve a sufficient bone thickness in the sinus cavity, thus allowing the dental implant placement followed by a successful prosthodontic rehabilitation in the posterior maxilla of totally or partially edentulous patients [6–18].

Prior and during sinus augmentation procedures, the surgeon should be aware of the several structures located in the sinus area, including posterior superior alveolar artery (PSAA) that runs caudally on the outside of the convexity of the maxillary tuberosity, bony projections called maxillary septa arising from the floor of the maxillary cavity, sinus mucosa thickness, sinus pathologies, maxillary ostium pattern, residual alveolar bone height and thickness, and also the dentist should analyze the volumetric features of the sinus augmentation surgery to achieve successful and effective outcomes [7, 9–11, 66].

Sinus augmentation or bone grafting in maxillary sinus has been performed for the placement of dental implants in edentulous maxillary sites for almost 30 years. Before and after sinus augmentation procedures, different radiographic techniques have been used to evaluate the maxillary posterior region including panoramic images, which provide 2 dimensional (2D) evaluation of the area, and distances may be affected by magnification or distortion, which may cause difficulties to make an accurate diagnosis. The evaluation of the oral and maxillofacial region can also be done with 3 dimensional (3D) radiographic methods, including medical computerized tomography (CT) with relatively high radiation dose levels compared with 2D imaging. In the last decade, cone beam computed tomography (CBCT) provides a lower radiation dose, easy accessibility and cost alternative. Innovations in imaging systems and increased usage of pre-operative CBCT evaluation have allowed dental practitioners to have a more accurate and close look at the anatomic structures, and variations and possible pathologies of the region. Various softwares, which enable pre-implant planning of the surgical sites, have also been developed, combining 3D images with a computer design that enables accurate diagnosis of the surgical area in a user friendly pre-surgical planning. With the support of 3D CBCT imaging and software tools, it is possible to make anatomic ridge mapping and diagnosis of pathologies of the jaws, teeth, and maxillofacial area. Pre-surgical 3D imaging of the surgical region is highly suggested to achieve favorable prosthetic angulations that will eventually result with esthetic and functional outcomes [13–18, 66–68].

One of the advanced surgical procedures is the sinus augmentation or known as sinus-lift procedure, is generally considered to be safe and has a low complication rate. The most common procedure-related complications are the perforation of the sinus membrane and bleeding during surgical intervention. It is therefore significant to predict possible sinus membrane perforation and bleeding possibilities before surgery, and by making a careful advanced diagnosis may also avoid post-operative inflammation/infection possibility of the augmented sinus. It is clear that several anatomic factors and/or pathologies have been implicated in the risk of these complications, some of which are residual ridge height, thin sinus membrane, tooth related and sinus originated pathologies, location of the posterior superior alveolar artery (PSAA), sinus septa formations and the obstruction of the maxillary sinus ostium [11, 12, 69, 70].

Recently, a significant interest in implant dentistry and 3D CBCT diagnosis is the use of volumetric evaluation of the maxillary sinus. Estimating the bone volume required prior to surgery for maxillary sinus floor augmentation may help in selecting the accurate donor site, minimizing the complications of the donor site after surgery, estimation of suitable bone substitute amount and cost, and also reducing hospital charges. Evaluation of the volumetric features of the maxillary sinus has been performed with different techniques in vitro and in vivo, including impression materials, 2D imaging and recently 3D CBCT diagnosis. It was concluded that 3D CBCT seemed to be a promising approach to quantify the volume of the sinus before surgery and also to understand the long-term changes in the augmented sinus regions [13, 15, 17, 18, 70–72].

One of the drawbacks of the above clinical imaging studies was the low number of samples measured, and many of which were clinical series. Based on limited publications evaluating human participants with 3D CBCT, the clarification about maxillary sinus anatomy, variations and pathologies of the sinus cavity and surrounding bony area, and further evaluating the volumetric pattern of the maxillary sinus seem to be essential before sinus augmentation and/or implant surgery.

1.4. Study IV

1.4.1. Classifications of jaw bone anatomy

The most popular classification systems for jaw anatomy (jaw shape and quality) for dental implant treatment was proposed by Lekholm and Zarb [73]. The quantity of jaw bone is divided into five groups, based on residual jaw shape following tooth extraction. There are presented drawings

of the jaws – jaw cross-sections, accompanied by text, and assessment methods. Similarly Cawood and Howell's [74] ridge classification presented as alveolar process resorption level jaw cross-sections and text. During all stages of the alveolar ridge atrophy, characteristic shapes result from the resorptive process.

The biggest shortcoming of previous classifications [74-80] is fact, that those classifications are two-dimensional representations and do not show the three-dimensionality of atrophic ridges. Nowadays clinician can combine three-dimensional jaw bone assessment and image-guided surgery by means of CBCT. Diagnostic and planning software are available to assist in implant planning to create diagnostic and surgical implant guidance stents (e.g., Virtual Implant Placement, Implant Logic Systems, Cedarhurst, USA; Simplant, Materialise, Belgium; Easy Guide, Keystone Dental, USA) [81].

Misch and Judy [82] classified available bone into 4 divisions: abundant, barely sufficient, compromised, and deficient (A-D). Abundant bone requires no augmentation and is greater than 5 mm in width, 10 to 13 mm in height, and 7 mm in length. Barely sufficient bone is 2.5 to 5 mm in width, greater than 10 to 13 mm in height, and greater than 12 mm in length and can be modified with osteoplasty or augmentation of hard or soft tissues, depending on the nature of the defect (B-w). Compromised bone necessitates osteoplasty and some form of hard or soft tissue augmentation depending on the extent of the defect in height (less than 10 mm, C-h) or width (less than 2.5 mm, C-w). Deficient bone requires substantial hard tissue augmentation from extraoral sites and is generally not amenable to implant rehabilitation. Unfortunately, aesthetic component in this classification is not considered. Implant rehabilitation is no longer just a vehicle to restore lost masticatory and phonetic function. It has become an integral part of modern implant dentistry for achieving structural and aesthetic pleasing outcomes [83]. It is well established that the soft tissue appearance is largely dependent upon the underlying bone topography [84]. Hence, it is important to assess hard tissue parameters, such as horizontal bone deficiency and interproximal bone height.

Current classifications also fail to assess mandibular canal anatomy variations and risk degree of inferior alveolar nerve injury. Worthington [85] showed that even after the accurate measurement of available bone, the nerve injury can occur as the result of over penetration of the drill owing to low resistance of the spongy bone; this can lead to slippage of the drill even by experienced surgeons.

Lekholm and Zarb [73] classify quality of residual alveolar bones into four types: type 1 = large homogenous cortical bone; type 2 = thick cortical layer surrounding a dense medullar bone; type 3 = thin cortical layer sur-

rounding a dense medullar bone; type 4 = thin cortical layer surrounding a sparse medullar bone). According to Ribeiro-Rotta et al. [86] and Bergkvist et al. [87] classification of quality of residual alveolar bones indicate a good correlation with bone mineral content. Trisi and Rao [88] proposed the system for bone quality assessment with three classes (dense, normal and soft bone).

Some authors proposed to evaluate jaw bone density in presurgical planning [89-91]. It is possible to assess jaw bone density using CT values (Hounsfield units: HU) and bone mineral densities obtained by medical CT. Norton and Gamble [90] measured the bone density in the posterior mandible using SimPlant software (3D Diagnostix, Boston, MA, USA) and concluded that the mean CT value was 669.6 HU. Misch [89] classified cancellous bone density into 5 grades: D1: > 1250 HU; D2: 850 to 1250 HU; D3: 350 to 850 HU; D4: 150 to 350 HU; and D5: < 150 HU. In the conversion of CT values (HU), the mean value in the molar region was 4.5×10^2 (D3): in the first molar region it was 5.2×10^2 (D3), in second molar region 4.3×10^2 (D3), and in the third molar region it was 0.7×10^2 (D5).

It is interesting to know that Başa and Dilek [92] assessed the risk of perforation of the mandibular canal by implant drill using density and thickness parameters. They investigated whether the resistance of the bone surrounding the mandibular canal had sufficient density and thickness to avoid perforation by implant drills. Study of the computed tomography (CT) images of 99 patients, showed that overall, average bone thickness in the premolar and molar regions was 0.87 ± 0.18 and 0.86 ± 0.18 mm, respectively, whereas the bone density in the premolar and molar regions was 649.18 ± 241.42 and 584.44 ± 222.73 HU, respectively ($p < 0.001$). It was concluded that the average density and thickness of the bone that surrounds the mandibular canal was not sufficient to resist the implant drill. Furthermore, in the posterior mandible, cancellous bone is more abundant and has bigger intratrabecular spaces and less dense than in anterior mandible [93, 94]. In some cases with low density bone, the twist drills may drop into intratrabecular spaces during preparation thus leads to the displacement of the implants deeper than planned [95].

The measurements of bone density in designed sites are important in presurgical planning when using CBCT for dental implant treatment. However, the pixel or voxel values obtained from CBCT images are not absolute values. Naitoh et al. [96] demonstrated a high-level correlation between voxel values of CBCT and bone mineral densities of multislice CT ($r = 0.965$). They concluded that voxel values of mandibular cancellous bone in CBCT could be used to estimate bone density. In contrast, Nackaerts et al. [97] and Parsa et al. [98] determined the grey value variation at the implant

site with different scan settings, including field of view (FOV), spatial resolution, number of projections, exposure time and dose selections in two CBCT systems and compared the results with those obtained from a multi-slice CT system. Authors concluded that grey-level values from CBCT images are influenced by device and scanning settings.

1.4.2. Radiological examination

The main goals of radiological jaw bone examination are to determine the quantity, quality and angulations of bone, selection of the potential implant sites, and to verify absence of pathology. Clinician should choose proper radiographic method which provides sufficient diagnostic information with the least possible radiation dose.

Periapical radiographs have been used for many years to assess the jaws pre- and post-implant placement [99]. Periapical radiographs commonly are used to evaluate the status of adjacent teeth, remaining alveolar bone in the mesiodistal dimension and vertical height. The long cone paralleling technique for taking periapical X-ray is the technique of choice for the following reasons: reduction of radiation dose; less magnification; a true relationship between the bone height and adjacent teeth is demonstrated [100]. If the paralleling technique is not used, periapical radiographs create an image with foreshortening and elongation [101–103]. Nevertheless, the biggest concern of periapical radiographs is in 28% of patients that mandibular canal could not be clearly identified in the second premolar and first molar regions [100] and mandibular foramen can be identified around 47–75% cases [104].

When a specific region (maxillofacial area, including many of the vital structures, such as maxillary sinus, inferior alveolar nerve and nasal fossa) that is too large to be seen on a periapical view, panoramic radiograph can be the method of choice. The major advantages of panoramic images are the broad coverage of oral structures, low radiation exposure (about 10% of a full-mouth radiographs), and relatively inexpensiveness of the equipment. The major drawbacks of panoramic imaging are: lower image resolution, high distortion, and presence of phantom images [105]. For example, Naitoh et al. [96] found that mandibular canal visibility on panoramic radiographs in superior and inferior wall was only 36.7%. Similarly, Lindh et al. [106] reported that the mandibular canal of specimen cadavers was clearly visible in 25% of panoramic radiographs (range 12 to 86%). Klinge et al. [107] also reported that the mandibular canal of specimen cadavers was not visible in 36.1% of panoramic radiographs. The location and configuration of mandi-

bular canal are important in imaging diagnosis for the proper dental implant placement in the mandible [108–110].

One of the most challenged regions for implantation in mandible is mental foramen region. This is because there are many variations with regards to the size, shape, location and direction of the opening of the mental foramen. After comparison of the anatomical and radiological assessment of 4 cadaver skulls, Yosue and Brooks [111] concluded that the panoramic and periapical films reflected the actual position of mental foramen in the skulls < 50% the time. Furthermore, Sonick et al. [112] found that the average linear errors occurred during routine bone assessments (n = 12) for panoramic films were 24% (mean 3 mm; range 0.5 to 7.5 mm), for periapical films were 14% (mean 1.9 mm; range 0.0 to 5.0 mm) and only 1.8% (mean 0.2 mm; range 0.0 to 0.5 mm) for CT scans. Kuzmanovic et al. [113], Ngeow and Yuzawati [114] and Jacobs et al. [22] similarly concluded that panoramic radiograph is not sufficient for anterior loop detection and presurgical implant planning in the mental region and there is a need for other additional images.

Even incisive canal detection is complicated using panoramic radiography. For example, Jacobs with co-workers [115] reported that the mandibular incisive canal was identified only in 15% of the 545 panoramic radiographs, with good visibility of only 1%. In contrast, canal was observed on 93% of CT scans with a good visibility in 22% of cases.

Peker et al. [116] showed that the measurements obtained from CT images are more consistent with direct measurements than the measurements obtained from panoramic radiographic images or conventional tomographic images. Furthermore, Rouas et al. [117] reported that the atypical mandibular canal such as bifid mandibular canal, in most cases can be identified using only three-dimensional imaging techniques. It was thought that the bifid mandibular canal is often left unrecognized [118]. Therefore, duplication or division of the canal by means of panoramic radiographs was found in about 1% of patients [119]. Naitoh et al. [120] reconstructed 122 two-dimensional images of the various planes in mandibular ramus region to the computer program using three-dimensional visualization and measurement software. Bifid mandibular canal in the mandibular ramus region was observed even in 65% of patients.

When the periapical radiography, panoramic radiography, tomography, or CT were compared for their efficiency in the identification of the mandibular canal, the CBCT seems to have the most potential while reduces radiation exposure considerably [121]. Similarly, CT scans are more accurate than conventional radiographs in mental foramen and anterior loop detection [22, 107, 112, 122, 123]. However, cross-sectional imaging have

following limitations: limited availability, high cost and the need for image interpretation [124, 125]. However, CBCT is often recommended for clinical usage, especially in cases where the vital structures are difficult to detect due to its high accuracy and low radiation exposure [126-128]. The main advantage of CBCT is a low dose scanning system, which has been specifically designed to produce three-dimensional images of the maxillo-facial skeleton. Hence, a major difference between CT and CBCT is how the data are gathered: CT acquires image data using rows of detectors, CBCT exposes the whole section of the patient over one detector [129, 130]. Furthermore, CBCT permits not only diagnosis, it facilitates image-guided surgery [81].

1.4.3. Inferior alveolar nerve injury risk

Inferior alveolar nerve injury is a serious complication with incidence ranged from 0 to 40% [2, 3, 24, 131–144]. As a result, many important functions such as speech, eating, kissing, make-up application, shaving and drinking were affected [136]. This influences patient's quality of life and often resulted in negative psychological adverse effects [138]. The most common causes of iatrogenic inferior alveolar nerve injuries are discrepancies of radiographs, surgeon's mistakes, low resistance of mandibular spongy bone and lack of mandibular canal superior wall.

The most severe types of injuries are caused by implant drills and implants themselves [85]. Many implant drills are slightly longer, for drilling efficiency, than their corresponding implants. Implant drill length varies and must be understood by the surgeon because the specified length may not reflect an additional millimetre so called "y" dimension [142]. Lack of knowledge about this may cause avoidable complications [145]. Damage to the inferior alveolar nerve can occur when the twist drill or implant encroaches, transects, or lacerates the nerve.

Over penetration of the drill (drill slippage) can be triggered by the low resistance of the spongy bone [85]. It was mentioned above that Başa and Dilek [92] assessed the risk of perforation of the mandibular canal by implant drill using density and thickness parameters. They investigated whether the resistance of the bone surrounding the mandibular canal had sufficient density and thickness to avoid perforation by implant drills. The results showed the risk of inferior alveolar nerve injury can be avoided by accurately determining the bone mass around the canal and avoid use excessive force when approaching the canal. Furthermore, Wadu et al. [146], studying mandibular canal appearance on the panoramic radiographs, found that the number of cases of radio-opaque border was either disrupted

or even absent. The superior border was more prone to disruption than the inferior border. It is evident that low resistance of the spongy mandibular bone and absence of mandibular canal superior wall is inauspicious anatomical combination which can lead to inferior alveolar nerve injury.

Juodzbaly et al. [144] stated that in 25% cases (n = 4) implant drill was identified as etiological factor with 2 cases caused by drill slippage during osteotomy preparation. The inferior alveolar nerve may be affected by perforation of the mandibular canal during drilling, or positioning the implant close to the canal and the subsequent formation of an adjacent hematoma that presses against the nerve [147]. Khawaja and Renton [148] indicated that “cracking” of the inferior alveolar nerve canal roof by its close proximity to preparation of the implant bed (millimetres) may cause haemorrhage into the canal or deposition of debris which may compress and cause ischemia of the nerve.

Limited evidence exists with regard to the proper distance between the implant and the mandibular canal to ensure the nerve’s integrity and physiologic activity. The proper distance should come from evaluation of clinical data as well as from biomechanical analyses [149, 150]. Sammartino et al. [149] created a numeric mandibular model based on the boundary element method to simulate a mandibular segment containing a threaded fixture so that the pressure on the trigeminal nerve, as induced by the occlusal loads, could be assessed. They found that the nerve pressure increased rapidly with a bone density decrease. A low mandibular cortical bone density caused a major nerve pressure increase. In conclusion, they suggested a distance of 1.5 mm to prevent implant damage to the underlying inferior alveolar nerve when biomechanical loading was taken into consideration.

1.4.4. Aesthetic considerations

It is generally agreed that implant success criteria should include an aesthetic component [151]. Although implant success, as measured through fixture osseointegration and restoration of function, is high, the procedures available to create aesthetic implant “success” are not always predictable [83]. To ensure optimal aesthetic implant rehabilitation, the following prerequisites are considered essential: adequate bone volume (horizontal, vertical, and, contour), optimal implant position (mesiodistal, apicocoronal, buccolingual, and angulation), stable and healthy perimplant soft tissues, aesthetic soft tissues contours, and ideal emergence profile [83, 152]. The level of bone support and the soft tissue dimensions around the implant-supported single-tooth restoration are factors suggested to be important for

the aesthetic outcome of implant therapy [153]. It has been demonstrated that presence or absence of bone crest influences the appearance of papillae between implants and adjacent teeth [154]. Furthermore, the implant-supported restoration should be in symmetry with the adjacent dentition [155].

The parameters of three-dimensional optimal implant position was defined by several authors [83, 151, 156, 157]. Mesio-distal dimension between adjacent teeth should be 6 to 9 mm to ensure minimal (1.5 mm) distance between implant fixture and adjacent teeth [156, 157]. Vela et al. [158] showed that it is possible to place platform-switched implant 1 mm from teeth while maintaining the bone level adjacent to them. Apicocoronal implant position should be 2 mm below the adjacent cervicoenamel line [151]. Natural buccal and proximal restorative contour can be ensured by correctly orienting the implant in a buccolingual position - 3 to 4 mm from outside buccal flange [83]. Minimum 2 mm of space should be maintained on the buccal side in front of the external implant collar surface.

It is necessary to mention that recommendations for successful results ideally require at least 1 mm of bone surrounding each implant [159].

1.5. Study V

Three-dimensional (3D) bone and soft tissue changes appear to be a natural consequence of tooth extraction [160]. It is generally agreed that the atrophy of alveolar process influences dental implant treatment planning [160, 161]. To correct the alveolar bone deficiencies, multiple treatments are often required which increase complication rate and may eventually impact on the long-term implant stability [160]. It has been reported that both hard and soft tissues quantity and quality are vital parameters for overall implant success. At this moment, various classifications were recommended for analyzing of the degree of anatomical deficiencies either in partially or totally edentulous jaws [73–76, 162, 163]. However, most of these classifications only described changes of jaw shapes but failed to adequately predict the actual measurements of planned surgical sites. Previously Juodzbalys et al. proposed clinical and radiological classification for more precise implant treatment planning [27]. However, this classification fails to take into consideration of mandibular canal (MC) anatomy variations which might increase the risk of inferior alveolar nerve injury. Recent advancement in radiographic technology, i.e. development of cone-beam computed tomography (CBCT), have made anatomical diagnoses more easily and precise, especially in the above situation.

As an attempt, we have recently proposed therapeutic anatomical based clinical and radiological classification for the dental implant treatment (Fig. 1.5.1, Table 1.5.1) [164].

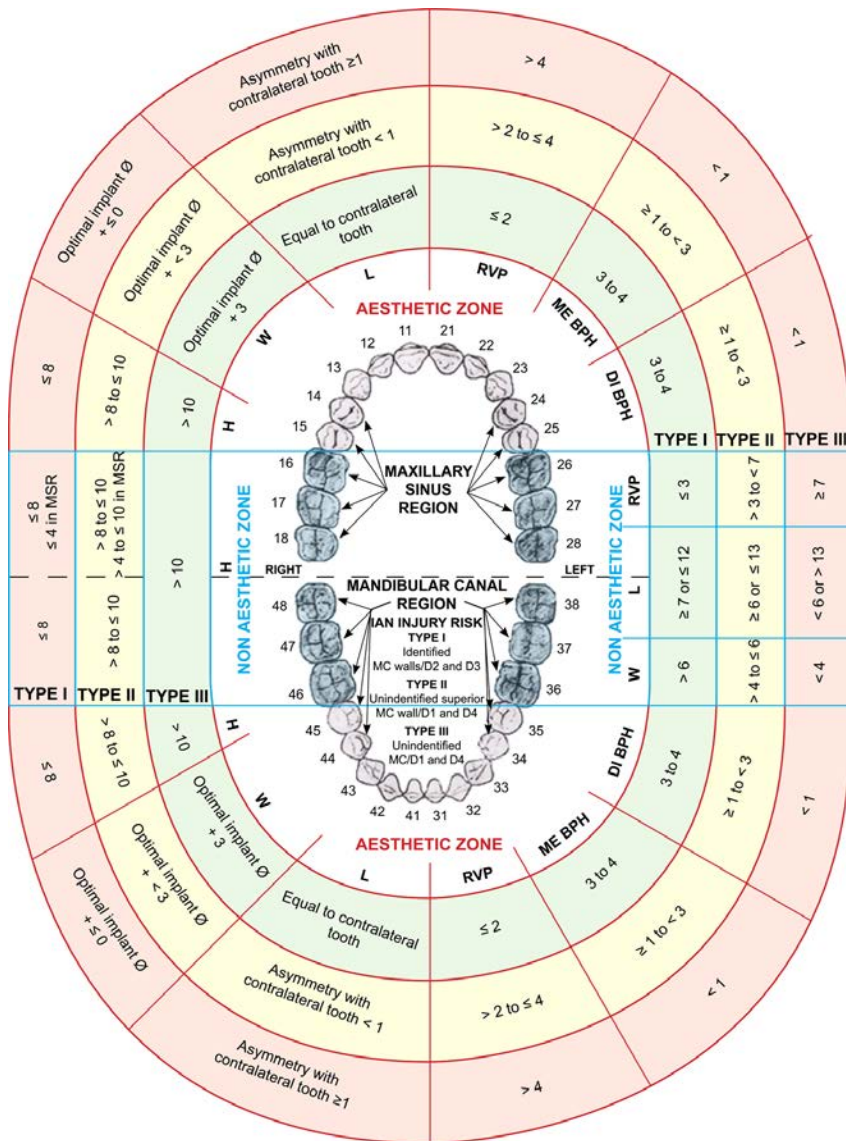


Fig. 1.5.1. Classification system of the jaw bone anatomy in endosseous dental implant treatment

H = height; W = width; L = length; RVP = Alveolar ridge vertical position; ME BPH = Mesial interdental bone peak height; DI BPH = Distal interdental bone peak height; MC = mandibular canal; IAN = inferior alveolar nerve; MSR = maxillary sinus region (all linear measurements are expressed in mm).

Table 1.5.1. Classification system of the jaw bone anatomy in endosseous dental implant treatment

Edentulous jaw segment parameters		Edentulous jaw segment types (risk degree)		
		Type I (low risk)	Type II (moderate risk)	Type III (high risk)
Non aesthetic zone				
Height (mm)	Maxilla	> 10	> 8 to ≤ 10 > 4 to ≤ 10 in MSR	≤ 8 ≤ 4 in MSR
	Mandible	> 10	> 8 to ≤ 10	≤ 8
Width (mm)		> 6	> 4 to ≤ 6	< 4
Length (mm)		≥ 7 or ≤ 12	≥ 6 or ≤ 13	< 6 or > 13
Alveolar ridge vertical position (mm)		≤ 3	> 3 to < 7	≥ 7
Aesthetic zone				
Height (mm)	Maxilla	> 10	> 8 to ≤ 10 > 4 to ≤ 10 in MSR	≤ 8 ≤ 4 in MSR
	Mandible	> 10	> 8 to ≤ 10	≤ 8
Width (mm)		Optimal implant diameter + 3	Optimal implant diameter + < 3	Optimal implant diameter + ≤ 0
Length (mm)		Equal to contralateral tooth	Asymmetry < 1 mm in comparison with contralateral tooth	Asymmetry ≥ 1 mm in comparison with contralateral tooth
Alveolar ridge vertical position (mm)		≤ 2	> 2 to ≤ 4	> 4
Interdental bone peak height (mm)	Mesial	3 to 4	≥ 1 to < 3	< 1
	Distal	3 to 4	≥ 1 to < 3	< 1
MC region (IAN injury risk degree)				
MC walls identification and jaw bone quality type ^a		Identified MC walls/D2 and D3	Unidentified superior MC wall/D1 and D4	Unidentified MC/D1 and D4

^aD = bone quality defined according to Lekholm and Zarb (1985).

MC = mandibular canal; IAN = inferior alveolar nerve; MSR = maxillary sinus region.

Identification of the maxillary sinus, MC and risk degree of inferior alveolar nerve injury were included. Equally important, we have also included aesthetic parameters. Briefly, edentulous jaw segments (EJSs) (Fig. 1.5.2) were classified into 3 types according to their assessment and risk degree of the dental implant treatment success. It is our belief that this will be an important tool for communication among dental specialists. However, this newly suggested classification needs to be verified in a prospective clinical trial.

Hence, it was the purpose of this study to validate the proposed therapeutic anatomical based clinical and radiological classification for the dental implant treatment.

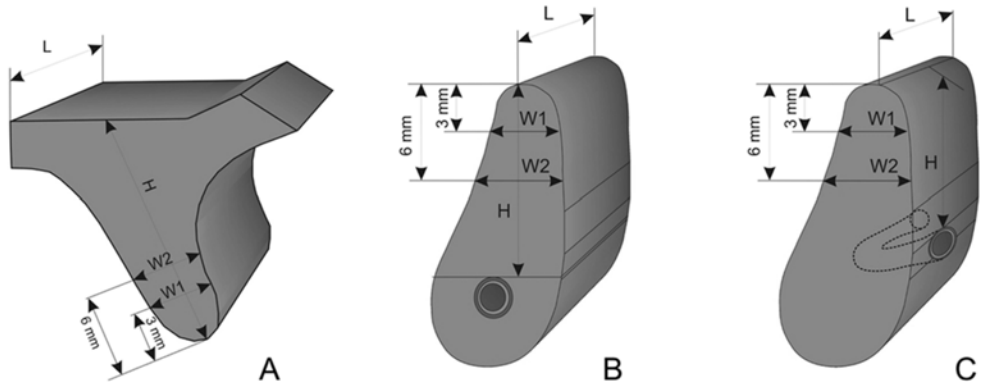


Fig. 1.5.2. Edentulous jaw segments (A = maxillary, B and C = mandibular) that consists of alveolar and basal bone

A = the vertical dimension (H) of the EJS is determined by the distance between the alveolar ridge crest and maxillary sinus. B = the vertical dimension (H) of the EJS is determined by the distance between the alveolar ridge crest and mandibular canal. C = the vertical dimension (H) of the planned implant is determined by the distance between the alveolar crestal ridge and mental foramen. The horizontal EJS dimensions: length (L) in all cases is determined by the distance between neighbouring teeth or implants and width (W) is determined by the alveolar process width measured at the level of 3 mm (W1) and 6 mm (W2) from the crest of alveolar process.

2. METHODS AND MATERIALS

2.1. Study I

2.1.1. Patient selection

Caucasian patients were selected randomly for the study at the Department of Oral and Maxillofacial Surgery from among patients needing panoramic imaging for preoperative planning of surgery. Patients were asked for medical and dental history to reveal any unsuitability for the study. All subjects had permanent dentition, were systematically healthy or with mild systemic diseases (American Society of Anaesthesiologists I or II), and had no history of mandibular traumas or surgical interventions in the regions of the evaluated JDSs (e.g. lateralization of IAN; the exception was removal of a tooth). Exclusion criteria were active periodontal diseases, current periodontal or orthodontic treatment, and inability to sign the informed consent. Ethical approval (No. BE-2-76) was retrieved from the Kaunas Regional Biomedical Research Ethics Committee (Lithuania). Permission for personal data management (No. 2R-4170) was achieved from the ethical State Data Protection Inspectorate. Written permissions to participate in the study were achieved from the randomly selected subjects.

2.1.2. Panoramic radiographs

All radiographs in this study were taken with a Kodak 9000 Extraoral Imaging System (Kodak Dental Systems, Carestream Health Inc., Rochester, NY, USA). According to the manufacturer's manual, 68–73 kV, 10–12 mA, and 6 mA were set, and the exposure time was 13.5–14.4 s. In this report, the technicians were calibrated to perform the technique prior to the study to reduce positional errors. Patients were positioned in a standardised manner according to manufacturer recommendations. Kodak Dental Imaging Software – 6.12.18.1 (Carestream Health Inc., Rochester, NY, USA) was used for image analysis. Evaluation was performed by one trained and calibrated oral surgeon on a 29.9" display (Coronis Fusion 4MP, Barco n.v, Kortrijk, Belgium) at a distance of 60 cm from the screen in dimmed room conditions. DPR inclusion criteria were based on image quality analysis: images considered optimal (high quality image providing sufficient information, with no errors from image taking procedure) and adequate (quality image providing sufficient information, from image taking procedure that does not affect the diagnosis) for diagnosis were suitable for further evaluation [4]. The main errors were positioning (for example, patient movement

or patient positioning asymmetry in any direction) and image taking or processing errors such as the image not being at the optimal contrast or density. If the DPR did not satisfy the mentioned quality requirements or had errors due to anatomical abnormalities, such as an unidentified mental foramen or a bifid MC, it was rejected from further evaluation.

2.1.3. MC visibility and JDS evaluation protocol

MC visibility assessment in relation to morphometric and densitometric parameters of the jaw bone on DPRs were made based on the JDS pattern [27]. This is defined as a vertically cut jaw segment including tooth, alveolar bone, and basal bone (Fig. 2.1.3.1).

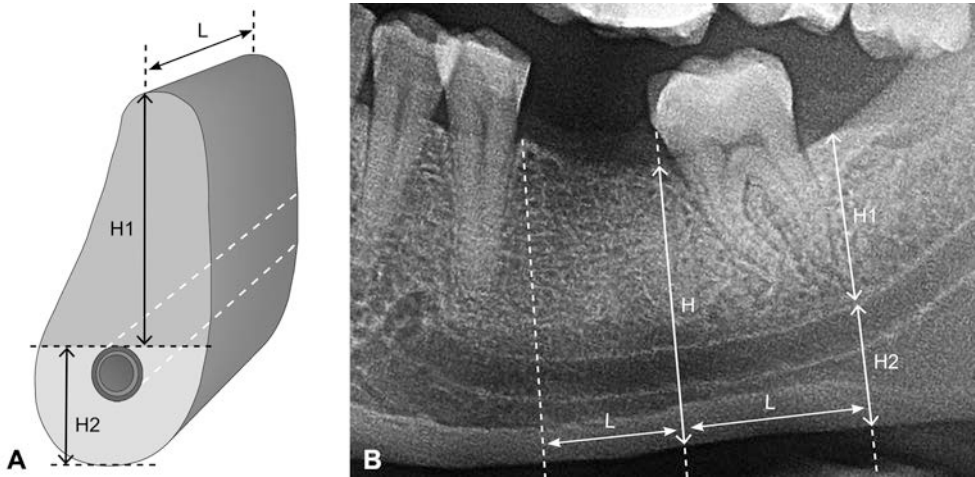


Fig. 2.1.3.1. *Jaw dental segment*

(a) Drawing and (b) digital panoramic radiograph showing JDS. H1, the alveolar bone: the distance from the crest of alveolar ridge to the MC superior border; H2, the basal bone: the distance from the superior border of the MC to the inferior ridge of the mandible; H, the height of the JDS: the distance between the crest of alveolar ridge and inferior ridge of the mandible; L, the length of the JDS: the distance between vertical lines that divides mesial and distal borders of the JDS between the evaluated JDS and the mesially and distally located JDSs borders respectively.

The location of bone suitable for implantation is identical with the former location of a tooth in the jaw. The number of the JDS describing the position of a planned implant in the jaw can be shown. If the JDS is edentulous, the term “edentulous jaw segment” is used. On DPR it is possible to assess only two-dimensional JDS parameters: height and length. The height of JDS is defined as the distance between the alveolar crest and inferior border of the mandible (Fig. 2.1.3.1). The mesial and distal borders of the JDS are vertical dividing lines between the evaluated JDS and the mesially and distally located JDS borders respectively.

JDS inclusion criteria were left and right mandibular first and second premolar (PM1 and PM2) and first and second molar (M1 and M2) jaw segments in which the MC was in an independent form condition that was dentate or edentulous. JDS exclusion criteria were the presence of mental foramen; impacted tooth or wisdom tooth; dental implant; overlapping JDSs; teeth with less than 1.0 mm distance between the lamina dura of neighbouring roots or less than 2.0 mm distance between the root apex and the MC; artefacts or bone pathology (e. g. cysts, inflammation-induced osteosclerosis) presented in any region of the JDS; less than 6 months since tooth extraction; longitudinal tooth axis and mandibular inferior ridge formed at an angle of less than 60 degrees; and mediolateral length of the edentulous JDS that did not correspond to the mediolateral length of the contralateral tooth crown (if the contralateral JDS was edentulous, then the average of the mediolateral crown values was used) [121].

2.1.4. MC visibility analysis

The radiographic image of the MC on DPR is defined as a dark ribbon between two white lines – the bony walls (borders) of the MC [26]. MC visibility was scored in a multifunction window (the “Measurements” tool was selected without additional settings) for each JDS in the four parts: mesial superior, mesial inferior, distal superior, and distal inferior (Fig. 2.1.4.1).

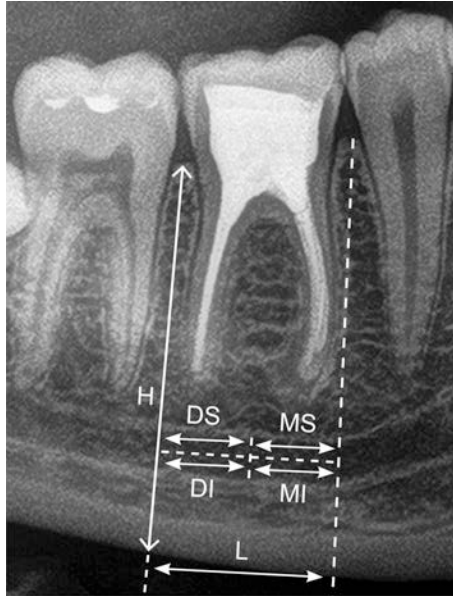


Fig. 2.1.4.1. *Jaw dental segment with mandibular canal parts for visibility evaluation*

MS, mesial superior part; DS, distal superior part; MI, mesial inferior part; DI, distal inferior part; H, the height of the JDS; L, the length of the JDS.

Since many anatomical variations can alter the common pattern of MC detection through the course, the visibility scores of the MC part for each JDS were characterised (Fig. 2.1.4.2) as 5 (good), 4 (moderate), 3 (poor), 2 (MC border is not visible, but visibility of the dark ribbon is good), or 1 (MC border is not visible, but visibility of the dark ribbon is moderate). An MC part with an identified MC border was scored as 5 or 4, while a detectable MC part with unidentified borders was scored as 2 or 1. An unidentified MC part was scored as 3.

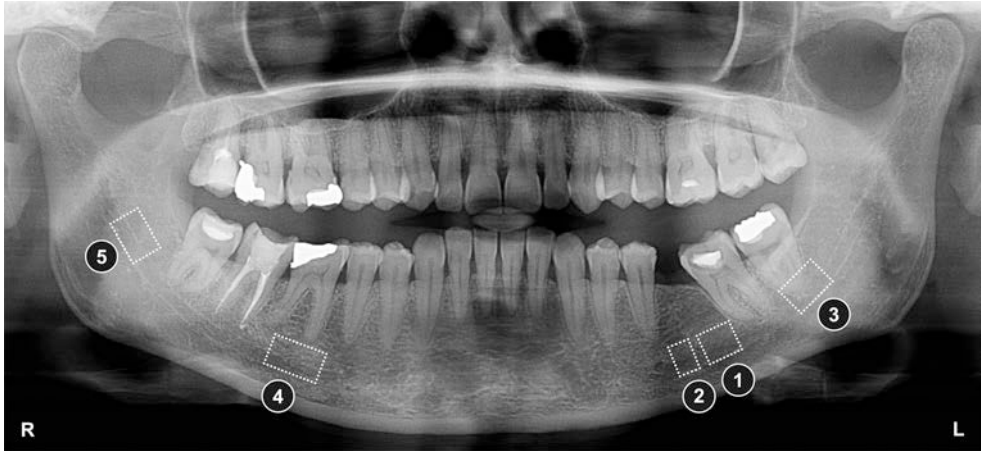


Fig. 2.1.4.2. Digital panoramic radiograph showing samples of MC parts' visibility scores

5, good; 4, moderate; 3, poor; 2, MC border is not visible, but visibility of the dark ribbon is good; 1, MC border is not visible, but visibility of the dark ribbon is moderate.

2.1.5. Morphometric analysis

Vertical JDS evaluation was performed using the “Measurements” tool without additional adjustments in the mesial and distal parts of the segment perpendicular to the inferior mandibular ridge. The centre of the JDS could not be evaluated properly according to the investigation protocol because dentate JDS contains root(s). Fig. 2.1.5.1 shows the vertical measurements that were assessed mesially and distally for each JDS: (a) the height (H) from the alveolar crest (AC) to the MC dark ribbon (H-AC-MC), including the superior MC border; (b) the height of the MC (H-MC), corresponding to the MC dark ribbon height; (c) the height from the lowest point of the MC dark ribbon to the superior border of the inferior cortical bone (IB) (H-MC-IB); (d) the height of the inferior cortical bone (H-IB); and (e) the height of the mandible (H-AC-IB). Measurement accuracy was ensured by periodical imaging system calibration according to the manufacturer recommendations and exclusion of the radiographs from investigation with patient positioning errors. Additional calibration was not made to reflect clinical conditions. Accepted measurement error was ± 0.1 mm.

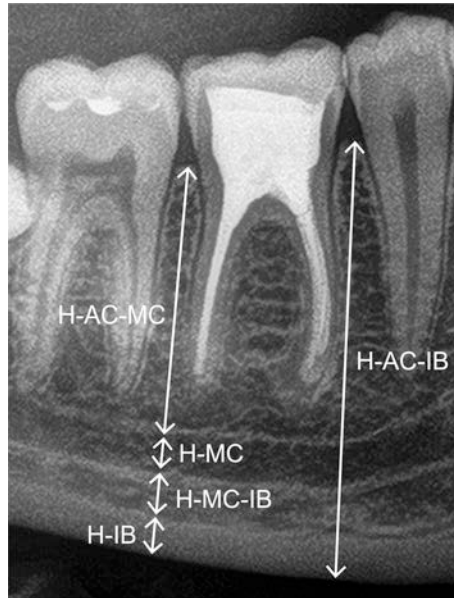


Fig. 2.1.5.1. Morphometric measurements

H-AC-MC, the height from the alveolar crest to the MC dark ribbon, including superior MC border; H-MC, the height of the MC, corresponding to the MC dark ribbon height; H-MC-IB, the height from the lowest point of the MC dark ribbon to the superior border of the inferior cortical bone; H-IB, the height of the inferior cortical bone; H-AC-IB, the height of the mandible.

2.1.6. Densitometric analysis

The analysis was made in a multifunction window with the “Densitometric analysis” tool selected. The “Sharp enhancement” tool was activated for standardisation of measurements, and no additional adjustments were used. Fig. 2.1.6.1 5 shows vertical and horizontal measurements in the region of the JDS. The following vertical (V) measurements were made mesially and distally: (a) from the alveolar crest in the trabecular bone to the bone 2.0 mm over the MC (AC-MC-V); (b) in the MC region (MC-V); (c) from the trabecular bone below the MC to the superior border of the inferior cortical bone (MC-IB-V); (d) in the inferior cortical bone region (IB-V); (e) from the alveolar crest in the trabecular bone to the end of the inferior cortical bone (AC-IB-V); and (f) at two bone density peaks, the superior MC peak (SMCP) and the inferior MC peak (IMCP), corresponding to the borders of the MC. Horizontal (Ho) densitometric measurements (Fig. 2.1.6.1) within JDS mediiodistal length were (a) 2.0 mm above the MC (AC-MC-Ho) (the measurement was not taken if the visibility of the superior MC border was poor (the border was not visible)); (b) the MC

region (MC-Ho); (c) the trabecular bone below the MC (MC-IB-Ho); (d) the inferior cortical bone region (IB-Ho); (e) 2.0 mm below the superior cortical bone of the edentulous JDS (or the mathematical average of horizontal measurements in the mesial and distal parts of the dentate JDS trabecular bone 2.0 mm below the superior cortical bone) when visibility of the MC superior border was poor (AC-MC-HoP). The vertical densitometric analysis line could not have an angle of more than 30 degrees and must be without overlapping lamina dura or tooth root when artefacts or anatomical structures were present in the region of measurement. Accepted measurement error was ± 5 relative measurement units.

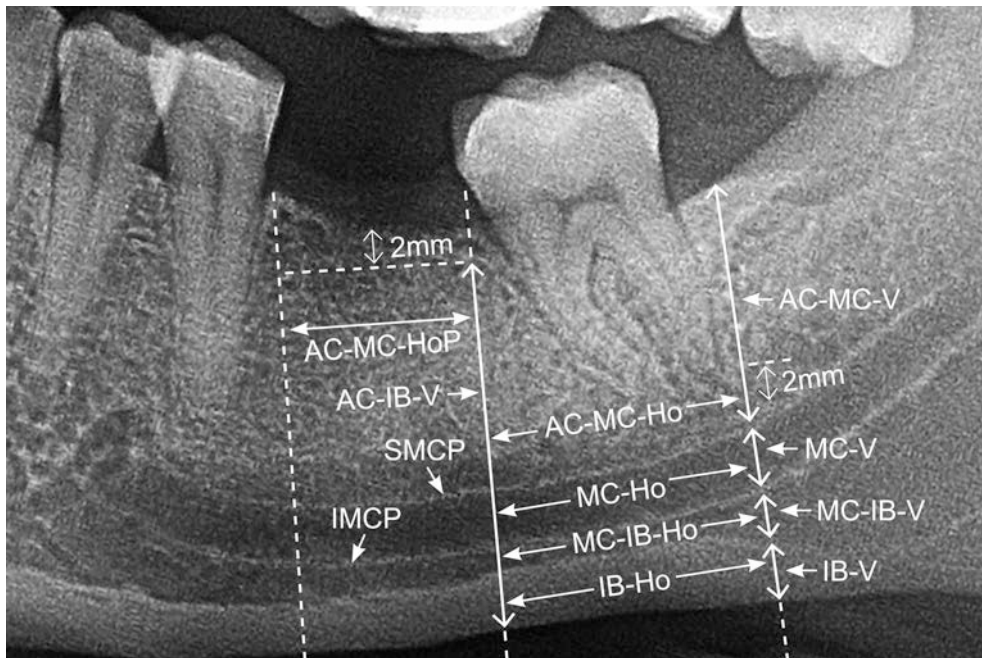


Fig. 2.1.6.1. Densitometric measurements

Vertical densitometric measurements: AC-MC-V, from the alveolar crest in the trabecular bone to the bone 2.0 mm over the MC; MC-V, in the MC region; MC-IB-V, from the trabecular bone below the MC to the superior border of the inferior cortical bone; IB-V, in the inferior cortical bone region; AC-IB-V, from the alveolar crest in the trabecular bone to the end of the inferior cortical bone; SMCP, at the superior MC peak corresponding to the border of the MC; IMCP, at the inferior MC peak corresponding to the border of the MC. Horizontal densitometric measurements: AC-MC-Ho, 2.0 mm above the MC; MC-Ho, the MC region; MC-IB-Ho, the trabecular bone below the MC; IB-Ho, the inferior cortical bone region; AC-MC-HoP, 2.0 mm below the superior cortical bone of the edentulous JDS (or mathematical average of horizontal measurements in mesial and distal parts of the dentate JDS trabecular bone 2.0 mm below the superior cortical bone) when visibility of the MC superior border is poor.

MC visibility, densitometric and morphometric analysis results were assessed additionally for possible significant differences between patients' age, gender, JDS condition, side of the mandible, or number.

Statistical analysis was performed by means of IBM SPSS 20.0 for Windows (SPSS Inc., Chicago, IL, USA). A Kolmogorov-Smirnov test was used for data (distribution of patients according to age) normality evaluation. The sample size was selected randomly using the criteria $\alpha = 0.05$ (confidence level) and $\beta = 0.8$ (power of the study). The sample size was calculated by means of a sample size calculator in the survey software (Creative Research System, Sebastopol, CA, USA). The three-sigma rule was applied for data inclusion before further analyses. The data are presented as mean \pm standard error (SE) in millimetres.

Repeated MC visibility evaluations were tested for agreement using Cohen's kappa coefficient. Investigation was simplified for intraobserver agreement evaluation: if an MC part was identified (previous scale grades of 5, 4, 2, or 1), then the visibility score was 1 (logical); if MC visibility was poor (previous scale grade of 3), then the score was 0 (logical).

Descriptive statistics was applied for the morphometric, densitometric, and MC visibility analysis. Fisher's exact test served for the MC border parts with the same visibility score comparison. A Pearson chi-square test was used to compare samples of categorical variables. Differences between the two independent samples were calculated using the Mann-Whitney U test.

Statistical significance was considered for p values less than 0.05.

2.2. Study II

A total of 639 partially dentulous and/or edentulous patients (266 men and 373 women, aged 18-83 years; mean 50 ± 14.18 years) scheduled for implant insertion in 5 dental clinics (185 CTs in Turkey, 173 CTs in Spain, 162 CTs in Cyprus-Turkey, 61 CTs in Lithuania, and 51 CTs in Saudi Arabia) were enrolled in this study. One thousand sixty-one lingual foramina of 639 patients were examined. One calibrated investigator at each center performed all the measurements. Spiral (Siemens AR-SP 40; Siemens, Munich, Germany) and CBCT scans (Imaging Sciences International, Hatfield, PA) achieved in these centers were used in the present study. A detailed research protocol was discussed and agreed before initiation of the study. Measurements were clarified on schematic diagrams between the calibrated investigators. CTs with low-quality imaging, such as scattering of the bony borders and pathology, were excluded. One thousand sixty-one lingual

foramen on axial mandibular CT sections were examined for the following measurements (Fig. 2.2.1):

1. Distance between crest and lingual foramen.
2. Distance between tooth apex and lingual foramen if tooth is present at the location of foramen.
3. Vertical distance from the mandibular border.
4. Diameter (vertical size) of lingual foramen.

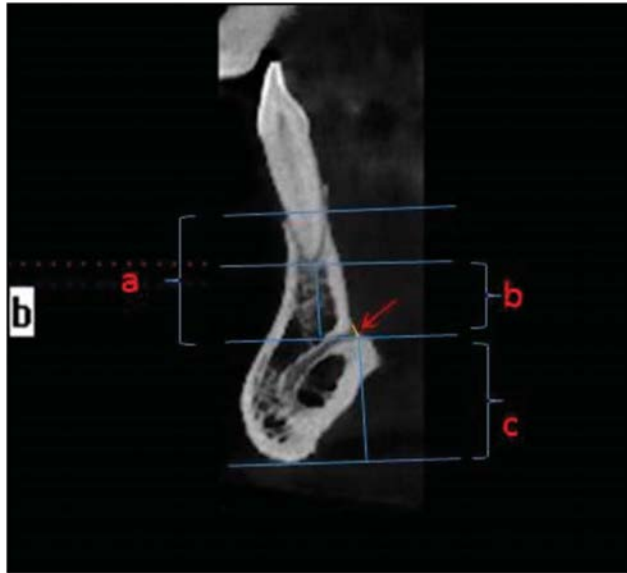


Fig. 2.2.1. Dimensional measurements on axial mandibular CT sections.

A, distance between crest and lingual foramen; B, distance between tooth apex and lingual foramen; C, vertical distance from the mandibular border to the lingual foramen. Arrow: diameter of lingual foramen.

Lingual vascular canal type was classified as mono, bifid, and triples if the number of bony canal inside the mandible in an axial CT section is only 1, 2, or 3, respectively. If more than 1 canal is detected, the mean measurements were calculated and recorded as 1 measurement. Occurrence of lingual foramen on both the sides of mandible was noted as bilateral, if not, unilateral. Anastomoses with incisive artery, mental artery, and alveolar inferior artery were evaluated. Dentition status of mandibles and location of lingual foramen were recorded. Location of foramen was determined as the tooth number, observed at the region of that tooth.

In the literature, lingual canal located in or near midline is called MLC and that located in premolar regions is called LLC [49]. A recent study included the canine teeth into LLC [49]. Cadaver studies named the canal/

foramen as “lateral” if it is not located at themidline [56]. In this study, the foraminaof the whole mandible was examined rather than the interforaminal area.

Statistical analyses were performed by the center at Hacettepe University with the SPSS for Windows 16.0 software (SPSS, Chicago, IL). Age and sex of the patients were recorded, and the measurements were analyzed according to the age and sex. Mean \pm SDs and frequency, percentage were calculated for numerical and categorical variables, respectively. Independent samples t test was used to compare the differences between the gender groups. The correlations between numerical variables were analyzed with Pearson correlation coefficient. Statistical significance was considered for p values less than 0.05.

2.3. Study III

Study III was purposed to be a retrospective clinical study with two subgroups EJSs (single tooth loss and multiple teeth loss) in the maxillary sinus region. In the study, a total of 597 adult patients with single EJS and 518 patients with multiple EJSs (1190 EJSs) in the maxillary sinus region were assessed to evaluate maxillary sinus anatomy, variations and pathologies of the sinus cavity and surrounding bony area (including alveolar process), and further evaluating the volumetric pattern of the maxillary sinus. The patients were those who were referred for oral surgery or dental implant treatments at six clinics internationally (Cyprus, Turkey, Lithuania, Spain, two centers in USA) and needed CBCT evaluation of the oral and maxillofacial area. The CBCT scans of each were transferred to a computer, and images were processed with a dedicated software on medical screen in a dimmed room.

2.3.1. Panoramic/Frontal view evaluations

2.3.1.1. The alveolar bone height and sinus membrane thickness measurements in mm [6]

Single tooth loos: the dimensions of bone between the root tips and sinus floor and the vertical bone height at the single-tooth gap (edentulous alveolar ridge) midway between the two neighboring teeth will be measured from the most crestal aspect to the sinus floor. The thickness of the sinus membrane will be evaluated at three sites: at the selected root tips of the mesial and distal neighboring teeth and at the single-tooth gap, starting at

the bony plate of the sinus and ending at the mucosal surface, perpendicular to the adjacent bone.

Multiple teeth loss: Presence of adjacent or opposing teeth to the edentulous span so that the location of the edentulous ridges in correspondence to the tooth site and size [165, 166] can be identified, and the panoramic section included the middle part of each missing tooth will be selected for alveolar ridge height and the sinus membrane thickness measurements.

2.3.1.2. Single or multi-rooted tooth/teeth in mm

The length of the neighboring dentitions' roots will also be measured from the cement-enamel junction (CEJ) to the most apical part of the root.

2.3.1.3. The morphology of the sinus membrane

It will be evaluated and classified in single tooth or multiple teeth loss [6], in scoring system:

- a) Healthy sinus membrane, no thickening = 1;
- b) Flat sinus membrane, thickening without well-defined outlines = 2;
- c) Semispherical membrane, thickening with well-defined outlines rising in an angle of greater than 30 degrees from the floor of the walls of the sinus = 3;
- d) Mucocele-like (complete opacification of the sinus) = 4;
- e) Mixed flat and semispherical thickenings = 5.

2.3.1.4. Vital and non-vital teeth classification for single tooth and multiple teeth loss [6] with scoring system

- a) The mesial and distal teeth are both vital = 1;
- b) The distal tooth is endodontically treated and the mesial tooth is vital = 2;
- c) The mesial tooth is endodontically treated and the distal tooth is vital = 3;
- d) Both neighbouring teeth are endodontically treated = 4;
- e) For no distal tooth but having mesial tooth: vital = 5;
- f) For no distal tooth but having mesial tooth: endodontically treated = 6;
- g) For no mesial tooth but having distal tooth: vital = 7;
- h) For no mesial tooth but having distal tooth: endodontically treated = 8.

2.3.1.5. Sinus augmentation classification for single tooth and multiple teeth loss [11] with scoring

- a) Abundant bone-1: Distance from cement-enamel junction (CEJ) to alveolar bone crest is ≤ 3 mm and alveolar bone height is > 10 mm = 1;
- b) Abundant bone-2: Distance from CEJ to alveolar bone crest is > 3 mm, and alveolar bone height is > 10 mm = 2;
- c) Barely sufficient bone-1: Distance from CEJ to alveolar bone crest is ≤ 3 mm, and alveolar bone height is 6–9 mm = 3;
- d) Barely sufficient bone-2: Distance from CEJ to alveolar bone crest is > 3 mm, and alveolar bone height is 6–9 mm = 4;
- e) Compromised bone-1: Distance from CEJ to alveolar bone crest is ≤ 3 mm, and alveolar bone height is ≤ 5 mm = 5;
- f) Compromised bone-2: Distance from CEJ to alveolar bone crest is > 3 mm, and alveolar bone height is ≤ 5 mm = 6.

2.3.1.6. Sinus septa morphology in single tooth or multiple teeth loss [12]

- a) Number of septa(s) that is anterior to zygomatic process;
- b) Number of septa(s) that is posterior to zygomatic process;
- c) Height of the septa in mm.

2.3.1.7. Sinus septa classification in single and multiple tooth loss [12] with scoring

- a) Single septa anterior to zygomatic process = 1;
- b) Single septa posterior to zygomatic process = 2;
- c) 2 or more septa anterior or posterior to zygomatic process = 3.

2.3.2. Sagittal view evaluations

2.3.2.1. Maxillary sinus ostium pattern in all sinus regions evaluated [7] with scoring:

- a) Patent (no obstruction) = 1;
- b) Obstructed = 2.

2.3.2.2. The vertical thickness of the sinus membrane morphological classification in all sinus regions evaluated [7] with scoring

- a) Healthy sinus membrane, no thickening = 1;
- b) Rounded = 2;
- c) Irregular = 3;
- d) Circumferential thickening = 4;
- e) Complete thickening = 5.

2.3.2.3. Sinus membrane thickness measurement [7]

Single tooth or Multiple teeth loss: Presence of adjacent or opposing teeth to the edentulous span so that the location of the edentulous ridges in correspondence to the tooth site and size [165, 166] can be identified, and the panoramic section included the middle part of each missing tooth will be selected for sinus membrane thickness measurements in mm.

2.3.2.4. Sinus membrane thickness classification of single tooth loss and multiple teeth loss [7]

Single tooth or Multiple teeth loss: Presence of adjacent or opposing teeth to the edentulous span so that the location of the edentulous ridges in correspondence to the tooth site and size [165, 166] can be identified, and the panoramic section included the middle part of each missing tooth will be selected for sinus membrane thickness measurements in mm, and then a score index will be used:

- a) Class 1: 0–5 mm = 1;
- b) Class 2: 5– 10 mm = 2;
- c) Class 3: 10– 15 mm = 3;
- d) Class 4: 15– 20 mm = 4;
- e) Class 5: greater than 20 mm = 5.

2.3.2.5. The location of the PSAA

It will be evaluated in single tooth loss and multiple teeth loss (the adjacent and opposing dentition will be used to understand the middle of each missing tooth, and measurements will be done for the each missing tooth separately) [9] with scoring system:

- a) No PSAA = 1;
- b) Intra-osseous = 2;
- c) Below sinus membrane = 3;
- d) On the outer cortex of the sinus wall = 4.

2.3.2.6. The diameter of the PSAA

It will be measured in single tooth loss and multiple teeth loss (the adjacent and opposing dentition will be used to understand the middle of each missing tooth, and measurements will be done for the each missing tooth separately) [9] with scoring system:

- a) No PSAA = 1;
- b) Smaller than 1 mm = 2;
- c) 1–2 mm = 3;
- d) Higher or equal to 2 mm = 4.

2.3.2.7. Bone length between the lower border of the PSAA to the alveolar ridge

It will be done in mm in single tooth and multiple teeth loss (the adjacent and opposing dentition will be used to understand the middle of each missing tooth, and measurements will be done for the each missing tooth separately) [9].

2.3.2.8. Buccal bone thickness at the upper border of the PSAA

The width of the buccal sinus wall [9] will be measured in mm (the adjacent and opposing dentition will be used as reference points to understand the middle of each missing tooth, and measurements will be done for the each missing tooth separately).

2.3.2.9. The height of the alveolar ridge

The dimension of the tooth/teeth gap(s) midway at the edentulous site will be measured from the most crestal aspect to the sinus floor, as residual alveolar ridge height in mm (the adjacent and opposing dentition will be used as reference points to understand the middle of each missing tooth, and measurements will be done for the each missing tooth separately) [10].

2.3.2.10. The width of the alveolar ridge

The sagittal section that included the middle part of each missing tooth (single or multiple tooth loss) will be selected for ridge width measurement including three measurements taken from the most coronal, middle and apical (where sinus floor is) parts, and as a fourth measurement an arithmetic mean will be calculated for each missing tooth/teeth [10].

2.3.2.11. The width of the maxillary sinus

The sagittal section that included the middle part of each missing tooth will be selected for sinus width measurements in mm between lateral to the mesial wall of the maxillary sinus: the sinus width will be measured at 5, 7, 10, 13 and 15 mm from the level of alveolar crest in single tooth loss or multiple teeth loss using referencing landmarks given above [10].

2.3.2.12. The edentulous sites classification according to the ridge height [10] with a scoring system

- a) Lower than 4 mm = 1;
- b) Lower or equal to 4 and lower than 7 mm = 2;
- c) Higher and equal to 7 or lower than 10 mm = 3.

2.3.2.13. Sinus septa morphology numbering and measurements [12]

- a) Number of septa(s) that is anterior to zygomatic process: how many septa (0, 1, 2 etc.);
- b) Number of septa(s) that is posterior to zygomatic process: how many septa (0, 1, 2 etc.);
- c) Mean height of the septa(s) that is anterior to zygomatic process in mm;
- d) Mean height of the septa(s) that is posterior to zygomatic process in mm.

2.3.2.14. Sinus septa classification [12] with a scoring system

- a) Septa located anterior to zygomatic process = 1;
- b) Septa located posterior to zygomatic process = 2.

2.3.3. Coronal/Transverse view evaluations

2.3.3.1. Maxillary sinus has relation to [167] with a scoring system

- a) Nothing = 1;
- b) Associated to peri-apical lesion = 2;
- c) Associated to bone graft = 3;
- d) Associated to implant fenestration = 4;
- e) Associated to tooth extraction = 5;
- f) Associated to bone graft + implant = 6;
- g) Associated to endodontic filling material = 7;
- h) Associated to foreign body = 8.

2.3.3.2. Maxillary sinus ostium pattern [8] with a scoring:

- a) Patent (not obstructed) = 1;
- b) Obstructed = 2.

Statistical analyses were performed by the center at Hacettepe University with the SPSS for Windows 16.0 software (SPSS, Chicago, IL). Age and sex of the patients were recorded, and the measurements were analyzed according to the age and gender, status of edentulous sites. Mean \pm SDs and frequency, percentage were calculated for numerical and categorical variables, respectively. Comparative statistics and statistical correlations were performed. Statistical significance was considered for p values less than 0.05.

2.4. Study IV

Literature was selected through a search of PubMed, Embase and Cochrane electronic databases. The keywords used for search were mandible; mandibular canal; alveolar nerve, inferior; anatomy, cross-sectional; dental implants; classification. The search was restricted to English language articles, published from 1972 to March 2013. Additionally, a manual search in the major anatomy and oral surgery books were performed. The publications there selected by including clinical and human anatomy studies.

Literature was selected through a search of PubMed, Embase and Cochrane electronic databases. The keywords used for search were mandible; mandibular canal; alveolar nerve, inferior; anatomy, cross-sectional; dental implants; classification. The search was restricted to English language articles, published from 1972 to March 2013. Additionally, a manual search in the major anatomy and oral surgery books were performed. The publications there selected by including clinical and human anatomy studies.

2.5. Study V

2.5.1. Patient selection

The study was done in two investigation centers: Department of Periodontology, Hacettepe University, and Department of Oral and Maxillofacial Surgery, Lithuanian University of Health Sciences. Subjects were sampled randomly from all patients who had appointments at the departments for dental implant treatment. Medical history was evaluated. CBCT, panoramic, or periapical radiography and clinical examinations were made for dental implant treatment. The inclusion criteria were as follows: adult people (at least 18 years old) with permanent dentition; subjects with one or more

single EJS, limited by neighboring teeth from both sides; patients did not wear any kind of removable prosthesis over the treatment area; adjacent teeth had to be intact or have no defective restorations over cemento-enamel junction; fractures and surgeries could not present in the regions of planned implant surgery; patients were systematically healthy or had mild systemic diseases (American Society of Anesthesiologists Physical Status Classification System: I and II); and patients had to sign the informed consent. Exclusion criteria were: heavy smokers (more than 10 cigarettes a day); pregnant or lactating mothers; active periodontal diseases; or other acute infection at the region of EJS; patients under current orthodontic or periodontal treatments; and patients with EJS in central and lateral lower incisors (individual case-related treatment planning).

The Non-Interventional Clinical Research Ethics Board (Hacettepe University, Ankara, Turkey) provided approval for the study (No. GO 14/283-10). The Kaunas Regional Biomedical Research Ethics Committee (Lithuania) provided ethical approval (No. BE-2-76) as well. State Data Protection Inspectorate (Lithuania) provided permission for personal data management (No. 2R-4170). The study was registered with ClinicalTrials.gov identifier: NCT02054676.

2.5.2. Study stages

The investigation object of suggested classification was the EJS in aesthetic or non-aesthetic zone (Table 1.5.1 in Chapter 1.5). Aesthetic zone contained incisors, canine, and premolar. First and second molar belongs to the non-aesthetic zone. Clinical parameters were assessed and compared at pre-, intra-, early post-, and late post-operative study stages. All graded measurements set overall risk for implantation at preoperative study stage (Appendix 1).

Separate numbers of clinical parameters were evaluated varying on anatomical location (aesthetic or non-aesthetic zone, MC region or not). Type I EJS had all parameters evaluated as low risk (Table 1.5.1 in Chapter 1.5). If at least one parameter was evaluated as being a moderate risk, overall EJS gradation was moderate risk or type II. If at least one parameter was evaluated as high risk, overall EJS gradation was high risk or Type III* (* – interdental bone peak height and alveolar ridge vertical position are aesthetic parameters). Type III EJS was not suitable for evaluation during the present study (exception: implant placement is possible in the EJS of aesthetic zone if aesthetic implant treatment success is not planned or not possible to be high). The results were collected during each evaluation stage (See Appendices). Corresponding parameters were compared after the data

collection to assess classification accuracy and predictability in dental implant treatment.

2.5.3. CBCT, panoramic, and periapical radiography

Panoramic or periapical radiography was primary common radiological investigation modality for implant treatment planning or for early postoperative EJS evaluation. Standardized digital panoramic radiographs were acquired by Kodak 9000 Extraoral Imaging System (Kodak Dental Systems, Carestream Health Inc., Rochester, NY, USA). According to the manufacturer's manual, 68–73 kV, 10–12 mA, and 6 mA were set, and the exposure time was 13.5–14.4 s. Patients were positioned in a standardised manner according to manufacturer recommendations. Kodak Dental Imaging Software – 6.12–18.1 (Carestream Health Inc., Rochester, NY, USA) was used for image analysis. All radiologic investigations were made by one experienced roentgen technician at each center.

CBCT examination was necessary before dental implant planning according to study protocol, despite two-dimensional (2D) imaging modality's significance in dentistry [168]. CBCT scans were obtained for 3D evaluation of EJS considering current guidelines [19, 21]. Patients were scanned with i-CAT[®] (Imaging Sciences International, Hatfield, Pennsylvania, USA) CBCT scanner. It has clinically accurate measurements and acceptable spatial resolution [169]. The exposure values were set at 120 kVp, 5 mA, with an exposure time of 26.9 s, a voxel size of 0.25 mm, and field of view of 16 cm (width) and 8 cm (height). CBCT images were analyzed by using the i-CATVision[™] (Imaging Sciences International, Inc., Hatfield, PA, USA) software.

Periapical radiographs using the long-cone paralleling technique were all made with Progeny dental preva (Midmark, Lincolnshire, IL, USA). Exposure parameters were adjusted individually. Image analysis was made with a Sopro imaging software (Sopro, Acteon Group, La Ciotat, France).

FDI (World Dental Association) dental notation system was used in this study for teeth or EJS numbering. The length measurement were registered in millimeters (mm) with used integer numbers (not with numbers after the comma, according to the mathematical rules). The images were viewed at each center by one trained and calibrated practitioner in dimmed room conditions 60 cm from Coronis Fusion 4MP (Barco n.v, Kortrijk, Belgium) medical display. Dedicated measurement tools were used for linear measurements. The investigators selected dental implant parameters for planned EJS region. At least 1–2 mm was recommended to be left from dental implant apex to vital structures of the jaws.

Non-linear measurements values were provided, such as: “+” meaning agreement and “-” meaning disagreement. Periodontal probe PCPUNC157 (Hu-Friedy Mfg. Co., LLC, Chicago, IL, USA) is recommended with 1 mm increments, grading for intraoperative stage measurements. The main variables of the classification and principle of the assessment are shown in Table 1.5.1 (Chapter 1.5).

2.5.4. Preoperative stage (Appendix 1)

This stage’s evaluation was done by using CBCT analysis software. If the EJS contained MC, an additional part of the data was filled. Basically, more detailed evaluation of MC region (Type III assessment). It was defined as follows: impossible to identify superior MC wall (dark ribbon is visible) and registered D2 or D3 bone quality parameters [73]. After this, the implant treatment risk degree (overall EJS type) was determined and assigned. The EJSs scored as Type I and II were suitable for subsequent stages of the study. Dental implant system was chosen with dental implant (height, width) and related parameters in Appendix 1.

2.5.5. Intraoperative stage (Appendix 2)

Surgery was planned according to preoperative evaluation results. Bone and soft tissue regeneration were performed individually if required after dental implant placement. Full mucoperiosteal flap was performed and aesthetic parameters related to implant treatment success were evaluated. Dental implant was then placed according to manufacturer recommendations. Dental implant placed in the non-aesthetic zone (central fossa region for molars in correspondence with long axis of imagined tooth) should be surrounded with at least 1 mm of bone to ensure successful treatment. If the operation is planned according to CBCT, implantation in the areas of MC requires that the apices of the implants be at least 1 mm away from mentioned anatomical structures (if a pilot drill is no longer than the planned corresponding dental implant) [142, 170]. Dental implant with added additional length (so-called “y” dimension) is assigned to be 1 mm away from anatomically important structures for more precise planning. As a result, we have placed dental implant at least 1–2 mm away from MC.

All implants placed in the aesthetic zone should have optimal three-dimensional position. An ideally placed dental implant is surrounded by bone at least 1 mm from the lingual side and at least 2 mm from the buccal side for successful treatment outcome [159, 171]. The dental implant is placed in the cingulum (for cuspids, incisors; for premolars, in the center of the central sulcus in correspondence with imagined tooth long axis) position

(in line with adjacent teeth), and planned implant tooth incisal edge position is in line with adjacent teeth incisal edge. In this ideal position, the implant collar is 2 mm below the cemento-enamel junction of the adjacent teeth apicocoronally or 3–4 mm below planned soft tissue margin, and at least 1.5 mm away from adjacent teeth mediolaterally. Natural buccal and proximal restorative contour is ensured by correctly orienting the implant in a buccolingual position: 3 to 4 mm from outside buccal flange. A minimum 2 mm of space should be maintained on the buccal side in front of the external implant collar surface. Primary implant stability was planned to be at least 15 Ncm (placed implant should be without lateral or vertical movements) [170].

2.5.6. Early postoperative stage (Appendix 2)

Postoperative digital radiological periapical radiograph evaluation was undertaken to assess postoperative implant apex distance to anatomically important vital structures [103, 172].

2.5.7. Late postoperative stage (Appendix 3)

This was the final step of the EJS aesthetic parameters evaluation. The evaluation was based on several parameters selected from complex aesthetic index (CEI) [173]. It was made during the placement of a single-tooth implant crown. Vertical soft tissue deficiency and mesial and distal papilla appearance (Appendix 3) evaluation of EJS was necessary for the accuracy of the classification assessment during final single-tooth implant crown placement in the aesthetic (both parameters are evaluated) and non-aesthetic zones (soft tissue vertical deficiency). The time after surgery was case dependent before provisional and final crown placement. Peri-implant soft tissue conditioning was recommended with screw-retained provisional single-tooth implant crown for approximately 4–8 weeks. Healing abutment placement after dental implant osseointegration was not recommended because of the treatment time saving.

IBM SPSS 20.0 for Windows (SPSS Inc., Chicago, IL, USA) served for statistical analysis of the study. Data (e.g. subjects distribution by the age in both centers) normality was checked by a Kolmogorov-Smirnov test. The representative sample size was selected randomly. It was calculated by application of the V. I. Paniotto formula ($n = 1/(\Delta^2 + 1/N)$, where n – representative sample size, Δ – sampling error, N – total sample size. The data were described as mean \pm standard deviation (SD). The following criteria were chosen: sampling error of 0.05 and confidence interval of 95%.

An independent samples test was used for the samples difference in age group evaluation. Descriptive statistics was used for the individual stages of the study. The samples of categorical variables were compared by using a Pearson chi-square test. Mann-Whitney U test was used for further categorical data evaluation. Analysis of variance tested differences between multiple means of variables. Fisher's exact test was used for comparison of variables in small samples. The linear relationship between nonparametric variables was evaluated using Spearman's rank correlation coefficient. Wilcoxon's signed ranks test or paired sample t-test was considered for match evaluation between pairs after normality evaluation of the samples. Statistical significance level was chosen of 0.05 to verify the hypotheses of the study.

3. RESULTS

3.1. Study I

The primary sample consisted of 101 patients of Caucasian race. Sixty-nine DPRs (68.3%) were scored less than “adequate for diagnosis” (diagnosable image, with some errors and partially unreadable region or diagnostically unacceptable poor quality image) according to Choi et al. [4] and were excluded from subsequent evaluation. Thirty-two panoramic radiographs (31.7%) met the requirements of the investigation (mean age of the patient in years 43.7 ± 2.0 , range 17–64 years). A total of 155 JDSs were evaluated from the 32 DPRs.

The Kolmogorov-Smirnov test showed normally distributed data ($d = 0.09$, $p > 0.05$) of the sample (distribution of patients by age). Distribution of patients of both genders by age was homogenous. No statistically significant differences ($p > 0.05$) were identified between JDS condition (edentulous or dentate) and JDS number.

3.1.1. MC visibility analysis results

Intraobserver agreement (Cohen’s kappa coefficient) for the MC visibility evaluation was almost perfect (Table 3.1.1.1).

Table 3.1.1.1. Cohen’s kappa coefficients for the MC parts’ visibility

MC part in JDS	κ	CI
Mesial superior	0.96 ^a	0.91–1.01
Mesial inferior	0.97 ^a	0.92–1.01
Distal superior	0.97 ^a	0.92–1.01
Distal inferior	0.88 ^a	0.80–0.97

MC part, mandibular canal part of the jaw dental segment (mesial superior, mesial inferior, distal superior, distal inferior); κ , Cohen’s kappa coefficient; CI, confidence interval by 95%. ^a almost perfect agreement = 0.81–0.99.

Table 3.1.1.2 shows the distribution of MC visibility scores according to the MC border part evaluation. The predominant MC visibility score was 4, with a mathematical average of 40.7%. The most frequent superior MC border visibility value was 4 (42.6–43.0%), and the most common inferior MC visibility value was 5 (43.9–49.5%). The most uncommon MC visibility value was 2 (1.0 to 7.0%).

Table 3.1.1.2. Mandibular canal visibility analysis results

Visibility Scores	MC part in JDS			
	Mesial Superior [I]	Mesial Inferior [II]	Distal Superior [III]	Distal Inferior [IV]
1	21.0%	7.1%	21.8%	2.0%
	I vs II, $p < 0.001$	II vs III, $p < 0.001$	III vs IV, $p < 0.001$	I vs IV, $p < 0.001$
2	7.0%	–	3.0%	1.0%
			III vs IV, $p = 0.16$	I vs IV, $p < 0.001$
3	22.0%	10.2%	24.7%	9.1%
	I vs II, $p < 0.01$	II vs III, $p < 0.03$	III vs IV, $p < 0.002$	I vs IV, $p < 0.006$
4	43.0%	38.8%	42.6%	38.4%
	I vs II, $p = 0.24$	II vs III, $p = 0.23$	III vs IV, $p = 0.23$	I vs IV, $p = 0.22$
5	7.0%	43.9%	7.9%	49.5%
	I vs II, $p < 0.001$	II vs III, $p < 0.001$	III vs IV, $p < 0.001$	I vs IV, $p < 0.001$

Visibility scores: 1, 2, 3, 4, 5; MC part in JDS: MC visibility was evaluated in four locations for each JDS (mesial superior [I], mesial inferior [II], distal superior [III], distal inferior [IV]).

Data are provided as a percentage (%) of the sum of visibility scores of the particular MC border part from all visibility scores of the particular border. Fisher’s exact test results (p value) between the indicated groups are provided below the percentage line.

Note. Statistically non-significant differences were identified between groups I vs III and II vs IV ($p > 0.05$) and were not provided in the table.

The mesial inferior MC part had no visibility value of 2. The superior MC border was not visible, more than twice as often as the inferior MC border was not visible. The superior MC border was not visible in 22.0% of the mesial parts and 24.7% of the distal parts in all evaluated JDSs. Statistically non-significant differences were identified between the visibility scores for the mesial and distal superior and the mesial and distal inferior MC border parts (Fisher’s exact test, $p > 0.05$). Statistically significant differences were identified between particular MC visibility scores for the mesial superior and mesial inferior MC border parts (Fisher’s exact test, $p < 0.01$), as well as between the distal superior and distal inferior MC border parts (Fisher’s exact test, $p < 0.01$) (Table 3.1.1.2).

No significant differences were identified between gender and MC visibility score ($p > 0.05$) or JDS number and MC visibility score ($p > 0.05$) in any MC visibility evaluation part. There were no differences in MC superior border visibility across ages ($p > 0.05$). Significant differences were identified between mean age and visibility scores of 4 and 5 for the mesial inferior border ($p = 0.02$). The visibility of the MC mesial and distal

superior border ($p > 0.05$) and distal inferior border ($p > 0.05$) was independent of JDS condition. MC mesial inferior border visibility evaluation scores 5 and 3 were dependent on the JDS condition (edentulous or dentate), i.e., statistically significant differences were identified (Fisher's exact test, $p = 0.04$, odds ratio [OR] = 5.67, 95% confidence interval [CI] = 4.05–7.94, p -two tailed = 0.02). No differences were revealed between JDSs' corresponding MC parts in the visibility evaluation of PM1 and PM2 ($p > 0.05$), PM2 and M1 ($p > 0.05$), or M1 and M2 ($p > 0.05$).

MC visibility of particular JDSs did not reveal differences in the MC visibility of corresponding JDSs in the contralateral mandible side ($p > 0.05$).

3.1.2. Morphometric analysis results and relations to MC visibility scoring

Table 3.1.2.1 provides morphometric measurement data. The highest SE values were found for the anatomically most variable measurements: H-AC-MC and H-AC-IB. The lowest values of SE were achieved for MC height as well as for inferior cortical bone height evaluation.

Table 3.1.2.1. JDS morphometric analysis results

Measurement Location	Measurement	Mean	SE
Mesially	H-AC-MC	15.6	0.4
	H-MC	2.4	0,1
	H-MC-IB	3.8	0.1
	H-IB	3.2	0.1
	H-AC-IB	25.4	0.4
Distally	H-AC-MC	14.1	0.5
	H-MC	2.3	0.1
	H-MC-IB	4.1	0.2
	H-IB	2.8	0.1
	H-AC-IB	23.3	0.4

Measurement location, JDS measurement location mesially and distally; Measurement: H-AC-MC, the height from the alveolar crest to the MC dark ribbon, including superior MC border; H-MC, the height of MC, corresponding to the MC dark ribbon height; H-MC-IB, the height from the lowest point of the MC dark ribbon to the superior border of the inferior cortical bone; H-IB, the height of the inferior cortical bone; H-AC-IB, the height of the mandible. The data are presented as mean, standard error (SE) in millimetres.

3.1.3. Morphometric analysis relations to MC visibility scoring

Analysis of the results revealed statistically non-significant differences between the visibility of the mesial superior ($p > 0.05$) as well as the mesial inferior MC ($p > 0.05$) part and the morphometric analysis results in the mesial part of JDS.

MC visibility revealed significant differences in particular morphometric analysis results (Table 3.1.3.1).

Table 3.1.3.1. Morphometric analysis relations to MC visibility scoring

MC part for visibility evaluation	JDS Part for Morphometric Analysis		
	H-AC-MC	H-MC	H-AC-IB
Distal Superior	1 (12.8 [0.9]) and 4 (15.2 [0.6]) ($p = 0.01$), 3 (10.2 [0.4]) and 4 (15.2 [0.6]) ($p = 0.04$)	1 (2.4 [0.1]) and 3 (1.7 [0.1]) ($p = 0.04$), 3 (1.7 [0.1]) and 4 (2.4 [0.1]) ($p = 0.04$)	1 (22.2 [0.7]) and 4 (24.2 [0.6]) ($p = 0.04$)
Distal Inferior	4 (13.3 [1.0]) and 5 (14.6 [0.6]) ($p = 0.04$)	–	–

MC part for visibility evaluation: JDS mandibular canal visibility evaluation in distal superior and distal inferior part (in visibility scores: 1, 2, 3, 4, 5); JDS part for morphometric analysis: JDS measurement part for morphometric analysis (measurement values are presented as mean [SE (standard error)] in millimetres): H-AC-MC, the height from the alveolar crest to the MC dark ribbon; H-MC, the height of the MC; H-AC-IB, the height of the mandible.

Statistically significant differences are presented: “visibility score (morphometric analysis value [SE])” and “visibility score (morphometric analysis value [SE])” “(p value)”; “–”, no statistically significant difference ($p > 0.05$).

3.1.4. Densitometric analysis results in relation to MC visibility scoring

Densitometric analysis results are provided in Table 3.1.4.1. Significant differences were identified ($p < 0.05$) between the corresponding results of mesial and distal densitometric analyses in the vertical direction of JDS.

Table 3.1.4.1. *JDS densitometric analysis results in vertical and horizontal directions*

Measurement Location	Measurement Direction	Measurement	Mean	SE
Mesially	Vertically	AC-MC-V	106.0	2.4
		MC-V	89.2	2.8
		MC-IB-V	89.2	2.8
		IB-V	97.7	2.7
		AC-IB-V	100.4	2.3
		SMCP	108.1	3.1
		IMCP	105.2	2.6
Distally	Vertically	AC-MC-V	122.7	2.5
		MC-V	103.1	2.8
		MC-IB-V	97.4	2.5
		IB-V	100.4	2.1
		AC-IB-V	109.8	2.0
		SMCP	117.8	3.1
		IMCP	114.1	2.6
	Horizontally	AC-MC-Ho	108.4	3.1
		MC-Ho	93.1	2.4
		MC-IB-Ho	92.3	2.6
		IB-Ho	101.5	2.2
		AC-MC-HoP	111.2	4.4

Measurement location, JDS measurement location mesially and distally; Measurement direction, vertically and horizontally; Measurement: AC-MC-V, from the alveolar crest in the trabecular bone to the bone 2.0 mm over the MC; MC-V, in the MC region; MC-IB-V, from the trabecular bone below the MC to the superior border of the inferior cortical bone; IB-V, in the inferior cortical bone region; AC-IB-V, from the alveolar crest in the trabecular bone to the end of the inferior cortical bone; SMCP, at the superior MC peak corresponding to the border of the MC; IMCP, at the inferior MC peak corresponding to the border of the MC; AC-MC-Ho, 2.0 mm above the MC; MC-Ho, the MC region; MC-IB-Ho, the trabecular bone below the MC; IB-Ho, the inferior cortical bone region; AC-MC-HoP, 2.0 mm below the superior cortical bone of the edentulous JDS (or mathematical average of horizontal measurements in mesial and distal parts of the dentate JDS trabecular bone 2.0 mm below the superior cortical bone) when visibility of the MC superior border is poor.

Measurement values are presented as mean, SE (standard error) in relative measurement units.

3.1.5. Vertical densitometric analysis in relation to MC visibility scoring

Non-significant differences were found between the visibility analysis results of the mesial superior MC and the densitometric analysis results of the vertical mesial part ($p > 0.05$). The results provided no statistically significant differences between the distally evaluated visibility of the inferior MC part and vertical densitometric analysis results in the distal part of the JDS ($p > 0.05$). Statistically significant differences between the MC visibility scores and the vertical densitometric analysis results are provided in Table 3.1.5.1.

Table 3.1.5.1. Vertical densitometric analysis in relation to MC visibility scoring

MC part for visibility evaluation	JDS part for vertical densitometric analysis						
	AC-MC-V	MC-V	MC-IB-V	IB-V	AC-IB-V	SMCP	IMCP
Mesial inferior	–	4 (97.1 [4.2]) and 5 (81.5 [3.9]) (p = 0.01)	–	1 (111.4 [5.6]) and 5 (89.6 [4.3]) (p = 0.03), 3 (121.2 [4.2]) and 4 (98.6 [4.2]) (p = 0.02), 3 (121.2 [4.2]) and 5 (89.6 [4.3]) (p = 0.01)	3 (115.7 [7.0]) and 5 (95.1 [3.5]) (p = 0.04)	1 (122.4 [7.5]) and 5 (99.3 [4.8]) (p = 0.04), 4 (114.3 [4.1]) and 5 (99.3 [4.8]) (p = 0.02)	–
Distal superior	4 (119.7 [3.5]) and 5 (142.0 [8.5]) (p = 0.03)	–	4 (91.7 [3.7]) and 5 (110 [7.6]) (p = 0.04)	4 (95.3 [3.2]) and 5 (111.5 [2.2]) (p = 0.04)	1 (107.0 [4.5]) and 5 (124.6 [5.4]) (p = 0.04), 4 (106.9 [2.6]) and 5 (124.6 [5.4]) (p = 0.01)	–	4 (110.3 [3.4]) and 5 (127.4 [6.8]) (p = 0.04)

MC part for visibility evaluation, JDS mandibular canal visibility evaluation in mesial inferior and distal superior parts (in visibility scores: 1, 2, 3, 4, 5); JDS part for vertical densitometric analysis: JDS measurement part for vertical densitometric analysis (measurement values are presented as mean [SE (standard error)] in relative measurement units): AC-MC-V, from the alveolar crest in the trabecular bone to the bone 2.0 mm over the MC; MC-V, in the MC region; MC-IB-V, from the trabecular bone below the MC to the superior border of the inferior cortical bone; IB-V, in the inferior cortical bone region; AC-IB-V, from the alveolar crest in the trabecular bone to the end of the inferior cortical bone; SMCP, at superior MC peak corresponding to the border of MC; IMCP, at inferior MC peak corresponding to the border of MC.

Statistically significant results are presented: “visibility score (vertical densitometric analysis value [SE])” and ”visibility score (vertical densitometric analysis value [SE])” “(p value)”; “–“, no statistically significant difference.

3.1.6. Horizontal densitometric analysis in relation to MC visibility scoring

The results provided statistically non-significant differences between the visibility of the mesial superior ($p > 0.05$) as well as distal inferior MC parts ($p > 0.05$) and the horizontal densitometric analysis results of the JDS.

MC visibility evaluation results were significantly different from particular horizontal densitometric analysis results ($p < 0.05$) (Table 3.1.6.1).

Table 3.1.6.1. Horizontal densitometric analysis in relation to MC visibility scoring

MC part for visibility evaluation	JDS Part for Horizontal Densitometric Analysis		
	MC-IB-Ho	IB-Ho	AC-MC-HoP
Mesial Inferior	–	1 (113.9 [6.5]) and 5 (94.5 [3.6]) ($p = 0.04$), 3 (112.2 [5.0]) and 5 (94.5 [3.6]) ($p = 0.02$)	1 (133.9 [12.0]) and 4 (96.0 [7.2]) ($p = 0.03$)
Distal Superior	4 (85.6 [3.6]) and 5 (108.2 [9.0]) ($p = 0.02$)	3 (106.7 [3.9]) and 4 (96.4 [3.1]) ($p = 0.04$)	–

MC part for visibility evaluation, JDS mandibular canal visibility evaluation in mesial inferior and distal superior parts (visibility scores [1, 2, 3, 4, 5] in pairs); JDS Part for Horizontal Densitometric Analysis, JDS measurement part for horizontal densitometric analysis: MC-IB-Ho, the trabecular bone below the MC; IB-Ho, the inferior cortical bone region; AC-MC-HoP, 2.0 mm below the superior cortical bone of the edentulous JDS (or mathematical average of horizontal measurements in mesial and distal parts of the dentate JDS trabecular bone 2.0 mm below the superior cortical bone) when visibility of the MC superior border is poor (measurement values are presented as mean [standard error (SE)] in relative measurement units).

Statistically significant results are presented: "visibility score (horizontal densitometric analysis value [SE])" and "visibility score (horizontal densitometric analysis value [SE])" "(p value)"; "–", no statistically significant difference.

3.2. Study II

From the 639 mandibular CTs examined, 1061 mandibular lingual foramina were detected. About 20.5% of the mandible was dentate, 10.2% was full edentate, and 69.3% was partially edentate. Foramen was found at a mean distance of 18.33 ± 5.45 mm below the bony crest and 17.40 ± 7.52 mm from the mandibular border. The differences were statistically significant for men and women ($p = 0.00$ and $p = 0.03$, respectively). Distance between tooth apex and lingual artery was 10.06 ± 4.38 mm; the distance

was significantly higher in men than women ($p = 0.00$). The mean diameter of lingual foramina was 0.89 ± 0.40 mm (Table 3.2.1).

Table 3.2.1. Descriptive statistics

	Women	Men	p	Total
Distance between crest and artery mm	17.64 ± 5.27	19.30 ± 5.57	0.000*	18.33 ± 5.45
Vertical distance from mandibular border mm	16.98 ± 8.35	17.97 ± 6.15	0.034*	17.40 ± 7.52
Distance between tooth apex and artery mm	9.44 ± 4.32	10.94 ± 4.33	0.000*	10.06 ± 4.38
Vertical size (diameter) of foramen mm	0.87 ± 0.42	0.91 ± 0.37	0.086	0.89 ± 0.40

One thousand sixty-one lingual foramen on axial mandibular CT sections were examined for the following measurements in Table 1. Statistically significant differences between men and women were detected in all parameters, except vertical size of the foramen. * $p < 0.05$.

We classified the diameter of foramina as ≤ 1 and > 1 mm to determine the risk of severe haemorrhage. Of the 1061 foramina, 802 were ≤ 1 mm and 259 were > 1 mm and these numbers corresponds to the 75.6% and 24.4% of wholeforamina, respectively, where 72.5% of male patients presented with ≤ 1 mm foramina and 27.5% were > 1 mm. It was 77.9% and 22.1%, respectively, in women. The distribution of diameters in 5 different countries was shown in Table 3.2.2.

Table 3.2.2. Vertical size (diameter) of foramen

	Men				Women				Total			
	≤ 1 mm		> 1 mm		≤ 1 mm		> 1 mm		≤ 1 mm		> 1 mm	
	n	%	n	%	n	%	n	%	n	%	n	%
Cyprus	23	27.1	62	72.9	23	26.4	64	73.6	46	26.7	126	73.3
Saudi Arabia	25	59.5	17	40.5	44	91.7	4	8.3	69	76.7	21	23.3
Spain	162	91.5	15	8.5	209	91.3	20	8.7	371	91.4	35	8.6
Lithuania	29	61.7	18	38.3	61	67	30	33	90	65.2	48	34.8
Turkey	85	88.5	11	11.5	141	88.7	18	11.3	226	88.6	29	11.4
Total	324	72.5	123	27.5	478	77.9	136	22.1	802	75.6	259	24.4

The distribution of diameters in 5 different countries was shown in this table. The diameter of foramina was classified as ≤ 1 and > 1 mm to determine the risk of severe hemorrhage. Of the 1061 foramina, 75.6% were ≤ 1 mm and 24.4% were > 1 mm.

The most prevalent lingual vascular canal type was mono (1 canal), determined in 76.8% of the canals. Approximately 20% was bifid and 3.2% of canals were triple. All the canals detected as bifid and triple were at the midline area. Distributions according to genders were listed in Table 3.2.3.

Table 3.2.3. Artery Type According to Gender

	Mono	Bifid	Triple
	%	%	%
Male	78.1	18.7	3.2
Female	75.9	20.9	3.2
Total	76.8	20.0	3.2

About 43.34% of the patients have 1 lingual foramen and 56.65% have more than 1. The most prevalent artery type was monotype in men and women, in percentages of 78.1% and 75.9%, respectively. The least artery type was triple type in both the genders.

About 277 (43.34%) patients have 1 lingual foramen and 362 (56.65%) have more than 1. About 362 patients having multiple foramina presented with the foramina mostly on both the right and the left sides of mandible (60.77% bilaterally and 39.22% unilaterally).

Vascular anastomoses were detected on CT sections in 38.1% of the arteries examined. The frequency of anastomoses, which could be seen with mental foramen, anterior loop, incisive canal, and mandibular canal were as follows: 2%, 4.5%, 3.7%, and 27.9%, respectively.

Three hundred thirty-one patients (51.8%) presented with foramina only in median part of the mandible, 135 patients (21.1%) only in lateral sides, and 173 patients (27.1%) in both. Regional frequency of lingual foramina was shown in Table 3.2.4.

Table 3.2.4. Regional Frequency of Lingual Foramen

	LLC						MLC				LLC						Total
	38	37	36	35	34	33	32	31	41	42	43	44	45	46	47	48	
Teeth	38	37	36	35	34	33	32	31	41	42	43	44	45	46	47	48	
%	0.3	0.1	1.1	4.4	6.3	6.9	5.0	26.9	24.5	3.9	7.3	7.7	3.8	1.4	0.3	0.2	100

Three hundred thirty-one patients presented with foramina only in median part of the mandible, 135 patients only in lateral sides, and 173 patients in both.

The measurements were examined for MLC and LLC separately (Table 3.2.5).

Table 3.2.5. Descriptive Statistics of MLC and LLC

	Median Lingual Foramen (MLC)		p	Lateral Lingual Foramen (LLC)		p	Total		p
	Men	Women		Men	Women		MLC	LLC	
Distance between crest and artery mm	19.42 ± 5.98	17.45 ± 5.46	0.000*	19.16 ± 5.04	17.03 ± 5.03	0.008*	18.24 ± 5.75	18.43 ± 5.07	0.575
Vertical distance from mandibular border mm	18.44 ± 5.98	17.18 ± 9.93	0.086	17.46 ± 6.30	16.60 ± 5.79	0.123	17.69 ± 8.58	16.99 ± 6.04	0.136
Distance between tooth apex and artery mm	11.62 ± 4.13	9.41 ± 3.81	0.000*	9.96 ± 4.42	9.62 ± 5.10	0.508	10.30 ± 4.09	9.77 ± 4.81	0.075
Vertical size (diameter) of foramen mm	0.95 ± 0.40	0.90 ± 0.47	0.187	0.87 ± 0.32	0.82 ± 0.35	0.113	0.92 ± 0.44	0.84 ± 0.34	0.002*

The only significant difference between MLC and LLC was detected in diameter of foramen; MLC was significantly larger than LLC. * $p < 0.05$.

Diameters of foramen were statistically larger in MLC ($p = 0.00$, $p = 0.00$, respectively). When MLC and LLC were examined according to gender, lingual foramina were found closer to alveolar crest and tooth apex in women on the median part of mandible ($p = 0.00$ for both distance between crest and artery, apex to artery). On the lateral part of the mandible, only distance between crest and artery was larger in men ($p = 0.01$).

The older the patients were, the shorter the vertical distance from mandibular border and distance between crest and foramen ($r = -0.178$, $p = 0.00$; $r = -0.242$, $p = 0.00$, respectively). Age was also negatively correlated with diameter of foramen ($r = -0.188$, $p = 0.00$). Vertical distance from mandibular border and distance between crest and foramen were positively correlated to each other ($r = 0.702$, $p = 0.00$). The distance from tooth apex to foramen was positively correlated with both vertical distance from mandibular border and distance between crest and foramen ($r = 0.340$, $p = 0.00$; $r = 0.559$, $p = 0.00$, respectively).

3.3. Study III

3.3.1. The subgroup of single tooth loss

Retrospective evaluation of the scans was conducted with CT images of 597 patients. The scans having single edentulism was evaluated as separate samples. The distribution of the centers, age and tooth regions are shown in Table 3.3.1.1.

Table 3.3.1.1. *Distribution of centers, age and tooth regions according to gender*

Center/Age/Area	Female	Male	Total
Cyprus, n (%)	31 (10.9)	53 (17.0)	84 (14.1)
Turkey, n (%)	41 (14.4)	46 (14.7)	87 (14.6)
Lithuania, n (%)	40 (14.0)	27 (8.7)	67 (11.2)
Spain, n (%)	102 (35.8)	112 (35.9)	214 (35.8)
University of Illinois (USA), n (%)	31 (10.9)	43 (13.8)	74 (12.4)
University of Michigan (USA), n (%)	40 (14.0)	31 (9.9)	71 (11.9)
Total, n (%)	285 (100)	312 (100)	597 (100)
Age, Mean \pm SD (Min-Max)	50.34 \pm 12.35 (20–84)	50.60 \pm 12.94 (18–79)	50.48 \pm 12.65 (18–84)
Area			
1 st premolar, n (%)	26 (9.1)	25 (8.0)	51 (8.5)
2 nd premolar, n (%)	85 (29.7)	51 (16.4)	136 (22.8)
1 st molar, n (%)	127 (44.4)	180 (57.9)	307 (51.4)
2 nd molar, n (%)	48 (16.8)	55 (17.7)	103 (17.3)
Total, n (%)	286 (100)	311 (100)	597 (100)

SD: Standard Deviation, Min: Minimum value, Max: Maximum value.

Main part of the scans belonged to Spain (35.8%) and other centers evaluated same percent of images (between 11.2% and 14.6%). The mean age of the participants was 50.48 ± 12.65 and male or female patients did not reveal different mean values ($p > 0.05$). The distribution of single tooth loss regions was also similar and single edentulism was predominantly detected at first molar area (51.4%).

Variables and their comparisons associated with membrane, dimensions, ostium, septa and relations of the sinus are given in Table 3.3.1.2.

Table 3.3.1.2. Variables associated with sinus membrane, dimensions, ostium, septa and relations

	Variable	Female	Male	Total	p value
Membrane	<i>Sinus membrane morphology (SMM)</i>				
	no thickening = 1, n (%)	167 (58.6)	152 (48.7)	319 (53.4)	0.059
	flat = 2, n (%)	46 (16.1)	73 (23.4)	119 (19.9)	
	semispherical = 3, n (%)	31 (10.9)	44 (14.1)	75 (12.6)	
	mucocoele-like = 4, n (%)	20 (7.0)	16 (5.1)	36 (6.0)	
	flat+semispherical = 5, n (%)	21 (7.4)	27 (8.7)	48 (8.0)	
	Total, n (%)	285 (100)	312 (100)	597 (100)	
	Sinus membrane thickness (dentate) (SMT-D)	3.45 ± 4.07 (0–28.9)	3.95 ± 4.99 (0–29.6)	3.73 ± 4.60 (0–29.6)	0.167
	Sinus membrane thickness (edentate) (SMT-E)	3.90 ± 5.11 (0–39.2)	4.19 ± 6.05 (0–36.3)	4.06 ± 5.65 (0–39.2)	0.163
	<i>Sinus membrane thickness classification (SMT-Class)</i>				
	0–5 mm = 1, n (%)	214 (75.1) ^a	240 (77.2) ^a	454 (76.2)	0.021
	5–10 mm = 2, n (%)	50 (17.5) ^a	33 (10.6) ^b	83 (13.9)	
	10–15 mm = 3, n (%)	10 (3.5) ^a	24 (7.7) ^b	34 (5.7)	
	15–20 mm = 4, n (%)	4 (1.4) ^a	2 (0.6) ^a	6 (1.0)	
	>20 mm = 5, n (%)	7 (2.5) ^a	12 (3.9) ^a	19 (3.2)	
	Total, n (%)	285 (100)	311 (100)	596 (100)	
	<i>Sinus membrane thickening (SM-Thickening)</i>				
no thickening = 1, n (%)	173 (60.9) ^a	156 (50.2) ^b	329 (55.3)	0.013	
rounded = 2, n (%)	34 (12.0) ^a	51 (16.4) ^a	85 (14.3)		
Irregular = 3, n (%)	38 (13.4) ^a	68 (21.9) ^b	106 (17.8)		
circumferential thickening = 4, n (%)	25 (8.8) ^a	27 (8.7) ^a	52 (8.7)		
complete thickening = 5, n (%)	14 (4.9) ^a	9 (2.9) ^a	23 (3.9)		
Total, n (%)	284 (100)	311 (100)	595 (100)		
Dimensions	<i>Sinus width (SW)</i>				
	at 5 th mm	11.12 ± 7.71 (0.00–37.42)	11.21 ± 7.71 (0.00–38.07)	11.17 ± 7.70 (0.00–38.07)	0.913
	at 7 th mm	12.89 ± 7.92 (0.00–8.44)	12.16 ± 7.60 (0.00–38.80)	12.49 ± 7.75 (0.00–38.80)	0.359
	at 10 th mm	13.75 ± 8.25 (0.00–42.07)	13.91 ± 7.39 (0.00–40.05)	13.84 ± 7.79 (0.00–42.07)	0.822
	at 13 th mm	15.40 ± 7.85 (2.40–39.30)	15.68 ± 7.25 (0.00–40.72)	15.55 ± 7.53 (0.00–40.72)	0.669

Table 3.3.1.2. Continued

	Variable	Female	Male	Total	p value
Dimensions (continued)	at 15 th mm	16.48 ± 8.06 (2.40–41.29)	16.78 ± 7.34 (0.00–41.66)	16.64 ± 7.68 (0.00–41.66)	0.642
	Mean	13.41 ± 7.20 (1.66–39.31)	13.51 ± 6.68 (0.00–39.76)	13.46 ± 6.92 (0.00–39.76)	0.859
	<i>Sinus augmentation classification (SA-Class-1)</i>				
	narrow = 1, n (%)	82 (31.2) ^a	58 (21.0) ^b	140 (26.0)	0.026
	average = 2, n (%)	98 (37.3) ^a	121 (43.8) ^a	219 (40.6)	
	wide = 3, n (%)	83 (31.6) ^a	97 (35.1) ^a	180 (33.4)	
	Total, n (%)	263 (100)	276 (100)	539 (100)	
Ostium	<i>Ostium pattern (OP)</i>				
	patent = 1, n (%)	226 (86.3)	261 (90.3)	487 (88.4)	0.138
	obstructed = 2, n (%)	36 (13.7)	28 (9.7)	64 (11.6)	
	Total, n (%)	262 (100)	289 (100)	551 (100)	
Septa	<i>Number of septa (NS)</i>				
	anterior of zyg process	0.35 ± 0.55 (0–2)	0.29 ± 0.55 (0–3)	0.32 ± 0.55 (0–3)	0.203
	posterior of zyg process	0.15 ± 0.38 (0–2)	0.16 ± 0.39 (0–3)	0.16 ± 0.39 (0–3)	0.630
	Anterior septa height (SH-A)	6.54 ± 3.77 (1.24–20.43)	6.37 ± 3.75 (1.09–27.63)	6.46 ± 3.75 (1.09–27.63)	0.775
	Posterior septa height (SH-P)	5.85 ± 3.46 (1.31–14.00)	4.36 ± 1.90 (1.35–8.12)	5.12 ± 2.88 (1.31–14.00)	0.076
	<i>Septa classification (S-Class)</i>				
	anterior single septum = 1, n (%)	51 (52.6)	43 (49.4)	94 (51.1)	0.082
	posterior single septum = 1, n (%)	28 (28.9)	36 (41.4)	64 (34.8)	
	anterior/posterior multiple septa = 2, n (%)	18 (18.6)	8 (9.2)	26 (14.1)	
	Total, n (%)	97 (100)	87 (100)	184 (100)	
Relations	<i>Sinus relation to (S-Relation)</i>				
	nothing = 1, n (%)	248 (87.0)	266 (85.3)	514 (86.1)	0.421
	periapical lesion = 2, n (%)	15 (5.3)	26 (8.3)	41 (6.9)	
	bone graft = 3, n (%)	1 (0.4)	4 (1.3)	5 (0.8)	
	implant fenestration = 4, n (%)	2 (0.7)	2 (0.6)	4 (0.7)	
	tooth extraction = 5, n (%)	12 (4.2)	9 (2.9)	21 (3.5)	

Table 3.3.1.2. Continued

Variable		Female	Male	Total	p value
Relations (continued)	bone graft+implant = 6, n (%)	3 (1.1)	4 (1.3)	7 (1.2)	
	endodontic filling material = 7, n (%)	2 (0.7)	1 (0.3)	3 (0.5)	
	foreign body = 8, n (%)	2 (0.7)	0 (0.0)	2 (0.3)	
	Total, n (%)	285 (100)	312 (100)	597 (100)	

^{a, b} – different superscripts indicate statistically different column proportions ($p < 0.05$) according to the Bonferroni adjusted z test for proportions; Quantitative variables were shown as Mean \pm SD (min-max); Qualitative variables were shown as n (%); Bold numbers indicate statistically significant differences.

Sinus membrane was evaluated with the variables regarding to membrane morphology and thickness. The membrane morphology did not show significant difference between male and female patients ($p > 0.05$). However, although millimetric thickness values were similar, the number of membranes demonstrating 5–10 mm thickness was higher ($p = 0.021$) whereas irregular thickening was significantly lower ($p = 0.013$) at female patients.

The dimensions of the sinus space were analyzed by using width measurements and augmentation class scores. Mean sinus width was 11.17 ± 7.70 for total study sample and as expected, gradually increased at higher millimeters. However, no intersexual difference was determined ($p > 0.05$) for this variable. On the other hand, according to augmentation classification scores, narrow sinus frequency was statistically higher at female patients ($p = 0.026$). The ostium of the patients was mostly patent (88.4% vs. 11.6%) and gender did not influence its pattern ($p > 0.05$).

Approximately, one-third of the patients had at least one sinus septum at the anterior of the zygomatic process and mean height of their septa was 6.46 ± 3.75 . The prevalence of septum at the posterior of the zygomatic process was around 16% and mean height these septa was relatively lower (5.12 ± 2.88 mm) compared to their anteriorly located counterparts. Septa classification scores also supported these findings and according to whole septa evaluation variables, gender did not affect the number and location of the septa ($p > 0.05$).

When the relationship between maxillary sinus and surrounding factors/materials including periapical lesion, bone graft, dental implant, endodontic materials and foreign bodies was considered, 86.1% of the patients did not show any kind of these contacts. The mostly encountered factor was repor-

ted as the presence of periapical lesion around the edentulous area (6.9%) and for all, no intersexual effect was detected ($p > 0.05$).

Variables associated with the height and width of the alveolar ridge was presented in Table 3.3.1.3.

Table 3.3.1.3. Variables associated with alveolar ridge

	Variable	Female	Male	Total	p value
Height	Alveolar bone height (edantate) (ABH-E)	7.90 ± 4.48 (0–1.3)	7.29 ± 4.67 (0.5–23.1)	7.58 ± 4.58 (0–23.1)	0.131
	<i>Edentulous site classification (ES-Class)</i>				
	< 4 mm = 1, n (%)	55 (19.5%)	75 (24.4%)	130 (22.0%)	0.186
	4 mm ≤ x < 7 mm = 2, n (%)	94 (33.3%)	109 (35.4%)	203 (34.4%)	
	7 mm ≤ x < 10 mm = 3, n (%)	133 (47.2%)	124 (40.3%)	257 (43.6%)	
	Total, n (%)	282 (100%)	308 (100%)	590 (100%)	
	<i>Sinus augmentation classification (SA-Class-2)</i>				
	abundant bone-1, n (%)	42 (14.8%)	32 (10.3%)	74 (12.4%)	0.064
	abundant bone-2, n (%)	46 (16.2%)	35 (11.3%)	81 (13.6%)	
	barely sufficient bone-1, n (%)	42 (14.8%)	36 (11.6%)	78 (13.1%)	
	barely sufficient bone-2, n (%)	62 (21.8%)	81 (26.0%)	143 (24.0%)	
	compromised bone-1, n (%)	34 (12.0%)	43 (13.8%)	77 (12.9%)	
	compromised bone-2, n (%)	58 (20.4%)	84 (27.0%)	142 (23.9%)	
	Total, n (%)	284 (100%)	311 (100%)	595 (100%)	
Distance from root tip to sinus floor (RT-SF)	3.14 ± 2.69 (0.00–12.20)	2.84 ± 2.68 (0.00–13.55)	2.98 ± 2.68 (0.00–13.55)	0.171	
Width	<i>Ridge width (RW)</i>				
	coronal	6.90 ± 2.44 (1.55–14.11)	7.47 ± 3.00 (2.30–17.22)	7.20 ± 2.76 (1.55–17.22)	0.011
	middle	9.04 ± 2.45 (2.00–16.21)	9.66 ± 2.82 (2.00–18.03)	9.35 ± 2.66 (2.00–18.03)	0.006
	apical	10.86 ± 2.53 (3.24–21.73)	11.59 ± 2.93 (3.80–24.09)	11.23 ± 2.76 (3.24–24.09)	0.003
	Mean	8.94 ± 2.17 (2.40–16.39)	9.69 ± 2.49 (2.97–16.85)	9.33 ± 2.37 (2.40–16.85)	<0.001

Quantitative variables were shown as Mean ± SD (min-max); Qualitative variables were shown as n (%); Bold numbers indicate statistically significant differences.

From these variables, only ridge width showed significant difference between genders and accordingly, male patients had thicker residual ridge

anatomies compared to females ($p < 0.001$). The difference was valid at all coronal ($p = 0.011$), middle ($p = 0.006$) and apical ($p = 0.003$) levels. On the contrary, ridge height parameters involving alveolar bone height and classifications of edentulous site and sinus augmentation did not reveal any significant differences in terms of gender ($p > 0.05$). Mean alveolar bone height was 7.58 ± 4.58 most of the patients exhibited barely sufficient or compromised bone amounts in their edentulous areas.

Table 3.3.1.4 shows the variables associated with PSAA and adjacent tooth root(s).

Table 3.3.1.4. Variables associated with PSAA and adjacent roots

Variable		Female	Male	Total	p value
Location	<i>PSAA location (PSAA-L)</i>				
	no PSAA = 1, n (%)	151 (54.9)	135 (45.8)	286 (50.2)	0.101
	intra-osseous = 2, n (%)	72 (26.2)	100 (33.9)	172 (30.2)	
	below sinus membrane = 3, n (%)	47 (17.1)	57 (19.3)	104 (18.2)	
	on the outer cortex of sinus wall = 4, n (%)	5 (1.8)	3 (1.0)	8 (1.4)	
	Total, n (%)	275 (100)	295 (100)	570 (100)	
Diameter	<i>PSAA diameter (PSAA-D)</i>				
	no PSAA = 1, n (%)	111 (50.5)	90 (40.0)	201 (45.2)	0.160
	< 1 mm = 2, n (%)	59 (26.8)	70 (31.1)	129 (29.0)	
	1–2 mm = 3, n (%)	49 (22.3)	63 (28.0)	112 (25.2)	
	≥ 2 mm = 4, n (%)	1 (0.5)	2 (0.9)	3 (0.7)	
	Total, n (%)	220 (100)	225 (100)	445 (100)	
Bone	PSAA to alveolar ridge (PSAA-ALV)	13.92 ± 6.19 (0–30.7)	14.35 ± 5.66 (0–29.7)	14.15 ± 5.91 (0–30.7)	0.519
	Buccal bone thickness above PSAA (PSAA-BBT)	1.22 ± 0.93 (0.00–5.5)	1.39 ± 0.88 (0.00–5.2)	1.31 ± 0.90 (0.00–5.5)	0.120
Length & Vitality	Root length (RL)	12.31 ± 2.15 (7.00–16.84)	12.27 ± 2.37 (7.00–18.79)	12.29 ± 2.27 (7.00–18.79)	0.823
	<i>Neighbouring tooth vitality (VIT)</i>				
	both vital = 1, n (%)	185 (65.4)	223 (71.7)	408 (68.7)	0.329
	mesial vital = 2, n (%)	26 (9.2)	28 (9.0)	54 (9.1)	
	distal vital = 3, n (%)	54 (19.1)	44 (14.1)	98 (16.5)	
	both devital = 4, n (%)	18 (6.4)	16 (5.1)	34 (5.7)	
	Total, n (%)	283 (100)	311 (100)	594 (100)	

Quantitative variables were shown as Mean ± SD (min-max). Qualitative variables were shown as n (%).

Nearly, half of the patients (50.2%) did not demonstrate any PSAA view at their sagittal cross-sections. Visible PSAA images were predominantly located at intra-osseous region (30.2%) or below (18.2%) the sinus membrane. Mean diameter of the arteries was < 1 mm or between 1 and 2 mm. Mean distance from PSAA to alveolar ridge was 14.15 ± 5.91 mm and the bone thickness above PSAA was 1.31 ± 0.90 mm. When the neighboring teeth were evaluated, their mean root length was 12.29 ± 2.27 mm and 68.7% of these roots are endodontically vital. From the gender perspective, no statistically difference was detected for the PSAA and adjacent root related variables ($p > 0.05$).

In the correlation analysis, only the correlations greater or equal to 0.05 were defined as “clinically meaningful correlation”; because very weak and clinically unimportant correlations tend to be statistically significant due to the high sample size. Accordingly, most of the sinus related variables including sinus membrane thickness, sinus membrane morphology, sinus membrane thickness classification, sinus membrane thickening exhibited significant correlations within themselves. Many of the variables representing the alveolar bone height (alveolar bone height at edentulous area, sinus augmentation class, distance between root-tip sinus floor, edentulous site classification) also showed significant correlations among each other. Moreover, posterior sinus septa height was correlated with number of septa and alveolar bone height at edentulous site. PSAA diameter and localization were also correlated between each other.

3.3.2. The subgroup of multiple teeth loss

1190 regions pertaining to CT scans of 518 patients were retrospectively evaluated in the study. Each edentulous tooth region was separately analyzed. The distribution of the centers, age and edentulous regions are given in Table 3.3.2.1.

Table 3.3.2.1. *Distribution of centers, age and tooth regions according to gender*

Center/Age/Area	Female	Male	Total
Cyprus, n (%)	48 (18.0)	68 (27.1)	116 (22.4)
Turkey, n (%)	68 (25.5)	45 (17.9)	113 (21.8)
Lithuania, n (%)	19 (7.1)	14 (5.6)	33 (6.4)
Spain, n (%)	78 (29.2)	75 (29.9)	153 (29.5)
University of Illinois (USA), n (%)	37 (13.9)	35 (13.9)	72 (13.9)
University of Michigan (USA), n (%)	17 (6.4)	14 (5.6)	31 (6.0)
Total, n (%)	267 (100)	251 (100)	518 (100)

Table 3.3.2.1. Continued

Center/Age/Area	Female	Male	Total
Age, Mean \pm SD (Min-Max)	52.36 \pm 12.53 (21–90)	51.77 \pm 11.53 (23–77)	52.06 \pm 12.02 (21–90)
<i>Area</i>			
1 st premolar, n (%)	75 (12.6)	69 (11.6)	144 (12.1)
2 nd premolar, n (%)	194 (32.6)	122 (20.5)	316 (26.6)
1 st molar, n (%)	185 (31.1)	241 (40.5)	426 (35.8)
2 nd molar, n (%)	141 (23.7)	163 (27.4)	304 (25.5)
Total, n (%)	595 (100)	595 (100)	1190 (100)

SD: Standard Deviation, Min: Minimum value, Max: Maximum value.

The mean age of the participants was 52.06 \pm 12.02. The distribution of edentulous areas was similar at female and male patients and first molar was the most frequently missing tooth (35.8%).

Comparison of the parameters regarding to sinus membrane, dimensions, ostium pattern, septa and surrounding factors/materials are shown in Table 3.3.2.2.

Table 3.3.2.2. Variables associated with sinus membrane, dimensions, ostium, septa and relations

Variable	Female	Male	Total	p value
<i>Sinus membrane morphology (SMM)</i>				
no thickening = 1, n (%)	169 (63.5) ^a	132 (52.5) ^b	301 (58.2)	0.005
flat = 2, n (%)	43 (16.2) ^a	57 (22.7) ^a	100 (19.3)	
semispherical = 3, n (%)	34 (12.8) ^a	28 (11.2) ^a	62 (12)	
mucocoele-like = 4, n (%)	2 (0.8) ^a	13 (5.2) ^b	15 (2.9)	
flat+semispherical = 5, n (%)	18 (6.8) ^a	21 (8.4) ^a	39 (7.5)	
Total, n (%)	266 (100)	251 (100)	517 (100)	
Sinus membrane thickness (dentate) (SMT-D)	2.83 \pm 3.53 (0–20)	4.13 \pm 5.52 (0–31.6)	3.47 \pm 4.66 (0–31.6)	
Sinus membrane thickness (edentate) (SMT-E)	3.30 \pm 4.60 (0–30)	4.71 \pm 6.66 (0–33.2)	3.98 \pm 5.73 (0–33.2)	0.006
<i>Sinus membrane thickness classification (SMT-Class)</i>				
0–5 mm = 1, n (%)	200 (75.5)	184 (73.3)	384 (74.4)	0.202
5–10 mm = 2, n (%)	40 (15.1)	28 (11.2)	68 (13.2)	
10–15 mm = 3, n (%)	9 (3.4)	11 (4.4)	20 (3.9)	
15–20 mm = 4, n (%)	5 (1.9)	10 (4.0)	15 (2.9)	

Table 3.3.2.2. Continued

	Variable	Female	Male	Total	p value
Membrane (continued)	>20 mm = 5, n (%)	11 (4.2)	18 (7.2)	29 (5.6)	
	Total, n (%)	265 (100)	251 (100)	516 (100)	
	<i>Sinus membrane thickening (SM-Thickening)</i>				
	no thickening = 1, n (%)	164 (61.9)	128 (51.0)	292 (56.6)	0.053
	rounded = 2, n (%)	31 (11.7)	43 (17.1)	74 (14.3)	
	irregular = 3, n (%)	38 (14.3)	37 (14.7)	75 (14.5)	
	circumferential thickening = 4, n (%)	24 (9.1)	26 (10.4)	50 (9.7)	
	complete thickening = 5, n (%)	8 (3.0)	17 (6.8)	25 (4.8)	
	Total, n (%)	265 (100)	251 (100)	516 (100)	
<i>Sinus width (SW)</i>					
Dimensions	at 5 th mm	3.51 ± 3.30 (0.0–19.5)	3.78 ± 3.36 (0.0–17.1)	3.64 ± 3.33 (0.0–19.5)	0.403
	at 7 th mm	4.45 ± 3.72 (0.0–20.2)	4.72 ± 3.54 (0.0–17.3)	4.58 ± 3.63 (0.0–20.2)	0.437
	at 10 th mm	5.75 ± 3.86 (0.0–21.0)	6.00 ± 3.70 (0.0–17.9)	5.87 ± 3.78 (0.0–21.0)	0.472
	at 13 th mm	6.96 ± 4.03 (0.0–21.9)	7.11 ± 3.68 (0.0–19.3)	7.03 ± 3.86 (0.0–21.9)	0.684
	at 15 th mm	7.85 ± 4.27 (0.0–22.3)	7.92 ± 3.80 (0.0–19.8)	7.89 ± 4.04 (0.0–22.3)	0.852
	Mean	10.88 ± 6.27 (0–42.0)	11.68 ± 6.11 (0–36.3)	11.27 ± 6.20 (0–42.0)	0.151
	<i>Sinus augmentation classification (SA-Class-1)</i>				
	narrow = 1, n (%)	30 (19.1)	19 (12.5)	49 (15.9)	0.230
	average = 2, n (%)	57 (36.3)	65 (42.8)	122 (39.5)	
	wide = 3, n (%)	70 (44.6)	68 (44.7)	138 (44.7)	
	Total, n (%)	157 (100)	152 (100)	309 (100)	
	<i>Ostium pattern (OP)</i>				
Ostium	patent = 1, n (%)	235 (91.4)	212 (86.9)	447 (89.2)	0.100
	obstructed = 2, n (%)	22 (8.6)	32 (13.1)	54 (10.8)	
	Total, n (%)	257 (100)	244 (100)	501 (100)	

Table 3.3.2.2. Continued

	Variable	Female	Male	Total	p value
Septa	<i>Number of septa (NS)</i>				
	anterior of zyg process	0.28 ± 0.58 (0–3)	0.35 ± 0.52 (0–2)	0.32 ± 0.55 (0–3)	0.187
	posterior of zyg process	0.15 ± 0.37 (0–2)	0.16 ± 0.38 (0–2)	0.15 ± 0.37 (0–2)	0.748
	Anterior septa height (SH-A)	7.06 ± 3.53 (2.1–22.0)	9.18 ± 5.64 (1.4–22.0)	8.38 ± 5.04 (1.4–22.0)	<0.001
	Posterior septa height (SH-P)	5.36 ± 2.27 (1.5–8.3)	6.87 ± 5.19 (1.0–24.7)	6.12 ± 4.02 (1.0–24.7)	0.068
	<i>Septa classification (S-Class)</i>				
	anterior single septum = 1, n (%)	30 (44.8)	62 (60.8)	92 (54.4)	0.159
	posterior single septum = 1, n (%)	26 (38.8)	28 (27.5)	54 (32.0)	
	anterior/posterior multiple septa = 2, n (%)	11 (16.4)	11 (10.8)	22 (13.0)	
	Total, n (%)	67 (100)	102 (100)	169 (100)	
Relations	<i>Sinus relation to (S-Relation)</i>				
	nothing = 1, n (%)	222 (83.5) ^a	210 (83.7) ^a	432 (83.6)	0.010
	periapical lesion = 2, n (%)	23 (8.6) ^a	7 (2.8) ^b	30 (5.8)	
	bone graft = 3, n (%)	2 (0.8) ^a	3 (1.2) ^a	5 (1.0)	
	implant fenestration = 4, n (%)	0 (0.0) ^a	0 (0.0) ^a	0 (0.0)	
	tooth extraction = 5, n (%)	17 (6.4) ^a	26 (10.4) ^a	43 (8.3)	
	bone graft+implant = 6, n (%)	0 (0.0) ^a	1 (0.4) ^a	1 (0.2)	
	endodontic filling material = 7, n (%)	2 (0.8) ^a	1 (0.4) ^a	3 (0.6)	
	foreign body = 8, n (%)	0 (0.0) ^a	3 (1.2) ^a	3 (0.6)	
	Total, n (%)	266 (100)	251 (100)	517 (100)	

^{a, b} – different superscripts indicate statistically different column proportions ($p < 0.05$) according to the Bonferroni adjusted z test for proportions; Quantitative variables were shown as Mean ± SD (min-max); Qualitative variables were shown as n (%); Bold numbers indicate statistically significant differences.

No (58.2%) or flat (19.3%) thickening morphology was detected at most of the sinus membranes. More tendencies were seen at male patients to membrane thickening and mucocele-like morphology was more prevalent for this gender ($p = 0.005$). Although sinus membrane thickness classifica-

tion scores did not show intersexual difference ($p > 0.05$), membrane thickness measurements also supported this issue ($p = 0.003$ and $p = 0.006$).

Sinus dimensions were determined with sinus width and sinus augmentation class measurements. Mean sinus width was relatively low (3.64 ± 3.33 mm) at 5 mm level and showed an expected increase towards upper levels. Most of the sinus spaces were dimensionally average (39.5%) or wide (44.7%) and no effect of gender was observed in terms of sinus dimensions ($p > 0.05$). Ostium was patent at 89.2% of the patients no gender did not influence its values ($p > 0.05$) (Table 3.3.2.2).

Nearly, one-third of the patients revealed at least one sinus septum at the anterior of the zygomatic process and mean height of their septa was 7.06 ± 3.53 . However, its prevalence decreased to 15% at the posterior of the process and mean height of these septa was 5.36 ± 2.27 mm. Anterior septa height was significantly higher at male patients ($p < 0.001$). Septa classification scores also supported these results gender did not affect classification scores ($p > 0.05$) (Table 3.3.2.2).

Despite high amount of patients demonstrating no relationship between maxillary sinus and surrounding factors/materials (83.6%), presence of tooth extraction (8.3%) and periapical lesion (5.8%) were the mostly encountered conditions and number of female patients demonstrating an adjacent periapical lesion was significantly higher than male patients ($p = 0.010$) (Table 3.3.2.2).

The variables regarding to alveolar bone dimensions are shown in Table 3.3.2.3.

Table 3.3.2.3. Variables associated with alveolar ridge

Variable		Female	Male	Total	p value
Height	Alveolar bone height (edantate) (ABH-E)	7.52 ± 4.75 (0–26.0)	6.73 ± 3.90 (1–24.2)	7.13 ± 4.37 (0–26.0)	0.041
	<i>Edentulous site classification (ES-Class)</i>				
	< 4 mm = 1, n (%)	81 (31.3) ^a	91 (36.8) ^a	172 (34.0)	0.010
	4 mm ≤ x < 7 mm = 2, n (%)	75 (29.0) ^a	89 (36.0) ^a	164 (32.4)	
	7 mm ≤ x < 10 mm = 3, n (%)	103 (39.8) ^a	67 (27.1) ^b	170 (33.6)	
	Total, n (%)	259 (100)	247 (100)	506 (100)	
	<i>Sinus augmentation classification (SA-Class-2)</i>				
	abundant bone-1, n (%)	29 (11.6) ^a	16 (7.0) ^a	45 (9.4)	0.015
	abundant bone-2, n (%)	38 (15.2) ^a	23 (10.1) ^a	61 (12.8)	
	barely sufficient bone-1, n (%)	23 (9.2) ^a	12 (5.3) ^a	35 (7.3)	
	barely sufficient bone-2, n (%)	51 (20.4) ^a	49 (21.5) ^a	100 (20.9)	

Table 3.3.2.3. Continued

Variable		Female	Male	Total	p value
Height (continued)	compromised bone-1, n (%)	31 (12.4) ^a	25 (11.0) ^a	56 (11.7)	
	compromised bone-2, n (%)	78 (31.2) ^a	103 (45.2) ^b	181 (37.9)	
	Total, n (%)	250 (100)	228 (100%)	478 (100)	
	Distance from root tip to sinus floor (RT-SF)	4.23 ± 3.66 (0–15.6)	3.69 ± 3.23 (0–13.7)	3.96 ± 3.46 (0–15.6)	0.103
Width	<i>Ridge width (RW)</i>				
	coronal	3.33 ± 1.47 (0.8–8.5)	3.41 ± 1.49 (0.7–9.9)	3.37 ± 1.47 (0.7–9.9)	0.531
	middle	4.06 ± 1.81 (0.9–10.5)	4.30 ± 1.89 (1.5–10.1)	4.18 ± 1.85 (0.9–10.5)	0.157
	apical	5.27 ± 2.17 (1.1–13.4)	5.11 ± 2.23 (1.5–15.6)	5.19 ± 2.20 (1.1–15.6)	0.448
	Mean	7.99 ± 2.23 (2.5–15.2)	8.34 ± 2.07 (3.8–15.1)	8.16 ± 2.16 (2.5–15.2)	0.066

^{a, b} – different superscripts indicate statistically different column proportions ($p < 0.05$) according to the Bonferroni adjusted z test for proportions; Quantitative variables were shown as Mean ± SD (min-max); Qualitative variables were shown as n (%); Bold numbers indicate statistically significant differences.

Mean alveolar bone height was 7.13 ± 4.37 mm and except the distance from adjacent root tip to above sinus floor, all variables related to increased alveolar bone height were significantly different for male and female patients (higher for female patients, $p = 0.041$, $p = 0.010$). Accordingly, most of the patients had compromised bone (37.9%) and the rate of this type of bone was significantly higher at male patients ($p = 0.015$). On the other hand, ridge width was clinically narrow (3.37 ± 1.47 mm) and expectedly increased towards the apical region. However, no gender-related difference was detected for this variable ($p > 0.05$).

When PSAA was considered, 63.0% of the patients did not reveal PSAA in their cross-sections and most of the PSAA visible images showed intraosseous alignment of the artery. Moreover, significant effect of the gender was observed to the presence and location of PSAA. While it was less visible in female patients, showed a tendency of intraosseous localization in male patients ($p = 0.001$). When present, the diameter of PSAA did not go beyond 2 mm and also did not be influenced by gender ($p > 0.05$). The mean length of the neighbouring teeth to the edentulous area was around 13 mm and they were rarely devital. While root length values were similar at different genders, only the number of devital teeth at distal

neighboring area was significantly higher at male patient group ($p = 0.038$) (Table 3.3.2.4).

Table 3.3.2.4. Variables associated with PSAA and neighbouring teeth

Variable		Female	Male	Total	p value
Location	<i>PSAA location (PSAA-L)</i>				
	no PSAA = 1, n (%)	169 (68.4) ^a	133 (57.3) ^b	302 (63.0)	0.001
	intra-osseous = 2, n (%)	42 (17.0) ^a	71 (30.6) ^b	113 (23.6)	
	below sinus membrane = 3, n (%)	34 (13.8) ^a	22 (9.5) ^a	56 (11.7)	
	on the outer cortex of sinus wall = 4, n (%)	2 (0.8) ^a	6 (2.6) ^a	8 (1.7)	
	Total, n (%)	247 (100)	232 (100)	479 (100)	
Diameter	<i>PSAA diameter (PSAA-D)</i>				
	no PSAA = 1, n (%)	58 (45.3)	55 (38.7)	113 (41.9)	0.533
	< 1 mm = 2, n (%)	44 (34.4)	57 (40.1)	101 (37.4)	
	1–2 mm = 3, n (%)	26 (20.3)	29 (20.4)	55 (20.4)	
	≥ 2 mm = 4, n (%)	0 (0)	1 (0.7)	1 (0.4)	
	Total, n (%)	128 (100)	142 (100)	270 (100)	
Bone	PSAA to alveolar ridge (PSAA-ALV)	14.46 ± 5.34 (0–24.7)	14.26 ± 4.72 (0–24.3)	14.35 ± 4.99 (0–24.7)	0.792
	Buccal bone thickness above PSAA (PSAA-BBT)	1.15 ± 0.65 (0–3.8)	1.32 ± 0.87 (0–4)	1.24 ± 0.78 (0–4)	0.162
Length & Vitality	Root length (RL)	12.71 ± 2.62 (6.0–20.0)	13.21 ± 3.05 (6.0–20.7)	12.96 ± 2.85 (6.0–20.7)	0.066
	<i>Neighbouring teeth vitality (VIT)</i>				
	both vital = 1, n (%)	128 (58.2) ^a	145 (66.5) ^a	273 (62.3)	0.038
	mesial vital = 2, n (%)	23 (10.5) ^a	10 (4.6) ^b	33 (7.5)	
	distal vital = 3, n (%)	58 (26.4) ^a	58 (26.6) ^a	116 (26.5)	
	both devital = 4, n (%)	11 (5) ^a	5 (2.3) ^a	16 (3.7)	
Total, n (%)	220 (100)	218 (100)	438 (100)		

^{a, b} – different superscripts indicate statistically different column proportions ($p < 0.05$) according to the Bonferroni adjusted z test for proportions; Quantitative variables were shown as Mean ± SD (min-max); Qualitative variables were shown as n (%); Bold numbers indicate statistically significant differences.

The correlations greater or equal to 0.05 were defined as “clinically meaningful correlation”; because very weak and clinically unimportant correlations tend to be statistically significant due to the high sample size. The

sinus related variables associated with thickness and morphology exhibited significant correlations within themselves. The variables representing the anatomy of edentulous ridge (alveolar bone height, sinus augmentation classification and edentulous site classification) also showed significant correlations among each other. Further, sinus septa height at posterior of the zygomatic process was correlated with sinus membrane thickness, sinus membrane thickness classification and bone thickness on the buccal surface of PSAA values. PSAA localization was also correlated with its diameter values.

3.4. Study IV

Classification system of the jaw bone anatomy in endosseous dental implant treatment and assessments

New classification system of the jaw bone anatomy in endosseous dental implant treatment is suggested taking into consideration previous Juodzbalys and Raustia [27] classification and literature review results (Fig. 1.5.1, 1.5.2 and Table 1.5.1 in Chapter 1.5).

Surgical dental implant installation requires understanding of associated anatomical structures. Planning should be done on three-dimensional edentulous jaw segment (EJS) pattern (Fig. 1.5.2).

This is because the EJS consists of alveolar and basal bone. In addition, EJS describes planned implant bed relation to present anatomical borders such as mandibular or maxillary vital structures. This is in coincidence with Ribeiro-Rotta et al. [86], they proposed that each implant site should be assessed and characterized knowing that bone characteristics vary within the same jaw [174]. All measurements should be obtained clinically and from CBCT and panoramic radiographic images. It should be done by identifying and depicting anatomical landmarks and position of important vital structures, when planning for dental implant operation.

There are two zones distinguished in the new classification system – aesthetic and non aesthetic and two regions – mandibular canal and maxillary sinus. EJSs are attributed to aesthetic and non aesthetic mandibular or maxillary zone, because the demands and risks of aesthetic result achievement differ significantly in aesthetic zone in comparison with non aesthetic zone. Mandibular canal and maxillary sinus regions are important because of the risk of injury of inferior alveolar nerve and maxillary sinus and implant operation planning peculiarities. Furthermore, all EJSs are divided into types (Types I to III) according to their assessment result and risk degree of planned surgical treatment success. This is in coincidence with Friberg et al. [1], they suggested that the justification for assessing jaw bone

tissue in endosseous dental implant treatment should be diagnostic tool to assess whether the jaw bone tissue is sufficient for implant treatment and a prognostic tool to predict the probability of success or failure.

The minimal dimensions of EJS for proper implantation were estimated according to the principles of threaded implant insertion.

3.4.1. Non aesthetic zone

3.4.1.1. The height of the alveolar process (H)

The distance between the crest of the alveolar process and the important vital structures of the jaws (maxillary sinus, mandibular canal, mental foramen, anterior loop of mental nerve). Several factors should be considered when estimating the minimal height of an alveolar process. In some cases the crest of alveolar process is thin and it is necessary to reduce it, so it can have wider base for the planned implant installation. In such cases, the heights of EJS will be shortened by 1 to 3 mm; this reduction had to be considered when calculating the available bone height [175] (Fig. 3.4.1.1.1).

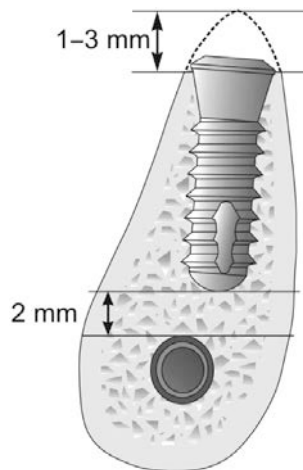


Fig. 3.4.1.1.1. Crestal ridge reduction

Thin crestal ridge could be reduced to create wide recipient bed for planned implant installation. In such cases, the heights of EJSs would have been shortened by 1 to 3 mm at least.

If the operation is planned according to the orthopantomograph, implantation in the areas of the mandibular canal mandated that the apices should be at least 2 mm away from those vital structures. A minimum of 1 mm is demanded if the operation is planned with CBCT [176]. Essentially, the minimal height of the Type I EJS is > 10 mm (Fig. 3.4.1.1.2).

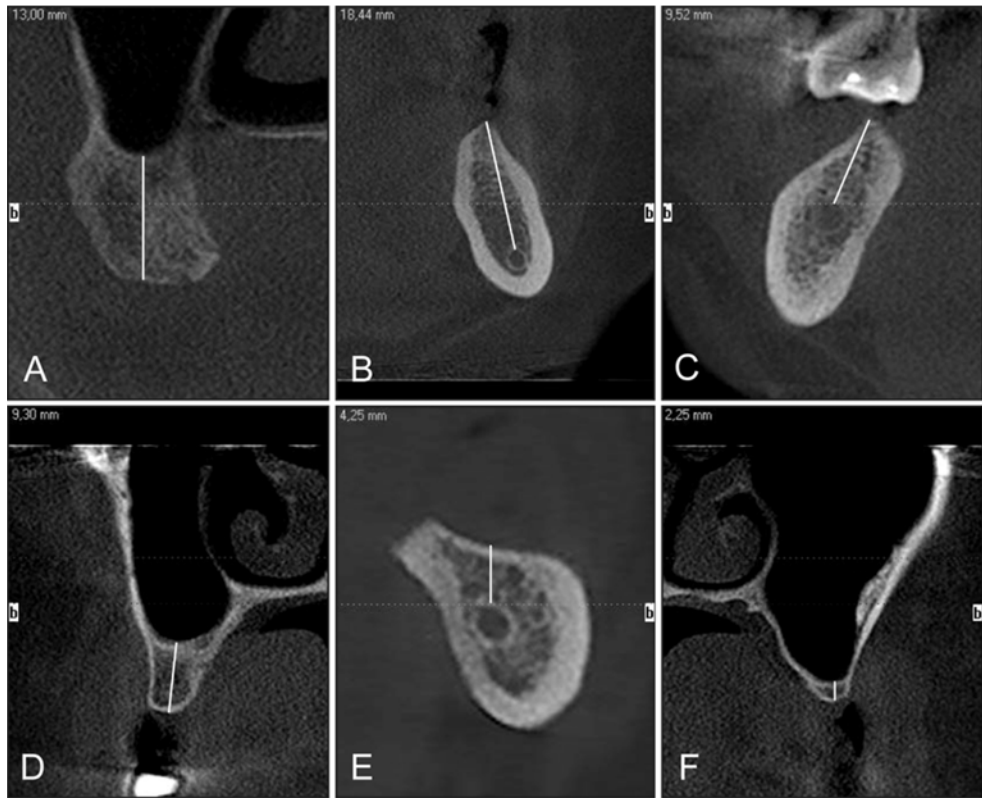


Fig. 3.4.1.1.2. The height of the alveolar process

A = Upper jaw first right molar EJS on CBCT cross-sectional image is more than 10 mm in height and classified as Type I with no requirement of vertical alveolar process bone height augmentation prior endosseous dental implant treatment (all CBCT images in this article were obtained with I-CAT® (Imaging Sciences International LLC, Hatfield, PA USA) CBCT, a letter “b” on cross-sectional CBCT image means buccal side).

B = Type I height (> 10 mm) of lower jaw first left molar EJS on CBCT cross-sectional image.

C = Type II height (> 8 to < 10 mm) of lower right first molar EJS on CBCT cross-sectional image. Simultaneous implantation with lateral bone augmentation are recommended.

D = Type II height (> 4 to < 10 mm) of upper right first molar EJS on CBCT cross-sectional image. Simultaneous implantation with vertical alveolar process augmentation are recommended.

E = Type III height (< 8 mm) of lower left second molar EJS on CBCT cross-sectional image. Vertical alveolar process augmentation and late implantation are recommended. Mandibular canal walls have proper identification with D2 bone quality.

F = Type III height (< 4 mm) of upper left premolar EJS on CBCT cross-sectional image. Sinus floor augmentation and late implantation are recommended.

EJS with the less height of > 8 to ≤ 10 mm (Fig. 3.4.1.1.2) and > 4 to ≤ 10 mm in maxillary sinus region (Fig. 3.4.1.1.2) were considered to be Type II. However, such height was found to be sufficient to ensure primary stability of implants [27]. Simultaneous implantation with vertical alveolar process augmentation or sinus floor augmentation is recommended. If EJS height was less than ≤ 8 mm and ≤ 4 mm in maxillary sinus region was categorized as Type III (Fig. 3.4.1.1.2). These measurements were considered to be insufficient for 8 mm length implant installation and primary stability achievement even in maxillary sinus region. Vertical alveolar process and/or sinus floor augmentation and late implantation are recommended.

3.4.1.2. The width of the alveolar process (W)

Determined by the alveolar process width measured at the level of 3 mm (W1) and 6 mm (W2) from the crest of alveolar process. The smallest measurement should be accepted as the width of the EJS. Recommendations for successful results ideally require at least 1 mm of bone surrounding each implant [159]. Most implant systems require bone widths of 5 to 7 mm [73, 159]. We estimated that for proper implantation the minimal width of an EJS (Type I) should be 6 mm (Fig. 3.4.1.2.1).

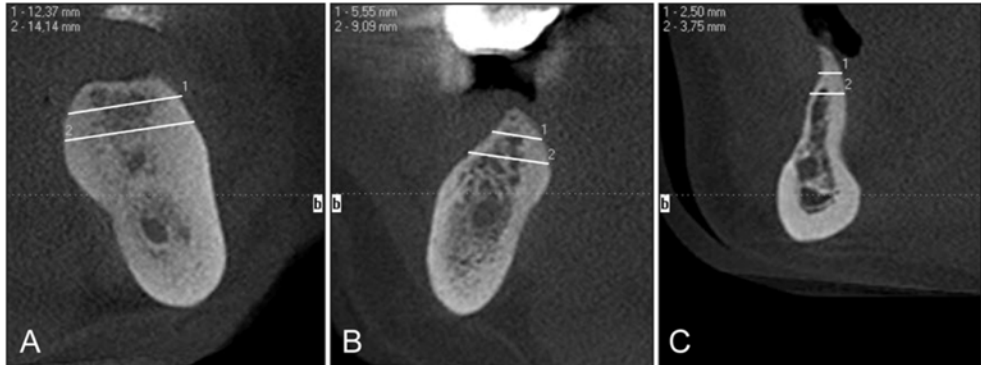


Fig. 3.4.1.2.1. The width of the alveolar process

A = Type I width (> 6 mm) of lower molar EJS on CBCT cross-sectional image at the level of 3 mm and 6 mm with no requirement of horizontal alveolar process augmentation prior endosseous dental implant treatment.

B = Type II width (> 4 to ≤ 6 mm) of lower right molar EJS on CBCT cross-sectional image. Endosseous dental implant treatment with simultaneous alveolar process horizontal augmentation are recommended.

C = Type III width of lower premolar EJS on CBCT cross-sectional image. Horizontal alveolar process augmentation and late implantation are recommended.

Alveolar processes with widths of > 4 to ≤ 6 mm were deemed insufficient (Type II) for proper implantation (Fig. 3.4.1.2.1). Despite such deficiencies, it is expected that the wider parts of the implants will be covered by bone after insertion and that primary stability would be achieved. Simultaneous implantation with alveolar process horizontal augmentation is recommended. EJS which width is less than 4 mm is categorized as Type III (Fig. 3.4.1.2.1). These measurements are considered to be insufficient for primary stability of implants. Horizontal alveolar process augmentation and late implantation is recommended.

3.4.1.3. The length of the EJS (L)

Is determined by the distance between equators of neighbouring teeth or implants. The minimal distance between 2 implants should be at least 3 mm [177], and minimal distances between implants and natural roots should be at least 1.5 mm [178] or in case of platform-switched implant 1 mm [158]. Considering that the optimal recommended diameter of implants in distal jaws segments is 4 to 5 mm, all EJS of Type I should be ≥ 7 or ≤ 12 mm in length (Fig. 3.4.1.3.1).



Fig. 3.4.1.3.1. The length of the EJS

The length of the EJS in non aesthetic zones on CBCT image (panoramic reconstruction): measurement “1” – Type I, measurement “2” – Type II, measurement “3” – Type III.

EJS which length is ≥ 6 or ≤ 13 mm is considered as Type II and < 6 or > 13 mm as Type III. In Type III EJS is impossible to install one or two proper diameter implants. Orthodontic treatment prior to implant treatment is recommended.

3.4.1.4. Alveolar ridge vertical position (RVP)

The distance between the lowest point of alveolar ridge crest to the labial/buccal surface cervicoenamel line of the adjacent teeth. This parameter is important for achieving of favourable implant/crown length ratio and adequate aesthetic result. Adequate distance for Type I EJS is estimated to be ≤ 3 mm. The alveolar ridge vertical position > 3 to < 7 mm is defined as Type II EJS. In case when EJS height is sufficient for implant primary stability achievement, simultaneous implantation with vertical alveolar process augmentation or sinus floor augmentation and vertical alveolar process augmentation is recommended (Fig. 3.4.1.4.1).

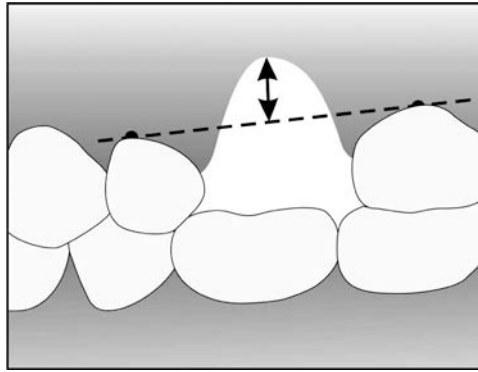


Fig. 3.4.1.4.1. Alveolar ridge vertical position in non aesthetic zone

The distance between the lowest point of the alveolar ridge crest to the cervicoenamel line of the adjacent teeth.

The alveolar ridge vertical position ≥ 7 mm is defined as Type III EJS with high risk of implant treatment success due to doubtful primary stability achievement. For Type III EJS vertical alveolar process augmentation and late implantation are recommended.

3.4.2. Aesthetic zone

3.4.2.1. The height of the alveolar process (H)

The distance between the crest of the alveolar process and the important vital structures of the jaws (nasal sinus floor, mental foramen, anterior loop of mental nerve). To facilitate a better implant/crown ratio, the minimal dental implant length in the aesthetic zone is 10 mm [179]. Hence, the alveolar process height for Type I EJS should be > 10 mm because the recommended apicocoronal position of the dental implant is 2 mm below the adjacent cemento-enamel junction [151]. A height for the alveolar process of > 8 to \leq

10 mm and > 4 to ≤ 10 mm in maxillary sinus region is defined as Type II EJS. Simultaneous implantation with vertical alveolar process augmentation or sinus floor augmentation is recommended. Alveolar process height ≤ 8 and ≤ 4 mm in maxillary sinus region is defined as Type III EJS. These measurements were considered to be insufficient for 8 mm length implant installation and primary stability achievement even in maxillary sinus region. Vertical alveolar process and/or sinus floor augmentation and late implantation are recommended.

3.4.2.2. The width of alveolar process (W)

Determined by the alveolar process width measured at the level of 3 mm (W1) and 6 mm (W2) from the crest of alveolar process. The smallest measurement should be accepted as the width of the EJS. It was taken into consideration that optimal implant diameter indicated for implantation in aesthetic zone can vary depending on tooth type and measurements. To make presented herein classification system more universal, it was considered to indicate proper alveolar process width for Type I EJS, as calculation of optimal implant diameter + 3 mm of the alveolar bone. It was mentioned above that it should be minimum 1 mm of bone surrounding each implant [159]. Hence, 3 mm in this case means that implant will be surrounded by minimum 1.5 mm of bone in buccal and lingual regions. The width of the alveolar process – optimal implant diameter + < 3 mm is defined as Type II EJS, and optimal implant diameter + ≤ 0 mm is defined as Type III EJS. For Type II EJS simultaneous implantation with alveolar process horizontal augmentation is recommended. For Type III EJS horizontal alveolar process augmentation and late implantation is recommended.

3.4.2.3. The length of the EJS (L)

It is determined by the least distance between neighbouring teeth or implants. The minimal distance between 2 implants should be at least 3 mm [177], and minimal distances between implants and natural roots should be at least 1.5 mm [178] or in case of platform-switched implant 1 mm [158]. To ensure optimal aesthetic implant rehabilitation, the implant-supported restoration should be in symmetry with the adjacent dentition [155]. Consequently, Type I EJS width must be equal to contralateral tooth. The alveolar process length characterised as asymmetry < 1 mm in comparison with contralateral tooth is defined as Type II EJS. Asymmetry ≥ 1 mm in comparison with contralateral tooth is defined as Type III EJS. In cases of Type II and III EJSs treatment choice depends on patient's aesthetic demands. If the patient wish to have adequate aesthetic result, orthodontic treatment for EJS

length optimisation should be recommended prior to dental implant surgical placement.

3.4.2.4. Alveolar ridge vertical position (RVP)

The distance between the lowest point of alveolar ridge crest to the cervicoenamel line of the adjacent teeth. This parameter is important for achieving of implant-supported restoration length equability to contralateral tooth (Fig. 3.4.2.4.1).

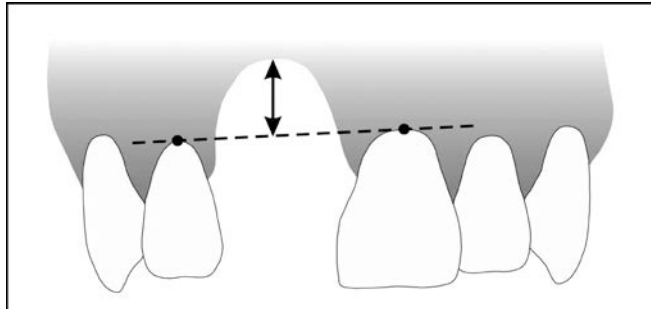


Fig. 3.4.2.4.1. Alveolar ridge vertical position in the aesthetic zone

The distance between the lowest point of alveolar ridge crest to the cervicoenamel line of the adjacent teeth.

Adequate distance for Type I EJS is estimated to be ≤ 2 mm. The alveolar ridge vertical position > 2 to ≤ 4 mm is defined as Type II EJS and distance > 4 mm is defined as Type III EJS. Simultaneous implantation with vertical alveolar process augmentation in case of Type II EJS is recommended. For Type III EJS vertical alveolar process augmentation and late implantation are recommended.

3.4.2.5. Mesial and distal interdental bone peak height (BPH)

The distance from the tip of the interdental bone peak to the alveolar crest midline. Distances of 3 to 4 mm, ≥ 1 to < 3 mm, and < 1 mm were defined as Types I, II and III, respectively (Fig. 3.4.2.5.1).

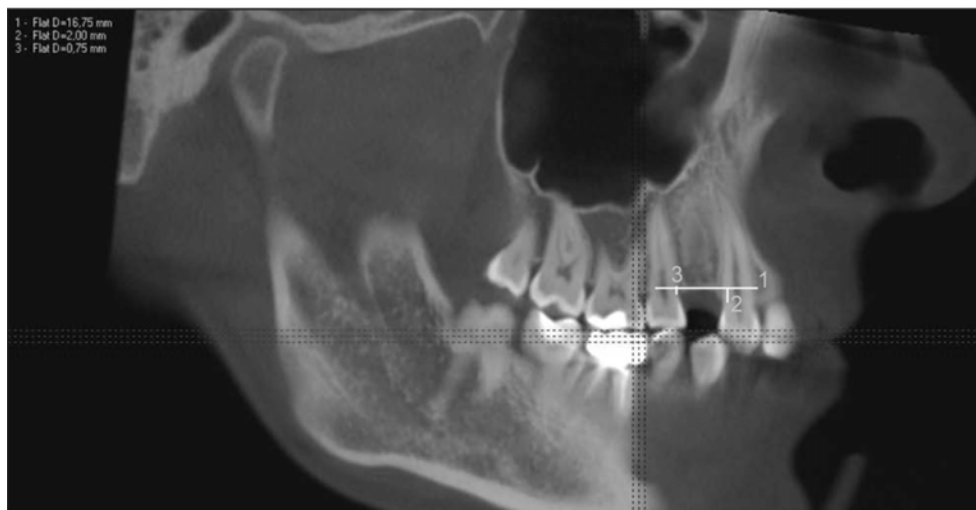


Fig. 3.4.2.5.1. Interdental bone peak height

Type II (measurement “2”) and Type III (measurement “3”) bone peak heights of the first upper premolar EJS on CBCT image reconstruction.

A study [154] demonstrated that the presence or absence of a bone crest influences the appearance of papillae between implants and adjacent teeth.

3.4.2.6. Mandibular canal walls (MCW) and jaw bone quality (JBQ) type identification

Mandibular canal walls are depicted on panoramic radiographs or CBCT images as radio-opaque white lines which are flanking as dark ribbon. The bone quality types are characterised according to Lekholm and Zarb classification (Fig. 3.4.2.6.1) [73].

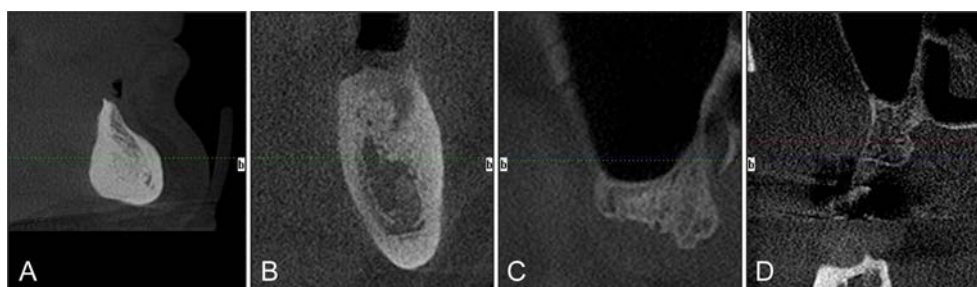


Fig. 3.4.2.6.1. Bone quality according to Lekholm and Zarb classification

A = D1 on the CBCT cross-sectional image (mental region EJS); B = D2 on the CBCT cross-sectional image (36 tooth EJS); C = D3 in the EJS of upper second molar (CBCT cross-sectional image); D = D4 in the EJS of 17 tooth on CBCT cross-sectional image.

The combination of identified MC walls and D2 or D3 bone quality types indicates Type I EJS with low risk of inferior alveolar nerve injury. In case when it is impossible to identify superior MC wall on X-ray and there is registered D1 or D4 bone quality type, Type II EJS with moderate inferior alveolar nerve injury risk is defined. The high inferior alveolar nerve injury risk and Type III EJS is considered when it is impossible to identify MC (Fig. 3.4.2.6.2.) and bone quality is registered as D1 or D4 type.

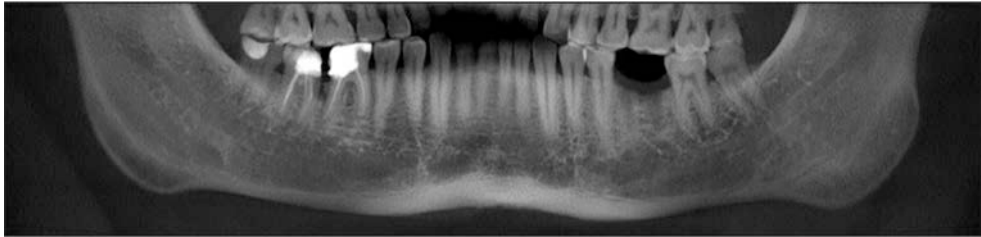


Fig. 3.4.2.6.2. The part of reconstructed panoramic radiograph with unidentified superior MC wall in the EJS

Unidentified superior MC wall in the EJS of 36 tooth (the same CBCT as Fig. 3.4.2.6.1).

3.5. Study V

The total sample size was 102 patients after the CBCT scanner. Eighty-one patients were included in the study after random selection. The mean of the patients' age was 40.3 ± 10.1 in years (range 21-62 years). The Kolmogorov-Smirnov test provided normal distribution of the patients by age ($p = 0.206$). Mean age in years of the patients in Lithuanian group (58 patients (71.6%)) was 40.4 ± 9.0 , in Turkish group (23 patient (28.4%)) 40.3 ± 12.8 ($p = 0.97$). Two age groups (the first group was patients less than 42 years old, and the second was patients 42 years and older) were distinguished, with 42 years as the median. Statistically, non-significant differences were identified between age groups and the investigation center ($p > 0.05$). The gender had no significant difference between any measured parameter in the study ($p > 0.05$).

There were 21 (25.9%) and 60 (74.1%) assessed EJSs in aesthetic and non-aesthetic zones respectively ($p < 0.05$). Statistically non-significant differences were identified between either investigation centers and zones ($p > 0.05$). Statistically, non-significant differences were identified between number of evaluated EJSs in both jaws (lower and upper jaw) and investigation center ($p > 0.05$). There was a non-significant difference between either position of the tooth and the investigation center ($p > 0.05$).

The chosen parameters did not differ significantly considering age groups and: investigation center, preoperative risk type, MC walls and jaw bone quality type identification, interdental bone peak height, soft tissue vertical deficiency, papilla appearance ($p > 0.05$).

3.5.1. Radiological EJS assessment during preoperative stage according to study protocol (Table 3.5.1.1)

Table 3.5.1.1. Preoperative parameters of edentulous jaw segment (EJS)

EJS parameters		Aesthetic zone	Non aesthetic zone	Total	p	
Height (mm (SD))		14.6 (2.6)	14.4 (4.3)	14.4 (3.9)	> 0.05	
Width (mm (SD))		6.5 (1.3)	7.6 (1.8)	7.3 (1.8)	< 0.05	
Length	Aesthetic	Equal, n (%)	17 (81.0)	Not measured	81.0	-
		Asymmetry < 1 mm, n (%)	4 (19.0)		19.0	
		Asymmetry \geq 1 mm, n (%)	-		-	
	Non aesthetic, mm (SD)	Not measured	9.6 (1.9)	9.6	-	
Alveolar ridge vertical position (mm (SD))		2.6 (1.2)	2.5 (1.3)	2.5 (1.2)	> 0.05	
MC walls identification and jaw bone quality type combination	Identified walls/ D2 and , n (%)		4 (100)	41 (85.4)	45 (86.5)	> 0.05
	Unidentified superior Wall/ D1 and D4, n (%)		-	4 (8.3)	4 (7.7)	
	Unidentified superior wall/ D2 and D3, n (%)		-	3 (6.3)	3 (5.8)	
	Unidentified MC/ D1 and D4, n (%)		-	-	-	
Planned dental implant parameters	Length, mm (SD)		11.3 (1.0)	10.9 (1.3)	11.0 (1.2)	> 0.05
	Diameter, mm (SD)		3.8 (0.5)	4.2 (0.4)	4.1 (0.5)	< 0.05

Table 3.5.1.1. Continued

EJS parameters		Aesthetic zone	Non aesthetic zone	Total	p
Implant threads coverage by the bone	Adequate, n (%)	13 (61.9)	50 (83.3)	63 (77.8)	< 0.05
	Deficient, n (%)	4 (19.0)	7 (11.7)	11 (13.6)	> 0.05
	Dehiscece, fenestration, n (%)	4 (19)	3 (5.0)	7 (8.6)	< 0.05
EJS Type	I, n (%)	8 (38.1)	31 (51.7)	39 (48.1)	> 0.05
	II, n (%)	12 (57.1)	29 (48.3)	41 (50.6)	> 0.05
	III, n (%)	1 (4.8)	–	1 (1.2)	> 0.05
Distance from implant apex to vital structures (mm (SD))		2.9 (2.0)	3.2 (1.8)	3.1 (1.9)	> 0.05

EJS = edentulous jaw segment; mean (SD) = mean (standard deviation) (for parametric variables); n (%) = number (%) (for non-parametric variables); D = bone quality; MC = mandibular canal; p = p value.

Additional results were provided below. Significant differences were identified between alveolar ridge height, width and tooth position ($p < 0.05$).

Cervical part(s) of the implant was not covered by the bone (dehiscence) in 7.4% (6 implants). Isolated implant part(s) was not covered by the bone (fenestration) in 1.2% (1) of implants.

Distance from implant apex to important vital structures had the mode value of 2.0 mm, and the median value of 2.0 mm range of 1.0–9.0 mm. Significant linear correlation was identified between EJS bone height and distance from implant apex to anatomically important vital structures ($r = 0.608$, $p < 0.001$). Significant correlation between mentioned variables was not identified for the upper jaw ($r = 0.155$, $p = 0.413$), but for the lower jaw it was registered ($r = 0.747$, $p < 0.001$). Significant linear correlation was identified between EJS bone height and distance from implant apex to anatomically important vital structures for aesthetic zone ($r = 0.879$, $p < 0.001$), as well for non-aesthetic zone ($r = 0.541$, $p < 0.001$).

Dental implants were planned for all EJSs (81 EJS). The range of dental implant length and diameter was 8.0–13.0 mm and 3.3–5.0 mm respectively.

3.5.2. Risk degree evaluation for proper implantation (Table 3.5.1.1)

Type II and Type III cases were combined (Type II/III) for statistical analysis, as just one case was high risk and was evaluated during subsequent stages. Statistically non-significant difference was assessed between numbers Type I and Type II/III ($p > 0.05$). Statistically non-significant difference was distinguished between risk degree (for two or three risk types) and aesthetic and non-aesthetic zone ($p > 0.05$).

3.5.3. Evaluation of the surgery during intraoperative and early postoperative stages according to study protocol: reliability of new proposed classification evaluation (Table 3.5.3.1)

Table 3.5.3.1. Differences between matching preoperative, intraoperative and early postoperative stages' parameters.

Parameter	Alveolar ridge vertical position	Alveolar ridge length (aesthetic zone)	Alveolar ridge length (non-aesthetic zone)	Placed implant diameter	Placed implant length	Implant threads coverage	Distance from implant apex to vital structures	Primary implant stability
p value	0.43**	1.00**	0.89**	0.66*	1.00*	1.00**	0.26*	1.00**

*paired sample t-test. **Wilcoxon signed ranks test. p = p value. $p > 0.05$, statistically non-significant difference between measurements.

Agreement (weighted kappa coefficient) between alveolar ridge vertical positions's preoperative and operative categorized measurements in non-aesthetic and aesthetic zone was 0.88 and 0.66 respectively.

Cohen's kappa coefficient for the length of EJS was 0.86 between preoperative and intraoperative categorized measurements for aesthetic zone, while for non-aesthetic zone it was 0.90.

Interdental bone peak height for mesial part of EJS was 2.4 ± 0.9 mm (range 0.0–4.0 mm). Mesial bone peak height categorization: 10 (47.6%) mesial bone peaks were Type I, 10 (47.6%) – Type II, 1 (4.8%) – Type III. Distal bone peak height categorization: 5 (23.8%) bone peaks were Type I, 13 (61.9%) – Type II, 3 (14.3%) – Type III.

All EJSs got implants during the intraoperative stage. Planned and placed implant length was identical. Mean dental implant width was 4.1 ± 0.5 mm

(range 3.3–5.0 mm). Paired non-significant differences 0.009 [–0,01–0,03] $p = 0.7$ were identified between planned and placed implant diameter. Mean dental implant length was 11.0 ± 1.2 mm (range 8.0–13.0 mm).

The agreement between preoperative and intraoperative implant threads' coverage by the bone was almost perfect (weighted kappa coefficient was 0.91).

Mean primary implant stability was 33.5 ± 9.3 Ncm (range 15–50 Ncm). Type I primary stability was identified in 63% of EJSs, while 37% were Type II. All placed implants corresponded to minimal requirements of primary implant stability. No significant difference was revealed between primary implant stability and zone ($p > 0.05$). No significant difference was identified between primary implant stability and MC walls/jaw bone quality type ($p > 0.05$). Significant linear correlation was identified between planned dental implant width and primary implant stability ($r = 0.409$, $p < 0.001$), as well between placed dental implant width and primary implant stability ($r = 0.432$, $p < 0.001$). Planned/placed implant length did not correlate significantly with primary implant stability ($r = -0.023$, $p = 0.839$).

Implant host sites' bony walls fractures, mandibular canal perforation, and inferior alveolar nerve direct mechanical injury by implant drill were not identified during the study. Excessive bleeding in the apical region of osteotomy was identified in only one case (1.2%) without clinical and radiological signs of MC damage or close-distance MC. Sign of perforation and inferior alveolar nerve direct mechanical injury by implant drill ("sudden give" or an "electric shock") was not identified in both investigation centers during intraoperative stage. Implant drill slippage deeper than planned or implant placement deeper than planned were not identified during implant surgery.

3.5.4. Implant treatment success evaluation at final crown placement

Vertical soft tissue deficiency was not identified (Type I) in 57 EJSs (70.4%). Soft tissue deficiency (Type II) was registered in 23 EJSs (28.4%), while compromised deficiency (Type III) was registered in 1 EJS (1.2%). Soft tissue vertical deficiency was not identified (Type I) in aesthetic zone for 8 EJSs (38.1%), while for non-aesthetic zone it was revealed in 49 EJSs (81.7%) ($p < 0.05$). Type II soft tissue vertical deficiency was assessed for 12 EJSs (57.1%) in the aesthetic zone, while 11 EJSs (18.3%) were identified in the non-aesthetic zone ($p < 0.05$). The highest soft tissue deficiency (Type III) was distinguished in 1 EJS (4.8%) for aesthetic zone, while no EJS was found within the non-aesthetic zone ($p > 0.05$).

Weighted kappa coefficients between categorized preoperative, intraoperative stage alveolar ridge vertical position and soft tissue vertical deficiency in aesthetic zone were 0.91 and 0.83 respectively. Weighted kappa coefficients were 0.94 and 0.83 between categorized preoperative, intraoperative stage alveolar ridge vertical position and soft tissue vertical deficiency in non-aesthetic zone EJSs.

Interdental mesial papilla complete fill was identified in 10 EJSs (47.6%), with partial fill in 11 EJSs (52.4%). No papilla was not observed. Agreement (weighted kappa coefficient) between categorized measurements (mesial interdental bone peak height and mesial papilla fill) was 0.55. Interdental distal papilla complete fill was defined in 6 EJSs (28.6%), partial fill in 13 EJSs (61.9%), and no papilla in 2 EJSs (9.5%). Weighted kappa coefficient was 0.73 between categorized distal interdental bone peak height and papilla fill.

The agreement between mesial and distal bone peak height (weighted kappa) was 0.43, while kappa value for mesial and distal interdental papilla fill agreement was 0.4.

4. DISCUSSION

4.1. Study I

The “as low as reasonably achievable” (ALARA) principle is of high importance for widespread dental implant surgery. The clinician can choose from several radiographic investigation methods to evaluate the alveolar ridge height and width for prosthetic implant placement. In many cases, a treatment plan cannot be composed without panoramic radiograph evaluation, even for an edentulous JDS in the region of MC, because the H-AC-MC distance must be measured [121]. Precise investigation requires more advanced investigation methods, like CBCT. Otherwise, there is still discussion about the application of panoramic radiography in clinical practice to facilitate treatment planning. Digital technologies are rapidly replacing analogue imaging techniques in dentistry. Updates to devices and software are periodically available. The software contains linear measurement tools, including a densitometric analysis tool. We noted the absence of investigations on the possibility of evaluating MC visibility using DPRs. Hence, we aimed to evaluate MC and the visibility of its walls by means of dedicated software (linear and densitometric analysis tools).

It is difficult to achieve optimal- or high-quality panoramic radiographs. Quality requirements were met in only 31.7% of the DPRs in our study. Similarly, Rumberg et al. [180] found 33% of their panoramic radiographs to be of acceptable quality. The percentage of the JDSs evaluated in the regions of PM₁, PM₂, M₁, and M₂ cannot be the same because of the study protocol requirements for inclusion. JDSs were not included in the study if they contained the mental foramen. A common horizontal position of the mental foramen (for Caucasian individuals) can be found in the premolar region [181].

Detailed MC evaluation was introduced due to variability of visibility through the course of MC. The 5-point scale (Fig. 2.1.4.2) was suggested during the present study for the comprehensive evaluation of the MC visibility for the mesial, distal, inferior, and superior parts of each JDS. Various 3-point, 4-point, and 5-point MC visibility rating scales have been proposed by investigators [22, 182, 183]. Oliveira-Santos et al. [26] used two scores for the evaluation of separate MC regions, while the overall MC visibility score was the sum of the six evaluated regions. MC depiction in another study was classified into three types for each implant site: visible in the superior and inferior walls, visible in the inferior walls and invisible in the superior walls, or invisible in the superior and inferior walls [184].

Agreement between observers' repeated MC visibility evaluations of one investigator's findings (Table 3.1.1.1) was almost perfect (a reflection of consistent measurements throughout the study) and coincided with the results of other investigators' data [26].

The different visibility of the MC borders in the mediobuccal and vertical directions was confirmed by the current study (Table 3.1.1.2). The most uncommon MC visibility score was 2 for the evaluation of the inferior and superior MC borders, and the MC tended to have better visibility when the borders were present. This tendency agrees with other investigations, showing the importance of the MC border for MC visibility [26, 146, 185]. The superior mesial and superior distal parts of the MC border had visibility score 3 in 22.0% and 24.7% of the sample, respectively, which is similar to data from Jung and Cho's investigation [186]. Naitoh et al. [184] found the MC superior wall to be invisible in 31.7% of designed implant sites, while Klinge et al's investigation [107] with specimen cadavers demonstrated an invisible MC in 36.1% (the superior and inferior borders of MC were not distinguished). Therefore, it could be concluded from our study that the three-dimensional evaluation of JDSs should be recommended for further analysis of MC in about 25% of JDSs if the identification of the superior MC border is obligatory. In comparison, the MC was not visible in 0.2% of the third molar (M_3) regions, 5.7% of the M_2 regions and 8.2% of the M_1 regions in the CBCT images [186]. Of more importance for this study was that the superior MC border could be identified in 75.3% of distal parts and 78.0% of mesial parts. We could not get data from the literature to make a clinical comparison with our results for the mesial and distal parts of the MC superior border.

It is interesting to know that anatomically trabeculated MC walls tend to be denser in the upper part than the lower part, but MC visibility does not have a similar tendency, according to our study and to that of Wadu et al. [146]. The last-mentioned sources supplement the statement that radiographic identification of the superior MC border cannot directly relate to MC border density and cannot have a prognostic value for MC damage during implant surgery. Furthermore, the multiple accessory canals directed toward root apices while leaving the MC could have a negative influence on trabeculation and the radiographic visibility of the superior MC border. However, our study results did not confirm the statement that superior or inferior MC border visibility is related to JDS condition in partially dentate lower jaws (with one exception between scores 5 and 3 for the visibility evaluation of the mesial and inferior parts of the MC border) and coincides with the CBCT study results [26].

The present study results confirmed (Table 3.1.1.2) that the superior MC border has lower visibility scores more often than the inferior MC border. Non-significant differences were identified between numbers of moderate visibility scores for both MC borders. Conversely, the superior border received the score 4 more than twice as often as the inferior border. These data tend to use the inferior MC border as a reference point for the identification of the imagined superior MC border in implant planning, while the diameter of the MC can be measured using other parts of the panoramic radiograph or by means of MC height (e.g., from our study). Indeed, this idea should be avoided because of the unreliable data. Wadu et al. [146] recognised and demonstrated a tendency to identify fine or non-existent structures. Furthermore, worldwide studies provide different mean MC diameters from 2 to about 5 mm with probable relation to race [110]. Even bifid MC can be identified in 0.08% to 65% of radiographs, depending on the investigation method [110]. The position of the mental foramen varies in horizontal and vertical planes and is related to race. The accessory mental foramen can be identified in 1.4% to 10% in patients of different populations [181]. Misidentification of these structures may lead to serious complications during implant surgery.

It is important to mention that the current study provides data with no difference between the visibility scores for the mesial and distal superior MC borders and the mesial and distal inferior MC borders (Table 3.1.1.2). It was considered that the clinician should not expect to observe differences in the visibility of corresponding MC parts of particular JDSs or even between neighbouring or other JDSs – that is, MC visibility did not change through the course, contrary to other investigators' results [26, 146, 186]. This statement could not be applied to the MC visibility in the mandibular ramus, the M₃ JDS region, or the mental canal region, as these regions were not included in our study protocol. There were no differences between any pair of corresponding bilateral JDSs in any of the four visibility evaluations of the MC parts. Similarly, researchers found no difference between MC visibility on the left and right sides [26, 186].

Our results revealed that MC visibility was not related to the subject's gender or age. Significant differences were only identified between the means of age groups with visibility scores of 4 and 5 for the mesial inferior MC border part, but this does not reflect a general tendency. This can be explained by the fact that patients included in the study were systematically healthy or had mild systemic diseases. The bone anatomy and endocrine system function could have influenced MC visibility [187].

It is interesting to know that we could not find any analogous studies confirming MC border visibility in relation to the region of each JDS and related regions.

A morphometric analysis of separate JDS parts (Fig. 2.1.5.1) was necessary before evaluating the relations between the morphometric analysis and the MC visibility scoring. Our measurements of MC height were within the range demonstrated in the summary Juodzbalyš et al. [110] provided of MC vertical linear evaluations made by various authors. We found that the mean distance from the alveolar crest to the MC was similar to the review results [110] and was the most variable linear height measurement (SE was 0.4–0.5 mm) in the present study. It confirms a widely known requirement for individual implant length planning while alveolar ridge height is variable.

It is important to consider that the morphometric measurements did not correlate with MC visibility in our study (Table 3.1.3.1). For example, no significant differences were identified between the mesially evaluated morphometric parameters of JDS and the corresponding MC visibility scores. In contrast, some differences were identified in the distally evaluated morphometric parameters of JDS.

The analysis of MC densitometric assessment data and visible MC depiction revealed controversial results. The corresponding vertical (Table 3.1.5.1) and horizontal (Table 3.1.6.1) densitometry did not provide statistically significant differences from the visibility analysis results in the mesial superior parts of the MC, but some differences were found in the distal superior parts. We expected to identify similar differences for the inferior MC border in the mediobuccal direction, but the results were the opposite: some significant differences were identified for the inferior mesial parts of JDS, while no significant differences were identified for the distal parts. The results might have differed for the superior and inferior MC borders due to significant differences in densitometric analysis results for mesial and distal JDS parts in the vertical direction. However, this would not explain the same differences when a comparison was made between MC visibility and horizontal densitometric analysis data. Based on these results, we concluded that the success in visually identifying MC borders did not correlate with the densitometric depiction of the MC borders (peaks).

Our investigation provides results indicating the limited accuracy of the densitometric tool for the possible improvement of radiographic MC identification. Naitoh et al. [184] found relations between MC depiction in digital panoramic radiographs and bone density in the alveolar region, but they evaluated bone density by multislice computed tomography (MSCT) in Hounsfield units (HUs). HUs give the relative density of tissue according to

a calibrated scale. HUs were found to be stable after quality phantom scanning with an MSCT scanner [97]. To our knowledge, there is no data in the literature regarding the investigation of the densitometric analysis tool used. The region of interest could not be modified (one standard line could be drawn without entering the desirable area). We found this to be a drawback, as a bigger and standardised region of interest should provide more stable results in the investigated region, especially in the region of MC with variable visibility. The densitometric analysis tool was tested with several enhancements that were provided prior to the investigation. The results varied and depended on the chosen enhancement tool. “Sharp enhancement” was chosen to standardize the measurements. We recommend conducting additional investigations for the validation of the densitometric tool with the inclusion of a quality control phantom. If the results are positive, a new investigation with a bigger sample is recommended.

In conclusion, evaluation of the visibility of the MC superior and inferior borders on digital panoramic radiographs depends on multiple factors without priority of gender, age, jaw dental segment location and condition, particular mandibular height parameter measurements, or anatomically specific area evaluation with the dedicated densitometric analysis tool. The MC visibility of particular JDSs does not change significantly from the MC visibility of mesially and distally located neighbouring JDSs. Particular differences between the visibility of the superior and inferior MC borders were identified to produce a clinically more important conclusion: the superior MC border was not visible more than twice as often as the inferior MC border.

4.2. Study II

Several case reports have pointed out the life-threatening haematoma in the floor of the mouth because of injury of mandibular lingual vessels mainly occurred in the interforaminal region [36–42, 44]. Profuse bleeding was reported in the premolar and molar region in some case reports but not well examined yet [47, 48]. In this study, we examined the whole lingual foramina with a large group of patients (639 patients with 1061 foramina) by means of CT and CBCT. The distance to the foramen from the alveolar bone crest was found to be 18.33 ± 5.45 mm, ranging between 1 and 31 mm (MLC, 18.24 ± 5.75 mm; LLC, 18.43 ± 5.07 mm). Mardinger et al. [188] found this range to be 2 to 26 mm in an anatomical study. The present results were consistent with this study. They dissected 12 hemimandibles, and in 10 of the mandibles, arteries were found in mental area, 9 in second

molars, and 12 in canine area; 2 mm distance was measured in mental and molar areas. Because mandibular resorption was unclassified in this study, it can be assumed that in cases of atrophic edentulous ridges, it should be even shorter. The mean distance from the mandibular border to the foramen was measured to be 17.40 ± 7.52 mm ranging from 1 to 31.2 mm in this study. Several CT studies gave different results [46, 49, 54, 58, 63]. Katakami et al [46] found a mean distance of 7.06 mm ranging between 0.75 and 15.28 mm on 181 patients. Other CT studies reported the mean results for median and LLCs separately. Tagaya et al. [58] showed a range from 1.1 to 18.4 mm in the mesial part and 7.7 mm (2.2–13.7 mm) mean distance from the mandibular border on the lateral side of 200 patients. Gültekin et al. [63] found a mean distance of 11.6 ± 3 mm for MLCs and 6 ± 1.3 mm for LLC in 26 patients. Kilic et al. [57] gave a range of 1 to 19 mm (median, 13 mm) for MLC and 2 to 35 mm (median, 7 mm) for LLC. The mean values were 10.2 ± 5.5 mm and 5.4 ± 3.8 mm for MLC and LLC, respectively, in another study of 32 patients [49]. In this study, the mean values were detected to be 17.69 ± 8.58 mm for MLC and 16.99 ± 6.04 mm for LLC. This higher distance could be because of the complex ethnicity of the study samples (5 different countries), and in our knowledge, this is the first study with such high sample group. We measured the distance between tooth apex and artery in this study. Immediate implantation into carefully selected extraction sockets shortens the time of therapy. About 3- to 5-mm bone beyond the apex is supportive for primary stability in immediate implantation procedures. The mean distance was measured as 10.06 ± 4.38 mm in this study. Thus, study results reveal that there is enough space for immediate procedures and it is safe with regard to the lingual vessels. However, Froum et al. [189] performed risk assessment in CT scans before extraction in the mandibular premolar and molar areas for immediate implant placement. For immediate implant placement, they determined that the amount of necessary bone in apical area should be 6 mm (4 mm for apical anchorage and 2 mm for safety zone). According to their results, 53% to 73% of mandibular premolars and molars presented with high risk when immediate implant treatment was considered. Therefore, one should suggest that presurgical CT scan evaluation is an obligation in this area when planning immediate implant placement treatment.

In accordance with the literature [49, 53, 63], vertical size of foramen was 0.89 ± 0.40 mm in this study. Similarly, Katakami et al. [46] reported a mean diameter of 0.88 ± 0.2 mm. They examined the lingual vascular canals of whole mandible similar to this study. A cadaver dissection study gave a mean diameter of 0.8 mm for perforating cortical branches of sublingual artery [51]. Another anatomical study with dry skull mandibles gave a mean

diameter of foramen on the lingual side of mandible as 0.8 ± 0.4 mm [56]. Rosano et al. [50] detected 0.8 to 0.9 mm diameter of genial foramen in the anatomical assessment of anterior mandible. The present study results obtained with CT sections are consistent with the anatomy. Vertical size of foramen was mostly reported for MLC and LLC in the literature in CT examinations or just reported for median part of the mandible. The present study results for MLC and LLC were 0.92 ± 0.44 mm and 0.84 ± 0.34 mm, respectively. Consistent with the previous reports, diameter of MLC was statistically higher than LLC in this study [49, 63]. Gültekin et al. [63] reported a mean value of 0.8 ± 0.2 mm for MLC and 0.6 ± 0.1 mm for LLC with 26 patients. Kilic et al. [57] reported 1.05 and 0.92 mm, respectively, in a study of 200 cases. These results were in accordance with each other. Gahleitner et al. [49] reported slightly smaller diameter, 0.7 ± 0.3 mm for MLC and 0.6 ± 0.3 mm for LLC.

We classified the foramen diameters as ≤ 1 and > 1 mm to give an idea about the risk of severe haemorrhage. Of the lingual foramen, 75.6% were ≤ 1 mm. Lustig et al. [5] identified the lingual artery in the anterior mandible, width, and blood flow by ultrasound/doppler measurement. Average size was reported to be 1.41 ± 0.34 mm and blood flow was 2.92 ± 3.19 ml/min. It was concluded that the artery is of sufficient size to give rise to hemorrhage in implant placement and procedures related to symphysis. Moreover, 25.9% arteries traveling in the sublingual space were located between the sublingual gland and the mandible [32]. In this pattern of course, blood vessels run parallel to the occlusal plane and assumed that the vessels lying perpendicular to the drill bit are at a greater risk for arterial injury [32]. Mylohyoid muscle separates the mouth floor like a diaphragm. In dentate mandibles, artery traveling above the muscle is more prone to cause haemorrhage, whereas in edentulous, one runs below the mylohyoid muscle [32]. Morphology of the mandible of the implant patient should be observed well because perforation of the lingual cortical plate may lead to the violation of sublingual/submandibular area. Several anastomoses of arteries take place in the body and oral cavity. Anastomosis of inferior alveolar artery and its branches, mental and incisive arteries, were found either with anatomical dissection or CT imaging [35, 46, 55]. Using a contrast medium, association between superior genial spinal foramen and incisive canal was examined in dry skulls. The association was seen in 41%, but the authors stated that leakage of the medium outside canals could not be totally prevented [190]. The observation of the anastomosis was reported; however, the frequency of this formation was given in only 1 study [46]. In this study, anastomoses of lingual artery with inferior alveolar artery and its branches could be detected with 38.1% of 1061 artery, whereas Katakami et al. [46]

showed 31 arterial anastomoses with 154 (20.12%) lingual artery, none was between intercanine area. We observed 3.7% anastomoses with incisive canal. The difference could be because of high number of samples investigated. Gender differences had an influence on examined parameters, except diameter of the foramen. But, number of foramen >1 mm diameter was higher in men. Distances between crest and foramen, tooth apex and foramen, and distance from the mandibular border were higher in men. Because the literature did not mention an evaluation about gender, on the parameters listed above, we cannot make a direct comparison. In a previous study, about tooth and dental arch dimensions, men had significantly larger dimensions [191]. Additionally, we observed gender differences in anatomical features of another bony canal and environmental bone of the jaws [67]. According to Lee et al. [192], one may suggest that by using the cone-beam CT and a laser intraoral scanner in virtual dental implant surgery, dentist may perform safer and successful implant surgeries and treatments.

4.3. Study III

The Rehabilitation of posterior maxilla is usually difficult due to maxillary sinus pneumatization and alveolar process resorbtion. The anatomical peculiarities of maxillary sinus region and related bony structures were provided by this investigation. Mainly, non-significant intersexual differences were observed for most variables. The study seems to be valuable in clinical practice for implant treatment planning. The further analysis of the data is needed.

4.4. Study IV and V

The pilot study had multiple variables and several stages for comprehensive evaluation of the newly proposed therapeutic anatomical based clinical and radiological classification for the dental implant treatment. Strict investigation protocol and limited indications for CBCT were the reasons of longer study duration. Furthermore, random selection of the patients reduced the sample size in comparison with a total number of treated patients. Despite an uneven amount of the included patients for both investigation centers, non-significant differences were identified considering patients' age, gender, jaw, tooth position, and aesthetic and non-aesthetic zone. The data could be used for further analysis. The inequality in evaluated EJSs amount for aesthetic and non-aesthetic zone should be justified with higher prevalence of dental caries in non-aesthetic zone teeth [193]

with the presumption of a subsequent higher rate of the various complications, including tooth extraction.

Multiple variables were required for evaluation of proposed classification, as it was composed for comprehensive implant treatment planning considering aesthetic and non-aesthetic zones. The aims were to assess both clinical and radiological parameters in aesthetic and non-aesthetic zone and then compared data at pre-, intra-, and early post- and late post-operative stages.

Preoperative stage evaluation results of anatomical peculiarities were similar in mandible and maxilla as well as in aesthetic and non-aesthetic zones (Table 3.5.1.1). The aesthetic zone included incisors, canines, and premolars, and it contained larger spectrum in comparison with non-aesthetic zone (first and second molar region). Otherwise, the mean alveolar process height did not differ between aesthetic and non-aesthetic zone, probably because of enlarged aesthetic zone (Table 3.5.1.1, 4.4.1).

Table 4.4.1. Edentulous jaw segments' height and width measurements depending on localization

Dental segments (maxilla)																	
		18	17	16	15	14	13	12	11	21	22	23	24	25	26	27	28
Width	Mean			8.40	7.33	6.20		4.00	5.00	5.00	7.00	5.00	6.67	8.00	8.88		
	SD			1.52	0.58	1.30		–	–	–	–	–	1.53	–	2.10		
Height	Mean			10.60	13.00	12.90		14.00	19.00	18.00	15.00	18.00	14.67	10.00	7.13		
	SD			2.54	1.73	1.82		–	–	–	–	–	2.08	–	2.80		
Dental segments (mandible)																	
		48	47	46	45	44	43	42	41	31	32	33	34	35	36	37	38
Width	Mean		10.00	7.26	6.33								6.00		7.14	8.00	
	SD		–	2.01	0.58								–		1.61	–	
Height	Mean		14.00	15.57	16.33								16.00		16.64	13.00	
	SD		–	3.27	2.08								–		2.34	–	

SD = standard deviation. All measurements are done in millimetres.

The height differences depending on tooth position were confirmed by the present study. It is interesting to know that our study did not support the statement that EJSs of non-aesthetic zone (in the region of the first maxillary molar) because of the lowest maxillary sinus floor position in that region [27].

The width of alveolar ridge supported the tendency to be wider in the EJSs with previously observed wider teeth and vice versa (Table 4.4.1) [194]. The EJS length evaluation was related with more strict requirements to aesthetic zone EJSs. The width of future restoration should be in symmetry with contralateral tooth [195]. The patients were informed about asymmetry in both zones and possible treatment options. The alveolar process height and width evaluation provided similar data to previous study results [27], but it has some discrepancies mainly due to the small sample size of the present study.

The results of the present study revealed the necessity of proposed classification updating, while additional combination of MC identification and bone density in Type III EJS was observed (unidentified superior MC wall and D2/D3 bone quality) (Table 3.5.1.1). Identification of MC was possible in all 52 EJSs containing MC, while bone quality varied. In comparison, Jung and Cho's [186] study revealed that MC was not visible in 0.2% of the third molar regions, 5.7% of the second molar regions, and 8.2% of the first molar regions on CBCT images. The absence of combination D1/D4 and unidentified MC (Type III EJS) could be explained by high accuracy of CBCT in MC identification. Furthermore, the D1 bone quality is more common for EJSs in anterior mandible while D4 more often can be observed in distal maxilla.

It was noted that if the alveolar process was higher, the distance between dental implant and anatomically vital structures was bigger. Observed correlation probably is related to the clinicians' wish to ensure a low risk of damage to vital structures and to install shorter, but optimal height (8–10 mm) implant [196, 197].

Implant planning was finished with overall EJS risk evaluation for implantation operation. Indeed, in order to reduce the risk, the clinicians use various soft and hard tissue regeneration methods. The final treatment's success and survival depends not just on preoperative stage results; it is the cumulative result of several treatment stages. The evaluation of the classification was distributed throughout the stages of the treatment in order to reflect classification's versatility and diminish the risk for treatment unreliable prognosis.

Intraoperative stage provided the biggest amount of study results (Appendix 2, Table 3.5.3.1). They confirmed the classification validity be-

cause of matching with preoperative stage results. The agreements between tested measurements in both periods ranged from substantial to almost perfect (range 0.66–0.91) by means of Cohen's and weighted kappa coefficients. All implants were installed in EJSs. Furthermore, planned dental implant parameters (length and width) were not significantly different from the installed implant parameters. It is important to consider that there was no correlation between dental implant length and primary stability, while it was observed between implant diameter and primary stability and is in coincidence with Urdaneta et al's study results [198].

The results revealed almost perfect agreement (kappa ranging from 0.83 to 0.94) between evaluated categorized peri-implant soft tissue vertical deficiency at late postoperative stage and alveolar ridge vertical position evaluated at preoperative and intraoperative stages. Lower requirements for vertical soft tissue deficiency evaluation parameters in non-aesthetic zone probably was the reason for the higher rate of Type I EJSs registered in comparison with aesthetic zone EJSs. Furthermore, soft tissue conditioning to some degree improved vertical soft tissue height evaluation results.

Correlations between interdental papilla and preoperative stage corresponding parameter assessment results were not analyzed because of possible discrepancies in preoperative evaluation of interdental bone peak height on CBCT. The kappa agreement between interdental papilla and interdental bone peak height assessed at final dental crown placement was in a range from moderate to substantial (0.55–0.73). The papilla height should increase in particular degree during longer conditioning time [199]. The papilla height depends not just on soft tissue height, as implant abutment and crown have individual profile and can be modified to some degree during manufacturing.

CONCLUSIONS

1. DPRs failed to provide MC visibility based on a single factor. Particular differences were identified between the levels of visibility of the superior and inferior MC borders. In less than 25% of JDSs the superior MC border was not visible, more than twice as often as the inferior MC border was not visible (about 10%).
2. Lingual foramina could be visualized and evaluated on CBCT. Vascular canals and several anastomoses exist in the anterior mandible extending through premolar and molar regions as well. It is imperative to consider these vessels with the CBCT before and during the mandibular surgery to prevent threatening haemorrhage.
3. Maxillary sinus and surrounding bone anatomical structures could be identified on CBCT. Anatomical variations were identified separately after single and multiple teeth loss in large group sample by providing implant treatment planning related information.
4. The new comprehensive classification system of the jaw bone anatomy in endosseous dental implant treatment planning was purposed with distinguished aesthetic and non-aesthetic zones, MC and maxillary sinus regions. Edentulous jaw segments were divided into three types (Types I to III) according to their assessment result and risk degree of planned surgical treatment success.
5. The therapeutic anatomical based clinical and radiological classification for dental implant treatment revealed reliability by confirmation of significant conformity between preoperative, intraoperative, and early postoperative implant treatment stages' parameters.

RECOMMENDATIONS FOR CLINICAL PRACTICE

1. DPRs failed to provide MC visibility based on a single factor (morphometric or densitometric assessment parameters, nor to age, gender, JDS location, condition, or the visibility of neighbouring MC parts or contralateral JDSs). The properly made DPRs could fail to provide superior MC border visibility in about 25% of JDSs. More advanced radiological investigation methods could be required for the evaluation of MC superior border.
2. Lingual vascular canals and anastomoses exist in the region of anterior and posterior mandible. The clinically important haemorrhage can be observed after injury of these relatively small diameter vessels. CBCT could be the tool for preoperative evaluation of lingual vascular canals.
3. Thorough maxillary sinus and surrounding bone evaluation is possible on CBCT, including maxillary ostium, posterior superior artery, sinus membrane, septa, alveolar bone, prior implant treatment and maxillary sinus augmentation surgeries.
4. The proposed classification system could be a helpful tool for immediate evaluation of the risk for implant treatment success. Treatment planning unification could be the step towards implant treatment standardization and better collaboration among specialists. Validated and updated classification system have more background for incorporation it in the daily clinical practice.

RECOMMENDATIONS FOR RESEARCH

1. Study I provided limited accuracy of the densitometric tool for the possible improvement of radiographic MC identification on DPRs. We recommend conducting additional investigations for the validation of the densitometric tool with the inclusion of a quality control phantom. If the results are positive, a new investigation with a bigger sample is recommended.
2. Study II and III provided general data internationally. We could recommend to perform studies with larger sample sizes nationally while anatomical peculiarities could be race and region at some degree dependent.
3. Periodically could be performed the literature analysis in order to evaluate new scientific data on implant treatment planning (study IV). Classification system could be updated and later validated to have helpful tool for planning of treatment strategy and collaboration among specialists.
4. Future studies with a larger sample size are needed to further validate the outcomes obtained in the pilot Study V.

REFERENCES

1. Friberg B, Jemt T, Lekholm U. Early failures in 4,641 consecutively placed Bråne-mark dental implants: a study from stage 1 surgery to the connection of completed prostheses. *Int J Oral Maxillofac Implants* 1991;6:142–6.
2. Juodzbaly G, Wang HL, Sabalys G. Injury of the Inferior Alveolar Nerve during Implant Placement: a Literature Review. *J oral Maxillofac Res* 2011;2:e1.
3. Tay AB, Zuniga JR. Clinical characteristics of trigeminal nerve injury referrals to a university centre. *Int J Oral Maxillofac Surg* 2007;36:922–7.
4. Choi BR, Choi DH, Huh KH, Yi WJ, Heo MS, Choi SC, et al. Clinical image quality evaluation for panoramic radiography in Korean dental clinics. *Imaging Sci Dent* 2012;42:183–90.
5. Lustig JP, London D, Dor BL, Yanko R. Ultrasound identification and quantitative measurement of blood supply to the anterior part of the mandible. *Oral Surg Oral Med Oral Pathol Oral Radiol Endod* 2003;96:625–9.
6. Schneider AC, Bragger U, Sendi P, Caversaccio MD, Buser D, Bornstein MM. Characteristics and dimensions of the sinus membrane in patients referred for single-implant treatment in the posterior maxilla: a cone beam computed tomographic analysis. *Int J Oral Maxillofac Implants* 2013;28:587–96.
7. Carmeli G, Artzi Z, Kozlovsky A, Segev Y, Landsberg R. Antral computerized tomography pre-operative evaluation: Relationship between mucosal thickening and maxillary sinus function. *Clin Oral Implants Res* 2011;22:78–82.
8. Shanbhag S, Karnik P, Shirke P, Shanbhag V. Cone-beam computed tomographic analysis of sinus membrane thickness, ostium patency, and residual ridge heights in the posterior maxilla: Implications for sinus floor elevation. *Clin Oral Implants Res* 2014;25:755–60.
9. Güncü GN, Yildirim YD, Wang HL, Tözüm TF. Location of posterior superior alveolar artery and evaluation of maxillary sinus anatomy with computerized tomography: A clinical study. *Clin Oral Implants Res* 2011;22:1164–7.
10. Chan HL, Suarez F, Monje A, Benavides E, Wang HL. Evaluation of maxillary sinus width on cone-beam computed tomography for sinus augmentation and new sinus classification based on sinus width. *Clin Oral Implants Res* 2014;25:647–52.
11. Wang H-L, Katranji A. ABC sinus augmentation classification. *Int J Periodontics Restorative Dent* 2008;28:383–9.
12. Wen SC, Chan HL, Wang HL. Classification and management of antral septa for maxillary sinus augmentation. *Int J Periodontics Restorative Dent* 2013;33:509–17.
13. Arias-Irimia O, Barona-Dorado C, Gómez Moreno G, Brinkmann JC, Martínez-González JM. Pre-operative measurement of the volume of bone graft in sinus lifts using CompuDent. *Clin Oral Implants Res* 2012;23:1070–4.
14. Yang SM, Park SI, Kye SB, Shin SY. Computed tomographic assessment of maxillary sinus wall thickness in edentulous patients. *J Oral Rehabil* 2012;39:421–8.
15. Arias-Irimia O, Barona-Dorado C, Martínez-Rodríguez N, Ortega-Aranegui R, Martínez-González JM. Pre-operative evaluation of the volume of bone graft in sinus lifts by means of CompuDent. *Med Oral Patol Oral Cir Bucal* 2010;15:e512–6.
16. Arasawa M, Oda Y, Kobayashi T, Uoshima K, Nishiyama H, Hoshina H, et al. Evaluation of bone volume changes after sinus floor augmentation with autogenous bone grafts. *Int J Oral Maxillofac Surg* 2012;41:853–7.
17. Kühl S, Brochhausen C, Götz H, Filippi A, Payer M, d’Hoedt B, et al. The influence

- of bone substitute materials on the bone volume after maxillary sinus augmentation: A microcomputerized tomography study. *Clin Oral Investig* 2013;17:543–51.
18. Klijn RJ, van den Beucken JJ, Bronkhorst EM, Berge SJ, Meijer GJ, Jansen JA. Predictive value of ridge dimensions on autologous bone graft resorption in staged maxillary sinus augmentation surgery using Cone-Beam CT. *Clin Oral Implants Res* 2012;23:409–15.
 19. SEDENTEXCT Project. Radiation protection: cone beam CT for dental and maxillofacial radiology. Evidence Based Guidelines. Radiation protection no. 172. Luxembourg: European Commission; 2012. Available from: http://www.sedentexct.eu/files/radiation_protection_172.pdf
 20. Bornstein MM, Scarfe WC, Vaughn VM, Jacobs R. Cone beam computed tomography in implant dentistry: a systematic review focusing on guidelines, indications, and radiation dose risks. *Int J Oral Maxillofac Implants* 2014;29 Suppl:55–77.
 21. Harris D, Horner K, Grondahl K, Jacobs R, Helmrot E, Benic GI, et al. E.A.O. guidelines for the use of diagnostic imaging in implant dentistry 2011. A consensus workshop organized by the European Association for Osseointegration at the Medical University of Warsaw. *Clin Oral Implants Res* 2012;23:1243–53.
 22. Jacobs R, Mraiwa N, Van Steenberghe D, Sanderink G, Quirynen M. Appearance of the mandibular incisive canal on panoramic radiographs. *Surg Radiol Anat* 2004;26:329–33.
 23. Devlin H, Yuan J. Object position and image magnification in dental panoramic radiography: a theoretical analysis. *Dentomaxillofac Radiol* 2013;42:29951683.
 24. Bartling R, Freeman K, Kraut RA. The incidence of altered sensation of the mental nerve after mandibular implant placement. *J Oral Maxillofac Surg* 1999;57:1408–12.
 25. Mehra A, Pai KM. Evaluation of dimensional accuracy of panoramic cross-sectional tomography, its ability to identify the inferior alveolar canal, and its impact on estimation of appropriate implant dimensions in the mandibular posterior region. *Clin Implant Dent Relat Res* 2012;14:100–11.
 26. Oliveira-Santos C, Capelozza AL, Dezzoti MS, Fischer CM, Poleti ML, Rubira-Bullen IR. Visibility of the mandibular canal on CBCT cross-sectional images. *J Appl Oral Sci* 2011;19:240–3.
 27. Juodzbaly G, Raustia AM. Accuracy of clinical and radiological classification of the jawbone anatomy for implantation--a survey of 374 patients. *J Oral Implantol* 2004;30:30–9.
 28. Gijbels F, De Meyer AM, Bou Serhal C, Van den Bossche C, Declerck J, Persoons M, et al. The subjective image quality of direct digital and conventional panoramic radiography. *Clin Oral Investig* 2000;4:162–7.
 29. Park HD, Min CK, Kwak HH, Youn KH, Choi SH, Kim HJ. Topography of the outer mandibular symphyseal region with reference to the autogenous bone graft. *Int J Oral Maxillofac Surg* 2004;33:781–5.
 30. Dym H, Huang D, Stern A. Alveolar Bone Grafting and Reconstruction Procedures Prior to Implant Placement. *Dent Clin North Am* 2012;56:209–18.
 31. Bavitz JB, Harn SD, Homze EJ. Arterial supply to the floor of the mouth and lingual gingiva. *Oral Surg Oral Med Oral Pathol* 1994;77:232–5.
 32. Katsumi Y, Tanaka R, Hayashi T, Koga T, Takagi R, Ohshima H. Variation in arterial supply to the floor of the mouth and assessment of relative hemorrhage risk in implant surgery. *Clin Oral Implants Res* 2013;24:434–40.

33. Martin D, Pascal JF, Baudet J, Mondie JM, Farhat JB, Athoum A, et al. The submental island flap: a new donor site. *Anatomy and clinical applications as a free or pedicled flap. Plast Reconstr Surg* 1993;92:867–73.
34. Kalpidis CD, Setayesh RM. Hemorrhaging associated with endosseous implant placement in the anterior mandible: a review of the literature. *J Periodontol* 2004;75:631–45.
35. Kawai T, Sato I, Yosue T, Takamori H, Sunohara M. Anastomosis between the inferior alveolar artery branches and submental artery in human mandible. *Surg Radiol Anat* 2006;28:308–10.
36. Del Castillo-Pardo de Vera JL, López-Arcas Calleja JM, Burgueño-García M. Hematoma of the floor of the mouth and airway obstruction during mandibular dental implant placement: a case report. *Oral Maxillofac Surg* 2008;12:223–6.
37. Felisati G, Saibene AM, Di Pasquale D, Borloni R. How the simplest dental implant procedure can trigger an extremely serious complication. *BMJ Case Rep* 2012; 2012.pii:bcr2012007373.
38. Flanagan D. Important arterial supply of the mandible, control of an arterial hemorrhage, and report of a hemorrhagic incident. *J Oral Implantol* 2003;29:165–73.
39. Mason ME, Triplett RG, Alfonso WF. Life-threatening hemorrhage from placement of a dental implant. *J Oral Maxillofac Surg* 1990;48:201–4.
40. Darriba MA, Mendonça-Caridad JJ. Profuse bleeding and life-threatening airway obstruction after placement of mandibular dental implants. *J Oral Maxillofac Surg* 1997;55:1328–30.
41. Givol N, Chaushu G, Halamish-Shani T, Taicher S. Emergency tracheostomy following life-threatening hemorrhage in the floor of the mouth during immediate implant placement in the mandibular canine region. *J Periodontol* 2000;71:1893–5.
42. Laboda G. Life-threatening hemorrhage after placement of an endosseous implant. *J Am Dent Assoc* 1990;121:599–600.
43. Fujita S, Ide Y, Abe S. Variations of Vascular Distribution in the Mandibular Anterior Lingual Region. *Implant Dent* 2012;21:259–64.
44. Jo JH, Kim SG, Oh JS. Hemorrhage related to implant placement in the anterior mandible. *Implant Dent* 2011;20:e33–7.
45. Lee CY, Yanagihara LC, Suzuki JB. Brisk, pulsatile bleeding from the anterior mandibular incisive canal during implant surgery: a case report and use of an active hemostatic matrix to terminate acute bleeding. *Implant Dent* 2012;21:368–73.
46. Katakami K, Mishima A, Kuribayashi A, Shimoda S, Hamada Y, Kobayashi K. Anatomical characteristics of the mandibular lingual foramina observed on limited cone-beam CT images. *Clin Oral Implants Res* 2009;20:386–90.
47. Kalpidis CD, Konstantinidis AB. Critical hemorrhage in the floor of the mouth during implant placement in the first mandibular premolar position: a case report. *Implant Dent* 2005;14:117–24.
48. ten Bruggenkate CM, Krekeler G, Kraaijenhagen HA, Foitzik C, Oosterbeek HS. Hemorrhage of the floor of the mouth resulting from lingual perforation during implant placement: a clinical report. *Int J Oral Maxillofac Implants* 1993;8:329–34.
49. Gahleitner A, Hofschneider U, Tepper G, Pretterklieber M, Schick S, Zauza K, et al. Lingual vascular canals of the mandible: evaluation with dental CT. *Radiology* 2001;220:186–9.
50. Rosano G, Taschieri S, Gaudy JF, Testori T, Del Fabbro M. Anatomic assessment of the anterior mandible and relative hemorrhage risk in implant dentistry: A cadaveric study. *Clin Oral Implants Res* 2009;20:791–5.

51. Loukas M, Kinsella CR, Kapos T, Tubbs RS, Ramachandra S. Anatomical variation in arterial supply of the mandible with special regard to implant placement. *Int J Oral Maxillofac Surg* 2008;37:367–71.
52. Choi DY, Woo YJ, Won SY, Kim DH, Kim HJ, Hu KS. Topography of the Lingual Foramen Using Micro-Computed Tomography for Improving Safety During Implant Placement of Anterior Mandibular Region. *J Craniofac Surg* 2013;24:1403–7.
53. Babiuc I, Tărlungeanu I, Păuna M. Cone beam computed tomography observations of the lingual foramina and their bony canals in the median region of the mandible. *Rom J Morphol Embryol* 2011;52:827–9.
54. Sheikhi M, Mosavat F, Ahmadi A. Assessing the anatomical variations of lingual foramen and its bony canals with CBCT taken from 102 patients in Isfahan. *Dent Res J* 2012;9:S45–51.
55. Nakajima K, Tagaya A, Otonari-Yamamoto M, Seki K, Araki K, Sano T, et al. Composition of the blood supply in the sublingual and submandibular spaces and its relationship to the lateral lingual foramen of the mandible. *Oral Surg Oral Med Oral Pathol Oral Radiol* 2014;117.
56. Liang X, Jacobs R, Lambrichts I, Vandewalle G. Lingual foramina on the mandibular midline revisited: A macroanatomical study. *Clin Anat* 2007;20:246–51.
57. Kilic E, Doganay S, Ulu M, Çelebi N, Yikilmaz A, Alkan A. Determination of lingual vascular canals in the interforaminal region before implant surgery to prevent life-threatening bleeding complications. *Clin Oral Implants Res* 2014;25.
58. Tagaya A, Matsuda Y, Nakajima K, Seki K, Okano T. Assessment of the blood supply to the lingual surface of the mandible for reduction of bleeding during implant surgery. *Clin Oral Implants Res* 2009;20:351–5.
59. Scaravilli MS, Mariniello M, Sammartino G. Mandibular lingual vascular canals (MLVC): Evaluation on dental CTs of a case series. *Eur J Radiol* 2010;76:173–6.
60. Liang H, Frederiksen NL, Benson BW. Lingual vascular canals of the interforaminal region of the mandible: Evaluation with conventional tomography. *Dentomaxillofac Radiol* 2004;33:340–1.
61. Tepper G, Hofschneider UB, Gahleitner A, Ulm C. Computed tomographic diagnosis and localization of bone canals in the mandibular interforaminal region for prevention of bleeding complications during implant surgery. *Int J Oral Maxillofac Implants* 2001;16:68–72.
62. Longoni S, Sartori M, Braun M, Bravetti P, Lapi A, Baldoni M, et al. Lingual vascular canals of the mandible: the risk of bleeding complications during implant procedures. *Implant Dent* 2007;16:131–8.
63. Gültekin S, Araç M, Celik H, Karaosmaoğlu AD, Işık S. [Assessment of mandibular vascular canals by dental CT]. *Tani Girişim Radyol* 2003;9:188–91. Turkish.
64. Gahleitner A, Watzek G, Imhof H. Dental CT: imaging technique, anatomy, and pathologic conditions of the jaws. *Eur Radiol* 2003;13:366–76.
65. Drago C, del Castillo R, Peterson T. Immediate Occlusal Loading in Edentulous Jaws, CT-Guided Surgery and Fixed Provisional Prosthesis: A Maxillary Arch Clinical Report. *J Prosthodont* 2011;20:209–17.
66. Busenlechner D, Huber CD, Vasak C, Dobsak A, Gruber R, Watzek G. Sinus augmentation analysis revised: The gradient of graft consolidation. *Clin Oral Implants Res* 2009;20:1078–83.
67. Güncü GN, Yildirim YD, Yılmaz HG, Galindo-Moreno P, Velasco-Torres M, Al-Hezaimi K, et al. Is there a gender difference in anatomic features of incisive canal and maxillary environmental bone? *Clin Oral Implants Res* 2013;24:1023–6.

68. Tözüm TF, Güncü GN, Yıldırım YD, Yılmaz HG, Galindo-Moreno P, Velasco-Torres M, et al. Evaluation of Maxillary Incisive Canal Characteristics Related to Dental Implant Treatment With Computerized Tomography: A Clinical Multicenter Study. *J Periodontol* 2012;83:337–43.
69. Yılmaz HG, Tözüm TF. Are Gingival Phenotype, Residual Ridge Height, and Membrane Thickness Critical for the Perforation of Maxillary Sinus? *J Periodontol* 2012;83:420–5.
70. Uchida Y, Goto M, Katsuki T, Soejima Y. Measurement of maxillary sinus volume using computerized tomographic images. *Int J Oral Maxillofac Implants* 1998;13:811–8.
71. Krenmair G, Krainhöfner M, Maier H, Weinländer M, Piehslinger E. Computerized tomography-assisted calculation of sinus augmentation volume. *Int J Oral Maxillofac Implants* 2006;21:907–13.
72. Mazzocco F, Lops D, Gobatto L, Lolato A, Romeo E, Del Fabbro M. Three-dimensional volume change of grafted bone in the maxillary sinus. *Int J Oral Maxillofac Implants* 2014;29:178–84.
73. Lekholm U, Zarb GA. In: Patient selection and preparation. Tissue integrated prostheses: osseointegration in clinical dentistry. Branemark PI, Zarb GA, Albrektsson T, editor. Chicago: Quintessence Publishing Company; 1985. p. 199–209.
74. Cawood JI, Howell RA. A classification of the edentulous jaws. *Int J Oral Maxillofac Surg* 1988;17:232–6.
75. Atwood DA. Reduction of residual ridges: A major oral disease entity. *J Prosthet Dent* 1971;26:266–79.
76. Mercier P, Lafontant R. Residual alveolar ridge atrophy: Classification and influence of facial morphology. *J Prosthet Dent* 1979;41:90–100.
77. Seibert JS. Reconstruction of deformed, partially edentulous ridges, using full thickness onlay grafts. Part I. Technique and wound healing. *Compend Contin Educ Dent* 1983;4:437–53.
78. Allen EP, Gainza CS, Farthing GG, Newbold DA. Improved technique for localized ridge augmentation. A report of 21 cases. *J Periodontol* 1985;56:195–9.
79. Eufinger H, Gellrich NC, Sandmann D, Dieckmann J. Descriptive and metric classification of jaw atrophy. An evaluation of 104 mandibles and 96 maxillae of dried skulls. *Int J Oral Maxillofac Surg* 1997;26:23–8.
80. Meyer U, Vollmer D, Runte C, Bourauel C, Joos U. Bone loading pattern around implants in average and atrophic edentulous maxillae: a finite-element analysis. *J craniomaxillofacial Surg* 2001;29:100–5.
81. Scarfe WC, Farman AG. Cone-Beam Computed Tomography. In: White SC, Pharoah MJ, editors. *Oral Radiology Principles and Interpretation*. 6th ed. St. Louis, Mo.: Mosby; 2009. p. 225–43.
82. Misch CE, Judy KW. Classification of partially edentulous arches for implant dentistry. *Int J Oral Implantol* 1987;4:7–13.
83. Kazor CE, Al-Shammari K, Sarment DP, Misch CE, Wang HL. Implant plastic surgery: a review and rationale. *J Oral Implantol* 2004;30:240–54.
84. Bianchi AE, Sanfilippo F. Single-tooth replacement by immediate implant and connective tissue graft: A 1-9-year clinical evaluation. *Clin Oral Implants Res* 2004; 15:269–77.
85. Worthington P. Injury to the inferior alveolar nerve during implant placement: a formula for protection of the patient and clinician. *Int J Oral Maxillofac Implants* 2004;19:731–4.

86. Ribeiro-Rotta RF, Lindh C, Pereira AC, Rohlin M. Ambiguity in bone tissue characteristics as presented in studies on dental implant planning and placement: A systematic review. *Clin Oral Implants Res* 2011;22:789–801.
87. Bergkvist G, Koh KJ, Sahlholm S, Klintström E, Lindh C. Bone density at implant sites and its relationship to assessment of bone quality and treatment outcome. *Int J Oral Maxillofac Implants* 2010;25:321–8.
88. Trisi P, Rao W. Bone classification: clinical-histomorphometric comparison. *Clin Oral Implants Res* 1999;10:1–7.
89. Misch C. Bone density: A key determinant for clinical success. In: Misch CE, editor. *Contemporary Implant Dentistry*. 2nd ed. St. Louis: Mosby; 1999. p. 109–18.
90. Norton MR, Gamble C. Bone classification: an objective scale of bone density using the computerized tomography scan. *Clin Oral Implants Res* 2001;12:79–84.
91. Naitoh M, Kurosu Y, Inagaki K, Katsumata A, Noguchi T, Arijji E. Assessment of mandibular buccal and lingual cortical bones in postmenopausal women. *Oral Surg Oral Med Oral Pathol Oral Radiol Endod* 2007;104:545–50.
92. Başa O, Dilek OC. Assessment of the risk of perforation of the mandibular canal by implant drill using density and thickness parameters. *Gerodontology* 2011;28:213–20.
93. Theisen FC, Shultz RE, Elledge DA. Displacement of a root form implant into the mandibular canal. *Oral Surg Oral Med Oral Pathol* 1990;70:24–8.
94. Fanuscu MI, Chang TL. Three-dimensional morphometric analysis of human cadaver bone: Microstructural data from maxilla and mandible. *Clin Oral Implants Res* 2004;15:213–8.
95. Schwarz MS, Rothman SL, Rhodes ML, Chafetz N. Computed tomography: part I. Preoperative assessment of the mandible for endosseous implant surgery. *Int J Oral Maxillofac Implant* 1987;2:137–41.
96. Naitoh M, Hirukawa A, Katsumata A, Arijji E. Evaluation of voxel values in mandibular cancellous bone: Relationship between cone-beam computed tomography and multislice helical computed tomography. *Clin Oral Implants Res* 2009;20:503–6.
97. Nackaerts O, Maes F, Yan H, Couto Souza P, Pauwels R, Jacobs R. Analysis of intensity variability in multislice and cone beam computed tomography. *Clin Oral Implants Res* 2011;22:873–9.
98. Parsa A, Ibrahim N, Hassan B, Motroni A, Der Van Stelt P, Wismeijer D. Influence of cone beam CT scanning parameters on grey value measurements at an implant site. *Dentomaxillofac Radiol* 2013;42.
99. van der Stelt PF. Filmless imaging: the uses of digital radiography in dental practice. *J Am Dent Assoc* 2005;136:1379–87.
100. Denio D, Torabinejad M, Bakland LK. Anatomical relationship of the mandibular canal to its surrounding structures in mature mandibles. *J Endod* 1992;18:161–5.
101. Benson BW, Shetty V. Dental Implants. In: White SC, Pharoah MJ, editors. *Oral Radiology Principles and Interpretation*. 6th ed. St. Louis, Mo.: Mosby; 2009. p. 597–612.
102. Chan HL, Misch K, Wang HL. Dental imaging in implant treatment planning. *Implant Dent* 2010;19:288–98.
103. Juodzbaly G, Wang HL. Guidelines for the Identification of the Mandibular Vital Structures: Practical Clinical Applications of Anatomy and Radiological Examination Methods. *J Oral Maxillofac Res* 2010;1:e1.
104. Phillips JL, Weller RN, Kulild JC. The mental foramen: Part I. Size, orientation, and positional relationship to the mandibular second premolar. *J Endod* 1990;16:221–3.

105. White SC, Heslop EW, Hollender LG, Mosier KM, Ruprecht A, ShROUT MK, et al. Parameters of radiologic care: An official report of the American Academy of Oral and Maxillofacial Radiology. *Oral Surg Oral Med Oral Pathol Oral Radiol Endod* 2001;91:498–511.
106. Lindh C, Petersson A, Klinge B. Measurements of distances related to the mandibular canal in radiographs. *Clin Oral Implant Res* 1995;6:96–103.
107. Klinge B, Petersson A, Maly P. Location of the mandibular canal: comparison of macroscopic findings, conventional radiography, and computed tomography. *Int J Oral Maxillofac Implants* 1989;4:327–32
108. Wyatt WM. Accessory mandibular canal: literature review and presentation of an additional variant. *Quintessence Int* 1996;27:111–3.
109. Kim IS, Kim SG, Kim YK, Kim JD. Position of the mental foramen in a Korean population: a clinical and radiographic study. *Implant Dent* 2006;15:404–11.
110. Juodzbaly G, Wang HL, Sabalys G. Anatomy of mandibular vital structures. Part I: mandibular canal and inferior alveolar neurovascular bundle in relation with dental implantology. *J Oral Maxillofac Res* 2010;1:e2.
111. Yosue T, Brooks SL. The appearance of mental foramina on panoramic radiographs. I. Evaluation of patients. *Oral Surg Oral Med Oral Pathol* 1989;68:360–4.
112. Sonick M, Abrahams J, Faiella RA. A comparison of the accuracy of periapical, panoramic, and computerized tomographic radiographs in locating the mandibular canal. *Int J Oral Maxillofac Implant* 1994;9:455–60.
113. Kuzmanovic DV, Payne AG, Kieser JA, Dias GJ. Anterior loop of the mental nerve: a morphological and radiographic study. *Clin Oral Implants Res* 2003;14:464–71.
114. Ngeow WC, Yuzawati Y. The location of the mental foramen in a selected Malay population. *J Oral Sci* 2003;45:171–5.
115. Jacobs R, Mraiwa N, vanSteenberghe D, Gijbels F, Quirynen M. Appearance, location, course, and morphology of the mandibular incisive canal: an assessment on spiral CT scan. *Dentomaxillofac Radiol* 2002;31:322–7.
116. Peker I, Alkurt MT, Michcioglu T. The use of 3 different imaging methods for the localization of the mandibular canal in dental implant planning. *Int J Oral Maxillofac Implants* 2008;23:463–70.
117. Rouas P, Nancy J, Bar D. Identification of double mandibular canals: Literature review and three case reports with CT scans and cone beam CT. *Dentomaxillofac Radiol* 2007;36:34–8.
118. Claeys V, Wackens G. Bifid mandibular canal: Literature review and case report. *Dentomaxillofac Radiol* 2005;34:55–8.
119. Sanchis JM, Peñarrocha M, Soler F, Penarrocha M, Soler F. Bifid mandibular canal. *J Oral Maxillofac Surg* 2003;61:422–4.
120. Naitoh M, Hiraiwa Y, Aimiya H, Arijji E. Observation of bifid mandibular canal using cone-beam computerized tomography. *Int J Oral Maxillofac Implants* 2009;24:155–9.
121. Angelopoulos C, Thomas SL, Hechler S, Parissis N, Hlavacek M. Comparison between digital panoramic radiography and cone-beam computed tomography for the identification of the mandibular canal as part of presurgical dental implant assessment. *J Oral Maxillofac Surg* 2008;66:2130–5.
122. Lindh C, Petersson A. Radiologic examination for location of the mandibular canal: a comparison between panoramic radiography and conventional tomography. *Int J Oral Maxillofac Implants* 1989;4:249–53.

123. Bou Serhal C, Jacobs R, Flygare L, Quirynen M, Van Steenberghe D. Perioperative validation of localisation of the mental foramen. *Dentomaxillofac Radiol* 2002;31:39–43.
124. Ekestubbe A, Gröndahl K, Gröndahl HG. The use of tomography for dental implant planning. *Dentomaxillofac Radiol* 1997;26:206–13.
125. Sakakura CE, Morais JA, Loffredo LC, Scaf G. A survey of radiographic prescription in dental implant assessment. *Dentomaxillofac Radiol* 2003;32:397–400.
126. Lascala CA, Panella J, Marques MM. Analysis of the accuracy of linear measurements obtained by cone beam computed tomography (CBCT-NewTom). *Dentomaxillofac Radiol* 2004;33:291–4.
127. Sato S, Arai Y, Shinoda K, Ito K. Clinical application of a new cone-beam computerized tomography system to assess multiple two-dimensional images for the preoperative treatment planning of maxillary implants: case reports. *Quintessence Int* 2004;35:525–8.
128. Loubele M, Guerrero ME, Jacobs R, Suetens P, van Steenberghe D. A comparison of jaw dimensional and quality assessments of bone characteristics with cone-beam CT, spiral tomography, and multi-slice spiral CT. *Int J Oral Maxillofac Implants* 2007;22:446–54.
129. Arai Y, Tammissalo E, Iwai K, Hashimoto K, Shinoda K. Development of a compact computed tomographic apparatus for dental use. *Dentomaxillofac Radiol* 1999;28:245–8.
130. Mozzo P, Procacci C, Tacconi A, Martini PT, Andreis IA. A new volumetric CT machine for dental imaging based on the cone-beam technique: preliminary results. *Eur Radiol* 1998;8:1558–64.
131. Delcanho RE. Neuropathic implications of prosthodontic treatment. *J Prosthet Dent* 1995;73:146–52.
132. Rubenstein JE, Taylor TD. Apical nerve transection resulting from implant placement: A 10-year follow-up report. *J Prosthet Dent* 1997;78:537–41.
133. Wismeijer D, Van Waas MA, Vermeeren JI, Kalk W. Patients' perception of sensory disturbances of the mental nerve before and after implant surgery: A prospective study of 110 patients. *Br J Oral Maxillofac Surg* 1997;35:254–9.
134. Dao TT, Mellor A. Sensory disturbances associated with implant surgery. *Int J Prosthodont* 1998;11:462–9.
135. Walton JN. Altered sensation associated with implants in the anterior mandible: A prospective study. *J Prosthet Dent* 2000;83:443–9.
136. Ziccardi VB, Assael LA. Mechanisms of trigeminal nerve injuries. *Atlas Oral Maxillofac Surg Clin North Am* 2001;9:1–11.
137. Von Arx T, Häfliger J, Chappuis V. Neurosensory disturbances following bone harvesting in the symphysis: A prospective clinical study. *Clin Oral Implants Res* 2005;16:432–9.
138. Abarca M, van Steenberghe D, Malevez C, De Ridder J, Jacobs R. Neurosensory disturbances after immediate loading of implants in the anterior mandible: An initial questionnaire approach followed by a psychophysical assessment. *Clin Oral Investig* 2006;10:269–77.
139. Greenstein G, Tarnow D. The mental foramen and nerve: clinical and anatomical factors related to dental implant placement: a literature review. *J Periodontol* 2006;77:1933–43.

140. Hegedus F, Diecidue RJ. Trigeminal nerve injuries after mandibular implant placement--practical knowledge for clinicians. *Int J Oral Maxillofac Implants* 2006;21:111-6.
141. Misch CE. Root form surgery in the edentulous anterior and posterior mandible: Implant insertion. In: Misch CE, editor. *Contemporary Implant Dentistry*. St. Louis, MO.: Mosby Elsevier; 2008. p. 221-6.
142. Alhassani AA, AlGhamdi AS. Inferior alveolar nerve injury in implant dentistry: diagnosis, causes, prevention, and management. *J Oral Implantol* 2010;36:401-7.
143. Misch CE, Resnik R. Mandibular nerve neurosensory impairment after dental implant surgery: management and protocol. *Implant Dent* 2010;19:378-86.
144. Juodzbalys G, Wang HL, Sabalys G, Sidlauskas A, Galindo-Moreno P. Inferior alveolar nerve injury associated with implant surgery. *Clin Oral Implants Res* 2013;24:183-90.
145. Kraut RA, Chahal O. Management of patients with trigeminal nerve injuries after mandibular implant placement. *J Am Dent Assoc* 2002;133:1351-4.
146. Wadu SG, Penhall B, Townsend GC. Morphological variability of the human inferior alveolar nerve. *Clin Anat* 1997;10:82-7.
147. Pelayo JL, Diago MP, Bowen EM, Diago MP. Intraoperative complications during oral implantology. *Med Oral Patol Oral Cir Bucal* 2008;13:239-43.
148. Khawaja N, Renton T. Case studies on implant removal influencing the resolution of inferior alveolar nerve injury. *Br Dent J* 2009;206:365-70.
149. Sammartino G, Marenzi G, Citarella R, Ciccarelli R, Wang HL. Analysis of the occlusal stress transmitted to the inferior alveolar nerve by an osseointegrated threaded fixture. *J Periodontol* 2008;79:1735-44.
150. Guan H, van Staden R, Loo YC, Johnson N, Ivanovski S, Meredith N. Influence of bone and dental implant parameters on stress distribution in the mandible: a finite element study. *Int J Oral Maxillofac Implants* 2009;24:866-76.
151. Saadoun AP, Landsberg CJ. Treatment classifications and sequencing for postextraction implant therapy: a review. *Pract periodontics aesthetic Dent* 1997;9: 933-41.
152. Jovanovic SA. Bone rehabilitation to achieve optimal aesthetics. *Pract Proced aesthetic Dent* 2007;19:569-76.
153. Belser UC, Buser D, Hess D, Schmid B, Bernard JP, Lang NP. Aesthetic implant restorations in partially edentulous patients - a critical appraisal. *Periodontol* 2000 1998;17:132-50.
154. Choquet V, Hermans M, Adriaenssens P, Daelemans P, Tarnow DP, Malevez C. Clinical and radiographic evaluation of the papilla level adjacent to single-tooth dental implants. A retrospective study in the maxillary anterior region. *J Periodontol* 2001;72:1364-71.
155. Fürhauser R, Florescu D, Benesch T, Haas R, Mailath G, Watzek G. Evaluation of soft tissue around single-tooth implant crowns: The pink esthetic score. *Clin Oral Implants Res* 2005;16:639-44.
156. Öhrnell L-O, Hirsch JM, Ericsson I, Brånemark PI. Single-tooth rehabilitation using osseointegration. A modified surgical and prosthodontic approach. *Quintessence Int* 1988;19:871-6.
157. Adell R, Eriksson B, Lekholm U, Brånemark PI, Jemt T. Long-term follow-up study of osseointegrated implants in the treatment of totally edentulous jaws. *Int J Oral Maxillofac Implants* 1990;5:347-59.

158. Vela X, Méndez V, Rodríguez X, Segalá M, Tarnow DP. Crestal bone changes on platform-switched implants and adjacent teeth when the tooth-implant distance is less than 1.5 mm. *Int J Periodontics Restorative Dent* 2012;32:149–55.
159. Allen F, Smith DG. An assessment of the accuracy of ridge-mapping in planning implant therapy for the anterior maxilla. *Clin Oral Implants Res* 2000;11:34–8.
160. Esposito M, Hirsch JM, Lekholm U, Thomsen P. Biological factors contributing to failures of osseointegrated oral implants. (II). Etiopathogenesis. *Eur J Oral Sci* 1998;721–64.
161. Oikarinen K, Raustia AM, Hartikainen M. General and local contraindications for endosseal implants--an epidemiological panoramic radiograph study in 65-year-old subjects. *Community Dent Oral Epidemiol* 1995;23:114–8.
162. Eufinger H, Gellrich NC, Sandmann D, Dieckmann J. Descriptive and metric classification of jaw atrophy. *Int J Oral Maxillofac Surg* 1997;26:23–8.
163. Jensen O. Site classification for the osseointegrated implant. *J Prosthet Dent* 1989;61:228–34.
164. Juodzbaly G, Kubilius M. Clinical and Radiological Classification of the Jawbone Anatomy in Endosseous Dental Implant Treatment. *J Oral Maxillofac Res* 2013;4:e2.
165. Hasegawa Y, Amarsaikhan B, Chinvipas N, Tsukada SI, Terada K, Uzuka S, et al. Comparison of mesiodistal tooth crown diameters and arch dimensions between modern Mongolians and Japanese. *Odontology* 2014;102:167–75.
166. Puri N, Pradhan KL, Chandna A, Sehgal V, Gupta R. Biometric study of tooth size in normal, crowded, and spaced permanent dentitions. *Am J Orthod Dentofac Orthop* 2007;132:279.e7-14.
167. Lana JP, Carneiro PM, Machado Vde C, de Souza PE, Manzi FR, Horta MC. Anatomic variations and lesions of the maxillary sinus detected in cone beam computed tomography for dental implants. *Clin Oral Implants Res* 2012;23:1398–403.
168. Suomalainen A, Pakbaznejad Esmaeili E, Robinson S. Dentomaxillofacial imaging with panoramic views and cone beam CT. *Insights Imaging* 2015;6:1–16.
169. Ballrick JW, Palomo JM, Ruch E, Amberman BD, Hans MG. Image distortion and spatial resolution of a commercially available cone-beam computed tomography machine. *Am J Orthod Dentofac Orthop* 2008;134:573–82.
170. Orenstein IH, Tarnow DP, Morris HF, Ochi S. Factors affecting implant mobility at placement and integration of mobile implants at uncovering. *J Periodontol* 1998;69:1404–12.
171. Spray JR, Black CG, Morris HF, Ochi S. The influence of bone thickness on facial marginal bone response: stage 1 placement through stage 2 uncovering. *Ann Periodontol* 2000;5:119–28.
172. Raes F, Renckens L, Aps J, Cosyn J, De Bruyn H. Reliability of circumferential bone level assessment around single implants in healed ridges and extraction sockets using cone beam CT. *Clin Implant Dent Relat Res* 2013;15:661–72.
173. Juodzbaly G, Wang HL. Esthetic index for anterior maxillary implant-supported restorations. *J Periodontol* 2010;81:34–42.
174. Lindh C, Obrant K, Petersson A. Maxillary bone mineral density and its relationship to the bone mineral density of the lumbar spine and hip. *Oral Surg Oral Med Oral Pathol Oral Radiol Endod* 2004;98:102–9.
175. Hardwick R, Scantlebury T, Sanchez R, Whitely N, Ambruster J. Membrane design criteria for guided bone regeneration of the alveolar ridge. In: Buser D, Dahlin C, Schenk RK, editors. *Guided bone regeneration in implant dentistry*. Hong Kong: Quintessence; 1994. p. 101–36.

176. Dula K, Mini R, van der Stelt PF, Buser D. The radiographic assessment of implant patients: decision-making criteria. *Int J Oral Maxillofac Implants* 2001;16:80–9.
177. Hobo S, Ichida E, Garcia LT. *Osseointegration and Occlusal Rehabilitation*, 1st ed. Chicago, Ill: Quintessence; 1989. p. 35.
178. Bauman GR, Mills M, Rapley JW, Hallmon WH. Clinical parameters of evaluation during implant maintenance. *Int J Oral Maxillofac Implants* 1992;7:220–7.
179. Davies SJ, Gray RJ, Young MP. Good occlusal practice in the provision of implant borne prostheses. *Br Dent J* 2002;192:79–88.
180. Rumberg H, Hollender L, Oda D. Assessing the quality of radiographs accompanying biopsy specimens. *J Am Dent Assoc* 1996;127:363–8.
181. Juodzbalys G, Wang HL, Sabalys G. Anatomy of Mandibular Vital Structures. Part II: Mandibular Incisive Canal, Mental Foramen and Associated Neurovascular Bundles in Relation with Dental Implantology. *J oral Maxillofac Res* 2010;1:e3.
182. Lindh C, Petersson A, Klinge B. Visualisation of the mandibular canal by different radiographic techniques. *Clin Oral Implants Res* 1992;3:90–7.
183. Yasar F, Yesilova E, Apaydin B. The effects of compression on the image quality of digital panoramic radiographs. *Clin Oral Investig* 2012;16:719–26.
184. Naitoh M, Katsumata A, Kubota Y, Hayashi M, Ariji E. Relationship between cancellous bone density and mandibular canal depiction. *Implant Dent* 2009;18:112–8.
185. Naitoh M, Yoshida K, Nakahara K, Gotoh K, Ariji E. Demonstration of the accessory mental foramen using rotational panoramic radiography compared with cone-beam computed tomography. *Clin Oral Implants Res* 2011;22:1415–9.
186. Jung YH, Cho BH. Radiographic evaluation of the course and visibility of the mandibular canal. *Imaging Sci Dent* 2014;44:273–8.
187. Mirza F, Canalis E. Management of Endocrine Disease: Secondary Osteoporosis: Pathophysiology and Management. *Eur J Endocrinol* 2015;173:R131–51.
188. Mardinger O, Manor Y, Mijiritsky E, Hirshberg A. Lingual perimandibular vessels associated with life-threatening bleeding: an anatomic study. *Int J Oral Maxillofac Implants* 2007;22:127–31.
189. Froum S, Casanova L, Byrne S, Cho SC. Risk assessment before extraction for immediate implant placement in the posterior mandible: a computerized tomographic scan study. *J Periodontol* 2011;82:395–402.
190. Vandewalle G, Liang X, Jacobs R, Lambrichts I. Macroanatomic and radiologic characteristics of the superior genial spinal foramen and its bony canal. *Int J Oral Maxillofac Implants* 2006;21:581–6.
191. Al-Khatib A, Rajion ZA, Masudi SM, Hassan R, Anderson PJ, Townsend GC. Tooth size and dental arch dimensions: A stereophotogrammetric study in Southeast Asian Malays. *Orthod Craniofac Res* 2011;14:243–53.
192. Lee CY, Ganz SD, Wong N, Suzuki JB. Use of Cone Beam Computed Tomography and a Laser Intraoral Scanner in Virtual Dental Implant Surgery. *Implant Dent* 2012;21:265–71.
193. Žemaitienė M, Grigalaušienė R, Vasiliauskienė I, Saldunaitė K, Razmienė J, Slabšinskienė E. Prevalence and severity of dental caries among 18-year-old Lithuanian adolescents. *Medicina (Kaunas)* 2016;52:54–60.
194. Stanley JN. Introduction to dental anatomy. In: *Wheeler's Dental Anatomy, Physiology, and Occlusion*. 10th ed. St. Louis, Mo.: Saunders Elsevier; 2015. p. 13.
195. Juodzbalys G, Sakavicius D, Wang HL. Classification of extraction sockets based upon soft and hard tissue components. *J Periodontol* 2008;79:413–24.
196. Lemos CA, Ferro-Alves ML, Okamoto R, Mendonça MR, Pellizzer EP. Short dental

- implants versus standard dental implants placed in the posterior jaws: A systematic review and meta-analysis. *J Dent* 2016;47:8–17.
197. Monje A, Chan HL, Fu JH, Suarez F, Galindo-Moreno P, Wang HL. Are Short Dental Implants (<10mm) Effective? A Meta-Analysis on Prospective Clinical Trials. *J Periodontol* 2012;1–11.
 198. Urdaneta RA, Leary J, Lubelski W, Emanuel KM, Chuang SK. The effect of implant size 5 × 8 mm on crestal bone levels around single-tooth implants. *J Periodontol* 2012;83:1235–44.
 199. Furze D, Byrne A, Alam S, Wittneben JG. Esthetic Outcome of Implant Supported Crowns With and Without Peri-Implant Conditioning Using Provisional Fixed Prosthesis: A Randomized Controlled Clinical Trial. *Clin Implant Dent Relat Res* 2016 Mar 16.

LIST OF THE AUTHOR'S PUBLICATIONS

Publications related to the results of dissertation:

1. Kubilius M, Kubilius R, Varinauskas V, Žalinkevičius R, Tözüm TF, Juodzbaly G. Descriptive Study of Mandibular Canal Visibility: Morphometric and Densitometric Analysis for Digital Panoramic Radiographs. *Dentomaxillofac Radiol* 2016; 20160079.
2. Yildirim YD1, Güncü GN, Galindo-Moreno P, Velasco-Torres M, Juodzbaly G, Kubilius M, Gervickas A, Al-Hezaimi K, Al-Sadhan R, Yilmaz HG, Asar NV, Karabulut E, Wang HL, Tözüm TF. Evaluation of mandibular lingual foramina related to dental implant treatment with computerized tomography: a multicenter clinical study. *Implant Dent* 2014;23:57-63.
3. Juodzbaly G, Kubilius M. Clinical and Radiological Classification of the Jawbone Anatomy in Endosseous Dental Implant Treatment. *J Oral Maxillofac Res* 2013;4:e2.

Other publications:

1. Kubilius M, Kubilius R, Gleiznys A. The preservation of alveolar bone ridge during tooth extraction. *Stomatologija*. 2012;14:3-11.
2. Varinauskas V, Diliūnas S, Kubilius M, Kubilius R. Influence of Cantilever Length on Stress Distribution in Fixation Screws of All-on-4 Full-arch Bridge. *Mechanika* 2013; 19:260-263.

Abstracts at scientific conferences

1. Juodzbaly G, Kubilius M. Inferior alveolar nerve injury associated with implant surgery. The 3rd International Baltic Osseointegration Academy Congress: 29 September – 1 October 2011 Kaunas, Lithuania.
2. Kubilius M, Juodzbaly G. Mandibular canal assessment analysis: analysis of digital orthopantomographs. The 4th International Baltic Osseointegration Academy Congress: 7-8 September 2012, Kaunas, Lithuania.
3. Juodzbaly G, Kubilius M, Daugela P. New look at three-dimensional jawbone anatomy evaluation: comprehensive clinical-radiological classifications. The 5th International Baltic Osseointegration Academy Congress: 13-14 September 2013, Kaunas, Lithuania.

4. Kubilius M, Juodzbaly G. Systematization of Patients Radiological Assessment in Implant Dentistry (Poster presentation). III CONGRESO INTERNACIONAL Sociedad Científica de Odontología Implantológica 27–29 de marzo de 2014 Granada: 27–29 March 2014, Granada, Spain.
5. Kubilius M, Juodzbaly G. Peculiarities of diagnostic imaging in posterior mandible. National Baltic Osseointegration Academy Conference: 05 September 2015, Kaunas, Lithuania.

MANUSCRIPTS

Manuscript I related to study I

Dentomaxillofacial Radiology (2016) 45, 20160079
© 2016 The Authors. Published by the British Institute of Radiology
birpublications.org/dmfr

RESEARCH ARTICLE

Descriptive study of mandibular canal visibility: morphometric and densitometric analysis for digital panoramic radiographs

¹Marius Kubilius, ¹Ričardas Kubilius, ²Vaidas Varinauskas, ³Rimantas Žalinkevičius, ⁴Tolga F Tözüm and ¹Gintaras Juodžbalys

¹Department of Oral and Maxillofacial Surgery, Faculty of Dentistry, Medical Academy, Lithuanian University of Health Sciences, Kaunas, Lithuania; ²DeoDental Clinic, Drogheda, Republic of Ireland; ³Institute of Endocrinology, Medical Academy, Lithuanian University of Health Sciences, Kaunas, Lithuania; ⁴Department of Periodontics, College of Dentistry, University of Illinois at Chicago, Chicago, IL, USA

Objectives: To assess the visibility of the mandibular canal (MC) morphology in different jaw dental segments (JDSs) in relation to morphometric and densitometric parameters on digital panoramic radiographs (DPRs).

Methods: 32 DPRs (155 JDSs) were selected randomly after retrieval. MC visibility in conjunction with superior and inferior border visibility was scored on a 5-point scale in four places on the JDS—that is, for the medial, distal, superior and inferior MC parts. Morphometric and densitometric analyses were made horizontally and vertically in the JDS region. Descriptive statistics, Fisher's exact test, Mann-Whitney *U* test and additional tests were performed.

Results: There was no significant difference in MC visibility for the superior, inferior, medial and distal parts of the JDSs. Statistically significant ($p < 0.05$) differences were identified between particular visibility scores of the superior and inferior MC borders. In 22.0–24.7% of JDSs, the superior MC border was not visible, more than twice as often as the inferior MC border was not visible (9.1–10.2%). The visibility of superior and inferior MC borders in JDSs was not related to the morphometric or densitometric assessment parameters, or to age, gender, JDS location, condition or the visibility of neighbouring MC parts or contralateral JDSs.

Conclusions: DPRs failed to provide MC visibility based on a single factor. Particular differences were identified between the levels of visibility of the superior and inferior MC borders. More advanced radiological investigation methods could be required for the evaluation of about 25% of JDSs when superior MC border identification is obligatory.

Dentomaxillofacial Radiology (2016) **45**, 20160079. doi: 10.1259/dmfr.20160079

Cite this article as: Kubilius M, Kubilius R, Varinauskas V, Žalinkevičius R, Tözüm TF, Juodžbalys G. Descriptive study of mandibular canal visibility: morphometric and densitometric analysis for digital panoramic radiographs. *Dentomaxillofac Radiol* 2016; **45**: 20160079.

Keywords: mandible; alveolar nerve, inferior; radiography, panoramic; densitometry; dental implants

Introduction

Dental implant surgery is a widely accepted and increasingly frequent treatment method in dentistry, but it can involve many complications. Injury to the inferior

alveolar nerve (IAN) is one of the most serious complications in implant dentistry. IAN injury is a predominantly iatrogenic complication with reported incidence of up to 40%.¹ Furthermore, IAN is the most commonly injured peripheral branch of the trigeminal nerve (64.4%).² Intraoperative pain, bleeding and

Correspondence to: Mr Marius Kubilius. E-mail: mariuskubilius@yahoo.com
Received 20 February 2016; revised 30 April 2016; accepted 9 May 2016

temporary or permanent post-operative anaesthesia, paraesthesia, hypaesthesia or dysaesthesia can follow such an injury. Pre-operative radiological planning is obligatory for interventions in the posterior mandible to minimize the IAN injury rate.

Opinion leaders and responsible organizations worldwide periodically provide guidelines for the application of diagnostic imaging in implant dentistry.³⁻⁶ The guidelines have been adapted many times in particular countries or regions based on particular scientific data and laws. The authors of the present study operated according to guidelines set forth by the European Commission and European Association for Osseointegration.^{3,5}

Panoramic imaging has a wide range of applications and is accepted for the evaluation of mandibular canal (MC) visibility despite the existence of more accurate investigation methods (e.g. CBCT).⁷ Panoramic imaging lacks three-dimensional visualization and suffers from vertical and horizontal magnification.⁸ A previous panoramic radiography quality evaluation study⁹ discusses possible positioning, image taking and processing errors as well as errors due to anatomical abnormalities, but these images commonly have normal or higher level quality⁹ and are recommended for examination in implant dentistry. Despite the possible shortcomings of panoramic imaging, accurate endosseous dental implant planning by means of panoramic radiographs reduces the risk for IAN injury and subsequent function impairment to a non-significant level.^{10,11} Treatment planning is exclusively unique because MC location and course are individual. MC visibility on panoramic radiographs changes from the mandibular foramen to the mental foramen.¹² The identification of fine anatomical structures on radiographs in the implant site is a delicate task for dental professionals. Juodzbaly and Raustia¹³ proposed to use the term "jaw dental segment" (JDS) for more accurate jaw segment identification and related investigations.

The use of digital panoramic imaging is becoming widespread due to improvements to image quality and after the introduction of dedicated software for image manipulation.¹⁴ Although MC visibility changes throughout the course of the MC, the more precise evaluation of JDS by means of dedicated digital panoramic radiographs (DPRs) could provide more details with regard to possibilities for MC visibility. Manufacturers even provide tools for densitometric analysis of bone density on panoramic radiographs. The clinician hopes to benefit from these technologies. Unfortunately, we could not find in the literature even one source for comprehensive MC region assessment with DPR using vertical morphometric measurements of the MC and surrounding bone nor a source using vertical or horizontal densitometric measurements of the MC and neighbouring regions to allow identification of the acquired parameters' relationship to MC visibility. Therefore, the present study was initiated to assess whether the morphometric measurements of the MC

and surrounding bone and specific patterns of densitometric value changes could be the guide for detecting the MC and its walls, even in cases of poor visibility.

The aim of the present study was to assess the visibility of the MC morphology in different JDSs in relation to morphometric and densitometric parameters on DPRs.

Methods and materials

Patient selection

Caucasian patients were selected randomly for the study at the Department of Oral and Maxillofacial Surgery (Lithuanian University of Health Sciences, Kaunas, Lithuania) from among patients needing panoramic imaging for pre-operative planning of surgery. Patients were asked for medical and dental history to reveal any unsuitability for the study. All subjects had permanent dentition, were systematically healthy or with mild systemic diseases (American Society of Anaesthesiologists I or II) and had no history of mandibular traumas or surgical interventions in the regions of the evaluated JDSs (e.g. lateralization of IAN; the exception was removal of a tooth). Exclusion criteria were active periodontal diseases, current periodontal or orthodontic treatment, and inability to sign the informed consent. Ethical approval (number BE-2-76) was retrieved from the Kaunas Regional Biomedical Research Ethics Committee (Lithuania). Permission for personal data management (number 2R-4170) was obtained from the ethical State Data Protection Inspectorate. Written permissions to participate in the study were obtained from randomly selected subjects.

Panoramic radiographs

All radiographs in this study were taken with a Kodak 9000[®] Extraoral Imaging System (Kodak Dental Systems, Carestream Health Inc., Rochester, NY). According to the manufacturer's manual, 68–73 kV, 10–12 mA and 6 mA were set, and the exposure time was 13.5–14.4 s. Patients were positioned in a standardized manner according to the manufacturer's recommendations to reduce positional errors. Kodak Dental Imaging Software v. 6.12.18.1 (Carestream Health Inc) was used for image analysis. Evaluation was performed by one trained and calibrated oral surgeon on a 29.9-inch display (Coronis Fusion 4MP; Barco N.V, Kortrijk, Belgium) at a distance of 60 cm from the screen in dimmed room conditions. DPR inclusion criteria were based on image quality analysis; images considered optimal and adequate for diagnosis were suitable for further evaluation.⁹ The main errors were positioning (e.g., patient movement or patient positioning asymmetry in any direction) and image taking or processing errors such as the image not being at the optimal contrast or density. If the DPR did not satisfy the mentioned quality requirements or had errors due to anatomical abnormalities, such as an unidentified

mental foramen or a bifid MC, it was rejected from further evaluation.

Mandibular canal visibility and jaw dental segment evaluation protocol

MC visibility assessment in relation to morphometric and densitometric parameters of the jaw bone on DPRs were made based on the JDS pattern.¹³ This is defined as a vertically cut jaw segment including tooth, alveolar bone and basal bone (Figure 1). The location of bone suitable for implantation is identical with the former location of a tooth in the jaw. The number of the JDS describing the position of a planned implant in the jaw can be shown. If the JDS is edentulous, the term “edentulous jaw segment” is used. On DPR, it is possible to assess only two-dimensional JDS parameters: height and length. The height of JDS is defined as the distance between the alveolar crest and inferior border of the mandible (Figure 1). The medial and distal borders of the JDS are vertical dividing lines between the evaluated JDS and the medially and distally located JDS borders, respectively.

JDS inclusion criteria were left and right mandibular first and second premolar (PM₁ and PM₂) and first and second molar (M₁ and M₂) jaw segments in which the MC was in an independent form condition that was dentate or edentulous. JDS exclusion criteria were the presence of mental foramen; impacted tooth or wisdom tooth; dental implant; overlapping JDSs; teeth with <1.0 mm distance between the lamina dura of neighbouring roots or <2.0 mm distance between the root apex and the MC; artefacts or bone pathology (e.g. cysts, inflammation-induced osteosclerosis) presented in any region of the JDS; less than 6 months since tooth extraction; longitudinal tooth axis and mandibular inferior ridge formed at an angle of <60°; and mediolateral

length of the edentulous JDS that did not correspond to the mediolateral length of the contralateral tooth crown (if the contralateral JDS was edentulous, then the average of the mediolateral crown values was used).¹⁵

Mandibular canal visibility analysis

The radiographic image of the MC on DPR is defined as a dark ribbon between two white lines—the bony walls (borders) of the MC.¹² MC visibility was scored in a multifunction window (the “measurements” tool was selected without additional settings) for each JDS in the four parts: medial superior, medial inferior, distal superior and distal inferior (Figure 2). Since many anatomical variations can alter the common pattern of MC detection through the course, the visibility scores of the MC part for each JDS were characterized (Figure 3) as 5 (good), 4 (moderate), 3 (poor), 2 (MC border is not visible, but visibility of the dark ribbon is good) or 1 (MC border is not visible, but visibility of the dark ribbon is moderate). A MC part with an identified MC border was scored as 5 or 4, whereas a detectable MC part with unidentified borders was scored as 2 or 1. An unidentified MC part was scored as 3.

Morphometric analysis

Vertical JDS evaluation was performed using the “measurements” tool without additional adjustments in the medial and distal parts of the segment perpendicular to the inferior mandibular ridge. The centre of the JDS could not be evaluated properly according to the investigation protocol because dentate JDS contains root (s). Figure 4 shows the vertical measurements that were assessed medially and distally for each JDS: (a) the height (H) from the alveolar crest (AC) to the MC dark ribbon (H-AC-MC), including the superior MC border; (b) the height of the MC (H-MC), corresponding to the MC dark ribbon height; (c) the height from the lowest

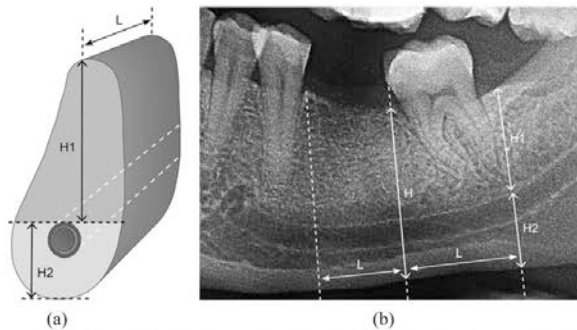


Figure 1 Jaw dental segment. (a) Drawing and (b) digital panoramic radiograph showing jaw dental segment (JDS). H, the height of the JDS: the distance between the crest of alveolar ridge and inferior ridge of the mandible; H1, the alveolar bone: the distance from the crest of alveolar ridge to the superior border of the mandibular canal (MC); H2, the basal bone: the distance from the superior border of the MC to the inferior ridge of the mandible; L, the length of the JDS: the distance between vertical lines that divides medial and distal borders of the JDS between the evaluated JDS and the medially and distally located JDSs borders, respectively.

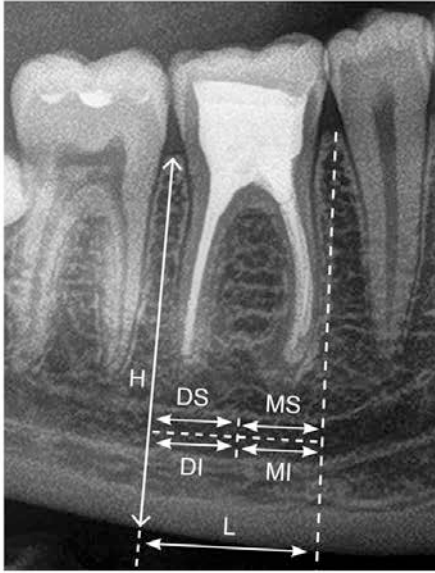


Figure 2 Jaw dental segment (JDS) with mandibular canal parts for visibility evaluation. DI, distal inferior part; DS, distal superior part; H, the height of the JDS; L, the length of the JDS; MI, medial inferior part; MS, medial superior part.

point of the MC dark ribbon to the superior border of the inferior cortical bone (IB) (H-MC-IB); (d) the height of the inferior cortical bone (H-IB); and (e) the height of the mandible (H-AC-IB). Accepted measurement error was ± 0.1 mm.

Densitometric analysis

The analysis was made in a multifunction window with the “densitometric analysis” tool selected. The “sharp



Figure 3 Digital panoramic radiograph showing samples of the visibility scores of mandibular canal (MC) parts: 5, good; 4, moderate; 3, poor; 2, MC border is not visible, but visibility of the dark ribbon is good; 1, MC border is not visible, but visibility of the dark ribbon is moderate.

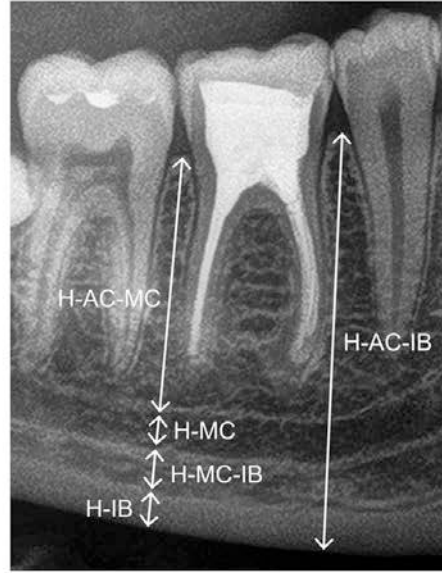


Figure 4 Morphometric measurements. H-AC-MC, the height from the alveolar crest to the mandibular canal (MC) dark ribbon, including superior MC border; H-MC, the height of the MC, corresponding to the MC dark ribbon height; H-MC-IB, the height from the lowest point of the MC dark ribbon to the superior border of the inferior cortical bone; H-IB, the height of the inferior cortical bone; H-AC-IB, the height of the mandible.

enhancement” tool was activated for standardization of measurements, and no additional adjustments were used. Figure 5 shows vertical and horizontal measurements in the region of the JDS. The following vertical (V) measurements were made medially and distally: (a) from the alveolar crest in the trabecular bone to the bone 2.0 mm over the MC (AC-MC-V); (b) in the MC region (MC-V); (c) from the trabecular bone below the MC to the superior border of the inferior cortical bone (MC-IB-V); (d) in the inferior cortical bone region (IB-V); (e) from the alveolar crest in the trabecular bone to the end of the inferior cortical bone (AC-IB-V); and (f) at two bone density peaks, the superior MC peak (SMCP) and the inferior MC peak (IMCP), corresponding to the borders of the MC. Horizontal (Ho) densitometric measurements (Figure 5) within JDS mediolateral length were (a) 2.0 mm above the MC (AC-MC-Ho) (the measurement was not taken if the visibility of the superior MC border was poor (the border was not visible)); (b) the MC region (MC-Ho); (c) the trabecular bone below the MC (MC-IB-Ho); (d) the inferior cortical bone region (IB-Ho); (e) 2.0 mm below the superior cortical bone of the edentulous JDS (or the

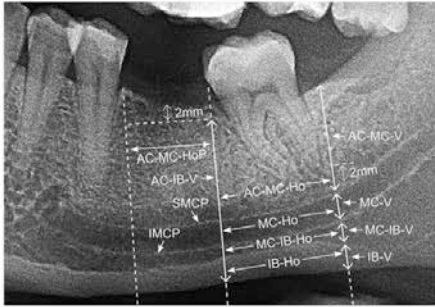


Figure 5 Densitometric measurements. Vertical densitometric measurements: AC-MC-V, from the alveolar crest in the trabecular bone to the bone 2.0 mm over the mandibular canal (MC); MC-V, in the MC region; MC-IB-V, from the trabecular bone below the MC to the superior border of the inferior cortical bone; IB-V, in the inferior cortical bone region; AC-IB-V, from the alveolar crest in the trabecular bone to the end of the inferior cortical bone; SMCP, at the superior MC peak corresponding to the border of the MC; IMCP, at the inferior MC peak corresponding to the border of the MC. Horizontal densitometric measurements: AC-MC-Ho, 2.0 mm above the MC; MC-Ho, the MC region; MC-IB-Ho, the trabecular bone below the MC; IB-Ho, the inferior cortical bone region; AC-MC-HoP, 2.0 mm below the superior cortical bone of the edentulous jaw dental segment (JDS) (or mathematical average of horizontal measurements in medial and distal parts of the dentate JDS trabecular bone 2.0 mm below the superior cortical bone) when visibility of the MC superior border is poor.

mathematical average of horizontal measurements in the medial and distal parts of the dentate JDS trabecular bone 2.0 mm below the superior cortical bone) when visibility of the MC superior border was poor (AC-MC-HoP). The vertical densitometric analysis line could not have an angle of $>30^\circ$ and must be without overlapping lamina dura or tooth root when artefacts or anatomical structures were present in the region of measurement. Accepted measurement error was ± 5 relative measurement units.

MC visibility and densitometric and morphometric analysis results were assessed additionally for possible significant differences between patients' age, gender, JDS condition, side of the mandible or number.

Data and statistical analysis

Statistical analysis was performed by means of IBM SPSS® v. 20.0 for Windows (IBM Corp., New York, NY; formerly SPSS Inc., Chicago, IL). A Kolmogorov–Smirnov test was used for data (distribution of patients according to age) normality evaluation. The sample size was selected randomly using the criteria $\alpha = 0.05$ (confidence level) and $\beta = 0.8$ (power of the study). The sample size was calculated by means of a sample size calculator in the survey software (Creative Research System, Sebastopol, CA). The three-sigma rule was applied for data inclusion before further analyses. The data are presented as mean \pm standard error (SE) in millimetres.

Repeated MC visibility evaluations were tested for agreement using Cohen's kappa coefficient. Investigation was simplified for intraobserver agreement evaluation: if an MC part was identified (previous scale grades of 5, 4, 2 or 1), then the visibility score was 1 (logical); if MC visibility was poor (previous scale grade of 3), then the score was 0 (logical).

Descriptive statistics was applied for the morphometric, densitometric and MC visibility analysis. Fisher's exact test served for the MC border parts with the same visibility score comparison. A Pearson χ^2 test was used to compare samples of categorical variables. Differences between the two independent samples were calculated using the Mann–Whitney *U* test.

Statistical significance was considered for *p*-values < 0.05 .

Results

The primary sample consisted of 101 patients of Caucasian race. 69 DPRs (68.3%) were scored less than “adequate for diagnosis”⁹ and were excluded from subsequent evaluation. 32 panoramic radiographs (31.7%) met the requirements of the investigation (mean age of the patient in years 43.7 ± 2.0 , range 17–64 years). A total of 155 JDSs were evaluated from the 32 DPRs.

The Kolmogorov–Smirnov test showed normally distributed data ($d = 0.09$, $p > 0.05$) of the sample (distribution of patients by age). Distribution of patients of both genders by age was homogeneous. No statistically significant differences ($p > 0.05$) were identified between JDS condition (edentulous or dentate) and JDS number.

Mandibular canal visibility analysis results

Intraobserver agreement (Cohen's kappa coefficient) for the MC visibility evaluation was almost perfect (Table 1).

Table 2 shows the distribution of MC visibility scores according to the MC border part evaluation. The predominant MC visibility score was 4, with a mathematical average of 40.7%. The most frequent superior MC border visibility value was 4 (42.6–43.0%), and the most common inferior MC visibility value was 5 (43.9–49.5%). The most uncommon MC visibility value was 2 (1.0–7.0%). The medial inferior MC part had no visibility value of 2. In 22.0–24.7% of JDSs, the superior

Table 1 Cohen's kappa coefficients (κ) for the visibility of the mandibular canal (MC) parts

MC part in JDS	κ	CI
Medial superior	0.96 ^a	0.91–1.01
Medial inferior	0.97 ^a	0.92–1.01
Distal superior	0.97 ^a	0.92–1.01
Distal inferior	0.88 ^a	0.80–0.97

CI, confidence interval by 95%; JDS, jaw dental segment.

^aAlmost perfect agreement = 0.81–0.99.

Table 2 Mandibular canal (MC) visibility analysis results

Visibility scores	MC part in JDS			
	Medial superior (I)	Medial inferior (II)	Distal superior (III)	Distal inferior (IV)
1	21.0% I vs II $p < 0.001$	7.1% II vs III $p < 0.001$	21.8% III vs IV $p < 0.001$	2.0% I vs IV $p < 0.001$
2	7.0%	–	3.0% III vs IV $p = 0.16$	1.0% I vs IV $p < 0.001$
3	22.0% I vs II $p < 0.01$	10.2% II vs III $p < 0.03$	24.7% III vs IV $p < 0.002$	9.1% I vs IV $p < 0.006$
4	43.0% I vs II $p = 0.24$	38.8% II vs III $p = 0.23$	42.6% III vs IV $p = 0.23$	38.4% I vs IV $p = 0.22$
5	7.0% I vs II $p < 0.001$	43.9% II vs III $p < 0.001$	7.9% III vs IV $p < 0.001$	49.5% I vs IV $p < 0.001$

JDS, jaw dental segment.

Data are provided as a percentage (%) of the sum of visibility scores of the particular MC border part from all visibility scores of the particular border. Fisher's exact test results (p -value) between the indicated groups are provided below the percentage line.

Statistically non-significant differences were identified between groups I vs III and II vs IV ($p > 0.05$) and were not provided in the table.

MC border was not visible, more than twice as often as the inferior MC border was not visible (9.1–10.2%). The superior MC border was not visible in 22.0% of the medial parts and 24.7% of the distal parts in all evaluated JDSs. Statistically non-significant differences were identified between the visibility scores for the medial and distal superior and the medial and distal inferior MC border parts (Fisher's exact test, $p > 0.05$). Statistically significant differences were identified between particular MC visibility scores for the medial superior and medial inferior MC border parts (Fisher's exact test, $p < 0.01$), as well as between the distal superior and distal inferior MC border parts (Fisher's exact test, $p < 0.01$) (Table 2).

No significant differences were identified between gender and MC visibility score ($p > 0.05$) or JDS number and MC visibility score ($p > 0.05$) in any MC visibility evaluation part. There were no differences in MC superior border visibility across ages ($p > 0.05$). Significant differences were identified between mean age and visibility scores of 4 and 5 for the medial inferior border ($p = 0.02$). The visibility of the MC medial and distal superior border ($p > 0.05$) and distal inferior border ($p > 0.05$) was independent of JDS condition. MC medial inferior border visibility evaluation scores 5 and 3 were dependent on the JDS condition (edentulous or dentate), *i.e.* statistically significant differences were identified (Fisher's exact test, $p = 0.04$, odds ratio = 5.67, 95% confidence interval = 4.05–7.94, p -value two-tailed = 0.02). No differences were revealed between the corresponding MC parts of the JDSs in the visibility evaluation of PM₁ and PM₂ ($p > 0.05$); PM₂ and M₁ ($p > 0.05$); or M₁ and M₂ ($p > 0.05$).

MC visibility of particular JDSs did not reveal differences in the MC visibility of corresponding JDSs in the contralateral mandible side ($p > 0.05$).

Morphometric analysis results and relations to mandibular canal visibility scoring

Table 3 provides morphometric measurement data. The highest SE values were found for the anatomically

most-variable measurements: H-AC-MC and H-AC-IB. The lowest values of SE were achieved for MC height as well as for inferior cortical bone height evaluation.

Morphometric analysis relations to mandibular canal visibility scoring

Analysis of the results revealed statistically non-significant differences between the visibility of the medial superior ($p > 0.05$) as well as the medial inferior MC ($p > 0.05$) part and the morphometric analysis results in the medial part of JDS.

MC visibility revealed significant differences in particular morphometric analysis results (Table 4).

Densitometric analysis results in relation to mandibular canal visibility scoring

Densitometric analysis results are provided in Table 5. Significant differences were identified ($p < 0.05$) between the corresponding results of medial and distal densitometric analyses in the vertical direction of JDS.

Table 3 Jaw dental segment (JDS) morphometric analysis results

Measurement location	Measurement	Mean	SE
Medially	H-AC-MC	15.6	0.4
	H-MC	2.4	0.1
	H-MC-IB	3.8	0.1
	H-IB	3.2	0.1
	H-AC-IB	25.4	0.4
Distally	H-AC-MC	14.1	0.5
	H-MC	2.3	0.1
	H-MC-IB	4.1	0.2
	H-IB	2.8	0.1
	H-AC-IB	23.3	0.4

SE, standard error.

Measurement location, JDS measurement location medially and distally; H-AC-MC, the height from the alveolar crest to the MC dark ribbon, including superior MC border; H-MC, the height of MC, corresponding to the MC dark ribbon height; H-MC-IB, the height from the lowest point of the MC dark ribbon to the superior border of the inferior cortical bone; H-IB, the height of the inferior cortical bone; H-AC-IB, the height of the mandible.

The data are presented as mean, SE in millimetres.

Vertical densitometric analysis in relation to mandibular canal visibility scoring

Non-significant differences were found between the visibility analysis results of the medial superior MC and the densitometric analysis results of the vertical medial part ($p > 0.05$). The results provided no statistically significant differences between the distally evaluated visibility of the inferior MC part and vertical densitometric analysis results in the distal part of the JDS ($p > 0.05$). Statistically significant differences between the MC visibility scores and the vertical densitometric analysis results are provided in Table 6.

Horizontal densitometric analysis in relation to mandibular canal visibility scoring

The results provided statistically non-significant differences between the visibility of the medial superior ($p > 0.05$) as well as distal inferior MC parts ($p > 0.05$) and the horizontal densitometric analysis results of the JDS.

MC visibility evaluation results were significantly different from particular horizontal densitometric analysis results ($p < 0.05$) (Table 7).

Discussion

The “as low as reasonably achievable” principle is of high importance for widespread dental implant surgery. The clinician can choose from several radiographic investigation methods to evaluate the alveolar ridge height and width for prosthetic implant placement. In many cases, a treatment plan cannot be composed without panoramic radiograph evaluation, even for an edentulous JDS in the region of MC, because the H-AC-MC distance must be measured.¹⁵ Precise investigation requires more advanced investigation methods, such as CBCT. Otherwise, there is still discussion about the application of panoramic radiography in clinical practice to facilitate treatment planning. Digital technologies are rapidly replacing

analogue imaging techniques in dentistry. Updates to devices and software are periodically available. The software contains linear measurement tools, including a densitometric analysis tool. We noted the absence of investigations on the possibility of evaluating MC visibility using DPRs. Hence, we aimed to evaluate MC and the visibility of its walls by means of dedicated software (linear and densitometric analysis tools).

It is difficult to achieve optimal- or high-quality panoramic radiographs. Quality requirements were met in only 31.7% of the DPRs in our study. Similarly, Rumberg et al¹⁶ found 33% of their panoramic radiographs to be of acceptable quality. The percentage of the JDSs evaluated in the regions of PM₁, PM₂, M₁ and M₂ cannot be the same because of the study protocol requirements for inclusion. JDSs were not included in the study if they contained the mental foramen. A common horizontal position of the mental foramen (for Caucasian individuals) can be found in the premolar region.¹⁷

Detailed MC evaluation was introduced due to variability of visibility through the course of the MC. The 5-point scale (Figure 3) was suggested during the present study for the comprehensive evaluation of MC visibility for the medial, distal, inferior and superior parts of each JDS. Various 3-, 4- and 5-point MC visibility rating scales have been proposed by investigators.^{7,18,19} Oliveira-Santos et al¹² used two scores for the evaluation of separate MC regions, whereas the overall MC visibility score was the sum of the six evaluated regions. MC depiction in another study was classified into three types for each implant site: visible in the superior and inferior walls; visible in the inferior walls and invisible in the superior walls; or invisible in the superior and inferior walls.²⁰

Agreement between observers' repeated MC visibility evaluations of one investigator's findings (Table 1) was almost perfect (a reflection of consistent measurements throughout the study) and coincided with the results of other investigators' data.¹²

Table 4 Morphometric analysis relations to mandibular canal (MC) visibility scoring

MC part for visibility evaluation	JDS part for morphometric analysis		
	H-AC-MC	H-MC	H-AC-IB
Distal superior	1 [12.8 (0.9)] and 4 [15.2 (0.6)] ($p = 0.01$), 3 [10.2 (0.4)] and 4 [15.2 (0.6)] ($p = 0.04$)	1 [2.4 (0.1)] and 3 [1.7(0.1)] ($p = 0.04$), 3 [1.7 (0.1)] and 4 [2.4 (0.1)] ($p = 0.04$)	1 [22.2 (0.7)] and 4 [24.2 (0.6)] ($p = 0.04$)
Distal inferior	4 [13.3 (1.0)] and 5 [14.6 (0.6)] ($p = 0.04$)	— ^a	— ^a

JDS, jaw dental segment.

MC part for visibility evaluation: JDS MC visibility evaluation in distal superior and distal inferior part (in visibility scores: 1, 2, 3, 4, 5); JDS part for morphometric analysis: JDS measurement part for morphometric analysis [measurement values are presented as mean [standard error (SE)] in millimetres]; H-AC-MC, the height from the alveolar crest to the MC dark ribbon; H-MC, the height of the MC; H-AC-IB, the height of the mandible.

Statistically significant differences are presented: “visibility score [morphometric analysis value (SE)]” and “visibility score [morphometric analysis value (SE)]” “(p -value)”.

“—^a” indicates no statistically significant difference ($p > 0.05$).

Table 5 Jaw dental segment (JDS) densitometric analysis results in vertical and horizontal directions

Measurement location	Measurement direction	Measurement	Mean	SE		
Medially	Vertically	AC-MC-V	106.0	2.4		
		MC-V	89.2	2.8		
		MC-IB-V	89.2	2.8		
		IB-V	97.7	2.7		
		AC-IB-V	100.4	2.3		
		SMCP	108.1	3.1		
		IMCP	105.2	2.6		
		Distally	Vertically	AC-MC-V	122.7	2.5
				MC-V	103.1	2.8
				MC-IB-V	97.4	2.5
IB-V	100.4			2.1		
AC-IB-V	109.8			2.0		
SMCP	117.8			3.1		
IMCP	114.1			2.6		
Horizontally	AC-MC-Ho			108.4	3.1	
	MC-Ho			93.1	2.4	
	MC-IB-Ho			92.3	2.6	
	IB-Ho	101.5	2.2			
		AC-MC-HoP	111.2	4.4		

SE, standard error.

Measurement location, JDS measurement location medially and distally; Measurement direction, vertically and horizontally; Measurement: AC-MC-V, from the alveolar crest in the trabecular bone to the bone 2.0 mm over the MC; MC-V, in the MC region; MC-IB-V, from the trabecular bone below the MC to the superior border of the inferior cortical bone; IB-V, in the inferior cortical bone region; AC-IB-V, from the alveolar crest in the trabecular bone to the end of the inferior cortical bone; SMCP, at the superior MC peak corresponding to the border of the MC; IMCP, at the inferior MC peak corresponding to the border of the MC; AC-MC-Ho, 2.0 mm above the MC; MC-Ho, the MC region; MC-IB-Ho, the trabecular bone below the MC; IB-Ho, the inferior cortical bone region; AC-MC-HoP, 2.0 mm below the superior cortical bone of the edentulous JDS (or mathematical average of horizontal measurements in medial and distal parts of the dentate JDS trabecular bone 2.0 mm below the superior cortical bone) when visibility of the MC superior border is poor.

Measurement values are presented as mean, SE (standard error) in relative measurement units.

The different visibility of the MC borders in the mediolateral and vertical directions was confirmed by the current study (Table 2). The most uncommon MC visibility score was two for the evaluation of the inferior and superior MC borders, and the MC tended to have

better visibility when the borders were present. This tendency agrees with other investigations, showing the importance of the MC border for MC visibility.^{12,21,22}

The superior medial and superior distal parts of the MC border had visibility score 3 in 22.0% and 24.7% of the

Table 6 Vertical densitometric analysis in relation to mandibular canal (MC) visibility scoring

MC part for visibility evaluation	JDS part for vertical densitometric analysis	AC-MC-V	MC-V	MC-IB-V	IB-V	AC-IB-V	SMCP	IMCP
Medial inferior	-	4 [97.1 (4.2)]	4 [97.1 (4.2)]	-	1 [111.4 (5.6)]	3 [115.7 (7.0)]	1 [122.4 (7.5)]	-
		and 5 [81.5 (3.9)] ($p = 0.01$)	and 5 [81.5 (3.9)] ($p = 0.01$)		and 5 [89.6 (4.3)] ($p = 0.03$) 3 [121.2 (4.2)] and 4 [98.6 (4.2)] ($p = 0.02$) 3 [121.2 (4.2)] and 5 [89.6 (4.3)] ($p = 0.01$)	and 5 [95.1 (3.5)] ($p = 0.04$)	and 5 [99.3 (4.8)] ($p = 0.04$) 4 [114.3 (4.1)] and 5 [99.3 (4.8)] ($p = 0.02$)	
Distal superior	-	4 [119.7 (3.5)]	4 [119.7 (3.5)]	4 [91.7 (3.7)]	4 [95.3 (3.2)]	1 [107.0 (4.5)]	-	4 [110.3 (3.4)]
		and 5 [142.0 (8.5)] ($p = 0.03$)	and 5 [142.0 (8.5)] ($p = 0.03$)	and 5 [110 (7.6)] ($p = 0.04$)	and 5 [111.5 (2.2)] ($p = 0.04$)	and 5 [124.6 (5.4)] ($p = 0.04$) 4 [106.9 (2.6)] and 5 [124.6 (5.4)] ($p = 0.01$)		and 5 [127.4 (6.8)] ($p = 0.04$)

JDS, jaw dental segment; SE, standard error.

MC part for visibility evaluation, JDS MC visibility evaluation in medial inferior and distal superior parts (in visibility scores: 1, 2, 3, 4, 5); JDS part for vertical densitometric analysis: JDS measurement part for vertical densitometric analysis [measurement values are presented as mean (SE) in relative measurement units]; AC-MC-V, from the alveolar crest in the trabecular bone to the bone 2.0 mm over the MC; MC-V, in the MC region; MC-IB-V, from the trabecular bone below the MC to the superior border of the inferior cortical bone; IB-V, in the inferior cortical bone region; AC-IB-V, from the alveolar crest in the trabecular bone to the end of the inferior cortical bone; SMCP, at superior MC peak corresponding to the border of MC; IMCP, at inferior MC peak corresponding to the border of MC.

Statistically significant results are presented: "visibility score [vertical densitometric analysis value (SE)]" and "visibility score [vertical densitometric analysis value (SE)]" " $(p\text{-value})$ ".

"-" indicates no statistically significant difference.

Table 7 Horizontal densitometric analysis in relation to mandibular canal (MC) visibility scoring

MC part for visibility evaluation	JDS part for horizontal densitometric analysis		
	MC-IB-Ho	IB-Ho	AC-MC-HoP
Medial inferior	— ^a	1 [113.9 (6.5)] and 5 [94.5 (3.6)] (<i>p</i> = 0.04), 3 [112.2 (5.0)] and 5 [94.5 (3.6)] (<i>p</i> = 0.02)	1 [133.9 (12.0)] and 4 [96.0 (7.2)] (<i>p</i> = 0.03)
Distal superior	4 [85.6 (3.6)] and 5 [108.2 (9.0)] (<i>p</i> = 0.02)	3 [106.7 (3.9)] and 4 [96.4 (3.1)] (<i>p</i> = 0.04)	— ^a

JDS, jaw dental segment.

MC part for visibility evaluation, JDS mandibular canal visibility evaluation in medial inferior and distal superior parts [visibility scores (1, 2, 3, 4, 5) in pairs]; JDS part for horizontal densitometric analysis, JDS measurement part for horizontal densitometric analysis; MC-IB-Ho, the trabecular bone below the MC; IB-Ho, the inferior cortical bone region; AC-MC-HoP, 2.0 mm below the superior cortical bone of the edentulous JDS (or mathematical average of horizontal measurements in medial and distal parts of the dentate JDS trabecular bone 2.0 mm below the superior cortical bone) when visibility of the MC superior border is poor (measurement values are presented as mean [standard error (SE)] in relative measurement units).

Statistically significant results are presented: “visibility score [horizontal densitometric analysis value (SE)]” and “visibility score [horizontal densitometric analysis value (SE)]” (“*p*-value”).

“—” indicates no statistically significant difference.

sample, respectively, which is similar to data from investigation of Jung and Cho.²³ Naitoh et al²⁰ found the MC superior wall to be invisible in 31.7% of designed implant sites, whereas the investigation of Klinge et al²⁴ with specimen cadavers demonstrated an invisible MC in 36.1% (the superior and inferior borders of MC were not distinguished). Therefore, it could be concluded from our study that the three-dimensional evaluation of JDSs should be recommended for further analysis of MC in about 25% of JDSs if the identification of the superior MC border is obligatory. In comparison, the MC was not visible in 0.2% of the third molar (M₃) regions, 5.7% of the M₂ regions and 8.2% of the M₁ regions in the CBCT images. Of more importance for this study was that the superior MC border could be identified in 75.3% of distal parts and 78.0% of medial parts. We could not get data from the literature to make a clinical comparison with our results for the medial and distal parts of the MC superior border.

It is interesting to know that anatomically trabeculated MC walls tend to be denser in the upper part than the lower part, but MC visibility does not have a similar tendency, according to our study and to that of Wadu et al.²¹ The last-mentioned sources supplement the statement that radiographic identification of the superior MC border cannot directly relate to MC border density and cannot have a prognostic value for MC damage during implant surgery. Furthermore, the multiple accessory canals directed toward root apices while leaving the MC could have a negative influence on trabeculation and the radiographic visibility of the superior MC border. However, our study results did not confirm the statement that superior or inferior MC border visibility is related to JDS condition in partially dentate lower jaws (with one exception between scores 5 and 3 for the visibility evaluation of the medial and inferior parts of the MC border) and coincide with the CBCT study results.¹²

The present study results confirmed (Table 2) that the superior MC border has lower visibility scores more

often than the inferior MC border. Non-significant differences were identified between numbers of moderate visibility scores for both MC borders. Conversely, the superior border received the score 4 more than twice as often as the inferior border. These data tend to use the inferior MC border as a reference point for the identification of the imagined superior MC border in implant planning, whereas the diameter of the MC can be measured using other parts of the panoramic radiograph or by means of MC height (e.g. from our study). Indeed, this idea should be avoided because of the unreliable data. Wadu et al²¹ recognized and demonstrated a tendency to identify fine or non-existent structures. Furthermore, worldwide studies provide different mean MC diameters from 2 to about 5 mm with probable relation to race.²⁵ Even bifid MC can be identified in 0.08–65% of radiographs, depending on the investigation method.²⁵ The position of the mental foramen varies in horizontal and vertical planes and is related to race. The accessory mental foramen can be identified in 1.4–10% in patients of different populations.¹⁷ Misidentification of these structures may lead to serious complications during implant surgery.

It is important to mention that the current study provides data with no difference between the visibility scores for the medial and distal superior MC borders and the medial and distal inferior MC borders (Table 2). It was considered that the clinician should not expect to observe differences in the visibility of corresponding MC parts of particular JDSs or even between neighbouring or other JDSs—that is, MC visibility did not change through the course, contrary to other investigators' results.^{12,21,23} This statement could not be applied to MC visibility in the mandibular ramus, the M₃ JDS region or the mental canal region, as these regions were not included in our study protocol. There were no differences between any pair of corresponding bilateral JDSs in any of the four visibility evaluations of the MC parts. Similarly, researchers found no difference between MC visibility on the left and right sides.^{12,23}

Our results revealed that MC visibility was not related to the subject's gender or age. Significant differences were only identified between the means of age groups with visibility scores of 4 and 5 for the medial inferior MC border part, but this does not reflect a general tendency. This can be explained by the fact that patients included in the study were systematically healthy or had mild systemic diseases. The bone anatomy and endocrine system function could have influenced MC visibility.²⁶

It is interesting to know that we could not find any analogous studies confirming MC border visibility in relation to the region of each JDS and related regions.

A morphometric analysis of separate JDS parts (Figure 4) was necessary before evaluating the relations between the morphometric analysis and the MC visibility scoring. Our measurements of MC height were within the range demonstrated in the summary that Juodzbalys et al²⁵ provided of MC vertical linear evaluations made by various authors. We found that the mean distance from the alveolar crest to the MC was similar to the review results²⁵ and was the most variable linear height measurement (SE was 0.4–0.5 mm) in the present study. It confirms a widely known requirement for individual implant length planning while alveolar ridge height is variable.

It is important to consider that the morphometric measurements did not correlate with MC visibility in our study (Table 4). For example, no significant differences were identified between the medially evaluated morphometric parameters of JDS and the corresponding MC visibility scores. By contrast, some differences were identified in the distally evaluated morphometric parameters of JDS.

The analysis of MC densitometric assessment data and visible MC depiction revealed controversial results. The corresponding vertical (Table 6) and horizontal (Table 7) densitometry did not provide statistically significant differences from the visibility analysis results in the medial superior parts of the MC, but some differences were found in the distal superior parts. We expected to identify similar differences for the inferior MC border in the mediobasal direction, but the results were the opposite: some significant differences were identified for the inferior medial parts of JDS, whereas no significant differences were identified for the distal parts. The results might have differed for the superior and inferior MC borders due to significant differences in densitometric analysis results for medial and distal JDS

parts in the vertical direction. However, this would not explain the same differences when a comparison was made between MC visibility and horizontal densitometric analysis data. Based on these results, we concluded that the success in visually identifying MC borders did not correlate with the densitometric depiction of the MC borders (peaks).

Our investigation provides results indicating the limited accuracy of the densitometric tool for the possible improvement of radiographic MC identification. Naitoh et al²⁰ found relations between MC depiction in DPRs and bone density in the alveolar region, but they evaluated bone density by multislice CT in HUs. HUs give the relative density of tissue according to a calibrated scale. HUs were found to be stable after quality phantom scanning with an multislice CT scanner.²⁷ To our knowledge, there is no data in the literature regarding the investigation of the densitometric analysis tool used. The region of interest could not be modified (one standard line could be drawn without entering the desirable area). We found this to be a drawback, as a bigger and standardized region of interest should provide more stable results in the investigated region, especially in the region of MC with variable visibility. The densitometric analysis tool was tested with several enhancements that were provided prior to the investigation. The results varied and depended on the chosen enhancement tool. "Sharp enhancement" was chosen to standardize the measurements. We recommend conducting additional investigations for the validation of the densitometric tool with the inclusion of a quality control phantom. If the results are positive, a new investigation with a bigger sample is recommended.

In conclusion, evaluation of the visibility of the MC superior and inferior borders on DPRs depends on multiple factors without priority of gender, age, JDS location and condition, particular mandibular height parameter measurements or anatomically specific area evaluation with the dedicated densitometric analysis tool. The MC visibility of particular JDSs does not change significantly from the MC visibility of medially and distally located neighbouring JDSs. Particular differences between the visibility of the superior and inferior MC borders were identified to produce a clinically more important conclusion: the superior MC border was not visible more than twice as often as the inferior MC border.

References

- Juodzbalys G, Wang HL, Sabalys G. Injury of the inferior alveolar nerve during implant placement: a literature review. *J Oral Maxillofac Res* 2011; 2: e1. doi: <http://dx.doi.org/10.5037/jomr.2011.2101>
- Tay AB, Zuniga JR. Clinical characteristics of trigeminal nerve injury referrals to a university centre. *Int J Oral Maxillofac Surg* 2007; 36: 922–7. doi: <http://dx.doi.org/10.1016/j.ijom.2007.03.012>
- SEDENTEXCT Project. Radiation protection: cone beam CT for dental and maxillofacial radiology. Evidence Based Guidelines. Radiation protection no. 172. Luxembourg: European Commission; 2012 [cited 17 May 2016]. Available from: http://www.sedentexct.eu/files/radiation_protection_172.pdf
- Tyndall DA, Price JB, Tetradis S, Ganz SD, Hildebolt C, Scarfe WC, et al. Position statement of the American Academy of Oral

- and Maxillofacial Radiology on selection criteria for the use of radiology in dental implantology with emphasis on cone beam computed tomography. *Oral Surg Oral Med Oral Pathol Oral Radiol* 2012; **113**: 817–26. doi: <http://dx.doi.org/10.1016/j.oooo.2012.03.005>
5. Harris D, Horner K, Gröndahl K, Jacobs R, Helmrot E, Benic GI, et al. E.A.O. guidelines for the use of diagnostic imaging in implant dentistry 2011. A consensus workshop organized by the European Association for Osseointegration at the Medical University of Warsaw. *Clin Oral Implants Res* 2012; **23**: 1243–53. doi: <http://dx.doi.org/10.1111/j.1600-0501.2012.02441.x>
 6. Bornstein MM, Scarfe WC, Vaughn VM, Jacobs R. Cone beam computed tomography in implant dentistry: a systematic review focusing on guidelines, indications, and radiation dose risks. *Int J Oral Maxillofac Implants* 2014; **29**: 55–77. doi: <http://dx.doi.org/10.11607/jomi.2014suppl.g1.4>
 7. Jacobs R, Mraiwa N, Van Steenberghe D, Sanderink G, Quirynen M. Appearance of the mandibular incisive canal on panoramic radiographs. *Surg Radiol Anat* 2004; **26**: 329–33. doi: <http://dx.doi.org/10.1007/s00276-004-0242-2>
 8. Devlin H, Yuan J. Object position and image magnification in dental panoramic radiography: a theoretical analysis. *Dentomaxillofac Radiol* 2013; **42**: 29951683. doi: <http://dx.doi.org/10.1259/dmfr/29951683>
 9. Choi BR, Choi DH, Huh KH, Yi WJ, Heo MS, Choi SC, et al. Clinical image quality evaluation for panoramic radiography in Korean dental clinics. *Imaging Sci Dent* 2012; **42**: 183–90. doi: <http://dx.doi.org/10.5624/isd.2012.42.3.183>
 10. Bartling R, Freeman K, Kraut RA. The incidence of altered sensation of the mental nerve after mandibular implant placement. *J Oral Maxillofac Surg* 1999; **57**: 1408–12. doi: [http://dx.doi.org/10.1016/S0278-2391\(99\)90720-6](http://dx.doi.org/10.1016/S0278-2391(99)90720-6)
 11. Mehra A, Pai KM. Evaluation of dimensional accuracy of panoramic cross-sectional tomography, its ability to identify the inferior alveolar canal, and its impact on estimation of appropriate implant dimensions in the mandibular posterior region. *Clin Implant Dent Relat Res* 2012; **14**: 100–11. doi: <http://dx.doi.org/10.1111/j.1708-8208.2009.00226.x>
 12. Oliveira-Santos C, Capelozza AL, Dezzoti MS, Fischer CM, Poletti ML, Rubira-Bullen IR. Visibility of the mandibular canal on CBCT cross-sectional images. *J Appl Oral Sci* 2011; **19**: 240–3. doi: <http://dx.doi.org/10.1590/S1678-77572011000300011>
 13. Juodzbalys G, Raustia AM. Accuracy of clinical and radiological classification of the jawbone anatomy for implantation—a survey of 374 patients. *J Oral Implantol* 2004; **30**: 30–9. doi: [http://dx.doi.org/10.1563/1548-1336\(2004\)030<0030:AOCARC>2.0.CO;2](http://dx.doi.org/10.1563/1548-1336(2004)030<0030:AOCARC>2.0.CO;2)
 14. Gijbels F, De Meyer AM, Bou Serhal C, Van den Bossche C, Declercq J, Persoons M, et al. The subjective image quality of direct digital and conventional panoramic radiography. *Clin Oral Investig* 2000; **4**: 162–7. doi: <http://dx.doi.org/10.1007/s007840000059>
 15. Angelopoulos C, Thomas SL, Hechler S, Parisis N, Hlavacek M. Comparison between digital panoramic radiography and cone-beam computed tomography for the identification of the mandibular canal as part of presurgical dental implant assessment. *J Oral Maxillofac Surg* 2008; **66**: 2130–5. doi: <http://dx.doi.org/10.1016/j.joms.2008.06.021>
 16. Rumberg H, Hollender L, Oda D. Assessing the quality of radiographs accompanying biopsy specimens. *J Am Dent Assoc* 1996; **127**: 363–8. doi: <http://dx.doi.org/10.14219/jada.archive.1996.0207>
 17. Juodzbalys G, Wang HL, Sabalys G. Anatomy of mandibular vital structures. Part II: mandibular incisive canal, mental foramen and associated neurovascular bundles in relation with dental implantology. *J Oral Maxillofac Res* 2010; **1**: e3. doi: <http://dx.doi.org/10.5037/jomr.2010.1103>
 18. Lindh C, Petersson A, Klinge B. Visualisation of the mandibular canal by different radiographic techniques. *Clin Oral Implants Res* 1992; **3**: 90–7. doi: <http://dx.doi.org/10.1034/j.1600-0501.1992.030207.x>
 19. Yasar F, Yesilova E, Apaydin B. The effects of compression on the image quality of digital panoramic radiographs. *Clin Oral Investig* 2012; **16**: 719–26. doi: <http://dx.doi.org/10.1007/s00784-011-0587-y>
 20. Naitoh M, Katsumata A, Kubota Y, Hayashi M, Ariji E. Relationship between cancellous bone density and mandibular canal depiction. *Implant Dent* 2009; **18**: 112–18. doi: <http://dx.doi.org/10.1097/ID.0b013e318198da7e>
 21. Wadu SG, Penhall B, Townsend GC. Morphological variability of the human inferior alveolar nerve. *Clin Anat* 1997; **10**: 82–7. doi: [http://dx.doi.org/10.1002/\(SICI\)1098-2353\(1997\)10:2<82::AID-CA2>3.0.CO;2-V](http://dx.doi.org/10.1002/(SICI)1098-2353(1997)10:2<82::AID-CA2>3.0.CO;2-V)
 22. Naitoh M, Yoshida K, Nakahara K, Gotoh K, Ariji E. Demonstration of the accessory mental foramen using rotational panoramic radiography compared with cone-beam computed tomography. *Clin Oral Implants Res* 2011; **22**: 1415–19. doi: <http://dx.doi.org/10.1111/j.1600-0501.2010.02116.x>
 23. Jung YH, Cho BH. Radiographic evaluation of the course and visibility of the mandibular canal. *Imaging Sci Dent* 2014; **44**: 273–8. doi: <http://dx.doi.org/10.5624/isd.2014.44.4.273>
 24. Klinge B, Petersson A, Maly P. Location of the mandibular canal: comparison of macroscopic findings, conventional radiography, and computed tomography. *Int J Oral Maxillofac Implants* 1989; **4**: 327–32.
 25. Juodzbalys G, Wang HL, Sabalys G. Anatomy of mandibular vital structures. Part I: mandibular canal and inferior alveolar neurovascular bundle in relation with dental implantology. *J Oral Maxillofac Res* 2010; **1**: e2. doi: <http://dx.doi.org/10.5037/jomr.2010.1102>
 26. Mirza F, Canalis E. Management of endocrine disease: secondary osteoporosis: pathophysiology and management. *Eur J Endocrinol* 2015; **173**: R131–51. doi: <http://dx.doi.org/10.1530/EJE-15-0118>
 27. Nackaerts O, Maes F, Yan H, Couto Souza P, Pauwels R, Jacobs R. Analysis of intensity variability in multislice and cone beam computed tomography. *Clin Oral Implants Res* 2011; **22**: 873–9. doi: <http://dx.doi.org/10.1111/j.1600-0501.2010.02076.x>



Evaluation of Mandibular Lingual Foramina Related to Dental Implant Treatment With Computerized Tomography: A Multicenter Clinical Study

Yagmur D. Yildirim, DDS, PhD,* Güliz N. Güncü, DDS, PhD,† Pablo Galindo-Moreno, DDS, PhD,‡ Miguel Velasco-Torres, DDS, PhD,§ Gintaras Juodzbalsys, DDS, PhD,|| Marius Kubilius, DDS,¶ Albinas Gervickas, DDS, PhD,‡ Khalid Al-Hezaimi, DDS, MS,** Ra'ed Al-Sadhan, DDS, MS,†† Hasan Güney Yılmaz, DDS, PhD,‡‡ Neset Volkan Asar, DDS, PhD,§§ Erdem Karabulut, PhD,||| Hom-Lay Wang, DDS, MS, PhD,¶¶ and Tolga F. Tözüm, DDS, PhD##

Dental implant placement is a routine and predictable technique for the replacement of missing teeth. Interforaminal region is a good choice for the implant placement to support fixed partial dentures or overdentures. Symphysis is one of the autologous donor graft area in the

Background: Bleeding can be one of the severe complications during implant placement or other surgeries. Presurgical assessment of the area should be performed precisely. Thus, we examined lingual vascular canals of the mandible using dental computerized tomography (CT); define the anatomical characteristics of canals and the relationship with mandibular bone.

Methods: One thousand sixty-one foramina in 639 patients, in 5 dental clinics, were included in this multicenter study. Distance between crest and lingual foramen, tooth apex and lingual foramen, distance from mandibular border, diameter of lingual foramen, canal type, anastomosis, and location of foramen were examined.

Results: Foramen was 18.33 ± 5.45 mm below the bony crest and 17.40 ± 7.52 mm from the mandibular border, with men showing

larger measurements. The mean diameter of lingual foramina was 0.89 ± 0.40 mm; 76.8% canal type was mono; 51.8% patients presented with median lingual canal-foramen (MLC) and 21.1% with lateral lingual foramen. Diameter of MLC was statistically larger.

Conclusions: With a large sample group, results represented that lingual foramina could be visualized with dental CT, providing useful data for mandibular implant surgeries. Findings suggest that vascular canals and several anastomoses exist in the anterior mandible extending through premolar and molar regions as well. It is imperative to consider these vessels with the dental CT before and during the mandibular surgery to prevent threatening hemorrhage. (Implant Dent 2014;23:57-63)

Key Words: dental implant, mandibula, anatomy, tomography, humans, surgery

*Clinical instructor, Department of Periodontology, Faculty of Dentistry, Hacettepe University, Ankara, Turkey.
 †Associate Professor, Department of Periodontology, Faculty of Dentistry, Hacettepe University, Ankara, Turkey.
 ‡Associate Professor, Department of Oral Surgery and Implant Dentistry, University of Granada, Granada, Spain.
 §Assistant Professor, Department of Oral Radiology, University of Granada, Granada, Spain.
 ¶Professor, Department of Maxillofacial Surgery, Lithuanian University of Health Sciences, Kaunas, Lithuania.
 **Research Investigator, Department of Maxillofacial Surgery, Lithuanian University of Health Sciences, Kaunas, Lithuania.
 ††Assistant Professor, Department of Maxillofacial Surgery, Lithuanian University of Health Sciences, Kaunas, Lithuania.
 ‡‡Associate Professor and Engineer Abdullah Bugshan Research Chair for Growth Factors and Bone Regeneration, Department of Periodontics, College of Dentistry, King Saud University, Riyadh, Saudi Arabia.
 §§Associate Professor, Department of Oral Medicine and Diagnostic Sciences, College of Dentistry, King Saud University, Riyadh, Saudi Arabia.
 ¶¶Associate Professor, Department of Periodontology, Faculty of Dentistry, Near East University, Mersin 10, Turkey.
 ##Clinical Instructor, Department of Prosthodontics, Faculty of Dentistry, Gazi University, Ankara, Turkey.
 †††Associate Professor, Department of Biostatistics, Faculty of Medicine, Hacettepe University, Ankara, Turkey.
 ‡‡‡Professor and Director, Department of Periodontics and Oral Medicine, School of Dentistry, The University of Michigan, Ann Arbor, MI.
 ####Professor, Department of Periodontology, Faculty of Dentistry, Hacettepe University, Ankara, Turkey.

Reprint requests and correspondence to: Tolga F. Tözüm, DDS, PhD, Department of Periodontology, Faculty of Dentistry, Hacettepe University, 3rd Floor, Sıhhiye, Ankara 06100, Turkey, Phone: +90-312-305-2237, Fax: +90-312-310 4440, E-mail: tozum@hacettepe.edu.tr

ISSN 1056-6183/14/02301-057
 Implant Dentistry
 Volume 23 • Number 1
 Copyright © 2014 by Lippincott Williams & Wilkins
 DOI: 10.1097/ID.000000000000012

oral cavity in need of excessive ridge augmentations.^{1,2} Submental branch of the facial artery and sublingual branch of the lingual artery supplies this area,

including the sublingual gland, mylohyoid, genioid and genioglossus muscles, mucous membranes of the mouth floor, and the lingual gingiva.^{3,4}



Fig. 1. Dimensional measurements on axial mandibular CT sections. **A**, Distance between crest and lingual foramen. **B**, Distance between tooth apex and lingual foramen. **C**, Vertical distance from the mandibular border to the lingual foramen. Arrow: diameter of lingual foramen.

The submental artery supplies the lymph nodes of the submandibular triangle, the anterior belly of the digastric muscle, and the mylohyoid muscle.^{3,5} Important arterial anastomoses are formed between sublingual and submental arteries and between sublingual and incisive arteries through multiple accessory lingual foramina.⁶ Mental artery, the branch of the inferior alveolar artery, was found to communicate with sublingual artery in the mental

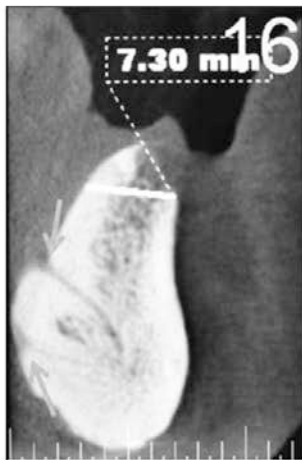


Fig. 2. Bifid lingual canal in the anterior mandible.

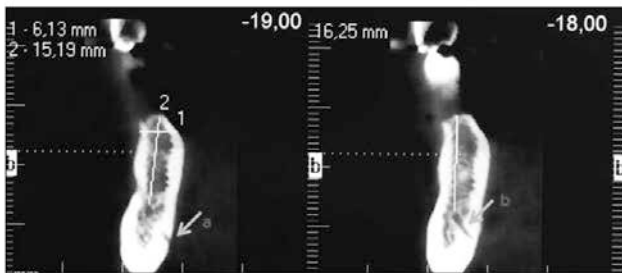


Fig. 3. Arrows: **A**, LLC, **B**, anastomosis between lingual and inferior alveolar artery.

region of the internal mandible.⁷ Although interforaminal region is a relatively safe area to place implants, perforation of the lingual cortex while placing dental implants can cause severe hemorrhage.⁸⁻¹⁷ Additionally with the arterial wound, if drilling ruptures lingual periosteum, damage to anatomical structures in the sublingual space may enhance the bleeding, resulting in the hematoma of the floor of the mouth.⁸ Besides the interforaminal region, the presence of lingual foramen in molar area has been reported as well.¹⁸ Severe hemorrhage was reported during drilling in molar and premolar areas.^{19,20}

Lingual vascular canals of the mandible have been investigated anatomically or by means of computerized tomography (CT).²¹⁻³⁵ Cadaver studies depicted that both submental and sublingual arteries perforate into the mandible through lingual foramen/foramina.^{4,30} Longoni et al³⁴ examined the interforaminal area in 100 CTs of the Caucasian patients. They reported 61% vascular canals ranging in entrance diameters

between 0.3 and 1.1 mm (mean, 0.6 ± 0.2 mm).³⁴ Katakami et al¹⁸ reported the presence of arterial in the molar area and measured a mean diameter of 0.88 ± 0.2 mm. Position of the foramen was reported to be 7.06 mm from the border of the mandible.¹⁸ Some authors classified the lingual foramina of the mandible as median lingual canal-foramen (MLC) and lateral lingual canal-foramen (LLC).^{5,21,34,35} LLC diameters were found slightly lower than the midline values.^{5,6,22}

After tooth extraction, bone loss is primarily horizontal from the labial side. This resorption pattern results in a linguo-angulated trajectory of mandible. If atrophic inclined mandible is not considered well before implant placement, risk of lingual perforations may increase. Moreover, there is an existing osseous concavity, sublingual fossa, extending to the first premolar region. Dental CT is a well-known and frequently used imaging technique to depict bony architecture and surrounding anatomical structures. It is a valuable tool for ridge mapping and diagnosis of pathologies of the jaws, teeth, and maxillofacial

Table 1. Descriptive Statistics

	Women	Men	P	Total
Distance between crest and artery mm	17.64 ± 5.27	19.30 ± 5.57	0.000*	18.33 ± 5.45
Vertical distance from mandibular border mm	16.98 ± 8.35	17.97 ± 6.15	0.034*	17.40 ± 7.52
Distance between tooth apex and artery mm	9.44 ± 4.32	10.94 ± 4.33	0.000*	10.06 ± 4.38
Vertical size (diameter) of foramen mm	0.87 ± 0.42	0.91 ± 0.37	0.086	0.89 ± 0.40

One thousand sixty-one lingual foramen on axial mandibular CT sections were examined for the following measurements in Table 1. Statistically significant differences between men and women were detected in all parameters, except vertical size of the foramen. * $P < 0.05$.

Table 2. Vertical Size (Diameter) of Foramen

	Men				Women				Total			
	≤1 mm		>1 mm		≤1 mm		>1 mm		≤1 mm		>1 mm	
	n	%	n	%	n	%	n	%	n	%	n	%
Cyprus	23	27.1	62	72.9	23	26.4	64	73.6	46	26.7	126	73.3
Saudi Arabia	25	59.5	17	40.5	44	91.7	4	8.3	69	76.7	21	23.3
Spain	162	91.5	15	8.5	209	91.3	20	8.7	371	91.4	35	8.6
Lithuania	29	61.7	18	38.3	61	67	30	33	90	65.2	48	34.8
Turkey	85	88.5	11	11.5	141	88.7	18	11.3	226	88.6	29	11.4
Total	324	72.5	123	27.5	478	77.9	136	22.1	802	75.6	259	24.4

The distribution of diameters in 5 different countries was shown in this table. The diameter of foramina was classified as ≤1 and >1 mm to determine the risk of severe hemorrhage. Of the 1061 foramina, 75.6% were ≤1 mm and 24.4% were >1 mm.

Table 3. Artery Type According to Gender

	Mono (%)	Bifid (%)	Triple (%)
Male	78.1	18.7	3.2
Female	75.9	20.9	3.2
Total	76.8	20.0	3.2

About 43.34% of the patients have 1 lingual foramen and 56.65% have more than 1. The most prevalent artery type was mono-type in men and women, in percentages of 78.1% and 75.9%, respectively. The least artery type was triple type in both the genders.

area.³⁶ Presurgical 3-dimensional assessment of the area is highly suggested to achieve favorable prosthetic angulations and avoid complications.^{24,37}

Thus, we aimed to examine lingual vascular canals of the mandible using reformatted 3-dimensional axial CT sections and define the anatomical characteristics of the canals and their relationship with mandibular bone to provide useful preoperative information.

MATERIALS AND METHODS

A total of 639 partially dentulous and/or edentulous patients (266 men and 373 women, aged 18–83 years; mean 50 ± 14.18 years) scheduled for implant insertion in 5 dental clinics (185 CTs in Turkey, 173 CTs in Spain, 162 CTs in Cyprus-Turkey, 61 CTs in Lithuania, and 51 CTs in Saudi Arabia) were enrolled in this study. One thousand sixty-one lingual foramina of 639 patients were examined. One calibrated

investigator (Y.D.Y., H.G.Y., M.V.-T., R.A.-S., and G.J.) at each center performed all the measurements. Spiral (Siemens AR-SP 40; Siemens, Munich, Germany) and cone-beam CT scans (Imaging Sciences International, Hatfield, PA) achieved in these centers were used in the present study. A detailed research protocol was discussed and agreed before initiation of the study. Measurements were clarified on schematic diagrams between the calibrated investigators (Y.D.Y., H.G.Y., M.V.-T., R.A.-S., and G.J.). CTs with low-quality imaging, such as scattering of the bony borders and pathology, were excluded. One thousand sixty-one lingual foramen on axial mandibular CT sections were examined for the following measurements (Figs. 1–3):

1. Distance between crest and lingual foramen.
2. Distance between tooth apex and lingual foramen if tooth is present at the location of foramen.
3. Vertical distance from the mandibular border.
4. Diameter (vertical size) of lingual foramen.

Lingual vascular canal type was classified as mono, bifid, and triples if the number of bony canal inside the mandible in an axial CT section is only 1, 2, or 3, respectively. If more than 1 canal

is detected, the mean measurements were calculated and recorded as 1 measurement. Occurrence of lingual foramen on both the sides of mandible was noted as bilateral, if not, unilateral. Anastomoses with incisive artery, mental artery, and alveolar inferior artery were evaluated. Dentition status of mandibles and location of lingual foramen were recorded. Location of foramen was determined as the tooth number, observed at the region of that tooth.

In the literature, lingual canal located in or near midline is called MLC and that located in premolar regions is called LLC.²¹ A recent study included the canine teeth into LLC.²¹ Cadaver studies named the canal/foramen as “lateral” if it is not located at the midline.²⁸ In this study, the foramina of the whole mandible was examined rather than the interforaminal area.

Statistical Analyses

All statistical analyses were performed with the center at Hacettepe University with the SPSS for Windows 16.0 software (SPSS, Chicago, IL). Age and sex of the patients were recorded, and the measurements were analyzed according to the age and sex. Mean ± SDs and frequency, percentage were calculated for numerical and categorical variables, respectively. Independent samples *t* test was used to compare the differences between the gender groups.

Table 4. Regional Frequency of Lingual Foramen

	LLC					MLC					LLC					Total	
	17	18	19	20	21	22	23	24	25	26	27	28	29	30	31		32
Teeth	17	18	19	20	21	22	23	24	25	26	27	28	29	30	31	32	
%	0.3	0.1	1.1	4.4	6.9	6.3	5.0	26.9	24.5	3.9	7.3	7.7	3.8	1.4	0.3	0.2	100

Three hundred thirty-one patients presented with foramina only in median part of the mandible, 135 patients only in lateral sides, and 173 patients in both.

Table 5. Descriptive Statistics of MLC and LLC

	Median Lingual Foramen (MLC)		P	Lateral Lingual Foramen (LLC)		P	Total	
	Men	Women		Men	Women		MLC	LLC
Distance between crest and artery mm	19.42 ± 5.98	17.45 ± 5.46	0.000*	19.16 ± 5.04	17.03 ± 5.03	0.003*	18.24 ± 5.75	18.43 ± 5.07
Vertical distance from mandibular border mm	18.44 ± 5.98	17.18 ± 9.93	0.086	17.46 ± 6.30	16.60 ± 5.79	0.123	17.69 ± 8.58	16.99 ± 6.04
Distance between tooth apex and artery mm	11.62 ± 4.13	9.41 ± 3.81	0.000*	9.96 ± 4.42	9.62 ± 5.10	0.508	10.30 ± 4.09	9.77 ± 4.81
Vertical size (diameter) of foramen mm	0.95 ± 0.40	0.90 ± 0.47	0.187	0.87 ± 0.32	0.82 ± 0.35	0.113	0.92 ± 0.44	0.84 ± 0.34

*The only significant difference between MLC and LLC was detected in diameter of foramen; MLC was significantly larger than LLC. P < 0.05.

The correlations between numerical variables were analyzed with Pearson correlation coefficient. $P < 0.05$ was considered statistically significant.

RESULTS

From the 639 mandibular CTs examined, 1061 mandibular lingual foramina were detected. About 20.5% of the mandible was dentate, 10.2% was full edentate, and 69.3% was partially edentate. Foramen was found at a mean distance of 18.33 ± 5.45 mm below the bony crest and 17.40 ± 7.52 mm from the mandibular border. The differences were statistically significant for men and women ($P = 0.000$ and $P = 0.034$, respectively). Distance between tooth apex and lingual artery was 10.06 ± 4.38 mm; the distance was significantly higher in men than women ($P = 0.000$). The mean diameter of lingual foramina was 0.89 ± 0.40 mm (Table 1).

We classified the diameter of foramina as ≤ 1 and > 1 mm to determine the risk of severe hemorrhage. Of the 1061 foramina, 802 were ≤ 1 mm and 259 were > 1 mm and these numbers corresponds to the 75.6% and 24.4% of whole foramina, respectively, where 72.5% of male patients presented with ≤ 1 mm foramina and 27.5% were > 1 mm. It was 77.9% and 22.1%, respectively, in women. The distribution of diameters in 5 different countries was shown in Table 2.

The most prevalent lingual vascular canal type was mono (1 canal), determined in 76.8% of the canals. Approximately 20% was bifid and 3.2% of canals were triple. All the canals detected as bifid and triple were at the midline area. Distributions according to genders were listed in Table 3. About 277 (43.34%) patients have 1 lingual foramen and 362 (56.65%) have more than 1. About 362 patients having multiple foramina presented with the foramina mostly on both the right and the left sides of mandible (60.77% bilaterally and 39.22% unilaterally).

Vascular anastomoses were detected on CT sections in 38.1% of the arteries examined. The frequency of anastomoses, which could be seen with mental foramen, anterior loop, incisive canal, and mandibular canal were as

follows: 2%, 4.5%, 3.7%, and 27.9%, respectively.

Three hundred thirty-one patients (51.8%) presented with foramina only in median part of the mandible, 135 patients (21.1%) only in lateral sides, and 173 patients (27.1%) in both. Regional frequency of lingual foramina was shown in Table 4. The measurements were examined for MLC and LLC separately (Table 5). Diameters of foramen were statistically larger in MLC ($P = 0.002$, $P = 0.000$, respectively). When MLC and LLC were examined according to gender, lingual foramina were found closer to alveolar crest and tooth apex in women on the median part of mandible ($P = 0.000$ for both distance between crest and artery, apex to artery). On the lateral part of the mandible, only distance between crest and artery was larger in men ($P = 0.008$).

The older the patients were, the shorter the vertical distance from mandibular border and distance between crest and foramen ($r = -0.178$, $P = 0.000$; $r = -0.242$, $P = 0.000$, respectively). Age was also negatively correlated with diameter of foramen ($r = -0.188$, $P = 0.000$). Vertical distance from mandibular border and distance between crest and foramen were positively correlated to each other ($r = 0.702$, $P = 0.000$). The distance from tooth apex to foramen was positively correlated with both vertical distance from mandibular border and distance between crest and foramen ($r = 0.340$, $P = 0.000$; $r = 0.559$, $P = 0.000$, respectively).

DISCUSSION

Several case reports have pointed out the life-threatening hematoma in the floor of the mouth because of injury of mandibular lingual vessels mainly occurred in the interforaminal region.^{8-14,16} Profuse bleeding was reported in the premolar and molar region in some case reports but not well examined yet.^{19,20} In this study, we examined the whole lingual foramina with a large group of patients (639 patients with 1061 foramina) by means of dental CT.

The distance to the foramen from the alveolar bone crest was found to be 18.33 ± 5.45 mm, ranging between 1 and 31 mm (MLC, 18.24 ± 5.75 mm; LLC,

18.43 ± 5.07 mm). Mardinger et al³⁸ found this range to be 2 to 26 mm in an anatomical study. The present results were consistent with this study. They dissected 12 hemimandibles, and in 10 of the mandibles, arteries were found in mental area, 9 in second molars, and 12 in canine area; 2 mm distance was measured in mental and molar areas. Because mandibular resorption was unclassified in this study, it can be assumed that in cases of atrophic edentulous ridges, it should be even shorter.

The mean distance from the mandibular border to the foramen was measured to be 17.40 ± 7.52 mm ranging from 1 to 31.2 mm in this study. Several CT studies gave different results.^{18,21,26,30,35} Katakami et al¹⁸ found a mean distance of 7.06 mm ranging between 0.75 and 15.28 mm on 181 patients. Other CT studies reported the mean results for median and LLCs separately. Tagaya et al³⁰ showed a range from 1.1 to 18.4 mm in the medial part and 7.7 mm (2.2–13.7 mm) mean distance from the mandibular border on the lateral side of 200 patients. Gültekin et al³⁵ found a mean distance of 11.6 ± 3 mm for MLCs and 6 ± 1.3 mm for LLC in 26 patients. Kilic et al²⁹ gave a range of 1 to 19 mm (median, 13 mm) for MLC and 2 to 35 mm (median, 7 mm) for LLC. The mean values were 10.2 ± 5.5 mm and 5.4 ± 3.8 mm for MLC and LLC, respectively, in another study of 32 patients.²¹ In this study, the mean values were detected to be 17.69 ± 8.58 mm for MLC and 16.99 ± 6.04 mm for LLC. This higher distance could be because of the complex ethnicity of the study samples (5 different countries), and in our knowledge, this is the first study with such high sample group.

We measured the distance between tooth apex and artery in this study. Immediate implantation into carefully selected extraction sockets shortens the time of therapy. About 3- to 5-mm bone beyond the apex is supportive for primary stability in immediate implantation procedures. The mean distance was measured as 10.06 ± 4.38 mm in this study. Thus, study results reveal that there is enough space for immediate procedures and it is safe with regard to the lingual vessels. However, Froum et al³⁹ performed risk assessment in CT scans

before extraction in the mandibular premolar and molar areas for immediate implant placement. For immediate implant placement, they determined that the amount of necessary bone in apical area should be 6 mm (4 mm for apical anchorage and 2 mm for safety zone). According to their results, 53% to 73% of mandibular premolars and molars presented with high risk when immediate implant treatment was considered. Therefore, one should suggest that presurgery CT scan evaluation is an obligation in this area when planning immediate implant placement treatment.

In accordance with the literature,^{21,25,35} vertical size of foramen was 0.89 ± 0.40 mm in this study. Similarly, Katakami et al¹⁸ reported a mean diameter of 0.88 ± 0.2 mm. They examined the lingual vascular canals of whole mandible similar to this study. A cadaver dissection study gave a mean diameter of 0.8 mm for perforating cortical branches of sublingual artery.²⁵ Another anatomical study with dry skull mandibles gave a mean diameter of foramen on the lingual side of mandible as 0.8 ± 0.4 mm.²⁸ Rosano et al²² detected 0.8 to 0.9 mm diameter of genial foramen in the anatomical assessment of anterior mandible. The present study results obtained with CT sections are consistent with the anatomy.

Vertical size of foramen was mostly reported for MLC and LLC in the literature in CT examinations or just reported for median part of the mandible. The present study results for MLC and LLC were 0.92 ± 0.44 mm and 0.84 ± 0.34 mm, respectively. Consistent with the previous reports, diameter of MLC was statistically higher than LLC in this study.^{21,35} Gültekin et al³⁵ reported a mean value of 0.8 ± 0.2 mm for MLC and 0.6 ± 0.1 mm for LLC with 26 patients. Kilic et al²⁹ reported 1.05 and 0.92 mm, respectively, in a study of 200 cases. These results were in accordance with each other. Gahleitner et al²¹ reported slightly smaller diameter, 0.7 ± 0.3 mm for MLC and 0.6 ± 0.3 mm for LLC.

We classified the foramen diameters as ≤1 and >1 mm to give an idea about the risk of severe hemorrhage. Of the lingual foramen, 75.6% were ≤1 mm. Lustig et al⁴⁰ identified the lingual

artery in the anterior mandible, width, and blood flow by ultrasound/doppler measurement. Average size was reported to be 1.41 ± 0.34 mm and blood flow was 2.92 ± 3.19 mL/min. It was concluded that the artery is of sufficient size to give rise to hemorrhage in implant placement and procedures related to symphysis. Moreover, 25.9% arteries traveling in the sublingual space were located between the sublingual gland and the mandible.⁴ In this pattern of course, blood vessels run parallel to the occlusal plane and assumed that the vessels lying perpendicular to the drill bit are at a greater risk for arterial injury.⁴ Mylohyoid muscle separates the mouth floor like a diaphragm. In dentate mandibles, artery traveling above the muscle is more prone to cause hemorrhage, whereas in edentulous, one runs below the mylohyoid muscle.⁴ Morphology of the mandible of the implant patient should be observed well because perforation of the lingual cortical plate may lead to the violation of sublingual/submandibular area.

Several anastomoses of arteries take place in the body and oral cavity. Anastomosis of inferior alveolar artery and its branches, mental and incisive arteries, were found either with anatomical dissection or CT imaging.^{7,18,27} Using a contrast medium, association between superior genial spinal foramen and incisive canal was examined in dry skulls. The association was seen in 41%, but the authors stated that leakage of the medium outside canals could not be totally prevented.⁴¹ The observation of the anastomosis was reported; however, the frequency of this formation was given in only 1 study.¹⁸ In this study, anastomoses of lingual artery with inferior alveolar artery and its branches could be detected with 38.1% of 1061 artery, whereas Katakami et al¹⁸ showed 31 arterial anastomoses with 154 (20.12%) lingual artery, none was between intercanine area. We observed 3.7% anastomoses with incisive canal. The difference could be because of high number of samples investigated.

Gender differences had an influence on examined parameters, except diameter of the foramen. But, number of foramen >1 mm diameter was higher in men. Distances between crest and

foramen, tooth apex and foramen, and distance from the mandibular border were higher in men. Because the literature did not mention an evaluation about gender, on the parameters listed above, we cannot make a direct comparison. In a previous study, about tooth and dental arch dimensions, men had significantly larger dimensions.⁴² Additionally, we observed gender differences in anatomical features of another bony canal and environmental bone of the jaws.⁴³

According to Lee et al,⁴⁴ one may suggest that by using the cone-beam CT and a laser intraoral scanner in virtual dental implant surgery, dentist may perform safer and successful implant surgeries and treatments.

CONCLUSIONS

Within the limitation of this study, lingual foramina of the mandible could be visualized with dental CT and provided useful data for mandibular implant surgeries. Findings suggest that vascular canals and several anastomoses exist in the anterior mandible extending through premolar and molar region as well. Size and prevalence of the arteria should not be underestimated. They are sufficient to enhance the risk of severe bleeding in many cases. It is imperative to consider these vessels, using the dental CT, before and during the mandibular surgery to prevent threatening hemorrhage.

DISCLOSURES

The authors claim to have no financial interest, either directly or indirectly, in the products or information listed in the article.

REFERENCES

1. Park HD, Min CK, Kwak HH, et al. Topography of the outer mandibular symphyseal region with reference to the autogenous bone graft. *Int J Oral Maxillofac Surg.* 2004;33:781-785.
2. Dym H, Huang D, Stern A. Alveolar bone grafting and reconstruction procedures prior to implant placement. *Dent Clin North Am.* 2012;56:209-218.
3. Bavitz JB, Harn SD, Homze EJ. Arterial supply to the floor of the mouth and lingual gingiva. *Oral Surg Oral Med Oral Pathol.* 1994;77:232-235.

4. Katsumi Y, Tanaka R, Hayashi T, et al. Variation in arterial supply to the floor of the mouth and assessment of relative hemorrhage risk in implant surgery. *Clin Oral Implants Res.* 2013;24:434-440.

5. Martin D, Pascal JF, Baudet J, et al. The submental island flap: A new donor site. Anatomy and clinical applications as a free or pedicled flap. *Plast Reconstr Surg.* 1993;92:867-873.

6. Kalpidis CD, Setayesh RM. Hemorrhaging associated with endosseous implant placement in the anterior mandible: A review of the literature. *J Periodontol.* 2004;75:631-645.

7. Kawai T, Sato I, Yosue T, et al. Anastomosis between the inferior alveolar artery branches and submental artery in human mandible. *Surg Radiol Anat.* 2006;28:308-310.

8. Del Castillo-Pardo de Vera JL, López-Arcas Calleja JM, Burguño-García M. Hematoma of the floor of the mouth and airway obstruction during mandibular dental implant placement: A case report. *Oral Maxillofac Surg.* 2008;12:223-226.

9. Felisati G, Saibene AM, Di Pasquale D, et al. How the simplest dental implant procedure can trigger an extremely serious complication. *BMJ Case Rep.* 2012;2012.

10. Flanagan D. Important arterial supply of the mandible, control of an arterial hemorrhage, and report of a hemorrhagic incident. *J Oral Implantol.* 2003;29:165-173.

11. Mason ME, Triplett RG, Alfonso WF. Life-threatening hemorrhage from placement of a dental implant. *J Oral Maxillofac Surg.* 1990;48:201-204.

12. Darriba MA, Mendonça-Caridad JJ. Profuse bleeding and life-threatening airway obstruction after placement of mandibular dental implants. *J Oral Maxillofac Surg.* 1997;55:1328-1330.

13. Givol N, Chaushu G, Halamish-Shani T, et al. Emergency tracheostomy following life-threatening hemorrhage in the floor of the mouth during immediate implant placement in the mandibular canine region. *J Periodontol.* 2000;71:1893-1895.

14. Laboda G. Life-threatening hemorrhage after placement of an endosseous implant: Report of case. *J Am Dent Assoc.* 1990;121:599-600.

15. Fujita S, Ide Y, Abe S. Variations of vascular distribution in the mandibular anterior lingual region: A high risk of vascular injury during implant surgery. *Implant Dent.* 2012;21:259-264.

16. Jo JH, Kim SG, Oh JS. Hemorrhage related to implant placement in the anterior mandible. *Implant Dent.* 2011;20:e33-e37.

17. Lee CY, Yanagihara LC, Suzuki JB. Brisk, pulsatile bleeding from the anterior

mandibular incisive canal during implant surgery: A case report and use of an active hemostatic matrix to terminate acute bleeding. *Implant Dent.* 2012;21:368-373.

18. Katakami K, Mishima A, Kuribayashi A, et al. Anatomical characteristics of the mandibular lingual foramina observed on limited cone-beam CT images. *Clin Oral Implants Res.* 2009;20:386-390.

19. Kalpidis CD, Konstantinidis AB. Critical hemorrhage in the floor of the mouth during implant placement in the first mandibular premolar position: A case report. *Implant Dent.* 2005;14:117-124.

20. ten Bruggenkate CM, Krekelor G, Kraaijenhagen HA, et al. Hemorrhage of the floor of the mouth resulting from lingual perforation during implant placement: A clinical report. *Int J Oral Maxillofac Implants.* 1993;8:329-334.

21. Gahleitner A, Hofschneider U, Tepper G, et al. Lingual vascular canals of the mandible: Evaluation with dental CT. *Radiology.* 2001;220:186-189.

22. Rosano G, Taschieri S, Gaudy JF, et al. Anatomic assessment of the anterior mandible and relative hemorrhage risk in implant dentistry: A cadaveric study. *Clin Oral Implants Res.* 2009;20:791-795.

23. Loukas M, Kinsella CR Jr, Kapos T, et al. Anatomical variation in arterial supply of the mandible with special regard to implant placement. *Int J Oral Maxillofac Surg.* 2008;37:367-371.

24. Choi DY, Woo YJ, Won SY, et al. Topography of the lingual foramen using micro-computed tomography for improving safety during implant placement of anterior mandibular region. *J Craniofac Surg.* 2013;24:1403-1407.

25. Babiuc I, Tărlungeanu I, Păuna M. Cone beam computed tomography observations of the lingual foramina and their bony canals in the median region of the mandible. *Rom J Morphol Embryol.* 2011;52:827-829.

26. Sheikh M, Mosavat F, Ahmadi A. Assessing the anatomical variations of lingual foramen and its bony canals with CBCT taken from 102 patients in Isfahan. *Dent Res J (Isfahan).* 2012;9(Suppl 1):S45-S51.

27. Nakajima K, Tagaya A, Otonari-Yamamoto M, et al. Composition of the blood supply in the sublingual and submandibular spaces and its relationship to the lateral lingual foramen of the mandible. *Oral Surg Oral Med Oral Pathol Oral Radiol.* 2012. Epub ahead of print. doi: 10.1016/j.oooo.2012.03.032

28. Liang X, Jacobs R, Lambrechts I, et al. Lingual foramina on the mandibular midline revisited: A macroanatomical study. *Clin Anat.* 2007;20:246-251.

29. Kilic E, Doganay S, Ulu M, et al. Determination of lingual vascular canals in the interforaminal region before implant

- surgery to prevent life-threatening bleeding complications. *Clin Oral Implants Res.* 2012. Epub ahead of print. doi: 10.1111/cir.12065.
30. Tagaya A, Matsuda Y, Nakajima K, et al. Assessment of the blood supply to the lingual surface of the mandible for reduction of bleeding during implant surgery. *Clin Oral Implants Res.* 2009;20:351-355.
31. Scaravilli MS, Mariniello M, Sammartino G. Mandibular lingual vascular canals (MLVC): Evaluation on dental CTs of a case series. *Eur J Radiol.* 2010;76:173-176.
32. Liang H, Frederiksen NL, Benson BW. Lingual vascular canals of the interforaminal region of the mandible: Evaluation with conventional tomography. *Dentomaxillofac Radiol.* 2004;33:340-341.
33. Tepper G, Hofschneider UB, Gahleitner A, et al. Computed tomographic diagnosis and localization of bone canals in the mandibular interforaminal region for prevention of bleeding complications during implant surgery. *Int J Oral Maxillofac Implants.* 2001;16:68-72.
34. Longoni S, Sartori M, Braun M, et al. Lingual vascular canals of the mandible: The risk of bleeding complications during implant procedures. *Implant Dent.* 2007;16:131-138.
35. Gültekin S, Araç M, Celik H, et al. Assessment of mandibular vascular canals by dental CT [in Turkish]. *Tani Girisim Radyol.* 2003;9:188-191.
36. Gahleitner A, Watzek G, Imhof H. Dental CT: Imaging technique, anatomy, and pathologic conditions of the jaws. *Eur Radiol.* 2003;13:366-376.
37. Drago C, del Castillo R, Peterson T. Immediate occlusal loading in edentulous jaws, CT-guided surgery and fixed provisional prosthesis: A maxillary arch clinical report. *J Prosthodont.* 2011;20:209-217.
38. Mardinger O, Manor Y, Mijiritsky E, et al. Lingual perimandibular vessels associated with life-threatening bleeding: An anatomic study. *Int J Oral Maxillofac Implants.* 2007;22:127-131.
39. Froum S, Casanova L, Byrne S, et al. Risk assessment before extraction for immediate implant placement in the posterior mandible: A computerized tomographic scan study. *J Periodontol.* 2011;82:395-402.
40. Lustig JP, London D, Dor BL, et al. Ultrasound identification and quantitative measurement of blood supply to the anterior part of the mandible. *Oral Surg Oral Med Oral Pathol Oral Radiol Endod.* 2003;96:625-629.
41. Vandewalle G, Liang X, Jacobs R, et al. Macroanatomic and radiologic characteristics of the superior genial spinal foramen and its bony canal. *Int J Oral Maxillofac Implants.* 2006;21:581-586.
42. Al-Khatib AR, Rajion ZA, Masudi SM, et al. Tooth size and dental arch dimensions: A stereo photogrammetric study in Southeast Asian Malays. *Orthod Craniofac Res.* 2011;14:243-253.
43. Güncü GN, Yıldırım YD, Yılmaz HG, et al. Is there a gender difference in anatomic features of incisive canal and maxillary environmental bone? *Clin Oral Implants Res.* 2013;24:1023-1026.
44. Lee CY, Ganz SD, Wong N, et al. Use of cone beam computed tomography and a laser intraoral scanner in virtual dental implant surgery: Part 1. *Implant Dent.* 2012;21:265-271.

Clinical and Radiological Classification of the Jawbone Anatomy in Endosseous Dental Implant Treatment

Gintaras Juodzbalyš¹, Marius Kubilius¹

¹Department of Maxillofacial Surgery, Lithuanian University of Health Sciences, Kaunas, Lithuania.

Corresponding Author:

Gintaras Juodzbalyš

Vainiku 12

LT- 46383, Kaunas

Lithuania

Phone: +370 37 29 70 55

Fax: +370 37 32 31 53

E-mail: gintaras@stilusoptimus.lt

ABSTRACT

Objectives: The purpose of present article was to review the classifications suggested for assessment of the jawbone anatomy, to evaluate the diagnostic possibilities of mandibular canal identification and risk of inferior alveolar nerve injury, aesthetic considerations in aesthetic zone, as well as to suggest new classification system of the jawbone anatomy in endosseous dental implant treatment.

Material and Methods: Literature was selected through a search of PubMed, Embase and Cochrane electronic databases. The keywords used for search were mandible; mandibular canal; alveolar nerve, inferior; anatomy, cross-sectional; dental implants; classification. The search was restricted to English language articles, published from 1972 to March 2013. Additionally, a manual search in the major anatomy and oral surgery books were performed. The publications there selected by including clinical and human anatomy studies.

Results: In total 109 literature sources were obtained and reviewed. The classifications suggested for assessment of the jawbone anatomy, diagnostic possibilities of mandibular canal identification and risk of inferior alveolar nerve injury, aesthetic considerations in aesthetic zone were discussed. New classification system of the jawbone anatomy in endosseous dental implant treatment based on anatomical and radiologic findings and literature review results was suggested.

Conclusions: The classification system proposed here based on anatomical and radiological jawbone quantity and quality evaluation is a helpful tool for planning of treatment strategy and collaboration among specialists. Further clinical studies should be conducted for new classification validation and reliability evaluation.

Keywords: mandible; alveolar nerve, inferior; anatomy, cross-sectional; dental implants; classification.

Accepted for publication: 12 June 2013

To cite this article:

Juodzbalyš G, Kubilius M. Clinical and Radiological Classification of the Jawbone Anatomy in Endosseous Dental Implant Treatment.

URL: <http://www.ejomr.org/JOMR/archives/2013/2/e2/v4n2e2ht.pdf>

doi: [10.5037/jomr.2013.4202](https://doi.org/10.5037/jomr.2013.4202)

INTRODUCTION

After the loss of teeth atrophy of the alveolar processes occurs in a vertical as well as a horizontal plane. The term atrophy is defined in the dictionary as "a wasting away; a diminution in the size of a cell, tissue, organ, or part" [1]. This process is starting and continuous throughout life because of the lack of stimuli (disuse atrophy) seen on alveolar process of the jaws [2].

Dental implants have become the most popular and reliable treatment option for restoring missing teeth. Nowadays there is a wide choice of screw-type implant systems. The success of dental implants depends on the jawbone quantity and quality [3]. Therefore, it is important to measure the alveolar process precisely so that the proper system may be chosen [4]. There are number of classifications suggested for assessment of the degree of atrophy of partially or fully edentulous jaws [5-11]. One of the most popular classification systems for jaw anatomy (jaw shape and quality) for dental implant treatment was proposed by Lekholm and Zarb in 1985 [12]. However, this classification, like many others, described changes only of jaw shapes in general and failed to indicate precise measurements [13]. Juodzbalys et al. in 2004 [14] proposed clinical and radiological classification of the jawbone anatomy for implantation based on edentulous jaw dental segment (eJDS) anatomy assessment. Nevertheless, this classification fails to assess mandibular canal anatomy variations and risk degree of inferior alveolar nerve injury. By means of the advancement of radiographic technology, i.e. development of cone beam computed tomography (CBCT), diagnostic possibilities are more precise, especially in the case of mandibular canal assessment [15-17]. In view of these considerations the purpose of present article was to review the classifications suggested for assessment of the jawbone anatomy, to evaluate the diagnostic possibilities of mandibular canal identification and risk of inferior alveolar nerve injury, aesthetic considerations in aesthetic zone, as well as to suggest new classification system of the jawbone anatomy in endosseous dental implant treatment.

MATERIAL AND METHODS

Literature was selected through a search of PubMed, Embase and Cochrane electronic databases. The keywords used for search were mandible; mandibular canal; alveolar nerve, inferior; anatomy, cross-sectional; dental implants; classification. The search was restricted to English language articles,

published from 1972 to March 2013. Additionally, a manual search in the major anatomy and oral surgery books were performed. The publications there selected by including clinical and human anatomy studies.

RESULTS

Classifications of jawbone anatomy

It was mentioned above that the most popular classification systems for jaw anatomy (jaw shape and quality) for dental implant treatment was proposed by Lekholm and Zarb [12]. The quantity of jawbone is divided into five groups, based on residual jaw shape following tooth extraction. There are presented drawings of the jaws – jaw cross-sections, accompanied by text, and assessment methods. Similarly Cawood and Howell's [9] ridge classification presented as alveolar process resorption level jaw cross-sections and text. During all stages of the alveolar ridge atrophy, characteristic shapes result from the resorptive process. The biggest shortcoming of previous classifications [5-11] is fact, that those classifications are two-dimensional representations and do not show the three-dimensionality of atrophic ridges. Nowadays clinician can combine three-dimensional jawbone assessment and image-guided surgery by means of CBCT. Diagnostic and planning software are available to assist in implant planning to create diagnostic and surgical implant guidance stents (e.g., Virtual Implant Placement, Implant Logic Systems, Cedarhurst, USA; Simplant, Materialise, Belgium; Easy Guide, Keystone Dental, USA) [18].

Misch and Judy [19] classified available bone into 4 divisions: abundant, barely sufficient, compromised, and deficient (A-D). Abundant bone requires no augmentation and is greater than 5 mm in width, 10 to 13 mm in height, and 7 mm in length. Barely sufficient bone is 2.5 to 5 mm in width, greater than 10 to 13 mm in height, and greater than 12 mm in length and can be modified with osteoplasty or augmentation of hard or soft tissues, depending on the nature of the defect (B-w). Compromised bone necessitates osteoplasty and some form of hard or soft tissue augmentation depending on the extent of the defect in height (less than 10 mm, C-h) or width (less than 2.5 mm, C-w). Deficient bone requires substantial hard tissue augmentation from extraoral sites and is generally not amenable to implant rehabilitation. Unfortunately, aesthetic component in this classification is not considered. Implant rehabilitation is no longer just a vehicle to restore lost masticatory and phonetic function. It has become an integral part of modern implant dentistry for achieving structural and aesthetic pleasing outcomes [20]. It is well established that

the soft tissue appearance is largely dependent upon the underlying bone topography [21]. Hence, it is important to assess hard tissue parameters, such as horizontal bone deficiency and interproximal bone height.

Current classifications also fail to assess mandibular canal anatomy variations and risk degree of inferior alveolar nerve injury. Worthington [22] showed that even after the accurate measurement of available bone, the nerve injury can occur as the result of over penetration of the drill owing to low resistance of the spongy bone; this can lead to slippage of the drill even by experienced surgeons.

Lekholm and Zarb [12] classify quality of residual alveolar bones into four types: type 1 = large homogenous cortical bone; type 2 = thick cortical layer surrounding a dense medullar bone; type 3 = thin cortical layer surrounding a dense medullar bone; type 4 = thin cortical layer surrounding a sparse medullar bone). According to Ribeiro-Rotta et al. [23] and Bergkvist et al. [24] classification of quality of residual alveolar bones indicate a good correlation with bone mineral content. Trisi and Rao [25] proposed the system for bone quality assessment with three classes (dense, normal and soft bone).

Some authors proposed to evaluate jawbone density in presurgical planning [26-28]. It is possible to assess jawbone density using CT values (Hounsfield units: HU) and bone mineral densities obtained by medical CT. Norton and Gamble [27] measured the bone density in the posterior mandible using SimPlant software (3D Diagnostix, Boston, MA, USA) and concluded that the mean CT value was 669.6 HU. Misch [26] classified cancellous bone density into 5 grades: D1: > 1250 HU; D2: 850 to 1250 HU; D3: 350 to 850 HU; D4: 150 to 350 HU; and D5: < 150 HU. In the conversion of CT values (HU), the mean value in the molar region was 4.5×10^2 (D3); in the first molar region it was 5.2×10^2 (D3), in second molar region 4.3×10^2 (D3), and in the third molar region it was 0.7×10^2 (D5).

It is interesting to know that Baša and Dilek [29] assessed the risk of perforation of the mandibular canal by implant drill using density and thickness parameters. They investigated whether the resistance of the bone surrounding the mandibular canal had sufficient density and thickness to avoid perforation by implant drills. Study of the computed tomography (CT) images of 99 patients, showed that overall, average bone thickness in the premolar and molar regions was 0.87 ± 0.18 and 0.86 ± 0.18 mm, respectively, whereas the bone density in the premolar and molar regions was 649.18 ± 241.42 and 584.44 ± 222.73 HU, respectively ($P < 0.001$). It was concluded that the average density and thickness of the bone that surrounds the mandibular canal

was not sufficient to resist the implant drill. Furthermore, in the posterior mandible, cancellous bone is more abundant and has bigger intratrabecular spaces and less dense than in anterior mandible [30,31]. In some cases with low density bone, the twist drills may drop into intratrabecular spaces during preparation thus leads to the displacement of the implants deeper than planned [32].

The measurements of bone density in designed sites are important in presurgical planning when using CBCT for dental implant treatment. However, the pixel or voxel values obtained from CBCT images are not absolute values. Naitoh et al. [33] demonstrated a high-level correlation between voxel values of CBCT and bone mineral densities of multislice CT ($r = 0.965$). They concluded that voxel values of mandibular cancellous bone in CBCT could be used to estimate bone density. In contrast, Nackaerts et al. [34] and Parsa et al. [35] determined the grey value variation at the implant site with different scan settings, including field of view (FOV), spatial resolution, number of projections, exposure time and dose selections in two CBCT systems and compared the results with those obtained from a multislice CT system. Authors concluded that grey-level values from CBCT images are influenced by device and scanning settings.

Radiological examination

The main goals of radiological jawbone examination are to determine the quantity, quality and angulations of bone, selection of the potential implant sites, and to verify absence of pathology. Clinician should choose proper radiographic method which provides sufficient diagnostic information with the least possible radiation dose.

Periapical radiographs have been used for many years to assess the jaws pre- and post-implant placement [36]. Periapical radiographs commonly are used to evaluate the status of adjacent teeth, remaining alveolar bone in the mesiodistal dimension and vertical height. The long cone paralleling technique for taking periapical X-ray is the technique of choice for the following reasons: reduction of radiation dose; less magnification; a true relationship between the bone height and adjacent teeth is demonstrated [37]. If the paralleling technique is not used, periapical radiographs create an image with foreshortening and elongation [38-40]. Nevertheless, the biggest concern of periapical radiographs is in 28% of patients that mandibular canal could not be clearly identified in the second premolar and first molar regions [41] and mandibular foramen can be identified around 47 - 75% cases [42].

When a specific region (maxillofacial area, including

many of the vital structures, such as maxillary sinus, inferior alveolar nerve and nasal fossa) that is too large to be seen on a periapical view, panoramic radiograph can be the method of choice. The major advantages of panoramic images are the broad coverage of oral structures, low radiation exposure (about 10% of a full-mouth radiographs), and relatively inexpensiveness of the equipment. The major drawbacks of panoramic imaging are: lower image resolution, high distortion, and presence of phantom images [43]. For example, Naitoh et al. [33] found that mandibular canal visibility on panoramic radiographs in superior and inferior wall was only 36.7%. Similarly, Lindh et al. [44] reported that the mandibular canal of specimen cadavers was clearly visible in 25% of panoramic radiographs (range 12 to 86%). Klinge et al. [45] also reported that the mandibular canal of specimen cadavers was not visible in 36.1% of panoramic radiographs. The location and configuration of mandibular canal are important in imaging diagnosis for the proper dental implant placement in the mandible [46-48].

One of the most challenged regions for implantation in mandible is mental foramen region. This is because there are many variations with regards to the size, shape, location and direction of the opening of the mental foramen. After comparison of the anatomical and radiological assessment of 4 cadaver skulls, Yosue and Brooks [49] concluded that the panoramic and periapical films reflected the actual position of mental foramen in the skulls < 50% of the time. Furthermore, Sonick et al. [50] found that the average linear errors occurred during routine bone assessments (n = 12) for panoramic films were 24% (mean 3 mm; range 0.5 to 7.5 mm), for periapical films were 14% (mean 1.9 mm; range 0.0 to 5.0 mm) and only 1.8% (mean 0.2 mm; range 0.0 to 0.5 mm) for CT scans. Kuzmanovic et al. [51], Ngeow and Yuzawati [52] and Jacobs et al. [53] similarly concluded that panoramic radiograph is not sufficient for anterior loop detection and presurgical implant planning in the mental region and there is a need for other additional images.

Even incisive canal detection is complicated using panoramic radiography. For example, Jacobs with co-workers [54] reported that the mandibular incisive canal was identified only in 15% of the 545 panoramic radiographs, with good visibility of only 1%. In contrast, canal was observed on 93% of CT scans with a good visibility in 22% of cases.

Peker et al. [55] showed that the measurements obtained from CT images are more consistent with direct measurements than the measurements obtained from panoramic radiographic images or conventional tomographic images. Furthermore, Rouas et al. [56] reported that the atypical mandibular canal such as

bifid mandibular canal, in most cases can be identified using only three-dimensional imaging techniques. It was thought that the bifid mandibular canal is often left unrecognized [57]. Therefore, duplication or division of the canal by means of panoramic radiographs was found in about 1% of patients [58]. Naitoh et al. [59] reconstructed 122 two-dimensional images of the various planes in mandibular ramus region to the computer program using three-dimensional visualization and measurement software. Bifid mandibular canal in the mandibular ramus region was observed even in 65% of patients.

When the periapical radiography, panoramic radiography, tomography, or CT were compared for their efficiency in the identification of the mandibular canal, the CBCT seems to have the most potential while reduces radiation exposure considerably [60]. Similarly, CT scans are more accurate than conventional radiographs in mental foramen and anterior loop detection [45,50,53,61,62]. However, cross-sectional imaging have following limitations: limited availability, high cost and the need for image interpretation [63,64]. However, CBCT is often recommended for clinical usage, especially in cases there the vital structures are difficult to detect due to its high accuracy and low radiation exposure [65,66,68]. The main advantage of CBCT is a low dose scanning system, which has been specifically designed to produce three-dimensional images of the maxillofacial skeleton. Hence, a major difference between CT and CBCT is how the data are gathered: CT acquires image data using rows of detectors, CBCT exposes the whole section of the patient over one detector [69,70]. Furthermore, CBCT permits not only diagnosis, it facilitates image-guided surgery [18].

Inferior alveolar nerve injury risk

Inferior alveolar nerve injury is a serious complication with incidence ranged from 0 to 40% [71-87]. As a result, many important functions such as speech, eating, kissing, make-up application, shaving and drinking were affected [77]. This influences patient's quality of life and often resulted in negative psychological adverse effects [79]. The most common causes of iatrogenic inferior alveolar nerve injuries are discrepancies of radiographs, surgeon's mistakes, low resistance of mandibular spongy bone and lack of mandibular canal superior wall.

The most severe types of injuries are caused by implant drills and implants themselves [22]. Many implant drills are slightly longer, for drilling efficiency, than their corresponding implants. Implant drill length varies and must be understood by the surgeon because the specified length may not reflect an additional millimetre so called

“y” dimension [84]. Lack of knowledge about this may cause avoidable complications [88]. Damage to the inferior alveolar nerve can occur when the twist drill or implant encroaches, transects, or lacerates the nerve. Over penetration of the drill (drill slippage) can be triggered by the low resistance of the spongy bone [22]. It was mentioned above that Baša and Dilek [29] assessed the risk of perforation of the mandibular canal by implant drill using density and thickness parameters. They investigated whether the resistance of the bone surrounding the mandibular canal had sufficient density and thickness to avoid perforation by implant drills. The results showed the risk of inferior alveolar nerve injury can be avoided by accurately determine the bone mass around the canal and avoid use excessive force when approaching the canal. Furthermore, Wadu et al. [93], studying mandibular canal appearance on the panoramic radiographs, found that the number of cases of radio-opaque border was either disrupted or even absent. The superior border was more prone to disruption than the inferior border. It is evident that low resistance of the spongy mandibular bone and absence of mandibular canal superior wall is inauspicious anatomical combination which can lead to inferior alveolar nerve injury.

Juodzbalys et al. [87] showed that in 25% cases ($n = 4$) implant drill was identified as etiological factor with 2 cases caused by drill slippage during osteotomy preparation. The inferior alveolar nerve may be affected by perforation of the mandibular canal during drilling, or positioning the implant close to the canal and the subsequent formation of an adjacent hematoma that presses against the nerve [89]. Khawaja and Renton [90] indicated that “cracking” of the inferior alveolar nerve canal roof by its close proximity to preparation of the implant bed (millimetres) may cause haemorrhage into the canal or deposition of debris which may compress and cause ischemia of the nerve.

Limited evidence exists with regard to the proper distance between the implant and the mandibular canal to ensure the nerve’s integrity and physiologic activity. The proper distance should come from evaluation of clinical data as well as from biomechanical analyses [91,92]. Sammartino et al. [91] created a numeric mandibular model based on the boundary element method to simulate a mandibular segment containing a threaded fixture so that the pressure on the trigeminal nerve, as induced by the occlusal loads, could be assessed. They found that the nerve pressure increased rapidly with a bone density decrease. A low mandibular cortical bone density caused a major nerve pressure increase. In conclusion, they suggested a distance of 1.5 mm to prevent implant damage to the underlying inferior alveolar nerve when biomechanical loading was taken into consideration.

Aesthetic considerations

It is generally agreed that implant success criteria should include an aesthetic component [94]. Although implant success, as measured through fixture osseointegration and restoration of function, is high, the procedures available to create aesthetic implant “success” are not always predictable [20]. To ensure optimal aesthetic implant rehabilitation, the following prerequisites are considered essential: adequate bone volume (horizontal, vertical, and, contour), optimal implant position (mesiodistal, apicocoronal, buccolingual, and angulation), stable and healthy periimplant soft tissues, aesthetic soft tissues contours, and ideal emergence profile [20,95]. The level of bone support and the soft tissue dimensions around the implant-supported single-tooth restoration are factors suggested to be important for the aesthetic outcome of implant therapy [96]. It has been demonstrated that presence or absence of bone crest influences the appearance of papillae between implants and adjacent teeth [97]. Furthermore, the implant-supported restoration should be in symmetry with the adjacent dentition [98].

The parameters of three-dimensional optimal implant position was defined by several authors [20,94,99,100]. Mesio-distal dimension between adjacent teeth should be 6 to 9 mm to ensure minimal (1.5 mm) distance between implant fixture and adjacent teeth [99,100]. Vela et al. [101] showed that it is possible to place platform-switched implant 1 mm from teeth while maintaining the bone level adjacent to them. Apicocoronal implant position should be 2 mm below the adjacent cervicoenamel line [94]. Natural buccal and proximal restorative contour can be ensured by correctly orienting the implant in a buccolingual position - 3 to 4 mm from outside buccal flange [20]. Minimum 2 mm of space should be maintained on the buccal side in front of the external implant collar surface.

It is necessary to mention that recommendations for successful results ideally require at least 1 mm of bone surrounding each implant [102].

Classification system of the jawbone anatomy in endosseous dental implant treatment and assessments

New classification system of the jawbone anatomy in endosseous dental implant treatment is suggested taking into consideration previous Juodzbalys and Raustia [14] classification and literature review results (Figure 1) (Table 1). Surgical dental implant installation requires understanding of associated anatomical structures. Planning should be done on three-dimensional edentulous jaw segment (EJS) pattern (Figure 2).

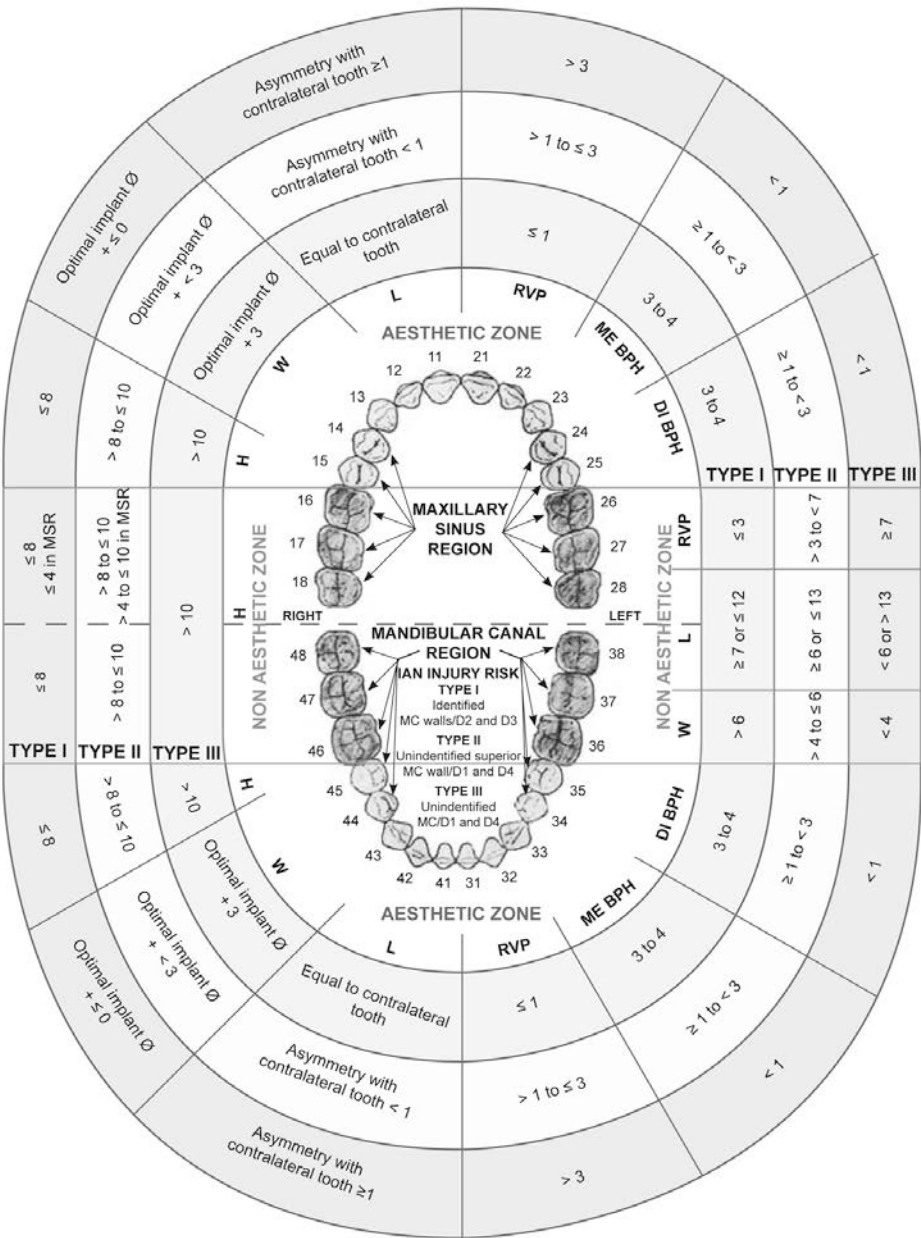


Figure 1. Classification system of the jawbone anatomy in endosseous dental implant treatment. H = height; W = width; L = length; RVP = Alveolar ridge vertical position; ME BPH = Mesial interdental bone peak height; DI BPH = Distal interdental bone peak height; MC = mandibular canal; IAN = inferior alveolar nerve; MSR = maxillary sinus region (all linear measurements are expressed in mm).

Table 1. Classification system of the jawbone anatomy in endosseous dental implant treatment

Edentulous jaw segment parameters		Edentulous jaw segment types (risk degree)		
		Type I (low risk)	Type II (moderate risk)	Type III (high risk)
Non aesthetic zone				
Height (mm)	Maxilla	> 10	> 8 to ≤ 10 > 4 to ≤ 10 in MSR	≤ 8 ≤ 4 in MSR
	Mandible	> 10	> 8 to ≤ 10	≤ 8
Width (mm)		> 6	> 4 to ≤ 6	< 4
Length (mm)		≥ 7 or ≤ 12	≥ 6 or ≤ 13	< 6 or > 13
Alveolar ridge vertical position (mm)		≤ 3	> 3 to < 7	≥ 7
Aesthetic zone				
Height (mm)	Maxilla	> 10	> 8 to ≤ 10 > 4 to ≤ 10 in MSR	≤ 8 ≤ 4 in MSR
	Mandible	> 10	> 8 to ≤ 10	≤ 8
Width (mm)		Optimal implant diameter + 3	Optimal implant diameter + 3	Optimal implant diameter + ≤ 0
Length (mm)		Equal to contralateral tooth	Asymmetry with contralateral tooth < 1	Asymmetry with contralateral tooth ≥ 1
Alveolar ridge vertical position (mm)		≤ 1	> 1 to ≤ 3	> 3
Interdental bone peak height (mm)	Mesial	3 to 4	≥ 1 to < 3	< 1
	Distal	3 to 4	≥ 1 to < 3	< 1
MC region (IAN injury risk degree)				
MC walls identification and jawbone quality type ^a combination		Identified MC walls/D2 and D3	Unidentified superior MC wall/D1 and D4	Unidentified MC/D1 and D4

^aD = bone quality defined according to Lekholm and Zarb (1985).
MC = mandibular canal; IAN = inferior alveolar nerve; MSR = maxillary sinus region.

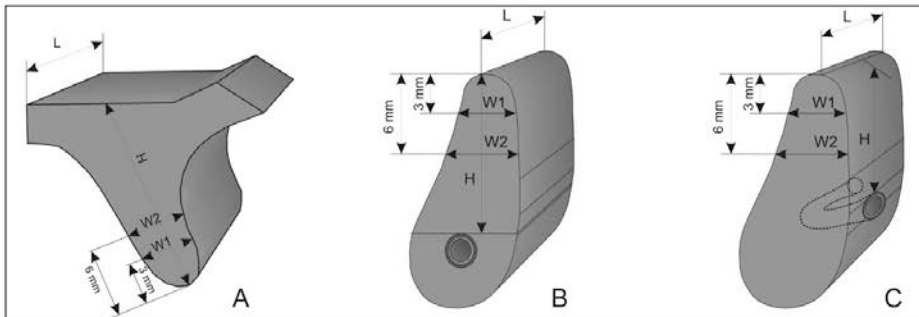


Figure 2. Edentulous jaw segments (A = maxillary, B and C = mandibular) that consists of alveolar and basal bone. A = the vertical dimension (H) of the EJS is determined by the distance between the alveolar ridge crest and maxillary sinus. B = the vertical dimension (H) of the EJS is determined by the distance between the alveolar ridge crest and mandibular canal. C = the vertical dimension (H) of the planned implant is determined by the distance between the alveolar crestal ridge and mental foramen. The horizontal EJS dimensions: length (L) in all cases is determined by the distance between neighbouring teeth or implants and width (W) is determined by the alveolar process width measured at the level of 3 mm (W1) and 6 mm (W2) from the crest of alveolar process.

This is because the EJS consists of alveolar and basal bone. In addition, EJS describes planned implant bed relation to present anatomical borders such as mandibular or maxillary vital structures. This is in coincidence with Ribeiro-Rotta et al. [23], they proposed that each implant site should be assessed and characterized

knowing that bone characteristics vary within the same jaw [103]. All measurements should be obtained clinically and from CBCT and panoramic radiographic images. It should be done by identifying and depicting anatomical landmarks and position of important vital structures, when planning for dental implant operation.

There are two zones distinguished in the new classification system - aesthetic and non aesthetic and two regions - mandibular canal and maxillary sinus. EJSs are attributed to aesthetic and non aesthetic mandibular or maxillary zone, because the demands and risks of aesthetic result achievement differ significantly in aesthetic zone in comparison with non aesthetic zone. Mandibular canal and maxillary sinus regions are important because of the risk of injury of inferior alveolar nerve and maxillary sinus and implant operation planning peculiarities. Furthermore, all EJSs are divided into types (Types I to III) according to their assessment result and risk degree of planned surgical treatment success. This is in coincidence with Friberg et al. [104], they suggested that the justification for assessing jawbone tissue in endosseous dental implant treatment should be diagnostic tool to assess whether the jawbone tissue is sufficient for implant treatment and a prognostic tool to predict the probability of success or failure.

The minimal dimensions of EJS for proper implantation were estimated according to the principles of threaded implant insertion.

Non aesthetic zone

The height of the alveolar process (H): the distance between the crest of the alveolar process and the important vital structures of the jaws (maxillary sinus, mandibular canal, mental foramen, anterior loop of mental nerve). Several factors should be considered when estimating the minimal height of an alveolar process. In some cases the crest of alveolar process is thin and it is necessary to reduce it, so it can have wider base for the planned implant installation. In such cases, the heights of EJS will be shortened by 1 to 3 mm; this reduction had to be considered when calculating the available bone height [105] (Figure 3). If the operation is planned according to the orthopantomograph, implantation in the areas of the mandibular canal mandated that the apices should be at least 2 mm away from those vital structures. A minimum of 1 mm is demanded if the operation is planned with CBCT [106]. Essentially, the minimal height of the Type I EJS is > 10 mm (Figures 4A, B). EJS with the less height of > 8 to ≤ 10 mm (Figure 4C) and > 4 to ≤ 10 mm in maxillary sinus region (Figure 4D) were considered to be Type II. However, such height was found to be sufficient to ensure primary stability of implants [14]. Simultaneous implantation with vertical alveolar process augmentation or sinus floor augmentation is recommended. If EJS height was less than ≤ 8 mm and ≤ 4 mm in maxillary sinus region was categorized as Type III (Figures 4E, F). These measurements were

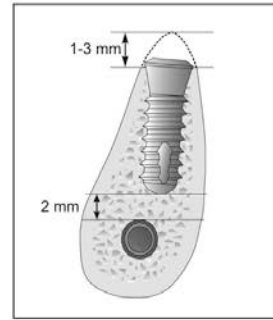


Figure 3. Thin crestal ridge was reduced to create wide recipient bed for planned implant installation. In such cases, the heights of EJSs would have been shortened by 1 to 3 mm at least.

considered to be insufficient for 8 mm length implant installation and primary stability achievement even in maxillary sinus region. Vertical alveolar process and/or sinus floor augmentation and late implantation are recommended.

The width of alveolar process (W): determined by the alveolar process width measured at the level of 3 mm (W1) and 6 mm (W2) from the crest of alveolar process. The smallest measurement should be accepted as the width of the EJS. Recommendations for successful results ideally require at least 1 mm of bone surrounding each implant [102]. Most implant systems require bone widths of 5 to 7 mm [12,102]. We estimated that for proper implantation the minimal width of an EJS (Type I) should be 6 mm (Figure 5A). Alveolar processes with widths of > 4 to ≤ 6 mm were deemed insufficient (Type II) for proper implantation (Figure 5B). Despite such deficiencies, it is expected that the wider parts of the implants will be covered by bone after insertion and that primary stability would be achieved. Simultaneous implantation with alveolar process horizontal augmentation is recommended. EJS which width is less than 4 mm is categorized as Type III (Figure 5C). These measurements are considered to be insufficient for primary stability of implants. Horizontal alveolar process augmentation and late implantation is recommended.

The length of the EJS (L): is determined by the distance between equators of neighbouring teeth or implants. The minimal distance between 2 implants should be at least 3 mm [107], and minimal distances between implants and natural roots should be at least 1.5 mm [108] or in case of platform-switched implant 1 mm [101]. Considering that the optimal recommended diameter of implants in distal jaws segments is 4 to 5 mm, all EJS of Type I should be ≥ 7 or ≤ 12 mm in length (Figure 6).



Figure 4. A = Upper jaw first right molar EJS on CBCT cross-sectional image is more than 10 mm in height and classified as Type I with no requirement of vertical alveolar process bone height augmentation prior endosseous dental implant treatment (all CBCT images in this article were obtained with I-CAT® (Imaging Sciences International LLC, Hatfield, PA USA) CBCT, a letter “b” on cross-sectional CBCT image means buccal side).
 B = Type I height (> 10 mm) of lower jaw first left molar EJS on CBCT cross-sectional image.
 C = Type II height (> 8 to ≤ 10 mm) of lower right first molar EJS on CBCT cross-sectional image. Simultaneous implantation with sinus floor augmentation are recommended.
 D = Type II height (> 4 to ≤ 10 mm) of upper right first molar EJS on CBCT cross-sectional image. Simultaneous implantation with vertical alveolar process augmentation are recommended.
 E = Type III height (≤ 8 mm) of lower left second molar EJS on CBCT cross-sectional image. Vertical alveolar process augmentation and late implantation are recommended. Mandibular canal walls have proper identification with D2 bone quality.
 F = Type III height (≤ 4 mm) of upper left premolar EJS on CBCT cross-sectional image. Sinus floor augmentation and late implantation are recommended.



Figure 5. A = Type I width (> 6 mm) of lower molar EJS on CBCT cross-sectional image at the level of 3 mm and 6 mm with no requirement of horizontal alveolar process augmentation prior endosseous dental implant treatment.
 B = Type II width (> 4 to ≤ 6 mm) of lower right molar EJS on CBCT cross-sectional image. Endosseous dental implant treatment with simultaneous alveolar process horizontal augmentation are recommended.
 C = Type III width of lower premolar EJS on CBCT cross-sectional image. Horizontal alveolar process augmentation and late implantation are recommended.



Figure 6. The length of EJS in non aesthetic zones on CBCT image (panoramic reconstruction): measurement "1" - Type I, measurement "2" - Type II, measurement "3" - Type III.

EJS which length is ≥ 6 or ≤ 13 mm is considered as Type II and < 6 or > 13 mm as Type III. In Type III EJS is impossible to install one or two proper diameter implants. Orthodontic treatment prior to implant treatment is recommended.

Alveolar ridge vertical position (RVP): the distance between the lowest point of alveolar ridge crest to the labial/buccal surface cervicoenamel line of the adjacent teeth. This parameter is important for achieving of favourable implant/crown length ratio and adequate aesthetic result. Adequate distance for Type I EJS is estimated to be ≤ 3 mm. The alveolar ridge vertical position > 3 to < 7 mm is defined as Type II EJS. In case when EJS height is sufficient for implant primary stability achievement, simultaneous implantation with vertical alveolar process augmentation or sinus floor augmentation and vertical alveolar process augmentation is recommended (Figure 7). The alveolar ridge vertical position ≥ 7 mm is defined as Type III EJS with high risk of implant treatment success due to doubtful primary stability achievement. For Type III EJS vertical alveolar process augmentation and late implantation are recommended.

Aesthetic zone

The height of the alveolar process (H): the distance between the crest of the alveolar process and the important vital structures of the jaws (nasal sinus floor, mental foramen, anterior loop of mental nerve). To facilitate a better implant/crown ratio, the minimal dental implant length in the aesthetic zone is 10 mm [109]. Hence, the alveolar process height for Type I EJS should be > 10 mm because the recommended

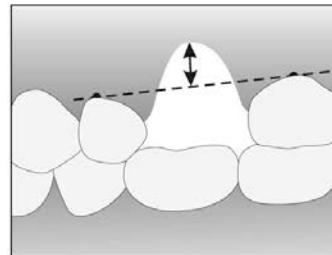


Figure 7. Alveolar ridge vertical position in non aesthetic zone: the distance between the lowest point of alveolar ridge crest to the cervicoenamel line of the adjacent teeth.

apicocoronal position of the dental implant is 2 mm below the adjacent cementoenamel junction [94]. A height for the alveolar process of > 8 to ≤ 10 mm and > 4 to ≤ 10 mm in maxillary sinus region is defined as Type II EJS. Simultaneous implantation with vertical alveolar process augmentation or sinus floor augmentation is recommended. Alveolar process height ≤ 8 and ≤ 4 mm in maxillary sinus region is defined as Type III EJS. These measurements were considered to be insufficient for 8 mm length implant installation and primary stability achievement even in maxillary sinus region. Vertical alveolar process and/or sinus floor augmentation and late implantation are recommended.

The width of alveolar process (W): determined by the alveolar process width measured at the level of 3 mm (W1) and 6 mm (W2) from the crest of alveolar process. The smallest measurement should be accepted as the width of the EJS. It was taken into consideration that optimal implant diameter indicated

for implantation in aesthetic zone can vary depending on tooth type and measurements. To make presented herein classification system more universal, it was considered to indicate proper alveolar process width for Type I EJS, as calculation of optimal implant diameter + 3 mm of the alveolar bone. It was mentioned above that it should be minimum 1 mm of bone surrounding each implant [102]. Hence, 3 mm in this case means that implant will be surrounded by minimum 1.5 mm of bone in buccal and lingual regions. The width of the alveolar process - optimal implant diameter + < 3 mm is defined as Type II EJS, and optimal implant diameter + ≤ 0 mm is defined as Type III EJS. For Type II EJS simultaneous implantation with alveolar process horizontal augmentation is recommended. For Type III EJS horizontal alveolar process augmentation and late implantation is recommended.

The length of the EJS (L): is determined by the least distance between neighbouring teeth or implants. The minimal distance between 2 implants should be at least 3 mm [107], and minimal distances between implants and natural roots should be at least 1.5 mm [108] or in case of platform-switched implant 1 mm [101]. To ensure optimal aesthetic implant rehabilitation, the implant-supported restoration should be in symmetry with the adjacent dentition [98]. Consequently, Type I EJS width must be equal to contralateral tooth. The alveolar process length characterised as asymmetry < 1 mm in comparison with contralateral tooth is defined as Type II EJS. Asymmetry ≥ 1 mm in comparison with contralateral tooth is defined as Type III EJS. In cases of Type II and III EJSs treatment choice depends on patient's aesthetic demands. If patient wish to have adequate aesthetic result, orthodontic treatment for EJS length optimisation should be recommended

prior to dental implant surgical placement.

Alveolar ridge vertical position (RVP): the distance between the lowest point of alveolar ridge crest to the cervicoenamel line of the adjacent teeth. This parameter is important for achieving of implant-supported restoration length equability to contralateral tooth (Figure 8). Adequate distance for Type I EJS is estimated to be ≤ 1 mm. The alveolar ridge vertical position > 1 to ≤ 3 mm is defined as Type II EJS and distance > 3 mm is defined as Type III EJS. Simultaneous implantation with vertical alveolar process augmentation in case of Type II EJS is recommended. For Type III EJS vertical alveolar process augmentation and late implantation are recommended.

Mesial and distal interdental bone peak height (BPH): the distance from the tip of the interdental bone peak to the alveolar crest midline. Distances of 3 to 4 mm, ≥ 1 to < 3 mm, and < 1 mm were defined as Types I, II and III, respectively (Figure 9). A study [97] demonstrated that the presence or absence of a bone crest influences the appearance of papillae between implants and adjacent teeth.

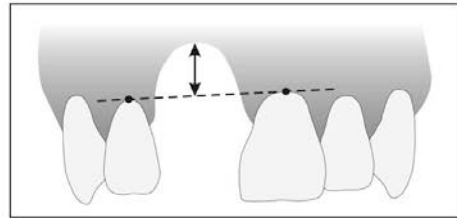


Figure 8. Alveolar ridge vertical position in aesthetic zone: the distance between the lowest point of alveolar ridge crest to the cervicoenamel line of the adjacent teeth.

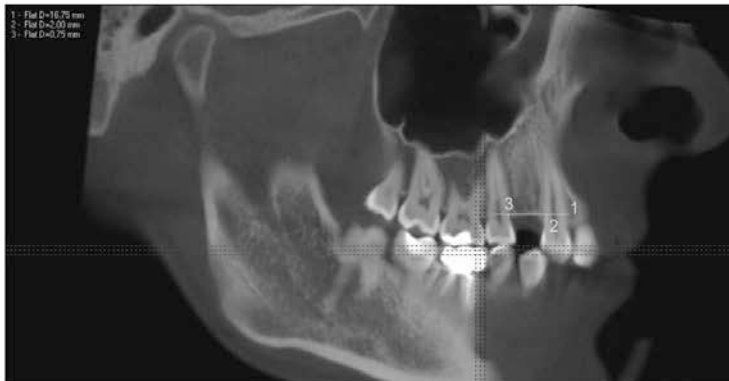


Figure 9. Type II (measurement “2”) and Type III (measurement “3”) bone peak heights of the first upper premolar EJS on CBCT image reconstruction.

Mandibular canal walls (MCW) and jawbone quality (JBQ) type identification: mandibular canal walls are depicted on panoramic radiographs or CBCT images as radio-opaque white lines which are flanking a dark ribbon. The bone quality types are characterised according to Lekholm and Zarb classification [12] (Figures 10A - D). The combination of identified MC walls and D2 or D3 bone quality types indicates Type I

EJS with low risk of inferior alveolar nerve injury. In case when it is impossible to identify superior MC wall on X-ray and there is registered D1 or D4 bone quality type, Type II EJS with moderate inferior alveolar nerve injury risk is defined. The high inferior alveolar nerve injury risk and Type III EJS is considered when it is impossible to identify MC (Figure 11) and bone quality is registered as D1 or D4 type.

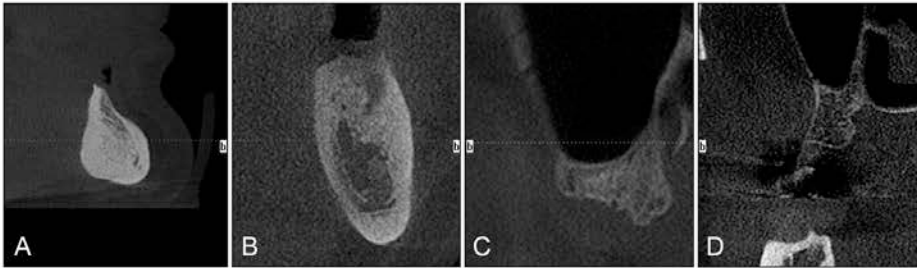


Figure 10. Bone quality according to Lekholm and Zarb classification.

A = D1 on the CBCT cross-sectional image (mental region EJS); B = D2 on the CBCT cross-sectional image (36 tooth EJS); C = D3 in the EJS of upper second molar (CBCT cross-sectional image); D = D4 in the EJS of 17 tooth on CBCT cross-sectional image.

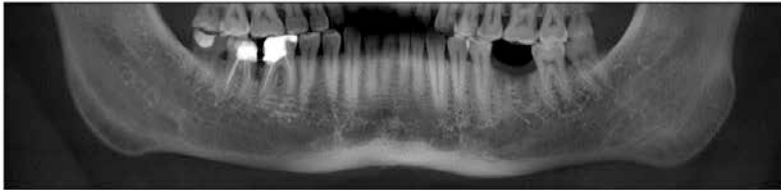


Figure 11. The part of reconstructed panoramic radiograph with unidentified superior MC wall in the EJS of 36 tooth (the same CBCT as Figure 10B).

CONCLUSIONS

New classification system of the jawbone anatomy in endosseous dental implant treatment, based on three-dimensional edentulous jaw segment pattern, is suggested. It is evident that the demands and risks of aesthetic result achievement differ significantly in aesthetic zone in comparison with non aesthetic zone. Mandibular canal and maxillary sinus regions are important anatomical vital structures of the jaws, because of the risk of injury of inferior alveolar nerve and maxillary sinus and implant operation planning peculiarities. In a result, two zones - aesthetic and non aesthetic and two regions - mandibular canal and maxillary sinus are distinguished in the new

classification system. Finally edentulous jaw segments are divided into three types (Types I to III) according to their assessment result and risk degree of planned surgical treatment success. The classification system proposed here based on anatomical and radiological jawbone quantity and quality evaluation is a helpful tool for planning of treatment strategy and collaboration among specialists. Further clinical studies should be conducted for new classification validation and reliability evaluation.

ACKNOWLEDGMENTS AND DISCLOSURE STATEMENTS

The authors report no conflicts of interest related to this study.

REFERENCES

1. The glossary of prosthodontic terms. *J Prosthet Dent.* 2005 Jul;94(1):10-92. [Medline: [16080238](#)] [doi: [10.1016/j.prosdent.2005.03.013](#)]
2. Tallgren A. The continuing reduction of the residual alveolar ridges in complete denture wearers: a mixed-longitudinal study covering 25 years. *J Prosthet Dent.* 1972 Feb;27(2):120-32. [Medline: [4500507](#)] [doi: [10.1016/0022-3913\(72\)90188-6](#)]
3. Esposito M, Hirsch JM, Lekholm U, Thomsen P. Biological factors contributing to failures of osseointegrated oral implants. (II). Etiopathogenesis. *Eur J Oral Sci.* 1998 Jun;106(3):721-64. [Medline: [9672097](#)] [doi: [10.1046/j.0909-8836.101.6.x](#)]
4. Oikarinen K, Raustia AM, Hartikainen M. General and local contraindications for endosseal implants--an epidemiological panoramic radiograph study in 65-year-old subjects. *Community Dent Oral Epidemiol.* 1995 Apr;23(2):114-8. [Medline: [7781299](#)]
5. Atwood DA. Reduction of residual ridges: a major oral disease entity. *J Prosthet Dent.* 1971 Sep;26(3):266-79. [Medline: [4934947](#)] [doi: [10.1016/0022-3913\(71\)90069-2](#)]
6. Mercier P, Lafontant R. Residual alveolar ridge atrophy: classification and influence of facial morphology. *J Prosthet Dent.* 1979 Jan;41(1):90-100. [Medline: [281529](#)] [doi: [10.1016/0022-3913\(79\)90363-9](#)]
7. Seibert JS. Reconstruction of deformed, partially edentulous ridges, using full thickness onlay grafts. Part I. Technique and wound healing. *Compend Contin Educ Dent.* 1983 Sep-Oct;4(5):437-53. [Medline: [6578906](#)]
8. Allen EP, Gainza CS, Farthing GG, Newbold DA. Improved technique for localized ridge augmentation. A report of 21 cases. *J Periodontol.* 1985 Apr;56(4):195-9. [Medline: [2987473](#)] [doi: [10.1902/jop.1985.56.4.195](#)]
9. Cawood JI, Howell RA. A classification of the edentulous jaws. *Int J Oral Maxillofac Surg.* 1988 Aug;17(4):232-6. [Medline: [3139793](#)] [doi: [10.1016/S0901-5027\(88\)80047-X](#)]
10. Eufinger H, Gellrich NC, Sandmann D, Dieckmann J. Descriptive and metric classification of jaw atrophy. An evaluation of 104 mandibles and 96 maxillae of dried skulls. *Int J Oral Maxillofac Surg.* 1997 Feb;26(1):23-8. [Medline: [9081248](#)] [doi: [10.1016/S0901-5027\(97\)80841-7](#)]
11. Meyer U, Vollmer D, Runte C, Bourauel C, Joos U. Bone loading pattern around implants in average and atrophic edentulous maxillae: a finite-element analysis. *J Craniomaxillofac Surg.* 2001 Apr;29(2):100-5. [Medline: [11465432](#)]
12. Lekholm U, Zarb GA. In: Patient selection and preparation. *Tissue integrated prostheses: osseointegration in clinical dentistry.* Branemark PI, Zarb GA, Albrektsson T, editor. Chicago: Quintessence Publishing Company; 1985. p. 199-209.
13. Jensen O. Site classification for the osseointegrated implant. *J Prosthet Dent.* 1989 Feb;61(2):228-34. [Medline: [2654368](#)] [doi: [10.1016/0022-3913\(89\)90380-6](#)]
14. Juodzbaly G, Raustia AM. Accuracy of clinical and radiological classification of the jawbone anatomy for implantation--a survey of 374 patients. *J Oral Implantol.* 2004;30(1):30-9. [Medline: [15008452](#)] [doi: [10.1563/1548-1336\(2004\)030<0030:AOCARC>2.0.CO;2](#)]
15. Kilic C, Kamburoglu K, Ozen T, Balcioglu HA, Kurt B, Kutoglu T, Ozan H. The position of the mandibular canal and histologic feature of the inferior alveolar nerve. *Clin Anat.* 2010 Jan;23(1):34-42. [Medline: [19918867](#)] [doi: [10.1002/ca.20889](#)]
16. de Oliveira-Santos C, Souza PH, de Azambuja Berti-Couto S, Stinkens L, Moyaert K, Rubira-Bullen IR, Jacobs R. Assessment of variations of the mandibular canal through cone beam computed tomography. *Clin Oral Investig.* 2012 Apr;16(2):387-93. Epub 2011 Mar 30. [Medline: [21448636](#)] [doi: [10.1007/s00784-011-0544-9](#)]
17. Chen JC, Lin LM, Geist JR, Chen JY, Chen CH, Chen YK. A retrospective comparison of the location and diameter of the inferior alveolar canal at the mental foramen and length of the anterior loop between American and Taiwanese cohorts using CBCT. *Surg Radiol Anat.* 2013 Jan;35(1):11-8. Epub 2012 Jun 5. [Medline: [22669484](#)] [doi: [10.1007/s00276-012-0986-z](#)]
18. Scarfe WC, Farman AG. Cone-Beam Computed Tomography. In: White SC, Pharoah MJ, editors. *Oral Radiology Principles and Interpretation.* St Louis: CV Mosby Company; 2009. p. 225-43.
19. Misch CE, Judy KW. Classification of partially edentulous arches for implant dentistry. *Int J Oral Implantol.* 1987;4(2):7-13. [Medline: [3269839](#)]
20. Kazor CE, Al-Shammari K, Sarment DP, Misch CE, Wang HL. Implant plastic surgery: a review and rationale. *J Oral Implantol.* 2004;30(4):240-54. Review. [Medline: [15453224](#)] [doi: [10.1563/0.637.1](#)]
21. Bianchi AE, Sanfilippo F. Single-tooth replacement by immediate implant and connective tissue graft: a 1-9-year clinical evaluation. *Clin Oral Implants Res.* 2004 Jun;15(3):269-77. [Medline: [15142088](#)] [doi: [10.1111/j.1600-0501.2004.01020.x](#)]
22. Worthington P. Injury to the inferior alveolar nerve during implant placement: a formula for protection of the patient and clinician. *Int J Oral Maxillofac Implants.* 2004 Sep-Oct;19(5):731-4. [Medline: [15508990](#)]
23. Ribeiro-Rotta RF, Lindh C, Pereira AC, Rohlin M. Ambiguity in bone tissue characteristics as presented in studies on dental implant planning and placement: a systematic review. *Clin Oral Implants Res.* 2011 Aug;22(8):789-801. Epub 2010 Dec 2. Review. [Medline: [21121957](#)] [doi: [10.1111/j.1600-0501.2010.02041.x](#)]
24. Bergkvist G, Koh KJ, Sahlholm S, Klintström E, Lindh C. Bone density at implant sites and its relationship to assessment of bone quality and treatment outcome. *Int J Oral Maxillofac Implants.* 2010 Mar-Apr;25(2):321-8. [Medline: [20369091](#)]

25. Trisi P, Rao W. Bone classification: clinical-histomorphometric comparison. *Clin Oral Implants Res.* 1999 Feb;10(1):1-7. [Medline: [10196784](#)]
26. Misch CE. Bone density: A key determinant for clinical success. In: Misch CE, editor. *Contemporary Implant Dentistry*, 2nd ed. St Louis: CV Mosby Company; 1999. p. 109-18.
27. Norton MR, Gamble C. Bone classification: an objective scale of bone density using the computerized tomography scan. *Clin Oral Implants Res.* 2001 Feb;12(1):79-84. [Medline: [11168274](#)] [doi: [10.1034/j.1600-0501.2001.012001079.x](#)]
28. Naitoh M, Kurosu Y, Inagaki K, Katsumata A, Noguchi T, Arijji E. Assessment of mandibular buccal and lingual cortical bones in postmenopausal women. *Oral Surg Oral Med Oral Pathol Oral Radiol Endod.* 2007 Oct;104(4):545-50. Epub 2007 Aug 6. [Medline: [17689117](#)] [doi: [10.1016/j.tripleo.2007.04.034](#)]
29. Başa O, Dilek OC. Assessment of the risk of perforation of the mandibular canal by implant drill using density and thickness parameters. *Gerodontology.* 2011 Sep;28(3):213-20. Epub 2010 Mar 4. [Medline: [20236331](#)]
30. Theisen FC, Shultz RE, Elledge DA. Displacement of a root form implant into the mandibular canal. *Oral Surg Oral Med Oral Pathol.* 1990 Jul;70(1):24-8. [Medline: [2196504](#)] [doi: [10.1016/0030-4220\(90\)90172-0](#)]
31. Fanuseu MI, Chang TL. Three-dimensional morphometric analysis of human cadaver bone: microstructural data from maxilla and mandible. *Clin Oral Implants Res.* 2004 Apr;15(2):213-8. [Medline: [15008933](#)] [doi: [10.1111/j.1600-0501.2004.00969.x](#)]
32. Schwarz MS, Rothman SL, Rhodes ML, Chafetz N. Computed tomography: Part I. Preoperative assessment of the mandible for endosseous implant surgery. *Int J Oral Maxillofac Implants.* 1987 Summer;2(3):137-41. [Medline: [3481354](#)]
33. Naitoh M, Hirukawa A, Katsumata A, Arijji E. Evaluation of voxel values in mandibular cancellous bone: relationship between cone-beam computed tomography and multislice helical computed tomography. *Clin Oral Implants Res.* 2009 May;20(5):503-6. [Medline: [19250241](#)] [doi: [10.1111/j.1600-0501.2008.01672.x](#)]
34. Nackaerts O, Maes F, Yan H, Couto Souza P, Pauwels R, Jacobs R. Analysis of intensity variability in multislice and cone beam computed tomography. *Clin Oral Implants Res.* 2011 Aug;22(8):873-9. Epub 2011 Jan 18. [Medline: [21244502](#)] [doi: [10.1111/j.1600-0501.2010.02076.x](#)]
35. Parsa A, Ibrahim N, Hassan B, Motroni A, van der Stelt P, Wismeijer D. Influence of cone beam CT scanning parameters on grey value measurements at an implant site. *Dentomaxillofac Radiol.* 2013;42(3):79884780. 1-7. Epub 2012 Aug 29. [Medline: [22933535](#)] [doi: [10.1259/dmfr/79884780](#)]
36. van der Stelt PF. Filmless imaging: the uses of digital radiography in dental practice. *J Am Dent Assoc.* 2005 Oct;136(10):1379-87. [Medline: [16255462](#)]
37. Denio D, Torabinejad M, Bakland LK. Anatomical relationship of the mandibular canal to its surrounding structures in mature mandibles. *J Endod.* 1992 Apr;18(4):161-5. [Medline: [1402570](#)] [doi: [10.1016/S0099-2399\(06\)81411-1](#)]
38. Benson BW, Shetty V. Dental Implants. In: White SC, Pharoah MJ, editors. *Oral Radiology Principles and Interpretation*. St Louis: CV Mosby Company; 2009. p. 597-612.
39. Chan HL, Misch K, Wang HL. Dental imaging in implant treatment planning. *Implant Dent.* 2010 Aug;19(4):288-98. [Medline: [20683285](#)] [doi: [10.1097/ID.0b013e3181e59ebd](#)]
40. Juodzbalys G, Wang HL. Guidelines for the Identification of the Mandibular Vital Structures: Practical Clinical Applications of Anatomy and Radiological Examination Methods. *J Oral Maxillofac Res.* 2010;1(2):e1. URL: <http://www.ejomr.org/JOMR/archives/2010/2/e1/e1ht.htm> [doi: [10.5037/jomr.2010.1201](#)]
41. Denio D, Torabinejad M, Bakland LK. Anatomical relationship of the mandibular canal to its surrounding structures in mature mandibles. *J Endod.* 1992 Apr;18(4):161-5. [Medline: [1402570](#)] [doi: [10.1016/S0099-2399\(06\)81411-1](#)]
42. Phillips JL, Weller RN, Kulild JC. The mental foramen: 1. Size, orientation, and positional relationship to the mandibular second premolar. *J Endod.* 1990 May;16(5):221-3. [Medline: [2074415](#)] [doi: [10.1016/S0099-2399\(06\)81674-2](#)]
43. White SC, Heslop EW, Hollender LG, Mosier KM, Ruprecht A, ShROUT MK; American Academy of Oral and Maxillofacial Radiology, ad hoc Committee on Parameters of Care. Parameters of radiologic care: An official report of the American Academy of Oral and Maxillofacial Radiology. *Oral Surg Oral Med Oral Pathol Oral Radiol Endod.* 2001 May;91(5):498-511. [Medline: [11346726](#)] [doi: [10.1067/moe.2001.114380](#)]
44. Lindh C, Petersson A, Klinge B. Measurements of distances related to the mandibular canal in radiographs. *Clin Oral Implants Res.* 1995 Jun;6(2):96-103. [Medline: [7578787](#)] [doi: [10.1034/j.1600-0501.1995.060205.x](#)]
45. Klinge B, Petersson A, Maly P. Location of the mandibular canal: comparison of macroscopic findings, conventional radiography, and computed tomography. *Int J Oral Maxillofac Implants.* 1989 Winter;4(4):327-32. [Medline: [2639861](#)]
46. Wyatt WM. Accessory mandibular canal: literature review and presentation of an additional variant. *Quintessence Int.* 1996 Feb;27(2):111-3. [Medline: [9063221](#)]
47. Kim IS, Kim SG, Kim YK, Kim JD. Position of the mental foramen in a Korean population: a clinical and radiographic study. *Implant Dent.* 2006 Dec;15(4):404-11. [Medline: [17172959](#)] [doi: [10.1097/01.id.0000243319.66845.15](#)]
48. Juodzbalys G, Wang HL, Sabalys G. Anatomy of Mandibular Vital Structures. Part I: Mandibular Canal and Inferior Alveolar Neurovascular Bundle in relation with Dental Implantology. *J Oral Maxillofac Res.* 2010;1(1):e2. URL: <http://www.ejomr.org/JOMR/archives/2010/1/e2/e2ht.htm> [doi: [10.5037/jomr.2010.1102](#)]
49. Yosue T, Brooks SL. The appearance of mental foramina on panoramic radiographs. I. Evaluation of patients. *Oral Surg Oral Med Oral Pathol.* 1989 Sep;68(3):360-4. [Medline: [2771380](#)] [doi: [10.1016/0030-4220\(89\)90224-7](#)]

50. Sonick M, Abrahams J, Faiella RA. A comparison of the accuracy of periapical, panoramic, and computerized tomographic radiographs in locating the mandibular canal. *Int J Oral Maxillofac Implants*. 1994;9:455-460.
51. Kuzmanovic DV, Payne AG, Kieser JA, Dias GJ. Anterior loop of the mental nerve: a morphological and radiographic study. *Clin Oral Implants Res*. 2003 Aug;14(4):464-71. [Medline: 12869009] [doi: 10.1034/j.1600-0501.2003.00869.x]
52. Ngeow WC, Yuzawati Y. The location of the mental foramen in a selected Malay population. *J Oral Sci*. 2003 Sep;45(3):171-5. [Medline: 14650583] [doi: 10.2334/josnusd.45.171]
53. Jacobs R, Mraiwa N, Van Steenberghe D, Sanderink G, Quirynen M. Appearance of the mandibular incisive canal on panoramic radiographs. *Surg Radiol Anat*. 2004 Aug;26(4):329-33. [Medline: 15197490] [doi: 10.1007/s00276-004-0242-2]
54. Jacobs R, Mraiwa N, vanSteenberghe D, Gijbels F, Quirynen M. Appearance, location, course, and morphology of the mandibular incisive canal: an assessment on spiral CT scan. *Dentomaxillofac Radiol*. 2002 Sep;31(5):322-7. [Medline: 12203132] [doi: 10.1038/sj.dmf.4600719]
55. Peker I, Alkurt MT, Michcioglu T. The use of 3 different imaging methods for the localization of the mandibular canal in dental implant planning. *Int J Oral Maxillofac Implants*. 2008 May-Jun;23(3):463-70. [Medline: 18700369]
56. Rouas P, Nancy J, Bar D. Identification of double mandibular canals: literature review and three case reports with CT scans and cone beam CT. *Dentomaxillofac Radiol*. 2007 Jan;36(1):34-8. [Medline: 17329586] [doi: 10.1259/dmfr/27374727]
57. Claeys V, Wäckens G. Bifid mandibular canal: literature review and case report. *Dentomaxillofac Radiol*. 2005 Jan;34(1):55-8. [Medline: 15709108] [doi: 10.1259/dmfr/23146121]
58. Sanchis JM, Pe-arrocha M, Soler F. Bifid mandibular canal. *J Oral Maxillofac Surg*. 2003 Apr;61(4):422-4. [Medline: 12684957] [doi: 10.1053/joms.2003.50004]
59. Naitoh H, Hiraiwa Y, Aimiya H, Ariji E. Observation of bifid mandibular canal using cone-beam computerized tomography. *Int J Oral Maxillofac Implants*. 2009 Jan-Feb;24(1):155-9. [Medline: 19344041]
60. Angelopoulos C, Thomas SL, Hechler S, Parissis N, Hlavacek M. Comparison between digital panoramic radiography and cone-beam computed tomography for the identification of the mandibular canal as part of presurgical dental implant assessment. *J Oral Maxillofac Surg*. 2008 Oct;66(10):2130-5. [Medline: 18848113] [doi: 10.1016/j.joms.2008.06.021]
61. Lindh C, Petersson A. Radiologic examination for location of the mandibular canal: a comparison between panoramic radiography and conventional tomography. *Int J Oral Maxillofac Implants*. 1989 Fall;4(3):249-53. [Medline: 2639123]
62. Bou Serhal C, Jacobs R, Flygare L, Quirynen M, van Steenberghe D. Perioperative validation of localization of the mental foramen. *Dentomaxillofac Radiol* 2002;31:39-43. [Medline: 11803387] [doi: 10.1038/sj.dmf.4600662]
63. Ekstubbe A, Gröndahl K, Gröndahl HG. The use of tomography for dental implant planning. *Dentomaxillofac Radiol*. 1997 Jul;26(4):206-13. [Medline: 9442610] [doi: 10.1038/sj.dmf.4600249]
64. Sakakura CE, Morais JA, Loffredo LC, Scaf G. A survey of radiographic prescription in dental implant assessment. *Dentomaxillofac Radiol*. 2003 Nov;32(6):397-400. [Medline: 15070843] [doi: 10.1259/dmfr/20681066]
65. Lascalca CA, Panella J, Marques MM. Analysis of the accuracy of linear measurements obtained by cone beam computed tomography (CBCT-NewTom). *Dentomaxillofac Radiol*. 2004 Sep;33(5):291-4. [Medline: 15585804] [doi: 10.1259/dmfr/25500850]
66. Sato S, Arai Y, Shinoda K, Ito K. Clinical application of a new cone-beam computerized tomography system to assess multiple two-dimensional images for the preoperative treatment planning of maxillary implants: case reports. *Quintessence Int*. 2004 Jul-Aug;35(7):525-8. [Medline: 15259967]
67. Almog DM, LaMar J, LaMar FR, LaMar F. Cone beam computerized tomography-based dental imaging for implant planning and surgical guidance, Part 1: Single implant in the mandibular molar region. *J Oral Implantol*. 2006;32(2):77-81. [Medline: 16704109] [doi: 10.1563/789.1]
68. Loubele M, Guerrero ME, Jacobs R, Suetens P, van Steenberghe D. A comparison of jaw dimensional and quality assessments of bone characteristics with cone-beam CT, spiral tomography, and multi-slice spiral CT. *Int J Oral Maxillofac Implants*. 2007 May-Jun;22(3):446-54. [Medline: 17622012]
69. Arai Y, Tammsalo E, Iwai K, Hashimoto K, Shinoda K. Development of a compact computed tomographic apparatus for dental use. *Dentomaxillofac Radiol*. 1999 Jul;28(4):245-8. [Medline: 10455389] [doi: 10.1038/sj.dmf.4600448]
70. Mozzo P, Procacci C, Tacconi A, Martini PT, Andreis IA. A new volumetric CT machine for dental imaging based on the cone-beam technique: preliminary results. *Eur Radiol*. 1998;8(9):1558-64. [Medline: 9866761] [doi: 10.1007/s003300050586]
71. Delcanho RE. Neuropathic implications of prosthodontic treatment. *J Prosthet Dent*. 1995 Feb;73(2):146-52. Review. [Medline: 7722929] [doi: 10.1016/S0022-3913(05)80154-4]
72. Rubenstein JE, Taylor TD. Apical nerve transection resulting from implant placement: a 10-year follow-up report. *J Prosthet Dent*. 1997 Dec;78(6):537-41. [Medline: 9421779] [doi: 10.1016/S0022-3913(97)70001-5]
73. Wismeijer D, van Waas MA, Vermeeren JI, Kalk W. Patients' perception of sensory disturbances of the mental nerve before and after implant surgery: a prospective study of 110 patients. *Br J Oral Maxillofac Surg*. 1997 Aug;35(4):254-9. [Medline: 9291263] [doi: 10.1016/S0266-4356(97)90043-7]
74. Dao TT, Mellor A. Sensory disturbances associated with implant surgery. *Int J Prosthodont* 1998 Sep-Oct;11(5):462-9. Review. [Medline: 9922738]

75. Bartling R, Freeman K, Kraut RA. The incidence of altered sensation of the mental nerve after mandibular implant placement. *J Oral Maxillofac Surg.* 1999 Dec;57(12):1408-12. [Medline: [10596660](#)] [doi: [10.1016/S0278-2391\(99\)90720-6](#)]
76. Walton JN. Altered sensation associated with implants in the anterior mandible: a prospective study. *J Prosthet Dent.* 2000 Apr;83(4):443-9. [Medline: [10756294](#)] [doi: [10.1016/S0022-3913\(00\)70039-4](#)]
77. Ziccardi VB, Assael LA. Mechanisms of trigeminal nerve injuries. *Atlas Oral Maxillofac Surg Clin North Am.* 2001 Sep;9(2):1-11. [Medline: [11665372](#)]
78. von Arx T, Häfliger J, Chappuis V. Neurosensory disturbances following bone harvesting in the symphysis: a prospective clinical study. *Clin Oral Implants Res.* 2005 Aug;16(4):432-9. [Medline: [16117767](#)] [doi: [10.1111/j.1600-0501.2005.01138.x](#)]
79. Abarca M, van Steenberghe D, Malevez C, De Ridder J, Jacobs R. Neurosensory disturbances after immediate loading of implants in the anterior mandible: an initial questionnaire approach followed by a psychophysical assessment. *Clin Oral Investig.* 2006 Dec;10(4):269-77. Epub 2006 Aug 26. [Medline: [16937108](#)] [doi: [10.1007/s00784-006-0065-0](#)]
80. Greenstein G, Tarnow D. The mental foramen and nerve: clinical and anatomical factors related to dental implant placement: a literature review. *J Periodontol.* 2006 Dec;77(12):1933-43. Review. [Medline: [17209776](#)] [doi: [10.1902/jop.2006.060197](#)]
81. Hegedus F, Diecidue RJ. Trigeminal nerve injuries after mandibular implant placement--practical knowledge for clinicians. *Int J Oral Maxillofac Implants.* 2006 Jan-Feb;21(1):111-6. Review. [Medline: [16519189](#)]
82. Tay AB, Zuniga JR. Clinical characteristics of trigeminal nerve injury referrals to a university centre. *Int J Oral Maxillofac Surg.* 2007 Oct;36(10):922-7. Epub 2007 Sep 17. [Medline: [17875382](#)] [doi: [10.1016/j.ijom.2007.03.012](#)]
83. Misch CE. Root form surgery in the edentulous anterior and posterior mandible: Implant insertion. In: Misch CE, editor. *Contemporary Implant Dentistry.* St. Louis, MO: Mosby Elsevier; 2008. p. 221-6.
84. Alhassani AA, AlGhamdi AS. Inferior alveolar nerve injury in implant dentistry: diagnosis, causes, prevention, and management. *J Oral Implantol.* 2010;36(5):401-7. Epub 2010 Jun 14. Review. [Medline: [20545547](#)] [doi: [10.1563/AID-JOI-D-09-00059](#)]
85. Misch CE, Resnik R. Mandibular nerve neurosensory impairment after dental implant surgery: management and protocol. *Implant Dent.* 2010 Oct;19(5):378-86. [Medline: [20881808](#)] [doi: [10.1097/ID.0b013e3181e1ffa92](#)]
86. Juodzbalys G, Wang HL, Sabalys G. Injury of the Inferior Alveolar Nerve during Implant Placement: a Literature Review. *J Oral Maxillofac Res.* 2011;2(1):e1. URL: <http://www.ejomr.org/JOMR/archives/2011/1/e1/v2n1e1ht.htm> [doi: [10.5037/jomr.2011.2101](#)]
87. Juodzbalys G, Wang HL, Sabalys G, Sidlauskas A, Galindo-Moreno P. Inferior alveolar nerve injury associated with implant surgery. *Clin Oral Implants Res.* 2013 Feb;24(2):183-90. Epub 2011 Nov 1. [Medline: [22092662](#)] [doi: [10.1111/j.1600-0501.2011.02314.x](#)]
88. Kraut RA, Chahal O. Management of patients with trigeminal nerve injuries after mandibular implant placement. *J Am Dent Assoc.* 2002 Oct;133(10):1351-4. [Medline: [12403537](#)]
89. Lamas Pelayo J, Pe-arrocha Diago M, Marti Bowen E, Pe-arrocha Diago M. Intraoperative complications during oral implantology. *Med Oral Patol Oral Cir Bucal.* 2008 Apr 1;13(4):E239-43. Review. [Medline: [18379448](#)]
90. Khawaja N, Renton T. Case studies on implant removal influencing the resolution of inferior alveolar nerve injury. *Br Dent J.* 2009 Apr 11;206(7):365-70. [Medline: [19357667](#)] [doi: [10.1038/sj.bdj.2009.258](#)]
91. Sammartino G, Marenzi G, Citarella R, Ciccarelli R, Wang HL. Analysis of the occlusal stress transmitted to the inferior alveolar nerve by an osseointegrated threaded fixture. *J Periodontol.* 2008 Sep;79(9):1735-44. [Medline: [18771376](#)] [doi: [10.1902/jop.2008.080030](#)]
92. Guan H, van Staden R, Loo YC, Johnson N, Ivanovski S, Meredith N. Influence of bone and dental implant parameters on stress distribution in the mandible: a finite element study. *Int J Oral Maxillofac Implants.* 2009 Sep-Oct;24(5):866-76. [Medline: [19865627](#)]
93. Wadu SG, Penhall B, Townsend GC. Morphological variability of the human inferior alveolar nerve. *Clin Anat.* 1997;10(2):82-7. [Medline: [9058013](#)] [doi: [10.1002/\(SICI\)1098-2353\(1997\)10:2<82::AID-CA2>3.0.CO;2-V](#)]
94. Saoudon AP, Landsberg TC. Treatment classifications and sequencing for post extraction implant therapy: A review. *Pract Periodontics Aesthet Dent.* 1997;9:933-941. [Medline: [9573848](#)]
95. Jovanovic SA. Bone rehabilitation to achieve optimal aesthetics. *Pract Periodontics Aesthet Dent.* 1997 Jan-Feb;9(1):41-51; quiz 52. [Medline: [9550059](#)]
96. Belsler UC, Buser D, Hess D, Schmid B, Bernard JP, Lang NP. Aesthetic implant restorations in partially edentulous patients--a critical appraisal. *Periodontol.* 2000. 1998 Jun;17:132-50. Review. [Medline: [10337321](#)] [doi: [10.1111/j.1600-0757.1998.tb00131.x](#)]
97. Choquet V, Hermans M, Adriaenssens P, Daelemans P, Tarnow DP, Malevez C. Clinical and radiographic evaluation of the papilla level adjacent to single-tooth dental implants. A retrospective study in the maxillary anterior region. *J Periodontol.* 2001 Oct;72(10):1364-71. [Medline: [11699478](#)] [doi: [10.1902/jop.2001.72.10.1364](#)]
98. Fürhauer R, Florescu D, Benesch T, Haas R, Mailath G, Watzek G. Evaluation of soft tissue around single-tooth implant crowns: the pink esthetic score. *Clin Oral Implants Res.* 2005 Dec;16(6):639-44. [Medline: [16307569](#)] [doi: [10.1111/j.1600-0501.2005.01193.x](#)]

99. Ohmell LO, Hirsch JM, Ericsson I, Brånemark PI. Single-tooth rehabilitation using osseointegration. A modified surgical and prosthodontic approach. *Quintessence Int.* 1988 Dec;19(12):871-6. [Medline: 3254544]
100. Adell R, Eriksson B, Lekholm U, Brånemark PI, Jemt T. Long-term follow-up study of osseointegrated implants in the treatment of totally edentulous jaws. *Int J Oral Maxillofac Implants.* 1990 Winter;5(4):347-59. [Medline: 2094653]
101. Vela X, Méndez V, Rodríguez X, Segalá M, Tarnow DP. Crestal bone changes on platform-switched implants and adjacent teeth when the tooth-implant distance is less than 1.5 mm. *Int J Periodontics Restorative Dent.* 2012 Apr;32(2):149-55. [Medline: 22292143]
102. Allen F, Smith DG. An assessment of the accuracy of ridge-mapping in planning implant therapy for the anterior maxilla. *Clin Oral Implants Res.* 2000 Feb;11(1):34-8. [Medline: 11168191] [doi: 10.1034/j.1600-0501.2000.011001034.x]
103. Lindh C, Öbrant K, Petersson A. Maxillary bone mineral density and its relationship to the bone mineral density of the lumbar spine and hip. *Oral Surg Oral Med Oral Pathol Oral Radiol Endod.* 2004 Jul;98(1):102-9. [Medline: 15243479] [doi: 10.1016/S1079-2104(03)00460-8]
104. Friberg B, Jemt T, Lekholm U. Early failures in 4,641 consecutively placed Brånemark dental implants: a study from stage I surgery to the connection of completed prostheses. *Int J Oral Maxillofac Implants.* 1991 Summer;6(2):142-6. [Medline: 1809668]
105. Hardwick R, Scantlebury TV, Sanchez R, Whitely N, Ambruster J. Membrane design criteria for guided bone regeneration of the alveolar ridge. In: Buser D, Dahlin C, Schenk RK, editors. *Guided bone regeneration in implant dentistry.* Hong Kong: Quintessence; 1994: p. b101-36.
106. Dula K, Mini R, van der Stelt PF, Buser D. The radiographic assessment of implant patients: decision-making criteria. *Int J Oral Maxillofac Implants.* 2001 Jan-Feb;16(1):80-9. [Medline: 11280366]
107. Hobo S, Ichida E, Garcia LT. *Osseointegration and Occlusal Rehabilitation*, 1st ed. Chicago, Ill: Quintessence; 1989. p. 35.
108. Bauman GR, Mills M, Rapley JW, Hallmon WH. Clinical parameters of evaluation during implant maintenance. *Int J Oral Maxillofac Implants.* 1992 Summer;7(2):220-7. Review. [Medline: 1398839]
109. Davies SJ, Gray RJ, Young MP. Good occlusal practice in the provision of implant borne prostheses. *Br Dent J.* 2002 Jan 26;192(2):79-88. Review. [Medline: 11841055] [doi: 10.1038/sj.bdj.4801298]

To cite this article:

Juodzbalyš G, Kubilius M. Clinical and Radiological Classification of the Jawbone Anatomy in Endosseous Dental Implant Treatment. *J Oral Maxillofac Res* 2013;4(2):e2
 URL: <http://www.ejomr.org/JOMR/archives/2013/2/e2/v4n2e2ht.pdf>
 doi: 10.5037/jomr.2013.4202

Copyright © Juodzbalyš G, Kubilius M. Accepted for publication in the JOURNAL OF ORAL & MAXILLOFACIAL RESEARCH (<http://www.ejomr.org>), 12 June 2013.

This is an open-access article, first published in the JOURNAL OF ORAL & MAXILLOFACIAL RESEARCH, distributed under the terms of the [Creative Commons Attribution-Noncommercial-No Derivative Works 3.0 Unported License](http://creativecommons.org/licenses/by-nc-nd/3.0/), which permits unrestricted non-commercial use, distribution, and reproduction in any medium, provided the original work and is properly cited. The copyright, license information and link to the original publication on (<http://www.ejomr.org>) must be included.

SANTRAUKA

(SUMMARY IN LITHUANIAN)

Ižanga

Dantų implantacija yra sėkmingas gydymo metodas, kurio sėkmės rodiklis yra apie 90 proc., bet šis metodas yra susijęs su keletu galimų komplikacijų. Apatinio alveolinio nervo (AAN) pažeidimas yra viena iš sunkiausių dantų implantacijos komplikacijų. AAN pažeidimas dažniausiai yra jatrogeninė komplikacija, jos dažnumas gali siekti iki 40 proc. Įdomu tai, kad AAN yra dažniausiai pažeidžiama trišakio nervo šaka (64,4 proc.). Prieš operaciją radiologinis ištyrimas ir planavimas yra privalomi, ypač apatinio žandikaulio distalinių segmentų, norint išvengti AAN pažeidimo. Gerėjant skaitmeninių panoraminių rentgenogramų (SPR) kokybei ir galimybei analizuoti rentgenogramą naudojant papildomus įrankius, tokius kaip densitometrija, šis metodas gana plačiai paplito. Panoraminių rentgenogramų kokybė priklauso nuo paciento pozicionavimo, nuotraukos registravimo ir apdorojimo proceso paklaidų. Įtakos gali turėti anatomiciniai paciento žandikaulių ypatumai. Nepaisant to, šios rentgenogramos yra pakankamai kokybiškos ir yra rekomenduojamos diagnozuojant ir planuojant dantų implantaciją. Kadangi apatinio žandikaulio kanalo (AŽK) matomumas keičiasi kanalui gilėjant, SPR gali suteikti radiologinę informaciją apie AŽK matomumą kiekvieno žandikaulio dantinio segmento (ŽDS) srityje. Būtų labai naudinga klinikinėje praktikoje, jeigu AŽK ir aplink esančio kaulo morfometriniu ir densitometriniu įvertinimo parametrų dinamika galėtų sukurti sistemą, kuri padėtų identifikuoti AŽK ir jo sienelės, netgi esant blogam kanalo matomumui.

Kraujavimas yra dar viena rimta komplikacija dantų implantacijos metu. Norint suprasti galimos komplikacijos svarbą santykinai saugiam apatinio žandikaulio priekiniame segmente, reikia pažymėti, kad vidutinis liežuvinės arterijos diametras yra 1,41 mm, o kraujo tekėjimo kiekis – apie 2,92 ml/min. Juolab kad šioje zonoje yra kaulinė žandikaulio įduba, poliežuvinė duobė, besitęsianti iki pirmojo kaplio. Klinikistas gali stebėti liežuvinį žandikaulio kanalą operacijos metu. Šiuo atveju yra nepaprastai svarbu įvertinti anatomicinius žandikaulio ypatumus naudojant labiausiai informatyvų rentgeno diagnostinį metodą. Daug žadantis ir vienas iš naujausių yra konusinio pluošto kompiuterinė tomografija (KPKT). Norint išsiaiškinti KPKT diagnostines galimybes, turėtų būti atliktas tarptautinis tyrimas su dideliu skaičiumi pacientų, kad būtų patobulinta liežuvinės ertmės diagnostika implantuojant dantis.

Viršutinio žandikaulio anatomiciniai ypatumai taip pat gali nulemti padidėjusį komplikacijų skaičių dantų implantacijos metu. Tinkamas kaulo kiekis ir kokybė yra svarbūs veiksniai, nulemiantys tinkamą chirurginį implantato instaliavimą. Implantacija viršutinio žandikaulio srityje paprastai yra susijusi su sinuso oringumo padidėjimu ir išsiskverbimu į alveolinę ataugą bei vertikaliu alveolinio kaulo deficitu. Šios aplinkybės paprastai sukelia rimtas problemas atliekant dantų implantaciją. Normalios viršutinio žandikaulio anatomijos ir galimų įvairių variacijų žinojimas yra esminiai sėkmingos sinuso dugno augmentacijos veiksniai. Prieš viršutinio žandikaulio sinuso augmentacijos procedūrą klinicistas turi atkreipti dėmesį į kai kurias sinuso anatomines struktūras: viršutinę galinę alveolinę arteriją (VGAA), sinuso angą, gleivinę, pertvaras. Ištyrus literatūros duomenis, nustatyta, kad tyrimų šia tema atlikta nedaug, o tiriamųjų skaičius nepakankamai didelis. Atsižvelgiant į tai, reikia konstatuoti, kad reikia plataus tarptautinio viršutinio žandikaulio sinuso anatomijos bei galimų variacijų ir patologijos, įskaitant ir aplinkinį kaulą, tyrimo taikant KPKT metodą. Kiekybinis ir kokybinis sinuso vertinimo šablonas yra būtinas diagnostikos ir planavimo patobulinimas atliekant dantų implantaciją.

Atsižvelgiant į sukauptų literatūros duomenų apie atliekamą diagnostiką prieš dantų implantaciją gausą ir sukauptą asmeninę klinikinę patirtį, natūraliai kyla idėja pateikti pasiūlymus, kurie pagerins diagnostiką ir planavimą. Klasifikacijos sistemos sukūrimas yra ta priemonė, kuri padėtų įgyvendinti aukščiau minėtą tikslą. Pirmieji trys lygiagrečiai vykdomi tyrimai buvo skirti įvertinti apatinio ir viršutinio žandikaulių anatomijos ypatumus, susijusius su dantų implantacijos planavimu. Kitas žingsnis buvo sukurti visa apimančią žandikaulių anatomijos klasifikaciją, skirtą endosalinei dantų implantacijai, paremtą literatūros duomenimis, gautų tyrimų rezultatais ir savo klinicine patirtimi. AŽK matomumo įvertinimas, morfometrinių ir densitometrinių apatinio žandikaulio dantinio segmento analizė ir kraujagyslių kanalų įvertinimas buvo įtraukti į naują detalią žandikaulių klasifikaciją. Ankstesnės klasifikacijos kaip tik ir neatsižvelgė į AŽK, kaulo kokybę, viršutinio žandikaulio sinuso srities įvertinimo bei estetinių parametru rezultatus. Reikia naujo tyrimo, kuris įvertintų sukurtos klasifikacijos patikimumą ir efektyvumą.

Prieš pradėdant gydymo procedūrą, yra atliekamas išsamus klinikinis ir radiologinis ištyrimas, norint sudaryti optimalų, gerai nuspėjamą gydymo planą. Ypač reikšmingi yra pirminio ištyrimo ir planavimo žingsniai, turintys įtakos ankstyviesiems ir tolimiesiems gydymo rezultatams bei paciento pasitenkinimui ir gerai klinikinio gydymo praktikai.

Šios santraukos išdėstymo seka atspindi dantų implantacijos chirurginės procedūros diagnostiką ir planavimą naudojant įvairius vaizduojamuosius

diagnostinius biomedicinos literatūroje aprašytus metodus ir įvertinant klinikinių bei radiologinių žandikaulių diagnostikos metodų tobulinimo būtinybę.

Darbo tikslai

Darbo tikslas: įvertinti ir patobulinti klinikinių ir radiologinių diagnostikos metodų, naudojamų endosalinės dantų implantacijos operacijai planuoti, patikimumą / efektyvumą, charakterizuojant konkrečią apatinio arba viršutinio žandikaulio sritį bei identifikuojant svarbius anatominius darinius.

Uždaviniai:

1. Įvertinti apatinio žandikaulio kanalo matomumą skaitmeninėje panoraminėje rentgenogramoje įvairiuose dantiniuose žandikaulio segmentuose, atsižvelgiant į morfometrinius ir densitometrinius rentgenogramos parametrus.
2. Įvertinti konusinio pluošto kompiuterinės tomografijos diagnostikos efektyvumą diagnozuojant apatinio žandikaulio liežuvinių kraujagyslių kanalus ir jų anatominius ypatumus.
3. Įvertinti konusinio pluošto kompiuterinės tomografijos diagnostikos efektyvumą tiriant viršutinio žandikaulio sinuso ir aplinkinio kaulo anatomines struktūras.
4. Sukurti naują klinikinę ir radiologinę žandikaulių anatomijos klasifikaciją, skirtą endosalinės dantų implantacijos operacijai planuoti.
5. Įvertinti naujos klinikinės ir radiologinės žandikaulių anatomijos klasifikacijos, skirtos endosalinės dantų implantacijos operacijai planuoti, patikimumą ir efektyvumą.

Darbo hipotezė

Išsamus dantinio segmento anatomijos vertinimas gerina dantų implantacijos diagnostiką ir planavimą.

Įvadas

Disertacija susideda iš šių tyrimų, kurie pažymėti tekste Romėniškais numeriais.

Romėniški numeriai:

I tyrimas (Descriptive study of mandibular canal visibility: morphometric and densitometric analysis for digital panoramic radiographs)

Kubilius M, Kubilius R, Varinauskas V, Žalinkevičius R, Tözüm TF, Juodzbaly G. Descriptive Study of Mandibular Canal Visibility: Morpho-

metric and Densitometric Analysis for Digital Panoramic Radiographs. *Dentomaxillofac Radiol* 2016;45: 20160079. doi: 10.1259/dmfr.20160079.

II tyrimas (Evaluation of mandibular lingual foramina related to dental implant treatment with computerized tomography: a multicenter clinical study).

Yildirim YD1, Güncü GN, Galindo-Moreno P, Velasco-Torres M, Juodzbaly G, Kubilius M, Gervickas A, Al-Hezaimi K, Al-Sadhan R, Yilmaz HG, Asar NV, Karabulut E, Wang HL, Tözüm TF. Evaluation of mandibular lingual foramina related to dental implant treatment with computerized tomography: a multicenter clinical study. *Implant Dent* 2014 Feb;23(1):57-63. doi: 10.1097/ID.000000000000012.

III tyrimas (Evaluation of maxillary sinus and surrounding bone anatomy with cone beam computed tomography).

IV tyrimas (Clinical and radiological classification of the jaw bone anatomy in endosseous dental implant treatment).

Juodzbaly G, Kubilius M. Clinical and Radiological Classification of the Jawbone Anatomy in Endosseous Dental Implant Treatment. *J Oral Maxillofac Res* 2013 (Apr-Jun);4(2):e2. doi: 10.5037/jomr.2013.4202).

V tyrimas (Validation of the therapeutic anatomy oriented classification in endosseous dental implant treatment: a pilot study).

Mokslinis naujumas

Buvo atlikti kompleksiniai tyrimai įvertinant ir patobulinant klinikinių ir radiologinių diagnostikos metodų efektyvumą atliekant endosalinės dantų implantacijos operacijos planavimą.

Nėra pakankamai AŽK matomumo skaitmeninėse panoraminėse rentgenogramose vertinimo tyrimų. Šiame darbe buvo atliktas detalus ŽDS ištyrimas naudojant SPR vertinimo įrankius, siekiant padidinti AŽK matomumo galimybes. Atliktas unikalus AŽK matomumo vertinimas keturiose ŽDS vietose, registruojant įvairius rodiklius, galinčius turėti įtakos AŽK matomumui (I).

Planuojant dantų implantaciją, maži kraujagysliniai apatinio žandikaulio kanalai nebuvo tirti KPKT metodu, įtraukiant didelį tiriamųjų skaičių. Atliktas tarptautinis tyrimas (II), kurio metu didelei tiriamųjų asmenų grupei buvo atlikta apatinio žandikaulio liežuvinių kraujagyslių kanalų vizualizacija ir analizė.

KPKT metodas viršutinio žandikaulio sinusui iširti jau yra naudojamas, tačiau yra atlikta nedaug tyrimų šia tema. Didžiausi šių tyrimų trūkumai yra mažas tiriamųjų skaičius ir ribotas svarbių anatominių darinių ištyrimas. Mūsų tyrimo metu (III) buvo įvertinti įvairūs anatominiai viršutinio žandi-

kaulio sinuso srities parametrai. Buvo išanalizuoti svarbūs dantų implantacijos viršutiniame žandikaulyje planavimo diagnostikos aspektai.

Buvo pasiūlyta detali klasifikacija, paremta literatūros duomenimis ir mūsų tyrimų rezultatais, skirta žandikaulių anatomijai įvertinti prieš dantų implantacijos operaciją (IV). Buvo pažymėta AŽK identifikavimo, atsižvelgiant į kaulo tankį ir AAN pažeidimo riziką bei estetinius reikalavimus estetinėje zonoje, svarba.

Buvo atliktas tarptautinis pilotinis tyrimas, siekiant įvertinti paskelbtos klasifikacijos patikimumą ir efektyvumą. Klasifikacijos trūkumai buvo identifikuoti ir išdiskutuoti. Klasifikacija buvo papildyta atsižvelgiant į pilotinio tyrimo rezultatus ir rekomendacijas (V).

Medžiaga ir metodai

I tyrimo metu Veido ir žandikaulių chirurgijos klinikoje atsitiktine tvarka atrinkti baltosios rasės pacientai, kuriems planuojant chirurginį gydymą reikėjo atlikti panoraminę rentgenogramą. Pacientų tinkamumas tyrimui buvo patvirtintas įvertinus jų medicininę ir odontologinę anamnezę. Į tyrimą neįtraukti pacientai, kuriems buvo nustatytos ūminės periodonto ligos ar skiriamas periodonto ar ortodontinių ligų gydymas. 32 SPR (155 specifiniai žandikaulio segmentai) buvo atrinktos atsitiktine tvarka planuojant chirurginį gydymą prieš operaciją. Kalibruotas ir standartizuotas tyrėjas atliko vertinimų serijas, naudodamas tam skirtą programinę įrangą ir medicininių monitorių. AŽK matomumas ir jo sąsaja su viršutine bei apatine siena buvo įvertintas (5 klasės) kiekvieno ŽDS keturiose srityse: medialinėje ir distalinėje, viršutinėje ir apatinėje AŽK dalyse. Suplanuotuose AŽK srityse horizontalia ir vertikalia kryptimis buvo atliktos radiomorfometrines ir radiodensitometrines analizės.

II tyrimo metu penkiose odontologinėse klinikose – Turkijoje, Ispanijoje, Lietuvoje, Saudo Arabijoje ir Kipre – atsitiktine tvarka buvo atrinkta 639 pacientai ir išanalizuota jų 1061 apatinio žandikaulio liežuvinė anga. Tyrimas buvo atliktas norint nustatyti atstumą tarp apatinio žandikaulio keteros ir liežuvinės angos. Taip pat buvo išmatuoti atstumai nuo liežuvinės angos iki danties viršūnės bei iki žandikaulio apatinio krašto, įvertintas liežuvinės angos diametras. Be to, tyrėjai vertino pacientų apatinio žandikaulio liežuvininių kraujagyslių kanalo tipą, anastomozes ir tikslią angos vietą.

III tyrimas buvo viršutinio žandikaulio sričių retrospektyvusis klinikinis tyrimas, kurį sudarė du bedančių žandikaulio segmentų (BŽS) pogrupiai (vieno netekto danties ir daugiau nei vieno netekto danties). Iš viso tirti 597 suaugę pacientai, kuriems buvo vienas BŽS, ir 518 pacientų, kuriems buvo keli BŽS (n = 1190 BŽS) viršutinio žandikaulio srityje, ir įvertinti viršutinio

žandikaulio sinuso srities anatomiciniai ypatumai bei alveolinė atauga. Atrinkti pacientai, kurie buvo nusiūsti burnos chirurginiam gydymui ar dantų implantacijai atlikti šešiose klinikose tarptautiniu mastu (Kipre, Turkijoje, Lietuvoje, Ispanijoje, dviejuose centruose JAV) ir kuriems reikėjo įvertinti burnos, veido ir žandikaulių sričių atliekant KPKT. Visų tiriamųjų KPKT tomogramos buvo perkeltos į kompiuterį ir vaizdai apdoroti medicininame monitoriuje tam skirta programine įranga.

IV tyrimo metu buvo atliekama literatūros paieška įvairiuose šaltiniuose ir elektroninėse duomenų bazėse, tarp jų *Cochrane*, *Embase* ir *PubMed*. Kai kurie iš svarbiausių ieškant literatūros naudotų raktinių žodžių buvo: klasifikacija; apatinis žandikaulis; apatinio žandikaulio kanalas; anatomija, skerspjuvio; alveolarinis nervas, apatinis; dantų implantai. Į tyrimą įtraukti straipsniai, parašyti anglų kalba ir publikuoti tarp 1972 m. ir 2013 m., siekiant originalumo ir informacijos aktualumo. Taip pat peržiūrėtos svarbiausios anatomijos ir chirurgijos knygos, turint omenyje, kad į jas įtraukti klinikiniai ir anatomiciniai tyrimai. Buvo peržiūrėtos ankstesnės klasifikacijos.

V tyrime dalyvavo 81 pacientas, kuriam buvo dalinė adentija. Jie buvo nusiūsti į dvi klinikas (Lietuvoje ir Turkijoje) implantuoti dantis atlikus KPKT. Į tyrimą įtraukti bendros sveikatos atžvilgiu sveiki ar nesunkiomis gretutinėmis ligomis sergantys ir papildomus reikalavimus atitikę suaugę žmonės. Tarptautinis tyrimas pagrįstas neseniai pasiūlyta klasifikacija. Pasiūlytos klasifikacijos tikslumas buvo vertintas po BDS vertinimo priešoperacinėje, intraoperacinėje, ankstyvoje pooperacinėje ir vėlyvoje pooperacinėje stadijoje. Tam tikrų estetinės ir neestetinės zonos parametrų atitikimo vertinimas skirtingais tyrimo etapais iš dalies skyrėsi. Atitinkami parametrai buvo palyginti po tyrimo duomenų surinkimo, norint patikrinti naujai pasiūlytą klinikinę ir radiologinę žandikaulių anatomijos klasifikaciją, skirtą dantų implantacijai.

Statistinė analizė

Tyrimo statistinei analizei atlikti buvo naudojami SPSS 20.0 arba 16.0 (*Statistical Package for Social Science for Windows*) programiniai paketai (*SPSS Inc., Chicago, IL, USA*), o duomenų pasiskirstymo normalumas buvo nustatomas Kolmogorovo-Smirnovo testu. Imčių dydžiai parinkti atsitiktinai. Jiems apskaičiuoti buvo pritaikoma V. I. Paniotto formulė arba naudojama imties dydžio skaičiuoklė tyrimo programiniame pakete (*Creative Research System, Sebastopol, CA, USA*). Buvo pasirinkti šie kriterijai: tyrimo paklaida 0,05, o pasikliautinis intervalas 95 proc. Duomenys buvo pateikiami kaip vidurkis ir standartinis nuokrypis (SN) arba vidurkis ir standartinė paklaida (SP). Įvairūs statistinės analizės metodai buvo taikyti tyrimo

grupėms, įskaitant aprašomąją statistiką, Pearsono chi kvadrato testą (*Pearson chi-square test*), Mano-Vitnio U testą (*Mann-Whitney U test*), Fišerio tikslųjį testą (*Fisher's exact test*), Spirmano koreliacijos koeficientą (*Spearman's rank correlation coefficient*), neparametrinį Vilkoksono testą (*Wilcoxon's signed ranks test*), porinių imčių t-testą (*paired sample t-test*), Koheno (*Cohen's Kappa coefficient*) ir svertinį (*Weighted Kappa coefficient*) Kappa koeficientus. Statistiniu reikšmingumu nuspręsta laikyti rezultatus, kai p reikšmės gaunamos mažesnės nei 0,05.

Rezultatai

Remiantis I tyrimo rezultatais, jokių statistiškai reikšmingų skirtumų tarp AŽK matomumo ŽDS viršutinėje medialinėje ir distalinėje dalyse, taip pat apatinėje medialinėje ir distalinėje dalyse rasta nebuvo ($p > 0,05$). Vis dėlto buvo statistiškai reikšmingų skirtumų tarp specifinių AŽK viršutinių ir apatinių ribų matomumo taškų ($p < 0,05$). Iki 24,7 proc. ŽDS viršutinė AŽK siena nebuvo matoma, ir tai yra daugiau nei du kartus dažniau nei kai nematoma apatinė AŽK siena (iki 10,2 proc.). Viršutinės ir apatinės AŽK sienos matomumas nebuvo susijęs su morfometriniiais ar densitometriniiais nustatymo parametrais, taip pat nebuvo susijęs su amžiumi, lytimi, ŽDS lokalizacija bei būkle. Viršutinės ir apatinės AŽK sienos matomumas ŽDS nebuvo susijęs su kaimyninių ar kontralateralinių ŽDS matomumu. II tyrimas patvirtino, kad anga nustatyta $18,33 \pm 5,45$ mm žemiau nei kaulinė ketera ir $17,40 \pm 7,52$ mm toliau nuo apatinio žandikaulio apatinio krašto, nors atstumas nuo angos iki danties viršūnės buvo $10,06 \pm 4,38$ mm (vyrams nustatyti reikšmingai didesni matmenys [$p < 0,05$]). Liežuvinė anga buvo vidutiniškai $0,89 \pm 0,40$ mm diametro. Dažniausiai pasitaikė monotipinis arterijos tipas (76,8 proc.), dvigubas kanalas buvo nustatytas 20,0 proc., o 3,2 proc. atvejų nustatyta triguba liežuvinė anga. Iš 1061 angų 75,6 proc. buvo ≤ 1 mm, o 24,4 proc. buvo > 1 mm, ir tai būtų siejama su didesne kraujavimo tikimybe. Liežuvinės angos, lokalizuotos šalia vidurio linijos, diametras buvo statistiškai reliatyviai didesnis nei angos, esančios lateraliau.

Bedančių zonų pasiskirstymas vyrams ir moterims buvo panašus, o dažniausiai trūko pirmojo krūminio danties (35,8 proc.) (III tyrimas). Daugumoje sinusų membranų nebuvo morfologinių pokyčių (58,2 proc.), o 19,3 proc. atvejų konstatuotas plokštuminis morfologinis sutankėjimas. Viršutinio žandikaulio sinuso anga buvo ryški 89,2 proc. pacientų, ir lytis neturėjo įtakos gautoms reikšmėms ($p > 0,05$). Vidutinis sinuso plotis pavienėse bedantėse zonose buvo $13,46 \pm 6,92$ mm. Vidutinis alveolinio kaulo aukštis nustatytas $7,13 \pm 4,37$ mm, kai plotis dantų šaknų viršūnių zonose siekė $5,19 \pm 2,2$ mm. Tiriant VGAA konstatuota, kad 63,0 proc. pacientų

VGAA nebuvo pastebima skerspjūviuose, o dauguma matomų VGAA vaizdų nurodė intraosalinę arterijos išsidėstymą.

IV tyrimas patvirtino 109 literatūros šaltinius, kurie buvo tinkami apžvalgai. Buvo pasiūlyta konkreti klasifikacija atskiriems BŽS parametrams įvertinti: žandikaulio kaulo anatomijai, AŽK identifikavimui ir AAN pažeidimų rizikos nustatymo galimybės, estetiniams sprendimams estetinėje zonoje. Sukurta nauja žandikaulių kaulo anatomijos klasifikacija, skirta dantų implantacijos diagnostikai ir planavimui, pagrįsta anatomiciais ir radiologiniais duomenimis, literatūros apžvalga, atliktų tyrimų rezultatais ir asmenine klinicine patirtimi. BŽS buvo padalinti į tris tipus (V tyrimas) pagal kietųjų ir minkštųjų audinių parametrus: I tipas – maža implantacijos rizika ir tinkami audinių parametrai, II tipas – vidutinė rizika ir kompromisiniai audinių parametrai, III tipas – rekomenduojama vėlyva implantacija, deficitiniai audinių parametrai. Išvados buvo patvirtintos priešoperacinėje, intraoperacinėje ir pooperacinėje stadijose be reikšmingų skirtumų tarp jokių matmenų.

Diskusija ir reikšmė perspektyvoje

Dantų implantacija yra svarbi gydomoji procedūra bedančiams pacientams ir gali būti sėkmingai atlikta naudojant vaizduojamuosius diagnostinius metodus. Diagnostiniai metodai, naudoti šiuose tyrimuose, yra lemiami planuojant odontologinę operaciją, taip pat ir intraoperaciniam bei pooperaciniam įvertinimui, norint išsiaiškinti gydymo sėkmę. Atlikus tyrimus ir apžvelgus literatūrą buvo nustatyta, kad KPKT metodas šiuo metu yra optimalus pasirinkimas dėl įvairių priežasčių, įskaitant tyrimo prieinamumą ir jo saugumą pacientui, turint omenyje gaunamą sąlyginai nedidelę radiacinę apšvitą. Vis dėlto diagnostiką svarbu pradėti nuo panoraminės rentgenogramos, intraoralinių rentgenologinių metodų, o aukštesnės vaizdo kokybės KPKT naudoti kaip paskutinį pasirinktiną metodą. Gydytojams naudinga informacija, gaunama iš skerspjūvio vaizdų, ypač kai reikalingi viso viršutinio žandikaulio ir apatinio žandikaulio vaizdai.

Išvados

1. Skaitmeninė panoraminė rentgenograma nebuvo pakankamai informatyvi nustatant apatinio žandikaulio kanalo matomumą įvairiuose dantiniuose segmentuose, priklausomai nuo morfometrinių ir densitometrinių parametrų. Du kartus dažniau (iki 25 proc.) buvo identifikuojama nematoma viršutinė kanalo sienelė, palyginti su apatine (apie 10 proc.).

2. Apatinio žandikaulio liežuvinės kraujagyslės kanalo anga gali būti identifikuojama tiriant konusinio pluošto kompiuteriniu tomografu. Kraujagysliniai kanalai ir keletas anastomozių nustatyta priekiniame apatinio žandikaulio segmente ir tęsiasi iki kaplių ir krūminių dantų. Yra būtina identifikuoti šias kraujagysles prieš atliekant chirurgines apatinio žandikaulio manipuliacijas, kad būtų išvengta intraoperacinio kraujavimo.
3. Viršutinio žandikaulio sinuso ir jį supančio kaulo anatomicinės struktūros gali būti identifikuojamos tiriant konusinio pluošto kompiuteriniu tomografu. Buvo įvertintos anatomicinės variacijos tiriant atskirai pavienių ir daugybinių dantų eilių defektų sritis didelei tiriamųjų grupei ir pateikta vertinga informacija danų implantacijos planavimui.
4. Buvo sukurta nauja žandikaulių anatomijos klasifikacija, skirta endosalinei dantų implantacijai planuoti, išskiriant estetinę ir neestetinę zonas bei apatinio žandikaulio kanalo ir viršutinio žandikaulio sinuso regionus. Bedančiai žandikaulių segmentai buvo suskirstyti į tris tipus pagal jų klinikinio ir radiologinio įvertinimo rezultatus ir planuojamo chirurginio gydymo rizikos laipsnį.
5. Tiriant naują klinikinę ir radiologinę žandikaulių anatomijos klasifikaciją nustatyta, kad klasifikacija yra patikima, kadangi statistiškai patikimai koreliavo įvairūs diagnostiniai parametrai, nustatyti priešoperaciniame, intraoperaciniame bei ankstyvajame ir vėlyvajame pooperaciniuose dantų implantacijos etapuose.

Rekomendacijos klinikinei praktikai

1. Kadangi SPR nebuvo pakankamai informatyvi nustatant AŽK matomumą įvairiuose dantiniuose segmentuose, atsižvelgiant į morfometrinius ir densitometrinius parametrus, amžių, lytį, ŽDS lokalizaciją ir kt., rekomenduojama taikyti pažangesnius radiologinio tyrimo metodus, norint efektyviau nustatyti AŽK viršutinę sienelę.
2. Liežuvinių kraujagyslių kanalai ir jų anastomozės yra nustatomi priekiniame ir galiniame apatinio žandikaulio segmentuose. Šių nedidelių kraujagyslių pažeidimas gali sukelti reikšmingą kraujavimą. Šiems kanalams nustatyti rekomenduojamas KPKT tyrimo metodas.
3. Prieš dantų implantaciją viršutinio žandikaulio sinuso regione arba sinuso dugno pakėlimo operaciją rekomenduojama iširti viršutinio žandikaulio sinuso (viršutinę galinę alveolinę arteriją, sinuso angą,

- gleivinę, pertvaras) ir jį supančio kaulo anatomines struktūras KPKT tyrimo metodu.
4. Nauja žandikaulių anatomijos klasifikacija, skirta endosalinei dantų implantacijai planuoti, gali pasitarnauti nustatant planuojamo chirurginio gydymo rizikos laipsnį. Gydymo planavimo unifikavimas yra žingsnis dantų implantacijos standartizavimo ir geresnio specialistų tarpusavio supratimo link. Kliniškai patikrinta ir papildyta klasifikacija yra patikimesnė ir gali būti naudojama kasdieninėje klinikinėje praktikoje.

Rekomendacijos moksliniams tyrimams

1. Kadangi I tyrimo metu buvo nustatyta, kad atlikti SPR densitometriniai matavimai, norint nustatyti AŽK, buvo netikslūs, mes rekomenduojame atlikti papildomus densitometrinio matavimo tyrimus, naudojant fantominį modelį kokybei kontroliuoti. Gavus teigiamą rezultatą, galima būtų atlikti naują tyrimą, įtraukiant didesnę tiriamųjų skaičių.
2. II ir III tyrimai buvo atlikti kelyse šalyse. Mes rekomenduojame atlikti nacionalinę studiją, įtraukiant didesnę tiriamųjų skaičių, nes anatominiai ypatumai dalinai gali būti priklausomi nuo rasės ir geografinės vietovės.
3. Periodiškai reikia atlikti literatūros analizę, kad būtų galima įvertinti naujus mokslinius duomenis, susijusius su dantų implantacijos planavimu (IV tyrimas). Klasifikacijos turėtų būti papildomos ir patikrinamos, kad turėtume planavimo ir geresnio specialistų tarpusavio supratimo priemonę.
4. Turėtų būti atliekami tolimesni tyrimai su didesne tiriamųjų imtimi, kad būtų patvirtinti V pilotinio tyrimo metu gauti rezultatai.

APPENDICES

Appendix I

IMPLANTATION RISK EVALUATION QUESTIONNAIRE

Observer:

Assessment series No:

Date:

The tooth was lost months/ year(s) before surgery.

Patients name and family name:

Gender: Male Female

Age:

Aesthetic zone Tooth No (*underline necessary*):

15 14 13 12 11 21 22 23 24 25 35 34 33 43 44 45

Non aesthetic zone tooth No (*underline necessary*):

17 16 26 27 37 36 46 47

Dental implant system and its peculiarities: _ _ _ _ _

- ADIN group dental implants (ADIN Dental Implant System Ltd., Afula, Israel)
- Bego group dental implants (Bego Implant Systems GmbH & Co. KG, Bremen, Germany)
- Biohorizons group dental implants (Biohorizons, Birmingham, AL, USA)
- EBI group dental implants (EBI, Gyeongsan-si, Gyeongsangbuk-do, South Korea)
- MIS group dental implants (MIS Implants Inc., Barlev, Israel)
- Nobel Biocare group dental implants (Nobel Biocare AB, Göteborg, Sweden)
- Straumann group dental implants (Straumann AG, Basel, Switzerland)
- Zimmer group dental implants (Zimmer Dental Inc., Carlsbad, CA, USA)

Edentulous jaw segment parameters		Edentulous jaw segment types (risk degree)					
		Type I (low risk)		Type II (moderate risk)		Type III (high risk)	
		Range	Value	Range	Value	Range	Value
Non aesthetic zone							
Height (mm)	Maxilla	> 10		> 8 to ≤ 10		≤ 8	
				> 4 to ≤ 10 in MSR		≤ 4 in MSR	
	Mandible	> 10		> 8 to ≤ 10		≤ 8	

Edentulous jaw segment parameters		Edentulous jaw segment types (risk degree)					
		Type I (low risk)		Type II (moderate risk)		Type III (high risk)	
		Range	Value	Range	Value	Range	Value
Width (mm)		> 6		> 4 to ≤ 6		< 4	
Length (mm)		≥ 7 or ≤ 12		≥ 6 or ≤ 13		< 6 or > 13	
Alveolar ridge vertical position (mm)		≤ 3		> 3 to < 7		≥ 7	
Aesthetic zone							
Height (mm)	Maxilla	> 10		> 8 to ≤ 10		≤ 8	
				> 4 to ≤ 10 in MSR		≤ 4 in MSR	
	Mandible	> 10		> 8 to ≤ 10		≤ 8	
Width (mm)		Optimal implant diameter + 3		Optimal implant diameter + < 3		Optimal implant diameter + ≤ 0	
Length (mm)		Equal to contralateral tooth		Asymmetry < 1 mm with contralateral tooth		Asymmetry ≥ 1 mm with contralateral tooth	
Alveolar ridge vertical position (mm)		≤ 2		> 2 to ≤ 4		> 4	
Mandibular canal (MC) region (inferior alveolar nerve injury risk degree)							
MC walls identification and jaw bone quality type combination		Identified MC walls/D2 and D3		Unidentified superior MC wall/D1 and D4		Unidentified MC/D1 and D4	
Planned dental implant		Height (mm) – Diameter (mm) –				Implant surgery is not planned	

Edentulous jaw segment parameters		Edentulous jaw segment types (risk degree)					
		Type I (low risk)		Type II (moderate risk)		Type III (high risk)	
		Range	Value	Range	Value	Range	Value
Planned implant threads coverage by the bone (mm)	Non aesthetic zone	≥ 1		Implant walls are covered by the bone < 1		Cervical or isolated part(s) of the implant is not covered by the bone	
	Aesthetic zone (buccal + lingual wall)	≥ 3		Total sum of implant coverage by the bone from buccal and lingual side < 3		Cervical or isolated part(s) of the implant is not covered by the bone	
Overall EJS type (risk degree)		Type I		Type II		Type III	
Distance from implant apex to anatomically important vital structures (mm)		≥ 1		< 1			

“+”, agreement; “-”, disagreement. MSR = maxillary sinus region; EJS = edentulous jaw segment. Linear measurement should be provided in millimeters; All appendices should be filled in capital letters.

INTRAOPERATIVE EVALUATION OF SURGERY AND EARLY POSTOPERATIVE STAGE EVALUATION QUESTIONNAIRE

Observer:

Assessment series No:

Date:

Patients name and family name:

Aesthetic zone Tooth No (*underline necessary*):

15 14 13 12 11 21 22 23 24 25 35 34 33 43 44 45

Non aesthetic zone tooth No (*underline necessary*):

17 16 26 27 37 36 46 47

Overall planned edentulous jaw segment type (risk degree):

I, II, III (*underline necessary type*)

Intraoperative surgery evaluation parameters		Agreement with implantation risk evaluation			
		No risk		Risk	
Alveolar ridge vertical position (mm)	Non aesthetic zone	≤ 3	> 3 to < 7		
			≥ 7		
	Aesthetic zone	≤ 2	> 2 to ≤ 4		
			> 4		
Bone peak height (mm)	Mesial	3 to 4	> 1 to ≤ 3		
			< 1		
	Distal	3 to 4	> 1 to ≤ 3		
			< 1		
Implant threads coverage by the bone (mm)	Non aesthetic zone	≥ 1	Implant walls are covered by the bone < 1		
			Cervical or isolated part(s) of the implant is not covered by the bone		
	Aesthetic zone (buccal + lingual wall)	≥ 3	Total sum of implant coverage by the bone from buccal and lingual side < 3		
			Cervical or isolated part(s) of the implant is not covered by the bone		

Intraoperative surgery evaluation parameters	Agreement with implantation risk evaluation		
	No risk		Risk
Implant host sites bony walls fractures	not present		present
Primary implant stability (Ncm)	≥ 35		≥ 15 to < 35
			< 15
Excessive bleeding in the apical region of osteotomy	not present		present
Mandibular canal perforation and inferior alveolar nerve direct mechanical injury by implant drill	“sudden give” or “electric shock” has not appeared		“sudden give” or “electric shock” has appeared
Implant drill slippage deeper than planned	not present		present
Implant placement deeper than planned	not present		present
Placed dental implant (height and width, mm)	Dental implant: height – width –		Dental implant was not placed
Distance from implant apex to anatomically important vital structures (mm)	≥ 1		< 1

“+”, agreement; “-”, disagreement. Linear measurement values should be provided in millimeters.

**EVALUATION QUESTIONNAIRE OF LATE POSTOPERATIVE STAGE
PARAMETERS**

Observer:

Assessment series No:

Date:

Patients name and family name:

Aesthetic zone Tooth No (*underline necessary*):

15 14 13 12 11 21 22 23 24 25 35 34 33 43 44 45

Non aesthetic zone tooth No (*underline necessary*):

17 16 26 27 37 36 46 47

Overall planned edentulous jaw segment type (risk degree):

I, II, III (*underline necessary type*)

Late postoperative evaluation parameters		Agreement with intraoperative stage risk evaluation			
		No risk		Risk	
Soft tissue vertical deficiency		0		1 to 2	
				> 2	
Papilla appearance (aesthetic zone parameter)	Mesial	Complete fill		Partial fill	
				None	
	Distal	Complete fill		Partial fill	
				None	

“+”, agreement; “-”, disagreement. Linear measurement should be provided in millimeters.



KAUNO REGIONINIS BIOMEDICININIŲ TYRIMŲ ETIKOS KOMITETAS

KMUK Eivenių 2, Centrinis korpusas, 71 kab., 50009 Kaunas, tel. +370 37 326168, faks. +370 37 326901, e-mail: cmefinfo@kmu.lt

LEIDIMAS ATLIKTI BIOMEDICININĮ TYRIMĄ

2010-12-13 Nr. BE-2-76

Biomedicininio tyrimo pavadinimas: „Viršutinio ir apatinio žandikaulių radiologiniai ištyrimai, vertinant dantis, nervų ir kraujagyslių pluoštus bei kaulines anatomines žandikaulių struktūras”.	
Pagrindinis tyrėjas:	Prof. Ričardas Kubilius Prof. Gintaras Juodžbalys
Biomedicininio tyrimo vieta:	KMUK Veido ir žandikaulių chirurgijos klinika
Įstaigos pavadinimas:	KMUK Dantų ir burnos ligų klinika
Adresas:	Eivenių g. 2, LT-50009 Kaunas

Išvada:

Kauno regioninio biomedicininis tyrimų etikos komiteto posėdžio, įvykusio **2010 m. gruodžio 7 d.** (protokolo Nr. 134/2010) sprendimu pritarta biomedicininio tyrimo vykdymui.

Mokslinio eksperimento vykdytojai įsipareigoja: (1) nedelsiant informuoti Kauno Regioninį biomedicininis Tyrimų Etikos komitetą apie visus nenumatytus atvejus, susijusius su studijos vykdymu, (2) iki sausio 15 dienos – pateikti metinį studijos vykdymo apibendrinimą bei, (3) per mėnesį po studijos užbaigimo, pateikti galutinį pranešimą apie eksperimentą.

Kauno regioninio biomedicininis tyrimų etikos komiteto nariai			
Nr.	Vardas, Pavardė	Veiklos sritis	Dalyvavo posėdyje
1.	Doc. Irena Marchertienė	anesteziologija	taip
2.	Doc. Romaldas Mačiulaitis	klinikinė farmakologija	taip
3.	Prof. Nijolė Dalia Bakšienė	pediatrija	taip
4.	Prof. Irayda Jakušovaite	filosofija	ne
5.	Dr. Eimantas Peičius	filosofija	taip
6.	Laima Vasiliauskaite	psichoterapija	taip
7.	Gintaras Česnauskas	chirurgija	ne
8.	Zelmanas Šapiro	terapija	ne
9.	Jurgita Laurinaitytė	bioteisė	ne

Kauno regioninis biomedicininis tyrimų etikos komitetas dirba vadovaudamasis etikos principais nustatytais biomedicininis tyrimų Etikos įstatyme, Helsinkio deklaracijoje, vaistų tyrinėjimo Geros klinikinės praktikos taisyklėmis.

Pirmininkė

Irena Marchertienė





VALSTYBINĖ DUOMENŲ APSAUGOS INSPEKCIJA

Lietuvos sveikatos mokslų universitetui
A. Mickevičiaus g. 9, LT-44307 Kaunas
(registruotu laišku ir el.p.marius.kubilius@yahoo.com)

SPRENDIMAS
DĖL LEIDIMO LIETUVOS SVEIKATOS MOKSLŲ UNIVERSITETUI ATLIKTI ASMENS
DUOMENŲ TVARKYMO VEIKSMUS

2013 m. spalio 13 d. Nr. 2R-1140 (2.6-1.)
Vilnius

Valstybinė duomenų apsaugos inspekcija, išnagrinėjusi Lietuvos sveikatos mokslų universiteto 2013-10-04 pateiktą pranešimą Nr. 1 dėl išankstinės patikros (toliau – Pranešimas) ir 2013-10-16 raštu pateiktą patikslintą Pranešimą (Inspekcijoje gauta 2013-10-09, reg. Nr. 1R-4625 ir 2013-10-18, reg. Nr. 1R-4794),

n u s t a t ė,

kad Lietuvos sveikatos mokslų universiteto Pranešime ir patikslintame Pranešime nurodyti asmens duomenų tvarkymo veiksmai atitinka Lietuvos Respublikos asmens duomenų teisinės apsaugos įstatyme (Žin., 1996, Nr. 63-1497; 2011, Nr. 65-3046) nustatytus asmens duomenų tvarkymo ir duomenų subjektų teisių įgyvendinimo reikalavimus, bei numatytos tinkamos organizacinės ir techninės duomenų saugumo priemonės.

Valstybinė duomenų apsaugos inspekcija, vadovaudamasi Lietuvos Respublikos asmens duomenų teisinės apsaugos įstatymo 33 straipsniu, Valstybinės duomenų apsaugos inspekcijos direktoriaus 2006 m. vasario 2 d. įsakymu Nr. 1T-6 (Žin., 2006, Nr. 18-653; 2009, Nr. 11-447) patvirtintų Išankstinės patikros atlikimo taisyklių 11 ir 18.1 punktais,

n u s p r e n d ė i a

Lietuvos sveikatos mokslų universitetui išduoti leidimą atlikti Pranešime ir patikslintame Pranešime nurodytą asmens duomenų apie sveikatą tvarkymo biomedicininio tyrimo „Viršutinio ir apatinio žandikaulių radiologiniai ištyrimai, vertinant dantis, nervų ir kraujagyslių pluoštus bei kaulines anatomines žandikaulių struktūras“ tikslu, veiksmus.

Direktorius



Algirdas Kuncinas

dr. Algirdas Kuncinas



EU2013.LT

V. Perednienė, tel. (8 5) 219 7279, el. p. vanda.peredniene@ada.lt;
A. Judinas, tel. (8 5) 219 7266, el. p. Arnoldas.judinas@ada.lt

Biudžetinė įstaiga
A. Juozapavičiaus g. 6
LT-09310 Vilnius

Tel. (8 5) 279 1445
Faks. (8 5) 261 9494
El. p. ada@ada.lt

Duomenys kaupiami ir saugomi
Juridinių asmenų registre
Kodas 188607912

CURRICULUM VITAE

Name, Surname: Marius Kubilius
Address: Lithuanian University of Health Sciences, Medical Academy,
Faculty of Odontology, Department of Maxillofacial surgery
Eivenių 2, LT-50009 Kaunas, Lithuania
Mobile phone: +37061804693
E-mail: mariuskubilius@yahoo.com

Education:

1999–2004 Program of Study in Odontology, Master of Dental Science and professional qualification of odontologist (Doctor of Dental Sciences), Kaunas University of Medicine, Faculty of Odontology, Kaunas, Lithuania

Postgraduate and further training:

2004–2005 Dental Internship program, Kaunas University of Medicine, Kaunas, Lithuania
2006–2009 Dental Residency Program in Oral Surgery, Doctor of Oral Surgery, Kaunas University of Medicine, Department of Maxillofacial surgery, Kaunas, Lithuania
2010–2016 PhD studies (Biomedical Sciences, Odontology), Lithuanian University of Health Sciences, Medical Academy, Department of Maxillofacial surgery, Kaunas, Lithuania

Position held:

2009–2015 Tutor in Oral Surgery, Department of Maxillofacial surgery, Kaunas University of Medicine (presently Lithuanian University of Health Sciences, Medical Academy, Department of Maxillofacial surgery, Kaunas, Lithuania)

Clinical work experience:

2005–2007 Dentist, UAB “Garliavos šeimos klinika”, Kaunas, Lithuania
2007 Dentist/oral surgeon, UAB “Aukštėja”, Kaunas, Lithuania
2008–2011 Dentist, UAB “Juvenalitas”, Vilnius, Lithuania
2009–2011 Dentist, UAB “Arinija”, Kaunas, Lithuania
2009–2013 Dentist/oral surgeon, T. Lingio IĮ dental clinic, Alytus, Lithuania
2011–2012 Oral surgeon, UAB “Dantėja”, Kaunas, Lithuania
2012 Dentist/oral surgeon, UAB “Raimisdent”, Kaunas, Lithuania
2013 Oral surgeon, UAB “Restauracinės odontologijos centras”, Kaunas, Lithuania

Activities related to dentistry:

2004–2005 Editor of the newspaper “Odontologo patarimai”

Scholarships and grants:

2008 Erasmus scholarship (Cardiff University, United Kingdom)

2014 The Open Fund of Lithuanian University of Health Sciences:
the grant

2014 The Research Council of Lithuania: scholarship (DOK-14529) for
academic achievements (for one year)

Membership of professional bodies:

National:

2005 Lithuanian Dental Chamber

2009 Society of Lithuanian Maxillofacial Surgeons

International:

2010 Baltic Osseointegration Academy

2007 ITI International Team of Implantology

ACKNOWLEDGEMENT

This dissertation was based on internationally made studies at Lithuanian University of Health Sciences (Lithuania), Hacettepe University (Turkey), University of Granada (Spain), King Saud University (Saudi Arabia), University of Illinois at Chicago (USA), Near East University (Turkey), Gazi University (Turkey) and University of Michigan (USA).

My work throughout the doctoral studies was influenced by many people who made their contribution in many different ways. Today I am delighted to finally have this opportunity to express my gratitude to every one of them for all the shared knowledge and experience.

I would like to express my deepest sense of gratitude to my mentor and academic advisor, Prof. Dr. Gintaras Juodžbalys, for his guidance in practical ways and his generous support. I have never seen a man so devoted to science. Thank you for your endless patience and trust, for all your corrections, recommendations and encouragement, which built my professional competence slowly but steadily. It has been so much easier to face the challenges knowing that help is always at hand, be it workday or weekend.

My very special thanks go to Prof. Dr. Ričardas Kubilius, Head of the Clinic, for his everlasting positive approach towards any assignment and his firm belief in happy endings. The truth is that indeed all ends well when he is around. And yet, trying your best is essential.

I often recall my very first steps in the world of science, and my mind always takes me back to those heart-to-hearts with the late Prof. Dr. Gintautas Sabalys. I am truly honored to have known this remarkable person.

I wish to express my gratitude to Irena Nedzelskienė and Assoc. Prof. Dr. Rimantas Žalinkevičius, who were my saviors and my teachers of mathematical statistics. Thanks to their contribution, the numbers in my papers started making sense.

I would like to thank all my foreign colleagues for the successfully implemented international researches, especially Assoc. Prof. Dr. Tolga F. Tözüm and Prof. Dr. Hom-Lay Wang. Engagement in this assignment helped me to realize how difficult it is to carry out a high quality large scale international research and how important it is to have a strong team with similar viewpoint towards the common goal. This was a true school of patience.

I am very grateful to my colleagues and employers who showed great interest in my work and patiently waited until I completed my creative endeavor.

I thank everyone who seamlessly helped me to develop my discreet demeanor and ability to balance between several totally different opinions.

My very special thanks to my well-meaning patients: if not for them, this thing would have not even started.

I remain forever grateful to my parents, Vilma and Daiva for always being by my side when I needed them.

To my wife and my closest friend Laura, and my little girls, who patiently coped with the constant lack of attention, my absent-mindedness and nervous tension, thank you for everything.